EMERGING TALENTS IN FRONTIERS IN PHARMACOLOGY: GASTROINTESTINAL AND HEPATIC PHARMACOLOGY 2022

EDITED BY: Laura Grasa, Thomas Brzozowski and Marilia Seelaender
COORDINATED BY: Andrea Bellés Miralles and Diego Aguirre Ramírez
PUBLISHED IN: Frontiers in Pharmacology

frontiers Research Topics

ISSN 1664-8714
ISBN 978-2-83250-707-0
DOI 10.3389/978-2-83250-707-0

About Frontiers

Frontiers is more than just an open-access publisher of scholarly articles: it is a pioneering approach to the world of academia, radically improving the way scholarly research is managed. The grand vision of Frontiers is a world where all people have an equal opportunity to seek, share and generate knowledge. Frontiers provides immediate and permanent online open access to all its publications, but this alone is not enough to realize our grand goals.

Frontiers Journal Series

The Frontiers Journal Series is a multi-tier and interdisciplinary set of open-access, online journals, promising a paradigm shift from the current review, selection and dissemination processes in academic publishing. All Frontiers journals are driven by researchers for researchers; therefore, they constitute a service to the scholarly community. At the same time, the Frontiers Journal Series operates on a revolutionary invention, the tiered publishing system, initially addressing specific communities of scholars, and gradually climbing up to broader public understanding, thus serving the interests of the lay society, too.

Dedication to Quality

Each Frontiers article is a landmark of the highest quality, thanks to genuinely collaborative interactions between authors and review editors, who include some of the world's best academicians. Research must be certified by peers before entering a stream of knowledge that may eventually reach the public - and shape society; therefore, Frontiers only applies the most rigorous and unbiased reviews.
Frontiers revolutionizes research publishing by freely delivering the most outstanding research, evaluated with no bias from both the academic and social point of view. By applying the most advanced information technologies, Frontiers is catapulting scholarly publishing into a new generation.

What are Frontiers Research Topics?

Frontiers Research Topics are very popular trademarks of the Frontiers Journals Series: they are collections of at least ten articles, all centered on a particular subject. With their unique mix of varied contributions from Original Research to Review Articles, Frontiers Research Topics unify the most influential researchers, the latest key findings and historical advances in a hot research area! Find out more on how to host your own Frontiers Research Topic or contribute to one as an author by contacting the Frontiers Editorial Office: frontiersin.org/about/contact

EMERGING TALENTS IN FRONTIERS IN PHARMACOLOGY: GASTROINTESTINAL AND HEPATIC PHARMACOLOGY 2022

Topic Editors:
Laura Grasa, University of Zaragoza, Spain
Thomas Brzozowski, Jagiellonian University Medical College, Poland
Marilia Seelaender, University of São Paulo, Brazil

Coordinator Editors:
Andrea Bellés Miralles, University of Zaragoza, Spain
Diego Aguirre Ramírez, University of Zaragoza, Spain

Citation: Grasa, L., Brzozowski, T., Seelaender, M., Miralles, A. B., Ramírez, D. A., eds. (2022). Emerging Talents in Frontiers in Pharmacology: Gastrointestinal and Hepatic Pharmacology 2022. Lausanne: Frontiers Media SA.
doi: 10.3389/978-2-83250-707-0

Table of Contents

frontiers | Frontiers in Pharmacology

TYPE Editorial
PUBLISHED 21 October 2022
DOI 10.3389/fphar.2022.1055030

OPEN ACCESS

EDITED AND REVIEWED BY
Angelo A. Izzo,
University of Naples Federico II, Italy

*CORRESPONDENCE
Laura Grasa,
lgralo@unizar.es

SPECIALTY SECTION
This article was submitted to Gastrointestinal and Hepatic Pharmacology, a section of the journal Frontiers in Pharmacology

RECEIVED 27 September 2022
ACCEPTED 10 October 2022
PUBLISHED 21 October 2022

CITATION
Grasa L, Brzozowski T and Seelaender M (2022), Editorial: Emerging talents in Frontiers in pharmacology: Gastrointestinal and hepatic pharmacology 2022.
Front. Pharmacol. 13:1055030.
doi: 10.3389/fphar.2022.1055030

Editorial: Emerging talents in Frontiers in pharmacology: Gastrointestinal and hepatic pharmacology 2022

Laura Grasa[1]*, Thomas Brzozowski[2] and Marilia Seelaender[3]

[1]Department of Pharmacology, Physiology and Legal and Forensic Medicine, University of Zaragoza, Zaragoza, Spain, [2]Department of Physiology, Jagiellonian University Medical College, Krakow, Poland, [3]Department of Surgery and LIM 25-HC, Faculdade de Medicina, University of São Paulo, São Paulo, Brazil

KEYWORDS

inflammatory bowel disease (IBD), irritable bowel syndrome (IBS), liver disease, cancer, pancreatitis

Editorial on the Research Topic
Emerging talents in Frontiers in pharmacology: Gastrointestinal and hepatic pharmacology 2022

This special edition of *Frontiers in Pharmacology* is dedicated to students from all over the world that undertake key research as part of education in Gastrointestinal and Hepatic Pharmacology. Here we present an article collection dedicated to highlighting the emerging talent of student researchers within the field of Gastrointestinal and Hepatic Pharmacology submitted on that occasion.

First, we present some articles related to the pharmacology of gastrointestinal diseases.

Zhang et al. overviewed and extended the discussion on the understanding of ulcerative colitis (UC) and postulated causes and mechanisms, while also providing biometric data on the last decade efforts to examine this disorder. The review stresses the need for collaborative work in Asia. Authors provide an insight into the mechanism of microbiome-induced inflammation, with major focus to NLRP3 inflammasome pathway, which has been one of the most explored and discussed "hot topics" in the scenario of this disease. They emphasized the potential of faecal microbiota transplants, anti-integrin treatment and the use of JAK inhibitor as the nowadays treatment options in patients with UC.

Li et al. performed and described a very diligent study showing that nintedanib, a new drug from the group of tyrosine kinase inhibitors, can be useful in the treatment of inflammatory bowel disease (IBD), by restoring intestinal permeability and the intestinal microbiota. Using advanced bioinformatics analysis and cellular and animal models of intestinal inflammation, they show that the action mechanism of this drug would involve the inhibition of the PCK1 and EFNA1 genes, which are regulated by the transcription factor CEBPB through two super-enhancers (sc-CHR20-57528535 and sc-CHR1-155093980). In addition, nintedanib improves the levels of beneficial microbiota for intestinal health.

Wang et al. presented an important dataset on the UK Biobank collection of over 100,000 adult irritable bowel syndrome (IBS) patients based on the incidence criteria and influencing factors, including pathogenesis and diagnosis criteria. They found that the majority of patients suffered from mixed IBS as the dominant subtype, followed by diarrhea-dominant IBS and constipation-dominant IBS. Precise analysis of the data showed that somatization and celiac disease were the main risk factors for IBS, and that risk factors such as gender differences in mental health are critical to physician diagnosis and treatment of particular IBS subtypes.

Guo et al. have determined the mechanism of cisplatin chemotherapy, which is known to induce nausea and vomiting in cancer patients suffering from depressive mood disorder. They developed experimental two animal models of chronic, unpredictable, mild stress that induced a depression-like phenotype in rats and a model resembling cisplatin-induced vomit, and investigated kaolin and food intake after administration of cisplatin. They found that chronic stress increased 5-HT and SP levels, accompanied by upregulation of 5-HT_3R, DA_2R, NK_1R and downregulation of CB_1R expression in the core extension. In contrast, chronic stress decreased the expression of 5-HT_3R, DA_2R, NK_1R and increased expression of CB_1R in the ileum. They concluded that anorexia and vomiting are exacerbated by chronic stress due to the activity of vomit-related molecules and their overexpression in the enteric nervous system (ENS).

Second, we present some articles of talented young researchers related to the pharmacology of liver and gallbladder diseases.

Ma et al. present novel and exciting results on the pharmacological regulation with Empagliflozin (EMPA) of Sestrin 2, a protein induced by stressing stimuli common to obesity-related diseases, such as nonalcoholic fatty liver disease (NAFLD). By performing *in vivo* and *in vitro* experiments, they provide further evidence showing this drug to prevent steatosis and hepatic inflammation. The authors elegantly demonstrate that, by inducing upregulation of Sestrin 2, EMPA modulates cell signaling via the AMPK/mTOR pathway. In addition to unveiling the mechanism of action of EMPA, they propose Sestrin 2 as target for further study of therapeutic strategies aiming at mitigating NAFLD.

Hou et al. presented the data of a clinical trial with regorafenib in the treatment for patients with hepatocellular carcinoma (HCC) who have progressive disease despite anti-tumor treatment with sorafenib. The results of this retrospective analysis in Chinese patients indicate that the second-line oral Regorafenib treatment is safe and can significantly improve overall survival of HCC patients.

Yang et al. have validated a novel model using aminotransferase (ALT) and total bilirubin dynamic evolution patterns to predict acute liver failure (ALF) in patients suffering from drug-induced liver injury. In comparison with other predictive models like Hy´s law or Robles-Diaz Model, this model has significantly higher capability of ALF prediction. In addition, the predictive potency of the model for ALF can be improved incorporating other parameters like the international normalized ratio (INR) and alkaline phosphatase (ALP).

Yan et al. have demonstrated a novel mode of action of the farnesoid X receptor (FXR) during the biliary obstruction. It is known that FXR is a key factor regulating hepatic bile acid synthesis and enterohepatic circulation. However, the authors show, for the first time, that the restoration of the FXR pathway improves both, the intestinal barrier damage and intestinal microbiota imbalance in rats with experimental bile-duct ligation. These findings provide a new, possibly translational potential target for clinical prevention of intestinal mucosal barrier injury in patients with obstructive jaundice.

Finally, we present an experimental study about the treatment of acute pancreatitis.

Yang et al. undertook *in vivo* and *in vitro* studies on the mechanism of the Chinese formula, Chaiqin chengqi decoction (CQCQD) against the development of acute pancreatitis (AP), introducing a new murine model of obesity-induced alcohol-AP. They assessed AP severity and its correlation with pancreas and fat using transcriptomic analysis and network pharmacology, as well as the interactions between CQCQD compounds and their key targets. They found that AP and systemic inflammation were attenuated by CQCQD through the activation of Nrf2/HO-1 antioxidant proteins and significant reduction of PI3K/Akt phosphorylation in pancreatic and adipose murine tissue. Moreover, CQCQD was effective in protecting freshly isolated acinar cells *in vitro* from oxidative stress-induced damage and necrotic cell death. These investigators conclude that CQCQD could alleviate AP severity by activating antioxidant proteins and reducing the PI3K/Akt signaling pathway in the pancreas and visceral adipose tissue associated with obesity.

Author contributions

All authors listed have made a substantial, direct, and intellectual contribution to the work and approved it for publication.

Conflict of interest

The authors declare that the research was conducted in the absence of any commercial or financial relationships that could be construed as a potential conflict of interest.

Publisher's note

frontiers | Frontiers in Pharmacology

ORIGINAL RESEARCH
published: 06 June 2022
doi: 10.3389/fphar.2022.917384

Real-Life Experience of Regorafenib in Patients With Advanced Hepatocellular Carcinoma

Jing-Yu Hou[1,2†], Ya-ting Xiao[3†], Jing-Bo Huang[4†], Xin-Hua Jiang[5], Kai Jiang[6], Xun Li[7], Li Xu[1,2] and Min-Shan Chen[1,2*]*

[1]Department of Liver Surgery, Sun Yat-sen University Cancer Center, Sun Yat-sen University, Guangzhou, China, [2]Collaborative Innovation Center for Cancer Medicine, State Key Laboratory of Oncology in South China, Guangzhou, China, [3]School of Molecular Medicine, Hangzhou Institute for Advanced Study, UCAS, Hangzhou, China, [4]Department of Hepatobiliary Surgery, The First Affiliated Hospital of Hunan Normal University (Hunan Provincial People's Hospital), Changsha, China, [5]Department of Radiology, Sun Yat-sen University Cancer Center, State Key Laboratory of Oncology in South China, Collaborative Innovation Center for Cancer Medicine, Guangzhou, China, [6]Department of Orthopaedics, The Second Xiangya Hospital, Central South University, Changsha, China, [7]School of Chemical Engineering, University of Chinese Academy of Sciences, Beijing, China

OPEN ACCESS

Edited by:
Laura Grasa,
University of Zaragoza, Spain

Reviewed by:
Eleonora Lai,
Azienda Ospedaliero Universitaria Cagliari, Italy
Rasha M. Allam,
National Research Centre, Egypt

***Correspondence:**
Li Xu
xuli@sysucc.org.cn
Min-Shan Chen
chenmsh@sysucc.org.cn

[†]These authors have contributed equally to this work and share first authorship

Specialty section:
This article was submitted to Gastrointestinal and Hepatic Pharmacology, a section of the journal Frontiers in Pharmacology

Received: 11 April 2022
Accepted: 16 May 2022
Published: 06 June 2022

Citation:
Hou J-Y, Xiao Y-t, Huang J-B, Jiang X-H, Jiang K, Li X, Xu L and Chen M-S (2022) Real-Life Experience of Regorafenib in Patients With Advanced Hepatocellular Carcinoma. Front. Pharmacol. 13:917384. doi: 10.3389/fphar.2022.917384

Background: The RESORCE trial reported that regorafenib was effective as the second-line treatment for patients with hepatocellular carcinoma (HCC) after progression on sorafenib. Real-world data are needed to assess clinical outcomes and adverse events in the setting of daily practice.

Objective: We aimed to evaluate the efficacy and safety of regorafenib after disease progression with sorafenib in Chinese patients with advanced HCC.

Patients and Methods: A total of 41 patients with advanced HCC who did not respond to sorafenib and followed a regorafenib regimen were enrolled in this retrospective study. Overall survival (OS), progression-free survival (PFS), radiological responses, and adverse events (AEs) were evaluated. Survival curves were compared by using the log-rank test and constructed with the Kaplan–Meier method.

Results: The median PFS with regorafenib was 6.6 months (range: 5.0–8.2 months), and the median OS with regorafenib was not reached. The 1-year OS rate of regorafenib was 66.4%. The median OS of sequential sorafenib to regorafenib treatment was 35.3 months [95% confidence interval (CI), 24.3–46.3], and the 2-year OS rate of sequential sorafenib to regorafenib treatment was 74.4%. The most common AEs of regorafenib treatment were elevated aspartate aminotransferase [17/41 patients (41.5%)], elevated alanine aminotransferase [16/41 patients (39%)] and hand-foot syndrome [14/41 patients (34.1%)].

Conclusion: Regorafenib appears to be safe and clinically effective in patients with advanced HCC who progressed on first-line sorafenib.

Keywords: hepatocellular carcinoma, prognosis, regorafenib, sorafenib, retrospective study

INTRODUCTION

In 2018, liver cancer became the sixth most common cancer and the fourth leading cause of cancer-related deaths worldwide, with China ranking first worldwide in terms of the incidence of liver cancer (Bray et al., 2018). Due to the early characteristic symptoms and signs are not obvious, most patients with hepatocellular carcinoma (HCC) are often diagnosed at an advanced stage (Truty and Vauthey, 2010). Currently, for patient with advanced HCC have the following variable treatment modalities: transcatheter arterial chemoembolization (TACE), chemotherapy, and targeted drug therapy (Liccioni et al., 2014). About 80% of patients with advanced HCC who have unresectable tumors, and many are not diagnosed until their tumors have grown to a large (>5.0 cm) or very large size (>10 cm). Molecular targeted drugs such as sorafenib have been shown to significantly extend overall survival (OS) and time to progression (TTP) in patient with advanced HCC (Truty & Vauthey, 2010; (Yeo et al., 2005; (Palmer, 2008). Although sorafenib has been the main treatment for advanced HCC in the past decade, the emergence of drug resistance is still inevitable (Huang et al., 2020). For HCC patients whose disease progresses after sorafenib treatment, second-line oral regorafenib can significantly improve overall survival (Bruix et al., 2017; (Duffy and Greten, 2017; (Bruix et al., 2013).

Regorafenib is an oral multikinase inhibitor that blocks the activation of multiple angiogenesis kinases and oncogenic kinases, including vascular endothelial growth factor receptors (VEGFR 1, VEGFR2, and VEGFR3), platelet-derived growth factor receptor β, and fibroblast growth factor receptor 1, and mutated oncogenic kinases RAS, MAPK, and KIT (Wilhelm et al., 2011; (Subramonian et al., 2020). Compared with sorafenib, regorafenib targets a wider range of kinases, and has a stronger pharmacological effect (Strumberg and Schultheis, 2012). However, the RESORCE trial did not report the baseline clinical data of patients when sorafenib treatment was initiated. We need real-world data to learn more about the differences between daily practice and clinical trials in patients. Regorafenib was approved for HCC in China in 2017. Therefore, in this study we aimed to evaluate the safety and efficacy of regorafenib after disease progression with sorafenib in Chinese patients with advanced HCC, with the aim of complementing phase III findings.

TABLE 1 | Baseline characteristics of patients with hepatocellular carcinoma treated with regorafenib after sorafenib (*n* = 41).

Characteristics	Patients
Age, years, median (range)	41 (31–80)
Sex, male, *n* (%)	33 (80.5)
Etiology, *n* (%)	
Hepatitis B virus	40 (97.6)
Hepatitis C virus	0 (0)
Alcohol	6 (14.6)
Unknown	1 (2.4)
BCLC stage, *n* (%)	
B	16 (39.0)
C	25 (61.0)
ECOG, 0/1/2, *n*	18/22/1
Child-Pugh class, *n* (%)	
A	25 (61.0)
B	16 (39.0)
Extrahepatic metastasis, *n* (%)	23 (53.5)
Macrovascular invasion, *n* (%)	9 (20.9)
AFP≥400 ng/ml, *n* (%)	20 (48.8)
Therapies prior regorafenib, *n* (%)	
Resection	36 (87.8)
Radiofrequency ablation	25 (61.0)
TACE	34 (82.9)
TAI	6 (14.6)
Radiation therapy	8 (19.5)
Sorafenib	41 (100)
Tumor number, *n* (%)	
≥3	9 (22.0)
<3	32 (78.0)
Tumor diameter, median (range),cm	3.3 (1.0–9.8)
TTP of sorafenib (month)	7.0
Tumor progression patterns of sorafenib, *n* (%)	
New intrahepatic lesion	11 (26.8)
Increase in intrahepatic tumor size	15 (36.6)
Increase in extrahepatic tumor size/new extrahepatic lesion	15 (36.6)

BCLC, barcelona clinic liver cancer; ECOG, eastern cooperative oncology group; TACE, transarterial chemoembolization; AFP, Alpha-fetoprotein; TAI, transcatheter arterial infusion; TTP, Time to progression.

METHODS

Study Population Selection and Regorafenib Treatment

The study was a single-center, single-arm study. Patients were enrolled who met the following criteria: 1) patients were 18–80 years of age and had confirmed advanced HCC; 2) none of the patients had a history of other malignant tumors before the discovery of HCC; 3) complete clinical, imaging and follow-up data of the patients are available. The exclusion criteria were as follows: 1) patients who were given regorafenib for less than one medication cycle; 2) patients with any of the following conditions within 12 months prior to taking the drug: myocardial infarction, severe/unstable angina, coronary artery bypass grafting, congestive heart failure, cerebrovascular accident (including transient ischemic attack), pulmonary embolism; 3) patients with other severe, acute, chronic physical illness that may increase the risk associated with participating in study treatment, or may not be considered appropriate for inclusion by the investigator; and 4) patients with an expected survival time of less than 3 months. The complete eligibility criteria are shown in the supplementary data.

After screening, we retrospectively collected clinical data of patients with advanced HCC who received sequential sorafenib-regorafenib treatment at our center before February 2019. Patients with radiological progression during sorafenib therapy are strongly recommended for treatment with regorafenib. A total of 41 patients in our center were enrolled in this study, and each cycle included 4 weeks. They took 160 mg regorafenib per day for the first 3 weeks, and stopped all the treatment in the last week of the cycle (Bruix et al., 2017). Dose adjustment of regorafenib was allowed depending on patient tolerance.

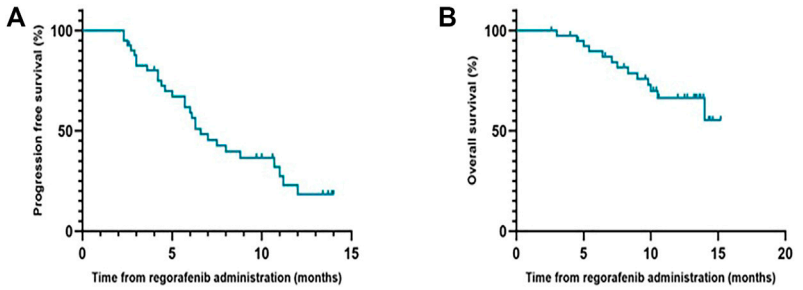

FIGURE 1 | Progression-free survival **(A)** and Overall survival **(B)** of regorafenib in patients with advanced hepatocellular carcinoma in Chinese clinical settings.

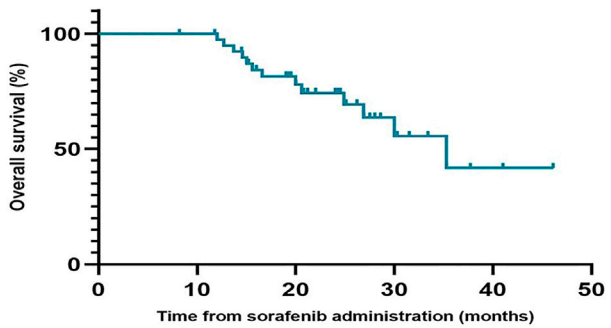

FIGURE 2 | Overall survival of patients receiving sequential sorafenib-regorafenib treatment.

Clinical Parameters and Evaluation

We collected clinical parameters such as etiology, age, sex, Child-Pugh class, alpha-fetoprotein (AFP), metastasis of primary HCC, macrovascular invasion, treatment prior to or combined with regorafenib and sorafenib initiation, initial and final sorafenib and regorafenib dosses, adverse events (AEs) after treatment with sorafenib and regorafenib, date of radiological progression, and date of death or last follow-up. Efficacy was evaluated every 2 months by computed tomography (CT) or magnetic resonance imaging (MRI) scans and blood indicator (AFP level) assessment. All patients received contrast-enhanced CT or MRI examinations, unless the administration of the contrast material was contraindicated. PET-CT was generally performed when systemic progression needed to be evaluated. All images were assessed by one of the authors (J.X.H) who had 10 years of experience. Tumor imaging response and disease progression were evaluated according to the Response Evaluation Criteria in Solid Tumors (RECIST) version 1.1 (Eisenhauer et al., 2009). Reported AEs were assessed in terms of type, causality, and severity as graded by Common Terminology Criteria for Adverse Events (CTCAE) Version 5.0.

TABLE 2 | Efficacy of regorafenib treatment.

Variable	Total (*n* = 41)
Response by RECIST v 1.1	
Complete response	0
Progressive disease	8 (19.5%)
Stable disease	29 (70.7%)
Objective response rate	4 (9.8%)
Disease control rate	33 (80.5%)
Progression-free survival, median	6.6 months (95% CI, 5.0–8.2 months)
Overall survival, median	Not reached
One-year overall survival rate	66.4% (95% CI, 50.72–82.08%)

CI, confidence interval.

Statistical Analysis

All study patients who met the eligibility criteria at baseline were included in the analyses. The primary endpoint for the study was OS and the secondary endpoint was progression-free survival (PFS). OS for regorafenib was defined as the time from the treatment of regorafenib to death from any cause. For sequential treatment with sorafenib-regorafenib, OS was defined as the time from the treatment of sorafenib to death from any cause. PFS was defined as the time from the initiation of regorafenib to the date of radiological assessment progression, or death. TTP was defined as the time from the initiation of sorafenib or regorafenib to the date of radiological assessment progression. OS, PFS, and TTP were estimated by using the Kaplan-Meier method with 95% confidence intervals (CIs). OS, PFS, and TTP were compared between different subgroups by means of the log-rank test. Analysis was performed using SPSS statistical software (version 24; SPSS-IBM, Chicago, IL, United States). $p < 0.05$ was considered statistically significant.

RESULTS

Patient Characteristics

A total of 41 patients with advanced HCC who did not respond to sorafenib and followed a regorafenib regimen were enrolled in our study. The median age was 42 (range: 25–75) years; Among them, 33 (80.5%) patients were male. Most patients had a history of local treatment prior to regorafenib included 25 (61.0%) patients undergo radiofrequency ablation, 40 (97.6%) patients received interventional therapy [include transarterial chemoembolization (TACE) and transcatheter arterial

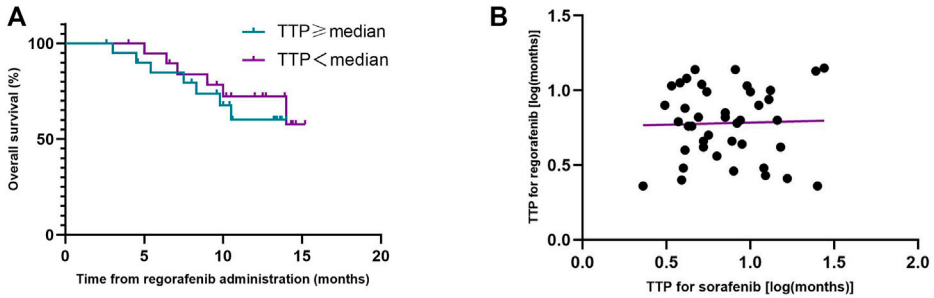

FIGURE 3 | Kaplan-Meier analyses of overall survival during treatment with regorafenib according to the time to progression (TTP) on prior sorafenib treatment **(A)**, and correlation diagram of TTP between sorafenib and regorafenib **(B)**.

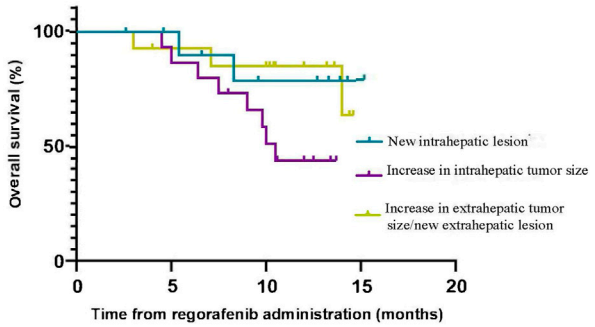

FIGURE 4 | Overall survival of patients with three tumor progression patterns of sorafenib.

infusion (TAI)] and eight patients (19.5%) received radiation therapy (RT). There were 9 (20.9%) patients had macrovascular invasion and 23 (53.5%) patients had extrahepatic metastasis. Most patients (78.0%) received a full dosage of sorafenib (800 mg). After sorafenib treatment failed, 28 patients (68.0%) received 160 mg once daily and 13 (32.0%) patients received 120 mg once daily as the starting dose of regorafenib. Of the 41 patients, 40 received other therapies as follows: TACE (n = 34), radiofrequency ablation (RFA) (n = 25), radiation therapy (n = 8), and transcatheter arterial infusion (TAI) (n = 1) during sequential sorafenib-regorafenib treatment. The baseline characteristics of patient are summarized in **Table 1**.

TABLE 3 | Adverse events (AEs) of regorafenib treatment (>10% of patients).

Adverse events	Any grades, *n* (%)
Treatment related AEs	33 (80.5)
Palmar-plantar erythrodyses-thesia	14 (34.1)
Diarrhea	12 (29.3)
Abdominal distension	5 (12.2)
Decreased appetite	6 (14.6)
Elevated aspartate aminotransferase	17 (41.5)
Elevated alanine aminotransferase	16 (39.0)
Hypertension	5 (12.2)

Efficacy of Regorafenib

During the follow-up period, the median PFS of patients who received regorafenib after sorafenib was 6.6 months (95% CI, 5.0–8.2 months), and the median OS was not reached (**Figure 1**). The 1-year OS rate of patients who received regorafenib after sorafenib was 66.4% (95% CI, 50.72–82.08%). The median OS of patients receiving sequential sorafenib-regorafenib treatment was 35.3 months (95% CI, 24.3–46.3) (**Figure 2**), and the 2-year OS rate of patients receiving sequential sorafenib-regorafenib treatment was 74.4% (95% CI, 59.7–89.1%). The objective response and disease control rate during treatment with regorafenib were 9.8% (n = 4) and 80.5% (n = 33), respectively (**Table 2**). In this study, the response was indicated at stable disease in 29 patients (70.7%) and progressive disease in eight patients (19.5%). OS was associated with baseline alpha fetoprotein levels (<400 vs. ≥ 400 ng/ml; p = 0.049), but not with extrahepatic metastasis (p = 0.844), the starting dose of regorafenib (160 mg or <160 mg) (p = 0.615), or the last dose of sorafenib (800 mg or <800 mg) (p = 0.172). However, we found that the PFS had a relationship with the starting dose of regorafenib (160 mg or <160 mg) (10.7 vs. 5.7 months, p = 0.006), but not with the starting dose of sorafenib (800 mg or <800 mg) (8.0 vs. 5.7 months, p = 0.084), baseline alpha fetoprotein levels (<400 vs. ≥ 400 ng/ml; p = 0.108), or extrahepatic metastasis (p = 0.107).

The median TTP (mTTP) with sorafenib was 7.0 months (95% CI, 4.2–9.8 months, suggesting that the mTTP with sorafenib is not relevant to the median OS of regorafenib (p = 0.552) (**Figure 3A**). We did not find any connection between these factors (R squared: 0.001) (**Figure 3B**). When we analyzed the tumor progression patterns of sorafenib, we found that the patients with an increase intrahepatic tumor size had the worst prognosis among those with disease progression (**Figure 4**).

Safety and Tolerability of Regorafenib and Correlation of Adverse Events Between Sorafenib and Regorafenib

During the observation period, there were no treatment-related deaths from sorafenib and regorafenib. The most common cause of regorafenib dose modification was hand-foot skin reaction in four patients (9%), and regorafenib doses were reduced to 120 mg

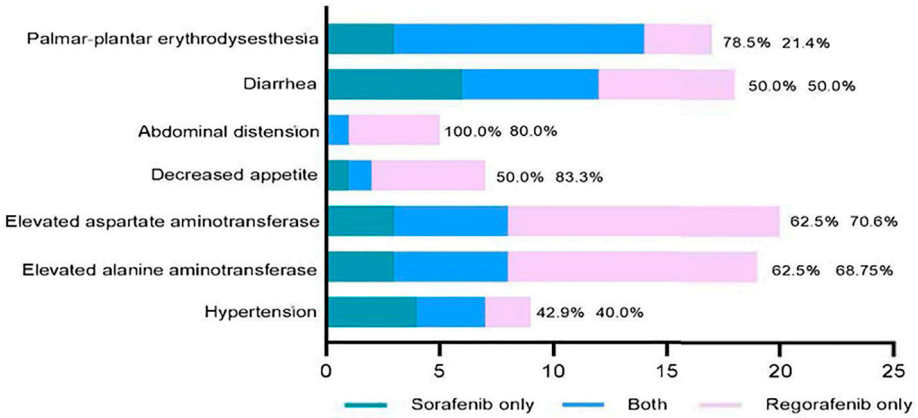

FIGURE 5 | Correlation of common adverse events between sorafenib and regorafenib in patients with advanced hepatocellular carcinoma. Reproducibility rates of regorafenib related adverse events during sorafenib therapy (left side) and occurrence rates of regorafenib related adverse events which did not found during sorafenib therapy (right side) are indicated in this figure.

or 80 mg. However, two patients increased the regorafenib dose from 120 to 160 mg due to disease progression. During the follow-up period, 33 patients had at least one treatment-related AEs, and the most common AE during regorafenib treatment were elevated aspartate aminotransferase [17/41 patients (41.5%)], elevated alanine aminotransferase [16/41 patients (39%)] and hand-foot syndrome [14/41 patients (34.1%)] (**Table 3**).

We also compared the adverse events during sorafenib and regorafenib treatment in 41 patients (**Figure 5**). All common sorafenib-related adverse events also emerged during regorafenib therapy. The most common adverse events that were observed during both sorafenib and regorafenib therapy were hand-foot syndrome and diarrhea. Conversely, 21.4% of the patients who did not have palmar-plantar erythrodyses-thesia during sorafenib therapy developed this adverse event during regorafenib therapy.

DISCUSSION

This study was a single center, retrospective analysis of Chinese patients who received regorafenib after progression disease of sorafenib. The results of this retrospective analysis not only demonstrate the efficacy and safety of sequential sorafenib-regorafenib therapy in Chinese patients with advanced HCC but also provide detailed clinical data that the RESORCE trial that did not provide. These results provide the first outcome data for sequential sorafenib-regorafenib treatment in patients with advanced HCC in China.

There was no linear relationship between the TTP of sorafenib and regorafenib. (R squared: 0.001). The result is similar to additional analyses from the phase III RESORCE trial (Finn et al., 2018). However, a study in Japan showed that after sorafenib, the group with TTP >4.6 months had a significantly longer TTP during regorafenib therapy than the group with TTP ≤4.6 months (Ogasawara et al., 2020). We compared the two groups of data and found that sorafenib had no significant effect on a group of Japanese patients, and disease progression occurred soon after the use of the drug. Even if they changed to regorafenib, the drug had no significant effect. However, this did not occur in Chinese patients, who responded differently to the two drugs.

In our cohort, the patients could adjust the dosage according to their tolerance, nine patients took sorafenib less than 800 mg every day, and 13 patients took regorafenib less than 160 mg every day. They chose dosage reduction because of AEs. The most frequent AEs during sorafenib treatment were hand-foot syndrome, diarrhea and elevated aspartate aminotransferase, but the most frequent AEs during regorafenib treatment were elevated aspartate aminotransferase, elevated alanine aminotransferase and hand-foot syndrome. Both drugs are oral multikinase inhibitors, so the patients had overlapping adverse-event profiles, and their tolerability to regorafenib was improved after treatment with sorafenib (Heo and Syed, 2018). The majority of these events were lower than grade 3 and can be alleviated by expectant treatment or by reducing the treatment dose. For example, the rate of hand-foot syndrome in our study was higher than that in the RESORCE trial, but we always advise the patients to use hand cream containing salicylic acid and take celecoxib or minocycline hydrochloride capsules to treat hand-foot syndrome (Rimassa et al., 2019; (Chen et al., 2020). Dose personalization of drugs and minimizing side effects could improve their tolerability to drugs (Rizzo et al., 2020).

In addition, we analyzed the tumor progression pattern and found that there were three tumor progression patterns of sorafenib: increase in intrahepatic tumor size, new intrahepatic lesion, and increase in extrahepatic tumor size/new extrahepatic lesion. The results suggested that patients with an increase in intrahepatic tumor size had the worst prognosis. This result is different from another study in which the prognosis of patients with radiologic tumor progression due to an increase in extrahepatic tumor size/new extrahepatic lesion (NEH) was the worst (Reig et al., 2013). When comparing the results of the previous imaging data with new imaging data, we also found that patients' liver function deteriorated (elevated aspartate

aminotransferase or alanine aminotransferase, increased total bilirubin, hypoproteinemia, ascites), when intrahepatic tumor size increased or new intrahepatic lesion occurred. But we are unable to treat patients with antitumor therapy because of their poor liver function (Terashima et al., 2018). In the end, antitumor therapy was not available for these patients, so their survival time was short. It is critical to preserve liver function so that patients are candidates for any antitumor therapy, as patients with poor performance status cannot obtain any survival benefit from HCC-directed therapy (Kirstein et al., 2020; (Piscaglia and Ogasawara, 2018; (Rich et al., 2017).

The median OS from initiation of sorafenib to regorafenib was 35.3 months, which was longer than that observed in the RESORCE trial. We compared the differences between the two groups, and the basic condition in our group was different from that in the RESORCE trial. For example, the proportion of patients with macrovascular invasion or BCLC stage C was lower than that in the RESORCE trial, and most patients in the RESORCE trial had extrahepatic disease. One study showed that among patients with advanced HCC after sorafenib, few patients with MVI or hypoalbuminemia at sorafenib initiation were able to undergo regorafenib treatment (Uchikawa et al., 2018). Hepatitis B is the main cause of HCC in China, and the majority of HCC patients have large HCC tumors (Truty and Vauthey, 2010; (Chen et al., 2019). The main cause of HCC in Europe and America is fatty liver and alcoholic liver disease, and the majority of HCC patients have small HCC tumors. This is also a basic difference between Chinese patients with HCC and HCC patients from other countries, so there are also differences in the treatment effect. Furthermore, our patients could receive many other treatments such as RFA, TACE, RT, and TAI, during sequential sorafenib-regorafenib treatment, and combining local therapies (RFA, TACE, RT) or systemic therapy (TAI) with drug treatment might have the potential to prolong OS. The variety of new treatments for patients with advanced HCC who do not respond to sorafenib means that multidisciplinary management could obtain an effect (Liu et al., 2018).

Furthermore, a series of exciting breakthroughs in HCC treatment will bring survival benefits to the majority of patients, and a revolution in advanced HCC treatment has been driven by combined therapy and immunotherapy in recent years (El-Khoueiry et al., 2017; (Kudo, 2018). The combination of regorafenib and immunotherapy drugs has also demonstrated synergistic antitumor effect (Wu et al., 2019; (Tsai et al., 2017; (Von Felden, 2020). Therefore, the combination of regorafenib and immunotherapy for HCC may be a good choice.

There are some limitations in our study need to be considered. Firstly, this study was retrospectively and carried out without randomization which may have resulted in selection bias and confounding. Second, as a single center study with small sample size, our results are limited in terms of generalization. The results of our study need further validation in the large-scale multi-center study and more randomized controlled trials.

CONCLUSION

In summary, the results of this retrospective analysis verified the efficacy and safety of regorafenib in patients with advanced HCC in China. Regorafenib combined with other treatments may bring survival benefits to patients. However, this is a retrospective and single-arm study without a control group. Moreover, this retrospective study had small sample size. Additional large-scale studies are needed to explore and expound on the specific treatment plan for patients.

DATA AVAILABILITY STATEMENT

The original contributions presented in the study are included in the article/supplementary material, further inquiries can be directed to the corresponding authors.

ETHICS STATEMENT

The studies involving human participants were reviewed and approved by An observational study of regofinib in hepatocellular carcinoma Ethics Committee of Cancer Center, Sun Yat-sen University. The patients/participants provided their written informed consent to participate in this study.

AUTHOR CONTRIBUTIONS

Study design: J-YH, Y-tX, LX, M-SC. Data collection: Jingyu Hou, Xinhua Jiang. Data analysis: J-YH, Y-tX, J-BH, LX, KJ, XL, M-SC. Draft writing: J-YH, Y-tX, LX, M-SC.

FUNDING

This work was funded by the National Science and Technology Major Project of China (2018ZX10302205, 2018ZX10723204).

ACKNOWLEDGMENTS

First, we thank Lin Xia for her guidance on this article. Second, we would like to thank Yao Wang, Qi Han, and He Min ke for their modification of this article. The content of this manuscript has been presented the abstract at the at the 14th International Liver Cancer Association (ILCA) in 2020, J-YH. Real-Life Experience of Regorafenib In Patients With Advanced Hepatocellular Carcinoma In China. 2020 ILCA, P-127.

REFERENCES

Bray, F., Ferlay, J., Soerjomataram, I., Siegel, R. L., Torre, L. A., and Jemal, A. (2018). Global Cancer Statistics 2018: GLOBOCAN Estimates of Incidence and Mortality Worldwide for 36 Cancers in 185 Countries. *CA Cancer J. Clin.* 68, 394–424. doi:10.3322/caac.21492

Bruix, J., Qin, S., Merle, P., Granito, A., Huang, Y. H., Bodoky, G., et al. (2017). Regorafenib for Patients with Hepatocellular Carcinoma Who Progressed on Sorafenib Treatment (RESORCE): a Randomised, Double-Blind, Placebo-Controlled, Phase 3 Trial. *Lancet* 389, 56–66. doi:10.1016/s0140-6736(16)32453-9

Bruix, J., Tak, W.-Y., Gasbarrini, A., Santoro, A., Colombo, M., Lim, H.-Y., et al. (2013). Regorafenib as Second-Line Therapy for Intermediate or Advanced Hepatocellular Carcinoma: Multicentre, Open-Label, Phase II Safety Study. *Eur. J. Cancer* 49, 3412–3419. doi:10.1016/j.ejca.2013.05.028

Chen, J. C., Wang, J. C., Pan, Y. X., Yi, M. J., Chen, J. B., Wang, X. H., et al. (2020). Preventive Effect of Celecoxib in Sorafenib-Related Hand-Foot Syndrome in Hepatocellular Carcinoma Patients, a Single-Center, Open-Label, Randomized, Controlled Clinical Phase III Trial. *Am. J. Cancer Res.* 10, 1467–1476.

Chen, W., Xia, C., Zheng, R., Zhou, M., Lin, C., Zeng, H., et al. (2019). Disparities by Province, Age, and Sex in Site-specific Cancer Burden Attributable to 23 Potentially Modifiable Risk Factors in China: a Comparative Risk Assessment. *Lancet Glob. Health* 7, e257–e269. doi:10.1016/s2214-109x(18)30488-1

Duffy, A. G., and Greten, T. F. (2017). Liver Cancer: Regorafenib as Second-Line Therapy in Hepatocellular Carcinoma. *Nat Rev Gastroenterol HepatolGastroenterology hepatology* 14, 141–142. doi:10.1038/nrgastro.2017.7

Eisenhauer, E. A., Therasse, P., Bogaerts, J., Schwartz, L. H., Sargent, D., Ford, R., et al. (2009). New Response Evaluation Criteria in Solid Tumours: Revised RECIST Guideline (Version 1.1). *Eur. J. Cancer* 45, 228–247. doi:10.1016/j.ejca.2008.10.026

El-Khoueiry, A. B., Sangro, B., Yau, T., Crocenzi, T. S., Kudo, M., Hsu, C., et al. (2017). Nivolumab in Patients with Advanced Hepatocellular Carcinoma (CheckMate 040): An Open-Label, Non-comparative, Phase 1/2 Dose Escalation and Expansion Trial. *Lancet* 389, 2492–2502. doi:10.1016/s0140-6736(17)31046-2

Finn, R. S., Merle, P., Granito, A., Huang, Y. H., Bodoky, G., Pracht, M., et al. (2018). Outcomes of Sequential Treatment with Sorafenib Followed by Regorafenib for HCC: Additional Analyses from the Phase III RESORCE Trial. *J. Hepatol.* 69, 353–358. doi:10.1016/j.jhep.2018.04.010

Heo, Y. A., and Syed, Y. Y. (2018). Regorafenib: A Review in Hepatocellular Carcinoma. *Drugs* 78, 951–958. doi:10.1007/s40265-018-0932-4

Huang, A., Yang, X. R., Chung, W. Y., Dennison, A. R., and Zhou, J. (2020). Targeted Therapy for Hepatocellular Carcinoma. *Signal Transduct. Target Ther.* 5, 146. doi:10.1038/s41392-020-00264-x

Kirstein, M. M., Scheiner, B., Marwede, T., Wolf, C., Voigtländer, T., Semmler, G., et al. (2020). Sequential Systemic Treatment in Patients with Hepatocellular Carcinoma. *Aliment. Pharmacol. Ther.* 52, 205–212. doi:10.1111/apt.15789

Kudo, M. (2018). Systemic Therapy for Hepatocellular Carcinoma: Latest Advances. *Cancers* 10 (11), 412. doi:10.3390/cancers10110412

Liccioni, A., Reig, M., and Bruix, J. (2014). Treatment of Hepatocellular Carcinoma. *Dig. Dis.* 32, 554–563. doi:10.1159/000360501

Liu, P. H., Huo, T. I., and Miksad, R. A. (2018). Hepatocellular Carcinoma with Portal Vein Tumor Involvement: Best Management Strategies. *Semin. Liver Dis.* 38, 242–251. doi:10.1055/s-0038-1666805

Ogasawara, S., Ooka, Y., Itokawa, N., Inoue, M., Okabe, S., Seki, A., et al. (2020). Sequential Therapy with Sorafenib and Regorafenib for Advanced Hepatocellular Carcinoma: a Multicenter Retrospective Study in Japan. *Invest New Drugs* 38, 172–180. doi:10.1007/s10637-019-00801-8

Palmer, D. H. (2008). Sorafenib in Advanced Hepatocellular Carcinoma. *N. Engl. J. Med.* 359, 2498–2499. author reply 2498-9.

Piscaglia, F., and Ogasawara, S. (2018). Patient Selection for Transarterial Chemoembolization in Hepatocellular Carcinoma: Importance of Benefit/Risk Assessment. *Liver cancer* 7, 104–119. doi:10.1159/000485471

Reig, M., Rimola, J., Torres, F., Darnell, A., Rodriguez-Lope, C., Forner, A., et al. (2013). Postprogression Survival of Patients with Advanced Hepatocellular Carcinoma: Rationale for Second-Line Trial Design. *Hepatology* 58, 2023–2031. doi:10.1002/hep.26586

Rich, N. E., Yopp, A. C., and Singal, A. G. (2017). Medical Management of Hepatocellular Carcinoma. *J. Oncol. Pract.* 13, 356–364. doi:10.1200/jop.2017.022996

Rimassa, L., Danesi, R., Pressiani, T., and Merle, P. (2019). Management of Adverse Events Associated with Tyrosine Kinase Inhibitors: Improving Outcomes for Patients with Hepatocellular Carcinoma. *Cancer Treat. Rev.* 77, 20–28. doi:10.1016/j.ctrv.2019.05.004

Rizzo, A., Nannini, M., Novelli, M., Dalia Ricci, A., Scioscio, V. D., and Pantaleo, M. A. (2020). Dose Reduction and Discontinuation of Standard-Dose Regorafenib Associated with Adverse Drug Events in Cancer Patients: a Systematic Review and Meta-Analysis. *Ther. Adv. Med. Oncol.* 12, 1758835920936932. doi:10.1177/1758835920936932

Strumberg, D., and Schultheis, B. (2012). Regorafenib for Cancer. *Expert Opin. Investig. Drugs* 21, 879–889. doi:10.1517/13543784.2012.684752

Subramonian, D., Phanhthilath, N., Rinehardt, H., Flynn, S., Huo, Y., Zhang, J., et al. (2020). Regorafenib Is Effective against Neuroblastoma *In Vitro* and *In Vivo* and Inhibits the RAS/MAPK, PI3K/Akt/mTOR and Fos/Jun Pathways. *Br. J. Cancer* 123, 568–579. doi:10.1038/s41416-020-0905-8

Terashima, T., Yamashita, T., Sunagozaka, H., Arai, K., Kawaguchi, K., Kitamura, K., et al. (2018). Analysis of the Liver Functional Reserve of Patients with Advanced Hepatocellular Carcinoma Undergoing Sorafenib Treatment: Prospects for Regorafenib Therapy. *Hepatol. Res.* 48, 956–966. doi:10.1111/hepr.13196

Truty, M. J., and Vauthey, J. N. (2010). Surgical Resection of High-Risk Hepatocellular Carcinoma: Patient Selection, Preoperative Considerations, and Operative Technique. *Ann. Surg. Oncol.* 17, 1219–1225. doi:10.1245/s10434-010-0976-5

Tsai, A. K., Khan, A. Y., Worgo, C. E., Wang, L. L., Liang, Y., and Davila, E. (2017). A Multikinase and DNA-PK Inhibitor Combination Immunomodulates Melanomas, Suppresses Tumor Progression, and Enhances Immunotherapies. *Cancer Immunol. Res.* 5, 790–803. doi:10.1158/2326-6066.Cir-17-0009

Uchikawa, S., Kawaoka, T., Aikata, H., Kodama, K., Nishida, Y., Inagaki, Y., et al. (2018). Clinical Outcomes of Sorafenib Treatment Failure for Advanced Hepatocellular Carcinoma and Candidates for Regorafenib Treatment in Real-World Practice. *Hepatol. Res.* 48, 814–820. doi:10.1111/hepr.13180

Von Felden, J. (2020). New Systemic Agents for Hepatocellular Carcinoma: an Update 2020. *Curr. Opin. Gastroenterol.* 36, 177–183. doi:10.1097/mog.0000000000000626

Wilhelm, S. M., Dumas, J., Adnane, L., Lynch, M., Carter, C. A., Schütz, G., et al. (2011). Regorafenib (BAY 73-4506): a New Oral Multikinase Inhibitor of Angiogenic, Stromal and Oncogenic Receptor Tyrosine Kinases with Potent Preclinical Antitumor Activity. *Int. J. Cancer* 129, 245–255. doi:10.1002/ijc.25864

Wu, R. Y., Kong, P. F., Xia, L. P., Huang, Y., Li, Z. L., Tang, Y. Y., et al. (2019). Regorafenib Promotes Antitumor Immunity via Inhibiting PD-L1 and Ido1 Expression in Melanoma. *Clin. Cancer Res.* 25, 4530–4541. doi:10.1158/1078-0432.Ccr-18-2840

Yeo, W., Mok, T. S., Zee, B., Leung, T. W., Lai, P. B., Lau, W. Y., et al. (2005). A Randomized Phase III Study of Doxorubicin versus Cisplatin/interferon Alpha-2b/doxorubicin/fluorouracil (PIAF) Combination Chemotherapy for Unresectable Hepatocellular Carcinoma. *J. Natl. Cancer Inst.* 97, 1532–1538. doi:10.1093/jnci/dji315

Conflict of Interest: The authors declare that the research was conducted in the absence of any commercial or financial relationships that could be construed as a potential conflict of interest.

frontiers | Frontiers in Pharmacology

ORIGINAL RESEARCH
published: 08 June 2022
doi: 10.3389/fphar.2022.896523

Transcriptomics and Network Pharmacology Reveal the Protective Effect of Chaiqin Chengqi Decoction on Obesity-Related Alcohol-Induced Acute Pancreatitis *via* Oxidative Stress and PI3K/Akt Signaling Pathway

Xinmin Yang[1], Linbo Yao[1], Mei Yuan[1], Xiaoying Zhang[1], Monika A. Jakubowska[2], Pawel E. Ferdek[3], Lei Dai[4], Jingyu Yang[1], Tao Jin[1], Lihui Deng[1], Xianghui Fu[4], Dan Du[5], Tingting Liu[1], David N. Criddle[6], Robert Sutton[7], Wei Huang[1,8] and Qing Xia[1]**

[1]Department of Integrated Traditional Chinese and Western Medicine, Sichuan Provincial Pancreatitis Centre and West China-Liverpool Biomedical Research Centre, West China Hospital, Sichuan University, Chengdu, China, [2]Malopolska Centre of Biotechnology, Jagiellonian University, Krakow, Poland, [3]Department of Cell Biology, Faculty of Biochemistry, Biophysics and Biotechnology, Jagiellonian University, Krakow, Poland, [4]State Key Laboratory of Biotherapy and Cancer Center, West China Hospital, Sichuan University and Collaborative Innovation Center of Biotherapy, Chengdu, China, [5]Advanced Mass Spectrometry Center, Research Core Facility, Frontiers Science Center for Disease-related Molecular Network, West China Hospital, Sichuan University, Chengdu, China, [6]Department of Cellular and Molecular Physiology, Institute of Translational Medicine, University of Liverpool, Liverpool, United Kingdom, [7]Liverpool Pancreatitis Research Group, Liverpool University Hospitals NHS Foundation Trust and Institute of Translational Medicine, University of Liverpool, Liverpool, United Kingdom, [8]Institutes for Systems Genetics & Immunology, Frontiers Science Center for Disease-related Molecular Network, West China Hospital, Sichuan University, Chengdu, China*

Obesity-related acute pancreatitis (AP) is characterized by increasing prevalence worldwide and worse clinical outcomes compared to AP of other etiologies. Chaiqin chengqi decoction (CQCQD), a Chinese herbal formula, has long been used for the clinical management of AP but its therapeutic actions and the underlying mechanisms have not been fully elucidated. This study has investigated the pharmacological mechanisms of CQCQD in a novel mouse model of obesity-related alcohol-induced AP (OA-AP). The mouse OA-AP model was induced by a high-fat diet for 12 weeks and subsequently two intraperitoneal injections of ethanol, CQCQD was administered 2 h after the first injection of ethanol. The severity of OA-AP was assessed and correlated with changes in transcriptomic profiles and network pharmacology in the pancreatic and adipose tissues, and further docking analysis modeled the interactions between compounds of CQCQD and their key targets. The results showed that CQCQD significantly reduced pancreatic necrosis, alleviated systemic inflammation, and decreased the parameters associated with multi-organ dysfunction. Transcriptomics and network pharmacology analysis, as well as further experimental validation, have shown that CQCQD induced Nrf2/HO-1 antioxidant protein response and decreased Akt phosphorylation in the pancreatic and adipose tissues. *In vitro*, CQCQD protected freshly isolated pancreatic acinar cells from H_2O_2-elicited oxidative stress and necrotic cell death. The docking results of AKT1 and the active compounds related to AKT1 in CQCQD showed high binding affinity. In

OPEN ACCESS

Edited by:
Thomas Brzozowski, Jagiellonian University Medical College, Poland

Reviewed by:
Qinghe Meng, Upstate Medical University, United States
Shiyu Song, Nanjing University, China
Qing Xia, Peking University, China

***Correspondence:**
Wei Huang
dr_wei_huang@scu.edu.cn
Qing Xia
xiaqing@medmail.com.cn

Specialty section:
This article was submitted to Gastrointestinal and Hepatic Pharmacology, a section of the journal Frontiers in Pharmacology

Received: *15 March 2022*
Accepted: *25 May 2022*
Published: *08 June 2022*

Citation:
Yang X, Yao L, Yuan M, Zhang X, Jakubowska MA, Ferdek PE, Dai L, Yang J, Jin T, Deng L, Fu X, Du D, Liu T, Criddle DN, Sutton R, Huang W and Xia Q (2022) Transcriptomics and Network Pharmacology Reveal the Protective Effect of Chaiqin Chengqi Decoction on Obesity-Related Alcohol-Induced Acute Pancreatitis via Oxidative Stress and PI3K/Akt Signaling Pathway. Front. Pharmacol. 13:896523. doi: 10.3389/fphar.2022.896523

conclusion, CQCQD ameliorates the severity of OA-AP by activating of the antioxidant protein response and down-regulating of the PI3K/Akt signaling pathway in the pancreas and visceral adipose tissue.

Keywords: Chaiqin chengqi decoction, obesity-related acute pancreatitis, pharmacology network analysis, transcriptomics, antioxidant protein response, PI3K/Akt pathway

INTRODUCTION

Acute pancreatitis (AP) is an inflammatory disease of the pancreas (Mederos et al., 2021), which shows a steady rise in the global incidence over the last 50 years (Iannuzzi et al., 2021). The clinical manifestation of AP varies from asymptomatic/mild to severe cases characterized by extensive pancreatic necrosis, multi-organ failure, and significant mortality (Garg and Singh, 2019). The pathogenesis of AP is complex, and includes several factors, such as premature trypsinogen activation, dysregulated calcium signaling, oxidative/endoplasmic reticulum stress, impaired autophagy, and mitochondrial dysfunction (Gukovskaya et al., 2017; Lee and Papachristou, 2019). Despite the significant prevalence of the disease, currently, there is no internationally-approved pharmacological treatment against AP (Moggia et al., 2017). Therefore, alternative therapeutic strategies to improve the outcomes of AP patients are urgently needed.

Obesity has emerged as an alarming health problem, particularly in developed countries. Overweight bears the risk of cardiometabolic complications, diabetes, cancer, and other diseases (Collaborators et al., 2017; Bluher, 2019), which may cause young-age disability or even death. A growing body of evidence associates obesity with the prevalence (Aune et al., 2021) and severity of AP (Dobszai et al., 2019). The risk factors related to obesity include the formation of gallstones, diabetes, hypertriglyceridemia, and weight loss interventions, all of which may promote lipolysis of the visceral adipose tissue and free fatty acid-mediated lipotoxicity, thus worsening the clinical outcomes of AP (Khatua et al., 2017). Inhibition of pancreatic lipase has been shown to decrease free fatty acid release and the severity of the disease (Navina et al., 2011; de Oliveira et al., 2020). Since visceral fat is implicated in obesity-related AP, new therapeutic strategies centered on the abdominal adipose tissue are an important medical avenue to explore.

Chaiqin chengqi decoction (CQCQD), is a classical traditional Chinese medicine-based herbal formula (Liang et al., 2021). This medicine has been routinely used to treat AP patients for over 40 years in the West China Hospital (Chengdu, Sichuan Province, China), one of the largest pancreatic centers, where more than 2000 AP patients are treated by an integrated approach that combines traditional Chinese and Western medicine (Jin et al., 2020; Li et al., 2020). Treatment with CQCQD can improve the outcomes of AP patients of different etiologies. However, the exact pharmacological mechanism still remains to be elucidated. In a mouse model of AP, our group has recently shown that CQCQD suppresses pancreatic inflammation, reduces acinar cell necrosis and systemic injury *via* modulation of the substance P/neurokinin-1 receptor (Han et al., 2021) and Toll-like four receptor/inflammasome (Wen et al., 2020) signaling pathways.

In the present study, we have investigated the pharmacological mechanisms of CQCQD in a newly established mouse model representing obesity and acute alcohol intake synergistically causes AP (Yang et al., 2022). By integrating the transcriptomic data from the pancreatic and adipose tissues, network pharmacology was constructed to identify the potential protein targets of CQCQD. Subsequently, key molecular mechanisms were validated *in vivo* and *in vitro*. Finally, the interactive activities between CQCQD components and the key target proteins were proposed as a result of docking analysis.

MATERIALS AND METHODS

Ethics and Animals

Male C57BL/6J mice were purchased from Beijing Huafukang Bioscience Co., Ltd (Beijing, China). Animals were maintained at 22 ± 2°C with a 12 h light-dark cycle. Mice received standard laboratory chow, and water was freely accessible throughout the experiment procedures. All animal experiments were approved by the Animal Ethics Committee of the West China Hospital, Sichuan University (20211086A).

Materials and Reagents

Chow diet (CD; 10 kcal % fat, H10010) and high-fat diet (HFD; 60 kcal % fat, H10060) were from Beijing Huafukang Bioscience Co., Ltd. Ethanol (Sigma-Aldrich) was dissolved in sterile saline at 37.5% concentration (v/v) before use. Substrate for myeloperoxidase (MPO) activity 3,3,5,5-tetramethylbenzidine was from Sigma-Aldrich. Interleukin (IL)-6 enzyme-linked immunosorbent assay was from R&D Systems (Shanghai, China). Propidium iodide (PI), hoechest 33,342, and CM-H2DCFDA were from Thermo Fisher Scientific (Shanghai). Hydrogen peroxide (H_2O_2) was from Sinopharm Chemical Reagent Co., Ltd (Shanghai). Anti-nuclear factor erythroid 2-related factor 2 (Nrf2) antibody and anti-heme oxygenase-1 (HO-1) antibody were from Abcam (Shanghai), Akt Rabbit mAb and phosphor-Akt Rabbit mAb were from CST (Shanghai), anti-β-actin antibody was from Proteintech (Shanghai). All other reagents were purchased from Sigma-Aldrich (Shanghai) if not stated otherwise.

CQCQD Preparation

The raw materia medica of CQCQD was resourced from Sichuan Hospital of Traditional Chinese Medicine (Chengdu, Sichuan, China). CQCQD formula consisted of *Rheum palmatum* L (Da

Huang in Chinese, 20 g), $Na_2SO_4.10H_2O$ (Mang Xiao, 20 g), *Magnolia officinalis* Rehd. et Wils (Hou Pu, 15 g), *Citrus aurantium* L (Zhi Shi, 15 g), *Bupleurum marginatum* Wall. ex DC (Chai Hu, 15 g), *Scutellaria baicalensis* Georgi (Huang Qin, 15 g), *Artemisia capillaris* Thunb (Yin Chen, 15 g), and *Gardenia jasminoides Ellis* (Zhi Zi, 20 g). The extraction process and the quality control of CQCQD (D8) has been evaluated by Ultra high-performance liquid chromatography (UHPLC) fingerprinting in our recent publication (Liang et al., 2021) (**Supplementary Figures S1A,B**).

AP Model Induction and Treatment

Mice of 4–5 weeks old were randomly assigned into CD and HFD groups, fed with normal chow or high-fat diet for 12 weeks, respectively. Then, ethanol (EtOH) at a dose of 2 g/kg was administered by two intraperitoneal injections 1 h apart, a slight modification of previous ethanol treatment regimens (Huang et al., 2014; Maleth et al., 2015; Wang et al., 2016). The acute EtOH administration in obese mice aimed to establish an obesity-related and alcohol-induced AP (OA-AP) model (Yang et al., 2022), which mimics a clinical scenario, whereby alcoholism increases the risk of developing AP in obese people (Lai et al., 2011). Control lean mice received equal volumes of saline injections. We have previously shown that EtOH alone at this range of doses only caused mild pancreatic edema in lean mice without discernible neutrophil infiltration and acinar cell necrosis (Huang et al., 2014). Therefore, we did not employ this group of control mice for the subsequent experiments.

Regarding the dose of CQCQD, it has been demonstrated in our recently published study that the single clinically-equivalent dose of CQCQD (5.5 g/kg) 3 times is more effective than other doses (Liang et al., 2021; Huang et al., 2022). Therefore, in the treatment group, obese mice were given oral gavage of CQCQD (5.5 g/kg) 3 times every 2 h, starting 2 h after the first EtOH injection. Animals were sacrificed 12 h after the first EtOH/saline injection, and the blood and relevant organs were collected for downstream analyses.

AP Severity Assessment

AP severity assessment including pancreatic histopathology (see detailed scoring system in **Supplementary Figure S2**), pancreatic and lung MPO activities, and serum IL-6 was described in detail in our previous studies (Huang et al., 2014; Huang et al., 2017; Wen et al., 2020; Han et al., 2021). Serum biochemical indices including urea, creatinine, alanine aminotransferase (ALT), aspartate aminotransferase (AST), lactate dehydrogenase (LDH), and ionized Ca^{2+} were determined using an automatic biochemical analyzer (Roche Cobas 8,000; Shanghai).

Transcriptome Analysis

Total RNA was isolated from the pancreas and epididymal adipose tissue using Trizol reagent. RNA degradation and contamination were monitored on 1% agarose gels. RNA purity was checked using the NanoPhotometer® spectrophotometer (IMPLEN, Westlake Village, CA). RNA integrity was assessed using the RNA Nano 6000 Assay Kit of the Bioanalyzer 2,100 system (Agilent Technologies, Santa Clara, CA). Then, sequencing libraries were generated using NEBNext® UltraTM RNA Library Prep Kit for Illumina® (New England Biolabs, Ipswich, MA) following the manufacturer's recommendations, and index codes were added to attribute sequences to each sample. The clustering of the index-coded samples was performed on a cBot Cluster Generation System using TruSeq PE Cluster Kit v3-cBot-HS (Illumina) according to the manufacturer's instructions. After cluster generation, the library preparations were sequenced on an Illumina Novaseq platform and 150 bp paired-end reads were generated.

For RNA-seq data analysis, raw data were filtered and adapters were cut using Trim galore software (0.6.6) and quality control was performed using fastp (0.20.1). Then clean reads were mapped to the GRCm38 mouse reference genome using the Star program (2.7.4a). Finally, the featureCounts (2.0.1) software was used to quantify reads. The difference analysis was carried out using the DEseq2 (1.30.0) package in R (4.0.1), and the statistical significance of differentially expressed genes (DEGs) was assessed by the adjusted P cutoff value of 0.05 and fold change cutoff value of 1.5. Gene Ontology (GO) and Kyoto Encyclopedia of Genes and Genomes (KEGG) enrichment analysis of DEGs was conducted using clusterProfiler (3.18.1).

Immunohistochemistry and Western Blot

Methods for immunohistochemical staining and Western blotting can be found in our previous studies (Wen et al., 2020; Han et al., 2021).

Network Pharmacology Analysis

A total of 22 Q-markers (synephrine, geniposidic acid, salidroside, coniferin, syringin, geniposide, rutin, narintin, naringin, hesperidin, sennoside A, baicalin, wogonoside, physcion, aloe emodin, bacalein, sinensetin, chrysin, rhein, honokiol, magnolol, and emodin) were identified in our recent study (Liang et al., 2021) and the concentration of each component is presented in the **Supplementary Table S1**. For each compound, putative targets were acquired from three databases: STITCH (Search Tool for Interactions of Chemicals, http://stitch.embl.de/), ETCM (http://www.tcmip.cn/ETCM/), and STP (SwissTargetPrediction, http://www.swisstargetprediction.ch). Targets obtained from the three databases were then combined and de-duplicated to obtain the final CQCQD targets. For disease target identification, OA-AP associated targets were obtained based on the transcriptome analysis. Genes related to AP were retrieved and integrated from four databases: GeneCards (https://www.genecards.org/), DisGeNET (https://www.disgenet.org/), OMIM (Online Mendelian Inheritance in Man, https://omim.org/), MalaCards (https://www.malacards.org/).

Network construction and functional enrichment analysis: CQCQD targets were further merged with OA-AP targets, and the overlapping targets identified as CQCQD-regulated OA-AP targets. Cytoscape (3.7.1, https://www.cytoscape.org/) was used to establish the "compound-target" network. In addition, the protein-protein interaction (PPI) network of overlapping

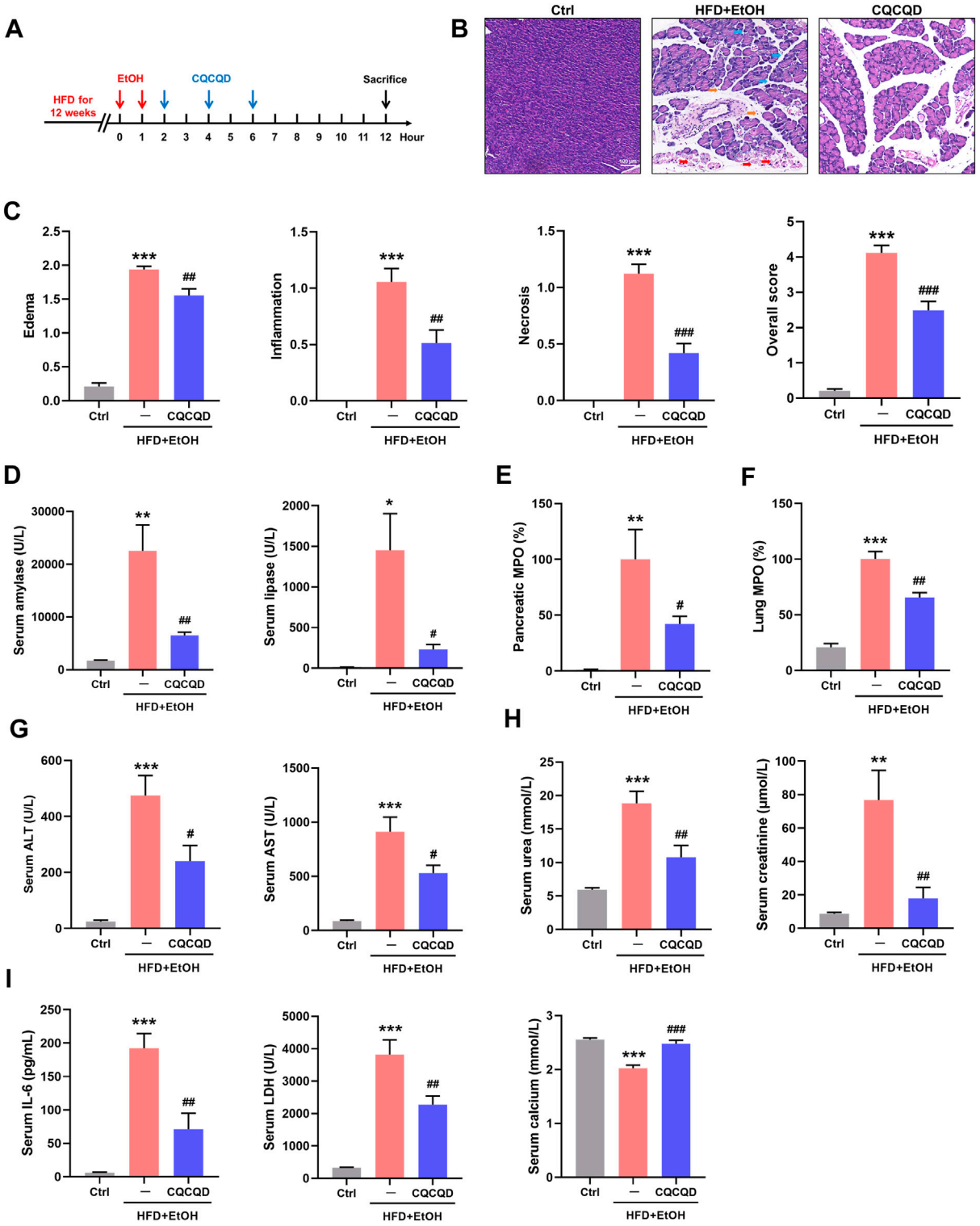

FIGURE 1 | CQCQD ameliorates the severity of OA-AP in a mouse model. **(A)** Experimental protocol of this study. **(B)** Representative H&E images of pancreatic sections (blue arrows indicate edema, orange arrows indicate inflammation, and red arrows indicate necrosis). **(C)** Pancreatic histopathology scores (edema, inflammatory infiltration, acinar cell necrosis, and the overall score). **(D)** Levels of serum amylase and lipase. **(E)** Pancreatic myeloperoxidase (MPO). **(F)** Lung MPO. **(G)** Serum alanine aminotransferase (ALT) and aspartate aminotransferase (AST). **(H)** Serum urea and creatinine levels. **(I)** Serum interleukin-6 (IL-6), lactate dehydrogenase (LDH), and ionized calcium. All data are presented as means ± SEM of 6–10 animals per group. Ctrl vs. OA-AP: $^{*}p < 0.05$, $^{**}p < 0.01$, $^{***}p < 0.001$; OA-AP vs. OA-AP + CQCQD: $^{\#}p < 0.05$, $^{\#\#}p < 0.01$, $^{\#\#\#}p < 0.001$.

targets was constructed by STRING database (https://string-db.org/), and then also visualized with Cytoscape. Functional enrichment analysis of overlapping targets, including GO and KEGG pathway enrichment analysis, was conducted by clusterProfiler (3.18.1) and R (4.0.3). $p < 0.05$ was considered statistically significant.

Acinar Cell Isolation, Treatment, and Cell Injury Assessment

Mouse pancreatic acinar cells were freshly isolated using a collagenase IV digestion procedure as previously described (Huang et al., 2014; Huang et al., 2017). Cells were pre-treated with CQCQD (5 mg/ml) (Wen et al., 2020) for 30 min, followed by co-incubation with H_2O_2 (1 mM) or solvent control for another 30 min with gentle shaking (50 rpm) at room temperature. Reactive oxygen species (ROS; H2-DCFDA, 10 μM) and necrotic cell death (PI, 1 μM) were measured using a plate reader (BMG CLARIOstar; Offenburg, Germany) as previously described (Du et al., 2018; Zhang et al., 2018).

Molecular Docking Studies

Molecular docking is a theoretical simulation method that models the interactions between compounds and proteins to predict the binding mode and affinity. Molecular docking studies were performed in AutoDock (4.2) and mgltools (1.5.6). The human AKT1 (P31749) protein structure was obtained from the alpha fold protein structure database (https://alphafold.ebi.ac.uk/). All small molecular structures were obtained from the TCMSP (Traditional Chinese Medicine Database and Analysis Platform, https://tcmsp-e.com/) in the corresponding mol2 file. During the pre-docking process, all the polar hydrogen atoms were added, and the water molecules were removed. Each molecule was docked with the protein for 50 times, and the lowest binding energy was selected to display the result at least once. The docking score was expressed as the binding energy. Lower binding energy reflects stronger interaction between the compound and protein. Finally, PyMOL software (2.4.1) was used to visualize the docking results. The python environment on which the above software depends is Python (3.7.4).

Statistical Analysis

All data are presented as means ± SEM. Statistical analysis was carried out using GraphPad Prism 8.4.1. For two-group comparisons, mean differences were analyzed by a two-tailed Student's *t*-test. For multi-group comparisons, mean differences were analyzed by one-way ANOVA with a Tukey's multiple comparison post-hoc test. p values <0.05 were considered significant.

RESULTS

CQCQD Reduces Pancreatitis Indices in OA-AP and Multi-Organ Dysfunction

The experimental pipeline of the OA-AP model and administration of CQCQD is shown in **Figure 1A**. Compared to the control mice, mice from the OA-AP group developed features of pancreatic injury (separated acinar lobules, intra-parenchymal neutrophil infiltration, and patchy acinar cell necrosis; **Figure 1B**), which was reflected by markedly increased corresponding histopathological scores (**Figure 1C**), the elevation of serum amylase and lipase levels (**Figure 1D**) as well as pancreatic MPO (**Figure 1E**). The OA-AP model was also associated with dramatically raised parameters of multiple organ dysfunction in the lung (**Figure 1F**), liver (**Figure 1G**), and kidney (**Figure 1H**); as well as deranged general severity indices (**Figure 1I**) including IL-6, LDH, and ionized calcium. Administration of CQCQD significantly ameliorated pancreatic injury (**Figures 1B–E**) and multi-organ dysfunction (**Figures 1F–H**) as well as normalized general severity indices (**Figure 1I**).

These data collectively show that CQCQD was protective against OA-AP, manifested as a reduction in pancreatic necrosis and protection against multi-organ dysfunction.

Transcriptome Analysis Reveals the Signaling Pathways Involved in the OA-AP Pathogenesis

We next carried out the transcriptome analysis in the pancreatic tissue to understand the molecular mechanisms underlying pancreatic injury during OA-AP progression. Compared to the control group (lean mice that received only saline injections), OA-AP induced different expressions of a total of 4,171 genes (DEGs) in the pancreas; of these DEGs, 2,114 were upregulated and 2057 were downregulated (**Figures 2A,B** and **Supplementary Table S2**). Further, unsupervised hierarchical clustering analysis of the top 500 DEGs showed a substantial difference between the OA-AP and the control pancreatic tissues (**Figure 2C**). Subsequently, GO enrichment analysis indicated the changes in biological processes related to mitochondrial organization, regulation of the apoptotic signaling pathway, processes utilizing autophagic mechanisms, autophagy, negative regulation of phosphorylation (all $p < 0.05$; **Figure 2D** and **Supplementary Figures S3A,B**). KEGG analysis revealed that neurodegeneration, the phosphatidylinositol 3-kinase-Akt (PI3K/Akt) signaling pathway, mitogen-activated protein kinase (MAPK) signaling pathway, focal adhesion, and oxidative phosphorylation were the top-ranked signaling pathways (all $p < 0.05$, **Figure 2E** and **Supplementary Figures S3C,D**).

Since the adipose tissue plays a crucial role in obesity-related AP, we included the adipose tissue transcriptomics to further clarify the potential pathological mechanisms of OA-AP. Volcano plot (**Figures 2F,G** and **Supplementary Table S3**) and heatmap (**Figure 2H**) analyses showed substantial differentiation between OA-AP and control visceral adipose tissues. GO enrichment analysis indicated the changes in the biological processes such as the positive regulation of cell adhesion, positive regulation of cytokine production, and others (**Figure 2I** and **Supplementary Figures S3E,F**). KEGG pathway analysis highlighted the involvement of the PI3K-Akt signaling pathway, cytokine-cytokine receptor interaction, MAPK signaling pathway, and focal adhesion (**Figure 2J** and **Supplementary Figures S3G,H**).

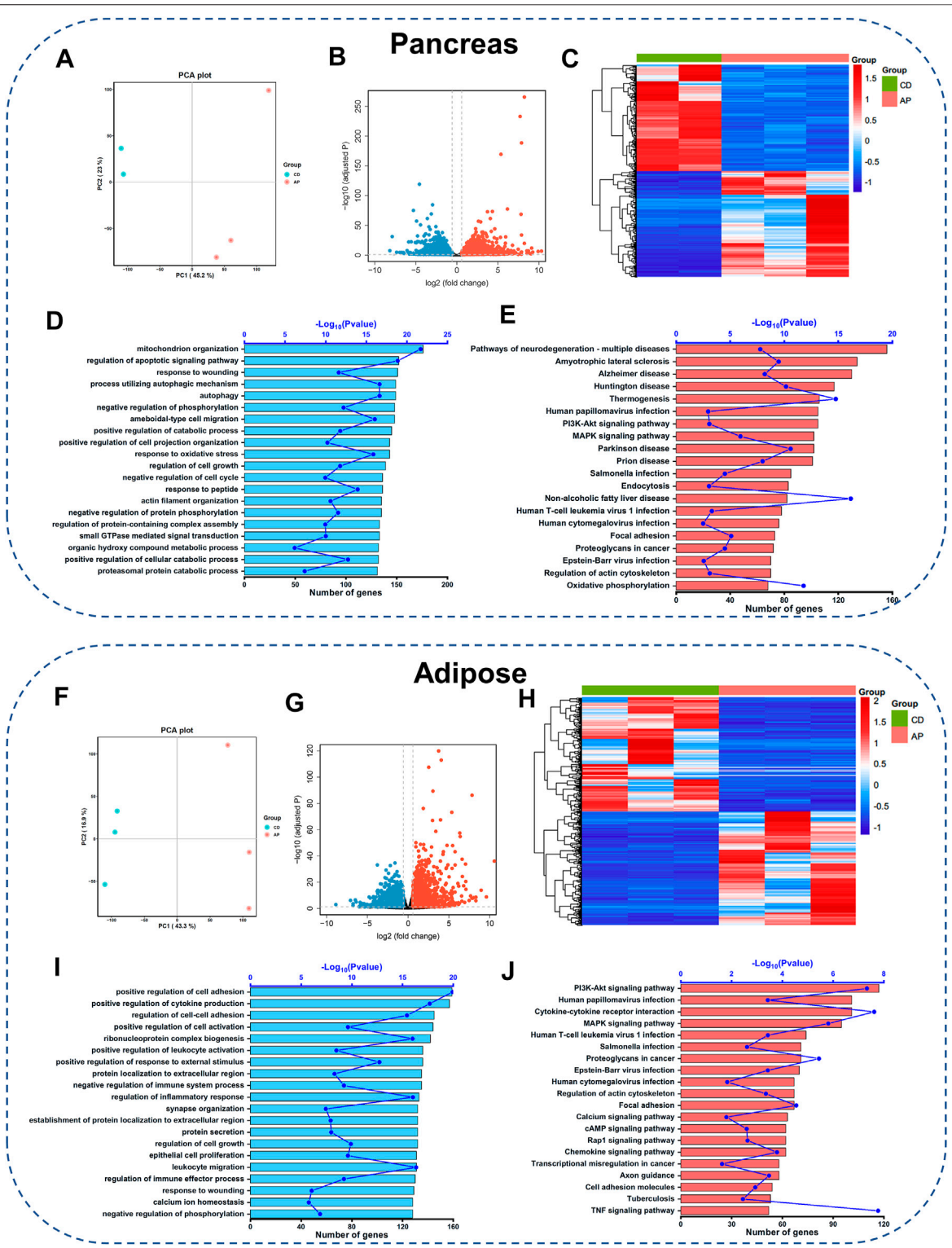

FIGURE 2 | Gene expression profiling in the pancreatic and adipose tissues of OA-AP mice. Transcriptome analysis of differentially expressed genes (DEGs) between OA-AP group and control group in the pancreatic tissue **(A–E)** and adipose tissue **(F–J)**, respectively. **(A,F)** Principal component analysis. **(B,G)** Volcano Plot. **(C,H)** Heatmap. **(D,I)** GO analysis shows the top 20 terms based on enrich factor arrangement. **(E,J)** KEGG pathway enrichment analysis shows the top 20 terms based on enrichment factor arrangement.

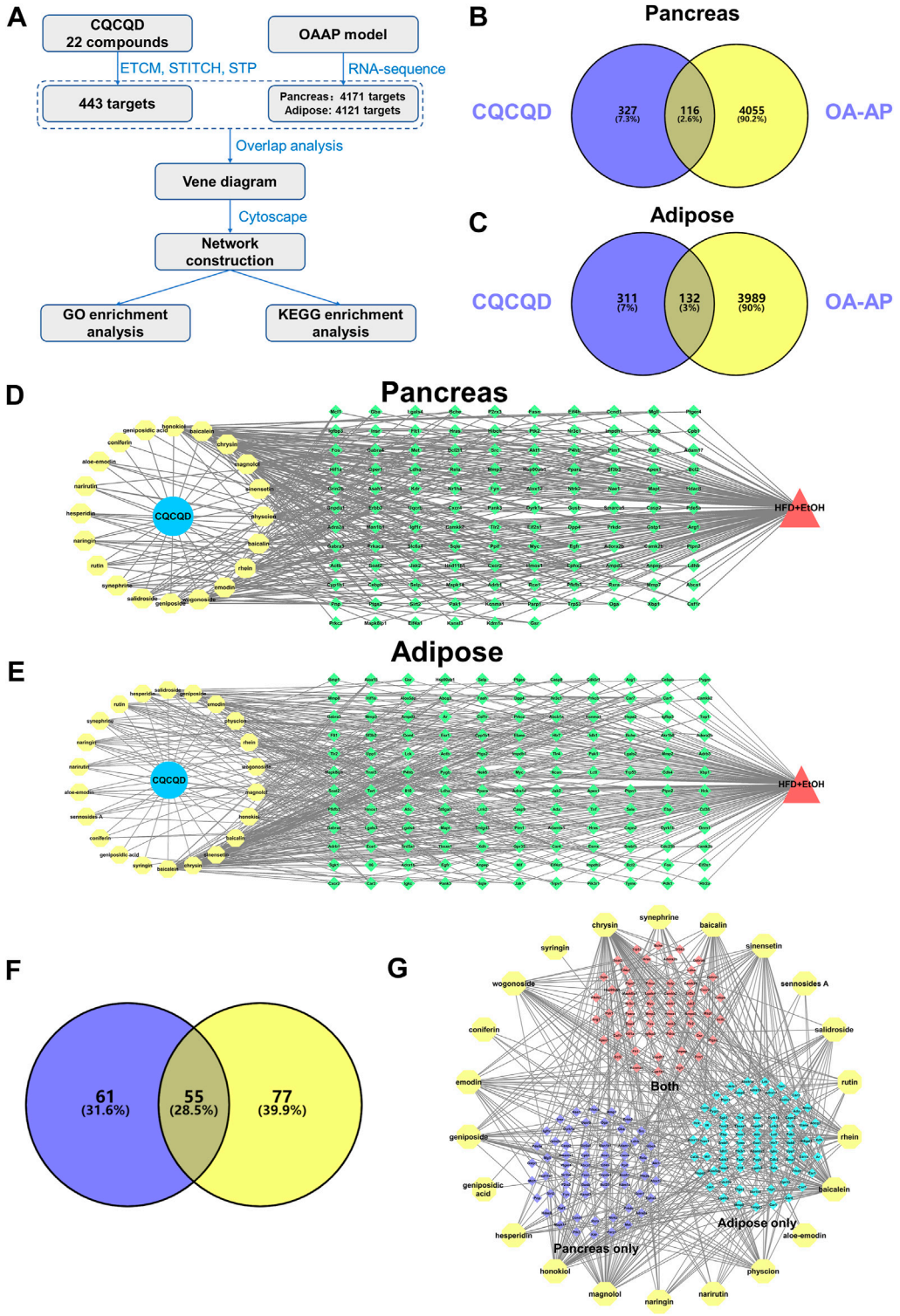

FIGURE 3 | Network targets of CQCQD on OA-AP both in the pancreatic and adipose tissues. **(A)** The protocol of network pharmacology analysis in this study. **(B,C)** Venn diagram shows overlapped targets between CQCQD and OA-AP in the pancreatic tissue **(B)** and adipose tissue **(C)**. **(D,E)** The compound-target network was established in the pancreatic tissue **(D)** and adipose tissue **(E)**. **(F)** Venn diagram shows overlapped CQCQD-regulated targets between the pancreatic tissue and adipose tissue. **(G)** The compound-target network is based on the pancreatic tissue and adipose tissue.

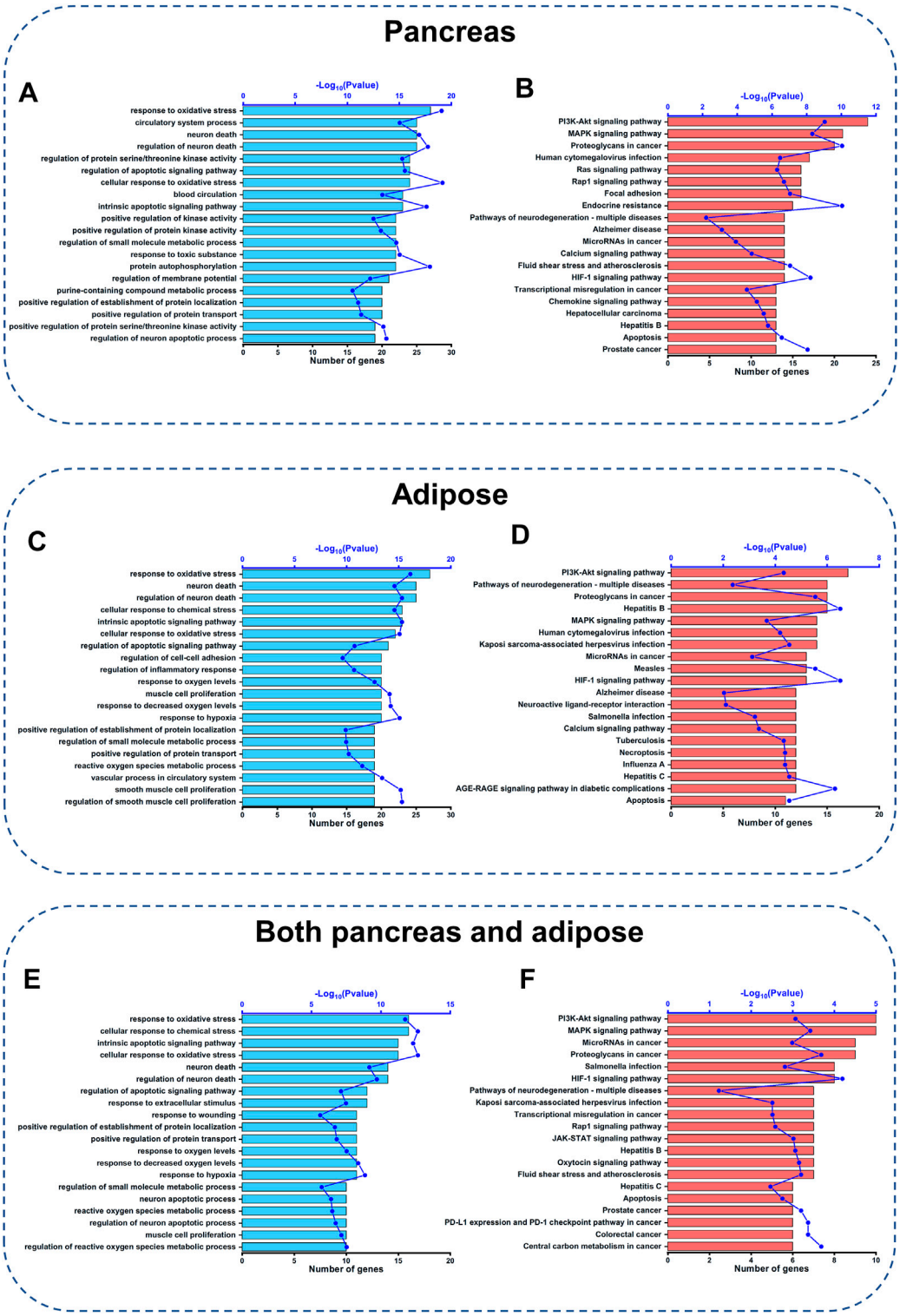

FIGURE 4 | GO function and KEGG pathway analysis of CQCQD-regulated targets. **(A,C,E)** Top 20 biological processes returned by the GO analysis of the pancreatic targets **(A)**, adipose tissue targets **(C)**, and common targets of the pancreatic tissue and adipose tissue **(E)**. **(B,D,F)** Top 20 KEGG pathways of the pancreatic targets **(B)**, and adipose tissue targets **(D)**, and common targets of the pancreatic tissue and adipose tissue **(F)**.

Pharmacology Network Construction Between CQCQD Targets and DEGs of OA-AP

In our study, we employed online databases that identified a total of 443 targets of 22 compounds from CQCQD (**Supplementary Table S4**), while the targets related to the disease were obtained from the transcriptomic analysis of the OA-AP model. The network pharmacology analysis was performed according to a pre-defined protocol (**Figure 3A**). Firstly, the Venn diagram showed overlapped targets between CQCQD and OA-AP. Based on these, a compound-target network was established, and related functional enrichment analysis was carried out. As a result, 116 and 132 overlapped targets were selected as potential therapeutic targets of CQCQD in the pancreatic (**Figure 3B**) and adipose tissues, respectively (**Figure 3C**). After discarding the compounds with no predicted target available, 20 compounds with 116 predicted targets were obtained in the pancreas (**Figure 3D**), and 22 compounds with 132 predicted targets in the adipose tissue (**Figure 3E**). In addition, we overlapped the targets of CQCQD from the pancreatic and adipose tissue (**Figure 3F**). There were 55 common targets, with the other 61 and 77 targets specific for the pancreas or adipose tissue, respectively. The network "compounds-targets-tissue" is shown in **Figure 3G**.

GO and KEGG Pathway Enrichment Analysis of CQCQD-Regulated Targets

To further investigate the detailed functions of the above CQCQD-regulated targets in the pancreas and adipose tissues, GO function and KEGG pathway enrichment analyses were carried out. For the targets specific for the pancreas, GO enrichment analysis mainly returned genes related to the response to oxidative stress, neuronal death, regulation of apoptotic signaling pathway, and other processes (**Figure 4A**). KEGG enrichment analysis showed that the pancreatic targets were closely related to the PI3K/Akt, MAPK, and Ras signaling pathways, hypoxia-inducible factor 1 signaling pathway, and apoptosis (**Figure 4B**). Concomitantly, GO enrichment analysis showed that the targets specific for the adipose tissue are potentially engaged in the response to oxidative stress, neuronal death, and cellular response to chemical stress (**Figure 4C**); whereas KEGG enrichment analysis highlighted the involvement of the PI3K/Akt and MAPK signaling pathways, calcium signaling and others (**Figure 4D**). Finally, GO enrichment analysis of the common targets of the pancreas and adipose tissue showed that these genes are engaged in the response to oxidative stress, cellular response to chemical stress, and intrinsic apoptotic signaling pathway (**Figure 4E**). KEGG enrichment analysis of those targets pointed towards pathways such as PI3K/Akt, MAPK, and Rap1 (**Figure 4F**). Interestingly, we also found that the response to oxidative stress and the PI3K/Akt signaling pathway were among the top20 ranked pathways returned by the GO and KEGG analyses of the targets common for both OA-AP and AP (**Supplementary Table S5** and **Supplementary Figures S4A–C**). Collectively, these results suggest that the protective effects of CQCQD against OA-AP were likely mediated by induction of antioxidant protein response and via reduced PI3K-Akt signaling.

CQCQD Decreases Oxidative Stress and Downregulates PI3K-Akt Signaling in Experimental OA-AP

To validate the findings from transcriptomics and pharmacology network analyses, we tested the expression of selected proteins involved in oxidative stress and the PI3K-Akt signaling pathway. Two indicators of oxidative stress were chosen: 1) an endogenous key anti-oxidative stress factor Nrf2, a master regulator of the antioxidant protein response; and 2) HO-1, an Nrf2-regulated detoxifying enzyme (Shapiro et al., 2007). Western blot images (**Figure 5A**) and the corresponding densitometric analysis (**Figure 5B**) demonstrated that the expression levels of pancreatic Nrf2 and HO-1 proteins were significantly up-regulated in the OA-AP mice compared to control. Following the CQCQD treatment, the expression levels of these proteins were further increased, indicating an enhanced anti-oxidant capacity against free radicals. This was further confirmed by the immunohistochemical staining for Nrf2 and HO-1 (**Figure 5C**). The control pancreata showed only very weak cytosolic staining patterns of Nrf2 and HO-1, essentially with no signal in the nuclei. In the OA-AP samples, both these proteins were expressed at a much higher level and were characterized by cytosolic and nuclear patterns of localization. The expression was even further elevated in the OA-AP groups treated with CQCQD (**Figure 5C**). The same patterns of Nrf2 and HO-1 expression were also observed in the visceral adipose tissues (**Figures 5D,E**).

To verify the involvement of the PI3K/Akt signaling pathway, two protein targets, Akt and phosphorylated-Akt (p-Akt), were selected and presented as the p-Akt/Akt ratio (Chen et al., 2020; Sarker and Steiger, 2020). While the p-Akt/Akt ratio was significantly increased in the OA-AP pancreata, CQCQD markedly decreased Akt phosphorylation to the levels in the OA-AP (**Figures 6A,B**). This was also evidenced by the immunohistochemical staining for p-Akt in the pancreatic tissue (**Figure 6C**). While Akt phosphorylation was not affected by OA-AP in the adipose tissue, CQCQD decreased the p-Akt/Akt ratio by approximately 75% compared to OA-AP without treatment (**Figures 6D,E**).

Both oxidative stress and the PI3K-Akt signaling pathway are associated with programmed death such as apoptosis (Cao et al., 2019). We found that apoptosis was involved in the top20 ranked pathways returned by the GO and KEGG analyses of the CQCQD-regulated targets in the pancreas and adipose tissues (**Figures 4A–F**). The expression of B-cell lymphoma-2 (Bcl2) and Bcl2-associated X protein of pancreatic tissues were detected to illustrate the effect of CQCQD on the acinar cells. While the Bax/Bcl2 ratio was significantly increased in the OA-AP pancreata, CQCQD markedly decreased this ratio in the OA-AP (**Supplementary Figures S5A,B**). The pancreatic TUNEL statining also supported CQCQD improved apoptosis in acinar cells (**Supplementary Figure S5C**).

These data collectively suggest that CQCQD reduced the severity of OA-AP by additional stimulation of the already activated antioxidant protein response (i.e., Nrf2/HO-1

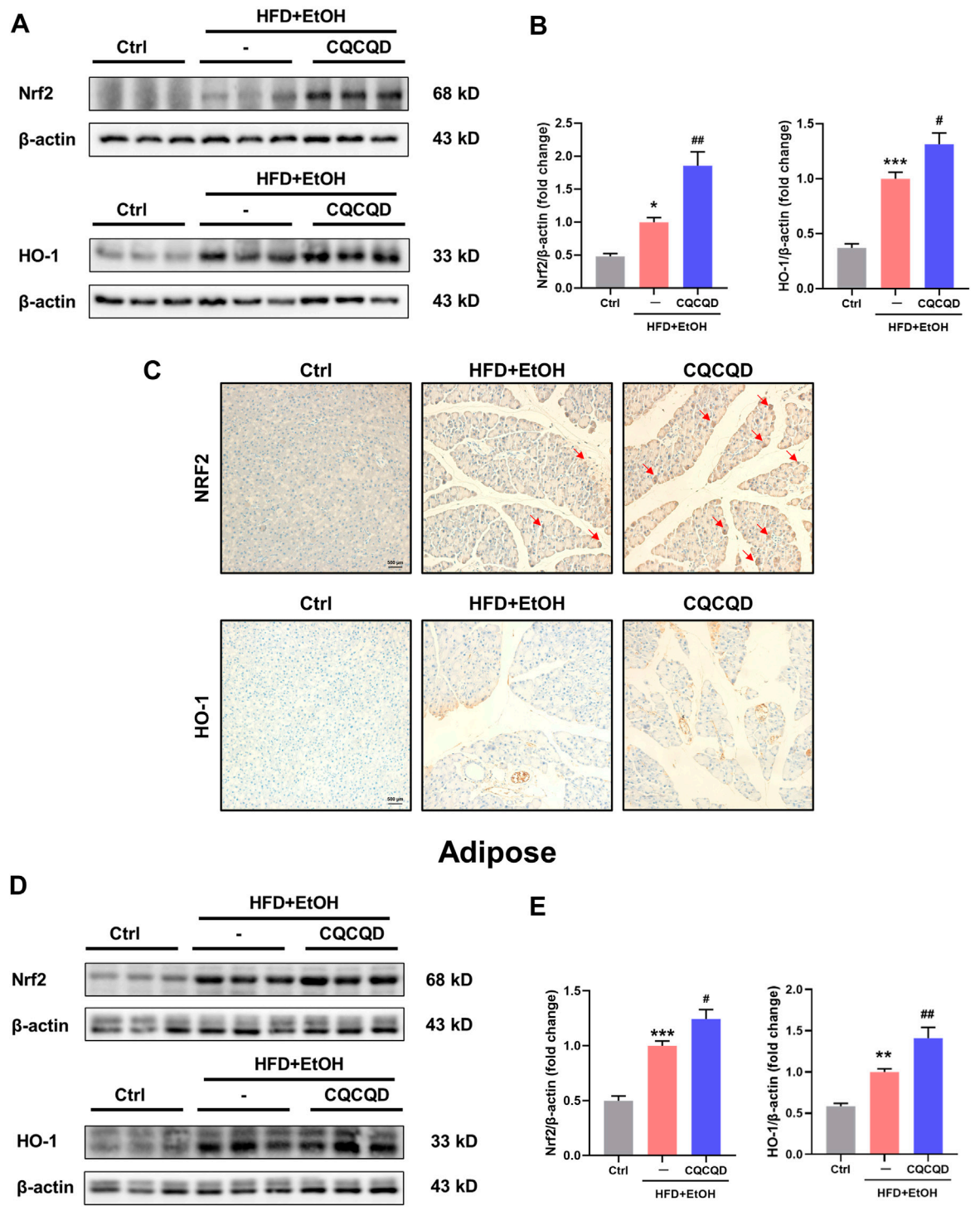

FIGURE 5 | CQCQD enhances the antioxidant protein response in the pancreas and adipose tissue from OA-AP mice. **(A,D)** Representative Western-blot images for Nrf2 and HO-1 in the pancreatic tissues **(A)** and adipose tissues **(D)**. **(B,E)** Quantification of Western-blot images for Nrf2 and HO-1 for the pancreatic tissues **(B)** and adipose tissues **(E)**. **(C)** Representative immunohistochemical staining for Nrf2 and HO-1 in the pancreatic tissue. All data are presented as means ± SEM of six samples per group. Ctrl vs. OA-AP: $^{*}p < 0.05$, $^{**}p < 0.01$, $^{***}p < 0.001$; OA-AP vs. OA-AP + CQCQD: $^{\#}p < 0.05$, $^{\#\#}p < 0.01$, $^{\#\#\#}p < 0.001$.

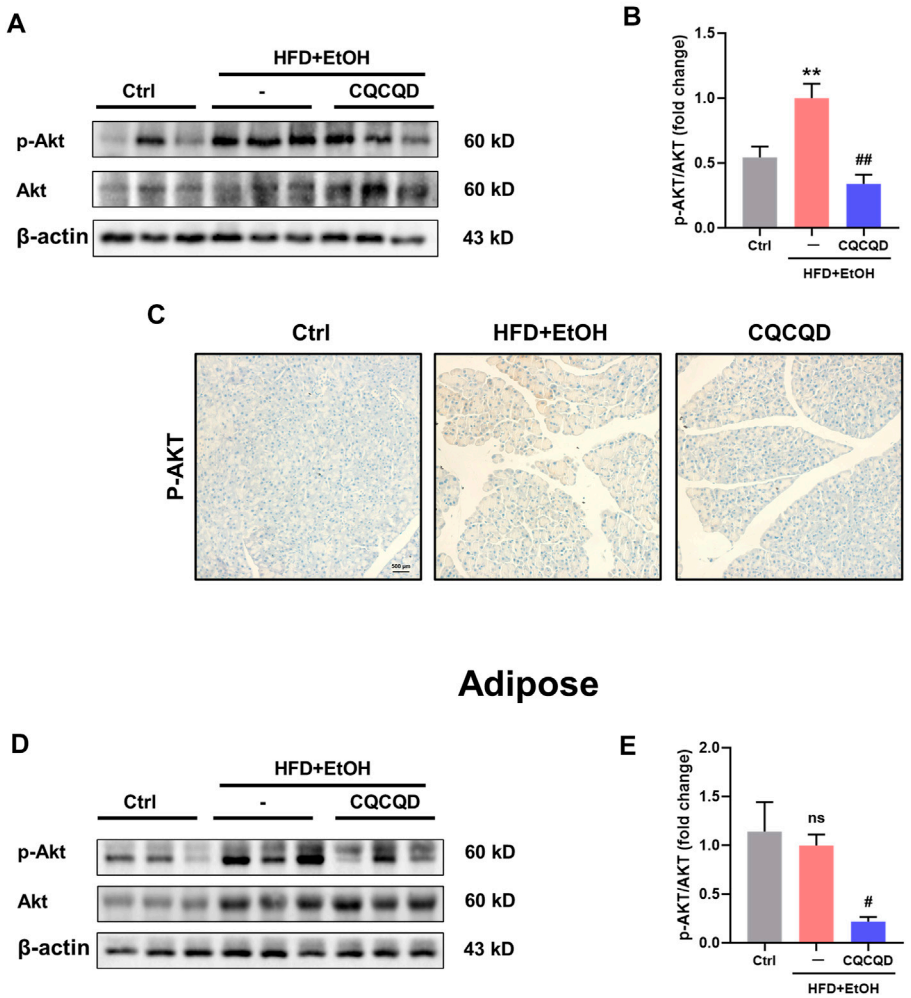

FIGURE 6 | CQCQD decreases Akt phosphorylation in the pancreas and adipose tissue from OA-AP mice. **(A,D)** Representative Western-blot images for p-Akt and total Akt in the pancreatic tissues **(A)** and adipose tissues **(D)**. **(B,E)** Quantification of Western-blot images for p-Akt/Akt of the pancreatic tissues **(B)** and adipose tissues **(E)**. **(C)** Representative immunohistochemical staining for p-Akt in the pancreatic tissue. All data are presented as means ± SEM of six samples per group. Ctrl vs. OA-AP: $^{**}p < 0.01$; OA-AP vs. OA-AP + CQCQD: $^{\#}p < 0.05$, $^{\#\#}p < 0.01$.

pathways) and at the same time suppressed the PI3K/Akt signaling pathway in the pancreatic and adipose tissues.

CQCQD Reduces Pancreatic Acinar Cell Death Elicited by Oxidative Stress

The effects of CQCQD were also tested *in vitro* in mouse pancreatic acinar cells. Acinar cells were isolated from lean mice and were pre-incubated with or without CQCQD, followed by treatment with H_2O_2 to induce oxidative stress (Huang et al., 2015). While H_2O_2 stimulation induced a steady increase in the reactive oxygen species (ROS) generation (**Figures 7A,B**) and triggered necrotic cell death of acinar cells (**Figures 7C,D**), CQCQD pre-incubation significantly reduced the recorded ROS signals as well as acinar cell necrosis (**Figures 7A–D**). The representative images of the PI staining of acinar cells are shown in **Figures 7E,F**. These results suggest that the protective effects of CQCQD against necrotic cell death in acinar cells are likely mediated by increased detoxification or scavenging of intracellular free radicals (Armstrong et al., 2018).

Docking Analysis Between CQCQD Compounds and AKT1

Finally, we narrowed down and explored the active compounds of CQCQD. A PPI network of 116 pancreatic targets of CQCQD was constructed by STRING database, which returned AKT1 as a target of the highest degree value (**Figure 8A**). Importantly, AKT1 was also one of the key targets common for OA-AP and AP (**Supplementary Figure S6**). Subsequently, a molecular docking approach was used to predict the

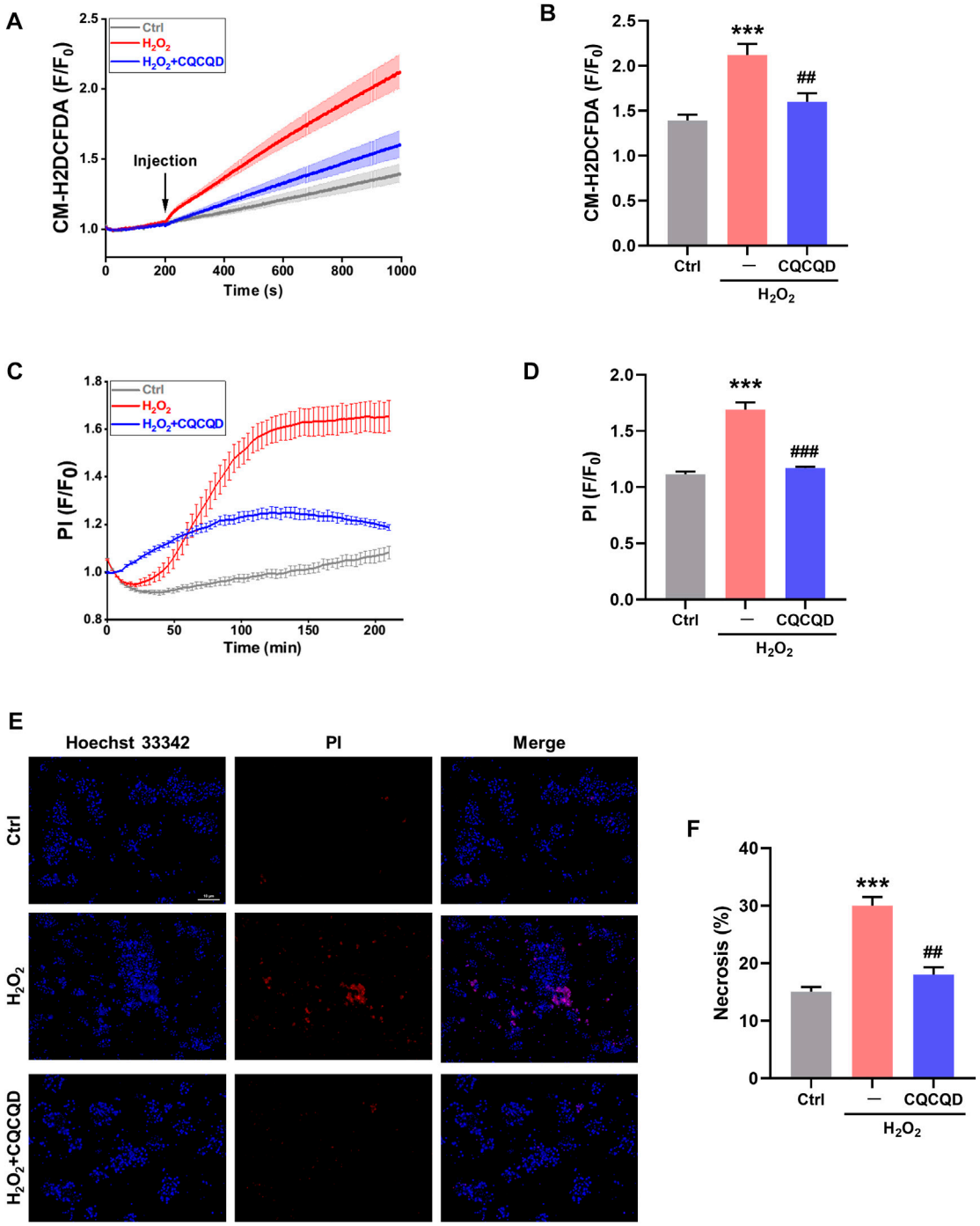

FIGURE 7 | CQCQD decreases ROS production and cell necrosis induced by H_2O_2 in mouse pancreatic acinar cells. **(A)** Average traces reflect intracellular ROS signals. **(B)** Summary quantification of ROS production (F/F_0). **(C)** Typical traces of cell necrosis. **(D)** Summary quantification of cell necrosis (F/F_0). **(E)** Representative images of pancreatic acinar cells stained with Hoechst 33,342 (blue) and PI (red). **(F)** Quantification of cell necrosis (%). All data are presented as means ± SEM of ≥ 3 repeats per group. Ctrl vs. OA-AP: $^{***}p < 0.001$; OA-AP vs. OA-AP + CQCQD: $^{\#\#}p < 0.01$, $^{\#\#\#}p < 0.001$.

interactive activities between CQCQD compounds and AKT1. Based on the network pharmacology, six compounds of CQCQD, i.e., baicalein, baicalin, chrysin, honokiol, magnolol, and salidroside, were found capable of high-affinity binding to AKT1 (**Figures 8B,C**).

DISCUSSION

This study has been inspired by promising clinical outcomes in AP patients treated with CQCQD in the West China Hospital. Since obesity is an important risk factor of AP and approximately 21% of

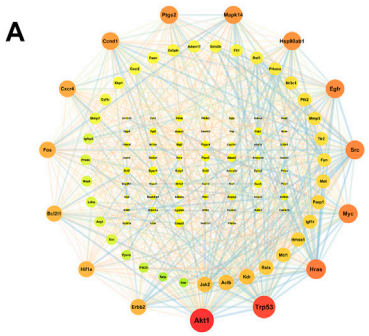

C

Compounds	△G (kj/mol)
Baicalein	-25.22952
Baicalin	-18.6188
Chrysin	-27.86544
Honokiol	-26.27552
Magnolol	-23.76512
Salidroside	-21.25472

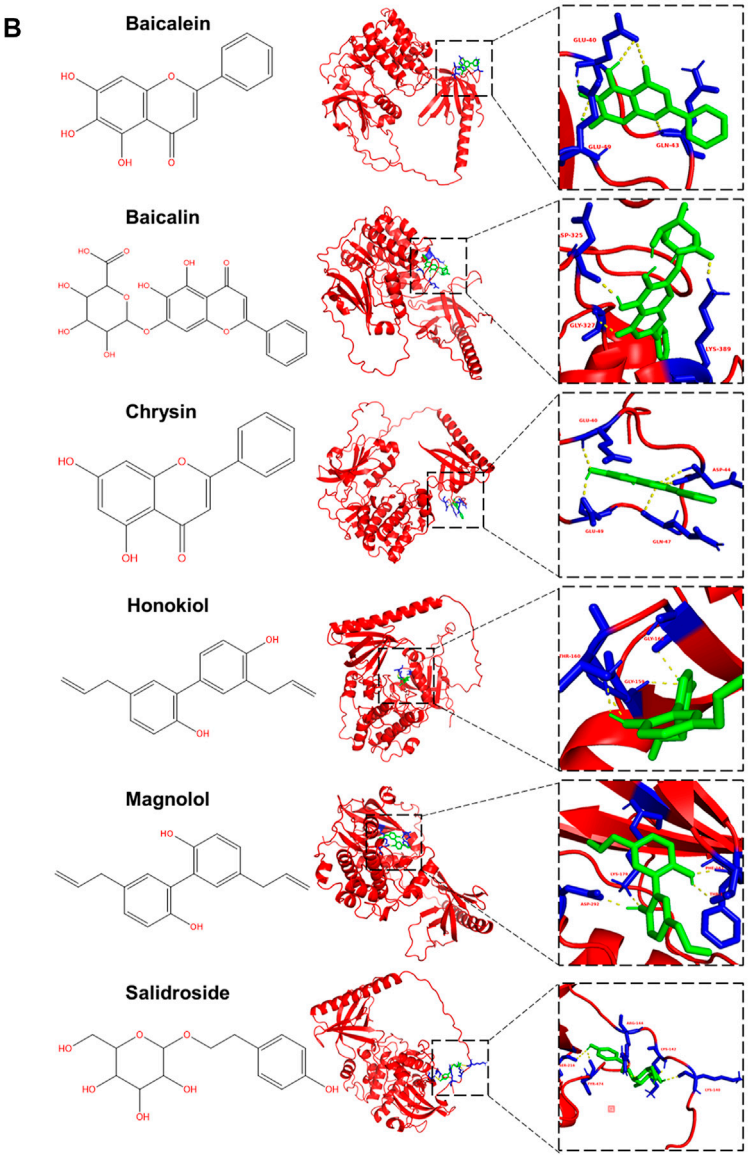

FIGURE 8 | Identification of interactions between CQCQD active compounds and the targets they regulate. **(A)** Interaction network of CQCQD-regulated targets in the pancreatic tissue. **(B)** Modeling interactions of CQCQD compounds and Akt1 by molecular docking. **(C)** The binding affinity between CQCQD compounds and Akt1.

all AP patients admitted to our center suffers from obesity-related AP (Jin et al., 2020; Li et al., 2020; Shi et al., 2020), we sought to shed some light on the pharmacological mechanisms underlying the clinical efficacy of CQCQD. For this purpose, we applied a new clinically-relevant mouse model of OA-AP along with transcriptome analysis of the pancreatic and adipose tissues to identify potential

gene targets and signaling pathways modulated by active compounds of CQCQD. Further, network pharmacology and molecular biology revealed that the protective effects of CQCQD on OA-AP are likely principally mediated by the antioxidant protein response and inhibition of the PI3K/Akt signaling pathway in both tissues. To the best of our knowledge, this is the first study that has linked the clinical effects of this traditional herbal formula with signaling in adipose tissue. Docking analysis further identified that CQCQD active compounds were capable of binding to Akt1, the protein kinase revealed by our *in silico* analyses.

Recently, obesity has been recognized as an important factor involved in the pathogenesis and progression of AP (Khatua et al., 2017). Alcohol consumption is another important risk factor for AP, although the pathology of alcoholic pancreatitis is still unclear (Alsamarrai et al., 2014; Samokhvalov et al., 2015). A recent epidemiological report (Lai et al., 2011) has shown an increased risk of AP in obesity-related metabolic conditions, such as type 2 diabetes combined with excessive alcohol consumption. Furthermore, previous preclinical studies have demonstrated that alcohol simultaneously supplied with free fatty acids can effectively induce AP in mice, rats, and hamsters (Huang et al., 2014; Maleth et al., 2015; Wang et al., 2016). The above has prompted us to apply a novel AP model induced by obesity and acute alcohol adminstration. Briefly, acute alcohol administration in obese mice caused pancreatic necrosis, systemic inflammation, and multi-organ dysfunction, while there were no significant changes in the histopathology of the pancreata from obese mice injected with saline alone or in lean mice injected with ethanol alone (Yang et al., 2022). This model may therefore reflect the pathophysiology underlying AP in obese patients, who are particularly vunlernable to progress to severe AP and poor clinical outcomes. However, OA-AP model is only suitable for obese mice, which may limit its use. And intraperitoneal injection of EtOH is still different from that of human drinking. Cerulein, a cholecystokinin analog, is the most widely used compound to induce AP (CER-AP) in rodents, which is characterized by overt pancreatic tissue edema, inflammatory cell infiltration, and a ceterin amount of acinar cell necrosis (Yang et al., 2020). Cerulein is often combined with lipopolysaccharide to increase the severity of CER-AP by exaggerating the inflammatory response and multi-organ dysfunction, mimicking AP-associated sepsis (Yang et al., 2020). Different from CER-AP, the OA-AP has much more increased indices for multi-organ dysfunction and the most significant pancreatic pathological change is a preferential acinar cell necrosis (Yang et al., 2022).

We found that in our OA-AP model, CQCQD administered at 5.5 g/kg, an equivalent dose to that regularly used in the clinic (Liang et al., 2021), decreased the pancreatic pathology score, local and systemic inflammation, and other organ injuries. Although previous reports have shown that CQCQD was effective in other preclinical models of AP, this study is the first to provide evidence on CQCQD efficacy in obesity-related pancreatic inflammation of alcoholic etiology.

In this study, we have applied transcriptomics and *in silico* analyses to identify DEGs in the pancreatic and adipose tissues from control and OA-AP mice. Modern methods of network pharmacology have been used to characterize active compounds of the traditional Chinese herbal formula. Predicted targets of 22 active compounds from CQCQD were overlapped with target genes differentially expressed in OA-AP and the "compound-target" network has been constructed. As a result, the antioxidant protein response and the PI3K/Akt signaling pathway have been identified as the key players in the CQCQD-mediated improvement of OA-AP outcomes. The same results were returned by the functional enrichment analysis of transcriptomics and network pharmacology both in the pancreas and adipose tissue. This is particularly important, since previous studies have demonstrated that oxidative stress and the PI3K/Akt signaling may underlie the pathogenesis of AP (Leung and Chan, 2009; Sarker and Steiger, 2020) and other acute inflammatory diseases (Manning and Toker, 2017).

Given that oxidative stress is implicated in AP (Tsai et al., 1998; Leung and Chan, 2009; Booth et al., 2011), antioxidant therapy can be a potential direction to explore further in AP treatment (Esrefoglu, 2012; Armstrong et al., 2013; Jiang et al., 2020). Nrf2/HO-1 pathway is the master regulator of cellular antioxidant responses (Kensler et al., 2007; Ma, 2013). Under stress conditions, Nrf2 translocates into the nucleus and activates antioxidant response elements that regulate gene expression of several enzymes including HO-1 (Kensler et al., 2007; Ma, 2013). Recently, natural or synthetic compounds capable of activating the Nrf2/HO-1 pathway in the pancreas have been reported to alleviate the severity of AP (Dong et al., 2016; Du et al., 2018; Liu et al., 2018). Similarly to cerulein-induced AP (Dong et al., 2016; Du et al., 2018; Liu et al., 2018), in our OA-AP model there was an up-regulation of Nrf2/HO-1, likely resulting from increased oxidative stress during the ongoing tissue inflammation. However, transcriptional activation of the Nrf2/HO-1 pathway by CQCQD, both in the pancreatic and adipose tissues, might be important for efficient detoxification of free radicals and thus could alleviate the progression of AP. In order to verify our findings experimentally, we first tested whether CQCQD could protect against oxidative stress in pancreatic acinar cells, in which premature activation of digestive enzymes causes autodigestion of the organ. CQCQD reduced the H_2O_2-elicited ROS signals and cell necrosis in acinar cells, thus confirming its protective anti-oxidant capacity in the cellular mediators of the sterile pancreatic inflammation. Although no clear benefit was found in the clinical trials of classical antioxidants in AP (Armstrong et al., 2013), our study provides the possibility of developing natural alternatives from traditional Chinese medicine.

The important role of the PI3K/Akt signaling pathway in the pathogenesis of inflammatory diseases, including AP, is well established (Lupia et al., 2014; Sarker and Steiger, 2020). Several previous studies implicated the PI3K/Akt pathway in trypsinogen activation, calcium overload, the nuclear translocation of NF-κB and cell apoptosis in the early course of AP, and strategies aim at PI3K inactivation to ameliorate the outcome of AP (Singh et al., 2001; Gukovsky et al., 2004; Abliz et al., 2015). On the other hand, Malagola et al. found that pharmacologic, or genetic inhibition of the Akt1 decreased acinar proliferation and exacerbated acinar-to-ductal metaplasia formation in the late course of AP following inflammatory insults (Chen et al., 2020). The PI3K/Akt pathway also plays an important role in insulin signaling cascade of adipose tissue by promoting glucose utilization, protein synthesis, and lipogenesis as well as inhibiting lipolysis (Huang et al., 2018).

Furthermore, PI3K/Akt pathway also modulated Nrf2 signaling by regulating Nrf2 phosphorylation, activity, and degradation (Yu and Xiao, 2021). In this study, we show that CQCQD markedly decreased Akt phosphorylation and thus inhibited the PI3K/Akt signaling our OA-AP model. Out of the active compounds of CQCQD, baicalein, baicalin, chrysin, honokiol, magnolol, and salidroside, all demonstrated marked potential for high affinity binding to AKT1, with chrysin being the most potent. While previous studies have reported that some of these compounds can improve AP in the *in vivo* or *in vitro* models (Li et al., 2018; Pu et al., 2019), the evidence that CQCQD components modulate oxidative stress or the PI3K/Akt pathway is marginal. In different diseases, honokiol was used as an inhibitor of Akt activation (Zhai et al., 2005), and chrysin was postulated to modulate the PI3K/Akt pathway (Zhou et al., 2021). In our study, out of a large pool of possible biological targets tested, it was the PI3K/Akt pathway that has emerged as the major mechanism regulated in OA-AP by the CQCQD active compounds.

CONCLUSION

This study is the first to explore how CQCQD herbal medicine, used in the pancreas clinics, ameliorates obesity-related and alcohol-induced AP via modulation of the antioxidant protein response and the PI3K/Akt pathway, in both the pancreatic and adipose tissues. Our findings provide a solid foundation for the applications of CQCQD or its modified formulas not only in traditional Chinese medicine but also in general clinical practice.

DATA AVAILABILITY STATEMENT

The datasets presented in this study can be found in online repositories. The names of the repository/repositories and accession number(s) can be found below: 220408 PM: https://www.ncbi.nlm.nih.gov; GSE200061.

ETHICS STATEMENT

The animal study was reviewed and approved by the Animal Ethics Committee of the West China Hospital, Sichuan University (20211086A).

AUTHOR CONTRIBUTIONS

WH, QX, and XY designed the study. QX and WH obtained funding and supervised students. XY and WH drafted the manuscript. XY, LY, MY, and XZ planned and conducted the major experiments and analyzed data. JY and DD identified the compounds of chaiqin chengqi decoction. XY and LY performed Network pharmacological analysis and molecular docking. LeD, TJ, LiD, and TL contributed to part of experiment. PF, MJ, and XF had important intellectual input. DC and RS critically revised the manuscript. All authors read and approved the final version of the article.

FUNDING

Program of Science and Technology Department of Sichuan Province (No. 2022YFS0406, to XY).National Nature Science Foundation of China (No. 81973632, to WH, No. 81800575, to TL; No. 81774120, to QX; No. 81970561,to XF). MJ and PF were supported by the HOMING/2017-3/23 (to MJ) and HOMING/2017-4/31 (to PF) project grants carried out within the HOMING program of the Foundation for Polish Science (Fundacja na rzecz Nauki Polskiej, FNP), cofinanced by the European Union under the European Regional Development Fund; and the OPUS project No. 2019/33/B/NZ3/02578 (to PF) of the National Science Center of Poland (Narodowe Centrum Nauki, NCN). UK NIHR Senior Investigator Award (to RS). Sichuan Provincial Key Research Project of Science and Technology of Traditional Chinese Medicine (No. 2020ZD004, to TJ).

SUPPLEMENTARY MATERIAL

The Supplementary Material for this article can be found online at: https://www.frontiersin.org/articles/10.3389/fphar.2022.896523/full#supplementary-material

Supplementary Figure S1 | Fingerprints and chemometric analysis of content in 22 Q-markers for CQCQD. **(A)** Ultra high-performance liquid chromatography(UHPLC) fingerprints for 10 batches (D1~D10) of CQCQD, and batch R is the simulated chromatogram (PMID: 33740732). **(B)** the representative total ion chromatograms (TIC) of CQCQD (D8, used in this study).

Supplementary Figure S2 | Pancreatic histopathology scoring system.

Supplementary Figure S3 | GO function and KEGG pathway analysis of the up-regulated genes and the down-regulated genes in the pancreatic and adipose tissues of OA-AP. Top 20 biological processes returned by the GO analysis of the up-regulated genes **(A)** and the down-regulated genes **(B)** in the pancreatic tissue. Top 20 KEGG pathways of the up-regulated genes **(C)** and the down-regulated genes **(D)** in the pancreatic tissue. Top 20 biological processes returned by the GO analysis of the up-regulated genes **(E)** and the down-regulated genes **(F)** in the adipose tissue. Top 20 KEGG pathways of the up-regulated genes **(G)** and the down-regulated genes **(H)** in the adipose tissue.

Supplementary Figure S4 | Comparison of the gene targets differentially regulated in AP and OA-AP. **(A)** Venn diagram shows common differentially regulated gene targets in AP and OA-AP. **(B)** KEGG pathway enrichment analysis shows the top 20 terms based on enrich factor arrangement. **(C)** GO analysis shows the top 20 terms based on enrich factor arrangement.

Supplementary Figure S5 | CQCQD improved the apoptosis of pancreatic acinar cells. **(A)** Representative Western-blot images for Bax and Bcl2 in the pancreatic tissues. **(B)** Quantification of Western-blot images for Bax and Bcl2 for the pancreatic tissues. **(C)** Representative TUNEL statining for apoptosis in the pancreatic tissue. All data are presented as means ± SEM of 6 samples per group. Ctrl vs. OA-AP: $^{*}p < 0.05$; OA-AP vs. OA-AP + CQCQD: $^{###}p < 0.001$.

Supplementary Figure S6 | Interaction network of common differentially regulated gene targets in AP and OA-AP.

REFERENCES

Abliz, A., Deng, W., Sun, R., Guo, W., Zhao, L., and Wang, W. (2015). Wortmannin, PI3K/Akt Signaling Pathway Inhibitor, Attenuates Thyroid Injury Associated with Severe Acute Pancreatitis in Rats. *Int. J. Clin. Exp. Pathol.* 8 (11), 13821–13833.

Alsamarrai, A., Das, S. L., Windsor, J. A., and Petrov, M. S. (2014). Factors that Affect Risk for Pancreatic Disease in the General Population: a Systematic Review and Meta-Analysis of Prospective Cohort Studies. *Clin. Gastroenterol. Hepatol.* 12 (10), 1635. doi:10.1016/j.cgh.2014.01.038

Armstrong, J. A., Cash, N., Soares, P. M., Souza, M. H., Sutton, R., and Criddle, D. N. (2013). Oxidative Stress in Acute Pancreatitis: Lost in Translation? *Free Radic. Res.* 47 (11), 917–933. doi:10.3109/10715762.2013.835046

Armstrong, J. A., Cash, N. J., Ouyang, Y., Morton, J. C., Chvanov, M., Latawiec, D., et al. (2018). Oxidative Stress Alters Mitochondrial Bioenergetics and Modifies Pancreatic Cell Death Independently of Cyclophilin D, Resulting in an Apoptosis-To-Necrosis Shift. *J. Biol. Chem.* 293 (21), 8032–8047. doi:10.1074/jbc.RA118.003200

Aune, D., Mahamat-Saleh, Y., Norat, T., and Riboli, E. (2021). High Body Mass Index and Central Adiposity Is Associated with Increased Risk of Acute Pancreatitis: A Meta-Analysis. *Dig. Dis. Sci.* 66 (4), 1249–1267. doi:10.1007/s10620-020-06275-6

Blüher, M. (2019). Obesity: Global Epidemiology and Pathogenesis. *Nat. Rev. Endocrinol.* 15 (5), 288–298. doi:10.1038/s41574-019-0176-8

Booth, D. M., Mukherjee, R., Sutton, R., and Criddle, D. N. (2011). Calcium and Reactive Oxygen Species in Acute Pancreatitis: Friend or Foe? *Antioxid. Redox Signal* 15 (10), 2683–2698. doi:10.1089/ars.2011.3983

Cao, Y., Li, Q., Liu, L., Wu, H., Huang, F., Wang, C., et al. (2019). Modafinil Protects Hippocampal Neurons by Suppressing Excessive Autophagy and Apoptosis in Mice with Sleep Deprivation. *Br. J. Pharmacol.* 176 (9), 1282–1297. doi:10.1111/bph.14626

Chen, R., Malagola, E., Dietrich, M., Zuellig, R., Tschopp, O., Bombardo, M., et al. (2020). Akt1 Signalling Supports Acinar Proliferation and Limits Acinar-To-Ductal Metaplasia Formation upon Induction of Acute Pancreatitis. *J. Pathol.* 250 (1), 42–54. doi:10.1002/path.5348

Collaborators, G. B. D. O., Afshin, A., Forouzanfar, M. H., Reitsma, M. B., Sur, P., Estep, K., et al. (2017). Health Effects of Overweight and Obesity in 195 Countries over 25 Years. *N. Engl. J. Med.* 377 (1), 13–27. doi:10.1056/NEJMoa1614362

de Oliveira, C., Khatua, B., Noel, P., Kostenko, S., Bag, A., Balakrishnan, B., et al. (2020). Pancreatic Triglyceride Lipase Mediates Lipotoxic Systemic Inflammation. *J. Clin. Invest.* 130 (4), 1931–1947. doi:10.1172/JCI132767

Dobszai, D., Mátrai, P., Gyöngyi, Z., Csupor, D., Bajor, J., Erőss, B., et al. (2019). Body-mass Index Correlates with Severity and Mortality in Acute Pancreatitis: A Meta-Analysis. *World J. Gastroenterol.* 25 (6), 729–743. doi:10.3748/wjg.v25.i6.729

Dong, Z., Shang, H., Chen, Y. Q., Pan, L. L., Bhatia, M., and Sun, J. (2016). Sulforaphane Protects Pancreatic Acinar Cell Injury by Modulating Nrf2-Mediated Oxidative Stress and NLRP3 Inflammatory Pathway. *Oxid. Med. Cell Longev.* 2016, 7864150. doi:10.1155/2016/7864150

Du, D., Yao, L., Zhang, R., Shi, N., Shen, Y., Yang, X., et al. (2018). Protective Effects of Flavonoids from Coreopsis Tinctoria Nutt. On Experimental Acute Pancreatitis via Nrf-2/are-Mediated Antioxidant Pathways. *J. Ethnopharmacol.* 224, 261–272. doi:10.1016/j.jep.2018.06.003

Esrefoglu, M. (2012). Experimental and Clinical Evidence of Antioxidant Therapy in Acute Pancreatitis. *World J. Gastroenterol.* 18 (39), 5533–5541. doi:10.3748/wjg.v18.i39.5533

Garg, P. K., and Singh, V. P. (2019). Organ Failure Due to Systemic Injury in Acute Pancreatitis. *Gastroenterology* 156 (7), 2008–2023. doi:10.1053/j.gastro.2018.12.041

Gukovskaya, A. S., Gukovsky, I., Algül, H., and Habtezion, A. (2017). Autophagy, Inflammation, and Immune Dysfunction in the Pathogenesis of Pancreatitis. *Gastroenterology* 153 (5), 1212–1226. doi:10.1053/j.gastro.2017.08.071

Gukovsky, I., Cheng, J. H., Nam, K. J., Lee, O. T., Lugea, A., Fischer, L., et al. (2004). Phosphatidylinositide 3-kinase Gamma Regulates Key Pathologic Responses to Cholecystokinin in Pancreatic Acinar Cells. *Gastroenterology* 126 (2), 554–566. doi:10.1053/j.gastro.2003.11.017

Han, C., Du, D., Wen, Y., Li, J., Wang, R., Jin, T., et al. (2021). Chaiqin Chengqi Decoction Ameliorates Acute Pancreatitis in Mice via Inhibition of Neuron Activation-Mediated Acinar Cell SP/NK1R Signaling Pathways. *J. Ethnopharmacol.* 274, 114029. doi:10.1016/j.jep.2021.114029

Huang, W., Booth, D. M., Cane, M. C., Chvanov, M., Javed, M. A., Elliott, V. L., et al. (2014). Fatty Acid Ethyl Ester Synthase Inhibition Ameliorates Ethanol-Induced Ca2+-dependent Mitochondrial Dysfunction and Acute Pancreatitis. *Gut* 63 (8), 1313–1324. doi:10.1136/gutjnl-2012-304058

Huang, W., Cane, M. C., Mukherjee, R., Szatmary, P., Zhang, X., Elliott, V., et al. (2017). Caffeine Protects against Experimental Acute Pancreatitis by Inhibition of Inositol 1,4,5-trisphosphate Receptor-Mediated Ca2+ Release. *Gut* 66 (2), 301–313. doi:10.1136/gutjnl-2015-309363

Huang, W., Cash, N., Wen, L., Szatmary, P., Mukherjee, R., Armstrong, J., et al. (2015). Effects of the Mitochondria-Targeted Antioxidant Mitoquinone in Murine Acute Pancreatitis. *Mediat. Inflamm.* 2015, 901780. doi:10.1155/2015/901780

Huang, X., Liu, G., Guo, J., and Su, Z. (2018). The PI3K/AKT Pathway in Obesity and Type 2 Diabetes. *Int. J. Biol. Sci.* 14 (11), 1483–1496. doi:10.7150/ijbs.27173

Huang, Y., Wen, Y., Wang, R., Hu, L., Yang, J., Yang, J., et al. (2022). Temporal Metabolic Trajectory Analyzed by LC-MS/MS Based Targeted Metabolomics in Acute Pancreatitis Pathogenesis and Chaiqin Chengqi Decoction Therapy. *Phytomedicine* 99, 153996. doi:10.1016/j.phymed.2022.153996

Iannuzzi, J. P., King, J. A., Leong, J. H., Quan, J., Windsor, J. W., Tanyingoh, D., et al. (2022). Global Incidence of Acute Pancreatitis Is Increasing over Time: A Systematic Review and Meta-Analysis. *Gastroenterology* 162, 122–134. doi:10.1053/j.gastro.2021.09.043

Jiang, X., Zheng, Y. W., Bao, S., Zhang, H., Chen, R., Yao, Q., et al. (2020). Drug Discovery and Formulation Development for Acute Pancreatitis. *Drug Deliv.* 27 (1), 1562–1580. doi:10.1080/10717544.2020.1840665

Jin, T., Li, L., Deng, L., Wen, S., Zhang, R., Shi, N., et al. (2020). Hemoconcentration Is Associated with Early Faster Fluid Rate and Increased Risk of Persistent Organ Failure in Acute Pancreatitis Patients. *JGH Open* 4 (4), 684–691. doi:10.1002/jgh3.12320

Kensler, T. W., Wakabayashi, N., and Biswal, S. (2007). Cell Survival Responses to Environmental Stresses via the Keap1-Nrf2-ARE Pathway. *Annu. Rev. Pharmacol. Toxicol.* 47, 89–116. doi:10.1146/annurev.pharmtox.46.120604.141046

Khatua, B., El-Kurdi, B., and Singh, V. P. (2017). Obesity and Pancreatitis. *Curr. Opin. Gastroenterol.* 33 (5), 374–382. doi:10.1097/MOG.0000000000000386

Lai, S. W., Muo, C. H., Liao, K. F., Sung, F. C., and Chen, P. C. (2011). Risk of Acute Pancreatitis in Type 2 Diabetes and Risk Reduction on Anti-diabetic Drugs: a Population-Based Cohort Study in Taiwan. *Am. J. Gastroenterol.* 106 (9), 1697–1704. doi:10.1038/ajg.2011.155

Lee, P. J., and Papachristou, G. I. (2019). New Insights into Acute Pancreatitis. *Nat. Rev. Gastroenterol. Hepatol.* 16 (8), 479–496. doi:10.1038/s41575-019-0158-2

Leung, P. S., and Chan, Y. C. (2009). Role of Oxidative Stress in Pancreatic Inflammation. *Antioxid. Redox Signal* 11 (1), 135–165. doi:10.1089/ars.2008.2109

Li, J., Zhou, R., Bie, B. B., Huang, N., Guo, Y., Chen, H. Y., et al. (2018). Emodin and Baicalein Inhibit Sodium Taurocholate-Induced Vacuole Formation in Pancreatic Acinar Cells. *World J. Gastroenterol.* 24 (1), 35–45. doi:10.3748/wjg.v24.i1.35

Li, L., Jin, T., Wen, S., Shi, N., Zhang, R., Zhu, P., et al. (2020). Early Rapid Fluid Therapy Is Associated with Increased Rate of Noninvasive Positive-Pressure Ventilation in Hemoconcentrated Patients with Severe Acute Pancreatitis. *Dig. Dis. Sci.* 65 (9), 2700–2711. doi:10.1007/s10620-019-05985-w

Liang, G., Yang, J., Liu, T., Wang, S., Wen, Y., Han, C., et al. (2021). A Multi-Strategy Platform for Quality Control and Q-Markers Screen of Chaiqin Chengqi Decoction. *Phytomedicine* 85, 153525. doi:10.1016/j.phymed.2021.153525

Liu, X., Zhu, Q., Zhang, M., Yin, T., Xu, R., Xiao, W., et al. (2018). Isoliquiritigenin Ameliorates Acute Pancreatitis in Mice via Inhibition of Oxidative Stress and Modulation of the Nrf2/HO-1 Pathway. *Oxid. Med. Cell Longev.* 2018, 7161592. doi:10.1155/2018/7161592

Lupia, E., Pigozzi, L., Goffi, A., Hirsch, E., and Montrucchio, G. (2014). Role of Phosphoinositide 3-kinase in the Pathogenesis of Acute Pancreatitis. *World J. Gastroenterol.* 20 (41), 15190–15199. doi:10.3748/wjg.v20.i41.15190

Ma, Q. (2013). Role of Nrf2 in Oxidative Stress and Toxicity. *Annu. Rev. Pharmacol. Toxicol.* 53, 401–426. doi:10.1146/annurev-pharmtox-011112-140320

Maléth, J., Balázs, A., Pallagi, P., Balla, Z., Kui, B., Katona, M., et al. (2015). Alcohol Disrupts Levels and Function of the Cystic Fibrosis Transmembrane Conductance Regulator to Promote Development of Pancreatitis. *Gastroenterology* 148 (2), 427. doi:10.1053/j.gastro.2014.11.002

Manning, B. D., and Toker, A. (2017). AKT/PKB Signaling: Navigating the Network. *Cell* 169 (3), 381–405. doi:10.1016/j.cell.2017.04.001

Mederos, M. A., Reber, H. A., and Girgis, M. D. (2021). Acute Pancreatitis: A Review. *JAMA* 325 (4), 382–390. doi:10.1001/jama.2020.20317

Moggia, E., Koti, R., Belgaumkar, A. P., Fazio, F., Pereira, S. P., Davidson, B. R., et al. (2017). Pharmacological Interventions for Acute Pancreatitis. *Cochrane Database Syst. Rev.* 4, CD011384. doi:10.1002/14651858.CD011384.pub2

Navina, S., Acharya, C., DeLany, J. P., Orlichenko, L. S., Baty, C. J., Shiva, S. S., et al. (2011). Lipotoxicity Causes Multisystem Organ Failure and Exacerbates Acute Pancreatitis in Obesity. *Sci. Transl. Med.* 3 (107), 107ra110. doi:10.1126/scitranslmed.3002573

Pu, W. L., Bai, R. Y., Zhou, K., Peng, Y. F., Zhang, M. Y., Hottiger, M. O., et al. (2019). Baicalein Attenuates Pancreatic Inflammatory Injury through Regulating MAPK, STAT 3 and NF-Kb Activation. *Int. Immunopharmacol.* 72, 204–210. doi:10.1016/j.intimp.2019.04.018

Samokhvalov, A. V., Rehm, J., and Roerecke, M. (2015). Alcohol Consumption as a Risk Factor for Acute and Chronic Pancreatitis: A Systematic Review and a Series of Meta-Analyses. *EBioMedicine* 2 (12), 1996–2002. doi:10.1016/j.ebiom.2015.11.023

Sarker, R. S., and Steiger, K. (2020). A Critical Role for Akt1 Signaling in Acute Pancreatitis Progression(dagger). *J. Pathol.* 251 (1), 1–3. doi:10.1002/path.5391

Shapiro, H., Singer, P., Halpern, Z., and Bruck, R. (2007). Polyphenols in the Treatment of Inflammatory Bowel Disease and Acute Pancreatitis. *Gut* 56 (3), 426–435. doi:10.1136/gut.2006.094599

Shi, N., Liu, T., de la Iglesia-Garcia, D., Deng, L., Jin, T., Lan, L., et al. (2020). Duration of Organ Failure Impacts Mortality in Acute Pancreatitis. *Gut* 69 (3), 604–605. doi:10.1136/gutjnl-2019-318241

Singh, V. P., Saluja, A. K., Bhagat, L., van Acker, G. J., Song, A. M., Soltoff, S. P., et al. (2001). Phosphatidylinositol 3-kinase-dependent Activation of Trypsinogen Modulates the Severity of Acute Pancreatitis. *J. Clin. Invest.* 108 (9), 1387–1395. doi:10.1172/JCI12874

Tsai, K., Wang, S. S., Chen, T. S., Kong, C. W., Chang, F. Y., Lee, S. D., et al. (1998). Oxidative Stress: an Important Phenomenon with Pathogenetic Significance in the Progression of Acute Pancreatitis. *Gut* 42 (6), 850–855. doi:10.1136/gut.42.6.850

Wang, Y., Kayoumu, A., Lu, G., Xu, P., Qiu, X., Chen, L., et al. (2016). Experimental Models in Syrian Golden Hamster Replicate Human Acute Pancreatitis. *Sci. Rep.* 6, 28014. doi:10.1038/srep28014

Wen, Y., Han, C., Liu, T., Wang, R., Cai, W., Yang, J., et al. (2020). Chaiqin Chengqi Decoction Alleviates Severity of Acute Pancreatitis via Inhibition of TLR4 and NLRP3 Inflammasome: Identification of Bioactive Ingredients via Pharmacological Sub-network Analysis and Experimental Validation. *Phytomedicine* 79, 153328. doi:10.1016/j.phymed.2020.153328

Yang, X., Yao, L., Fu, X., Mukherjee, R., Xia, Q., Jakubowska, M. A., et al. (2020). Experimental Acute Pancreatitis Models: History, Current Status, and Role in Translational Research. *Front. Physiol.* 11, 614591. doi:10.3389/fphys.2020.614591

Yang, X., Yao, L., Dai, L., Yuan, M., He, W., Liu, T., et al. (2022). Alcohol Predisposes Obese Mice to Acute Pancreatitis via Adipose Triglyceride Lipase-dependent Visceral Adipocyte Lipolysis. *Gut*. doi:10.1136/gutjnl-2022-326958

Yu, C., and Xiao, J. H. (2021). The Keap1-Nrf2 System: A Mediator between Oxidative Stress and Aging. *Oxid. Med. Cell Longev.* 2021, 6635460. doi:10.1155/2021/6635460

Zhai, H., Nakade, K., Oda, M., Mitsumoto, Y., Akagi, M., Sakurai, J., et al. (2005). Honokiol-induced Neurite Outgrowth Promotion Depends on Activation of Extracellular Signal-Regulated Kinases (ERK1/2). *Eur. J. Pharmacol.* 516 (2), 112–117. doi:10.1016/j.ejphar.2005.04.035

Zhang, X., Jin, T., Shi, N., Yao, L., Yang, X., Han, C., et al. (2018). Mechanisms of Pancreatic Injury Induced by Basic Amino Acids Differ between L-Arginine, L-Ornithine, and L-Histidine. *Front. Physiol.* 9, 1922. doi:10.3389/fphys.2018.01922

Zhou, Y. J., Xu, N., Zhang, X. C., Zhu, Y. Y., Liu, S. W., and Chang, Y. N. (2021). Chrysin Improves Glucose and Lipid Metabolism Disorders by Regulating the AMPK/PI3K/AKT Signaling Pathway in Insulin-Resistant HepG2 Cells and HFD/STZ-Induced C57BL/6J Mice. *J. Agric. Food Chem.* 69 (20), 5618–5627. doi:10.1021/acs.jafc.1c01109

Conflict of Interest: The authors declare that the research was conducted in the absence of any commercial or financial relationships that could be construed as a potential conflict of interest.

Publisher's Note: All claims expressed in this article are solely those of the authors and do not necessarily represent those of their affiliated organizations, or those of the publisher, the editors and the reviewers. Any product that may be evaluated in this article, or claim that may be made by its manufacturer, is not guaranteed or endorsed by the publisher.

frontiers | Frontiers in Pharmacology

ORIGINAL RESEARCH
published: 13 June 2022
doi: 10.3389/fphar.2022.906452

Effects of Intestinal FXR-Related Molecules on Intestinal Mucosal Barriers in Biliary Tract Obstruction

Meng Yan[1,2†], Li Hou[1†], Yaoyao Cai[1], Hanfei Wang[1], Yujun Ma[1], Qiming Geng[1], Weiwei Jiang[1] and Weibing Tang[1]**

[1]Department of Pediatric Surgery, Children's Hospital of Nanjing Medical University, Nanjing, China, [2]Department of Pediatrics, Huai'an Maternal And Child Health Care center, Huai'an, China

Background: The farnesoid X receptor (FXR) is a key factor regulating hepatic bile acid synthesis and enterohepatic circulation. Repression of bile acid synthesis by the FXR is a potential strategy for treating cholestatic liver disease. However, the role of intestinal FXR on the intestinal barrier and intestinal microbiota needs further investigation.

Materials: Intestinal tissues were collected from patients with biliary atresia or without hepatobiliary disease. Then, intestinal mRNA levels of FXR-related molecules were determined. To investigate the effect of FXR activation, bile-duct-ligation rats were treated with obeticholic acid [OCA (5 mg/kg/day)] or vehicle (0.5% methyl cellulose) per oral gavage for 14 days. The mRNA levels of intestinal FXR, SHP, TNF-α, FGF15 and bile acid transporter levels were determined. In addition, the intestinal permeability, morphologic changes, and composition of the intestinal microbiota were evaluated. Gut Microbiome was determined by 16S rDNA MiSeq sequencing, and functional profiling of microbial communities was predicted with BugBase and PICRUSt2. Finally, the role of OCA in injured intestinal epithelial cell apoptosis and proliferation was examined by pretreatment with lipopolysaccharide (LPS) in Caco-2 cells.

Results: The downstream of the FXR in ileum tissues was inhibited in biliary obstruction. Activation of the FXR signaling pathway by OCA significantly reduced liver fibrosis and intestinal inflammation, improved intestinal microbiota, and protected intestinal mucosa in BDL rats. OCA also altered the functional capacities of ileum microbiota in BDL rats. Significant differences existed between the controls and BDL rats, which were attenuated by OCA in the alpha diversity analysis. Principal coordinates analysis showed that microbial communities in BDL rats clustered separately from controls, and OCA treatment attenuated the distinction. Bugbase and PICRUSt2 analysis showed that OCA changed the composition and structure of the intestinal microbiota and improved the metabolic function of the intestinal microbiota by increasing the relative abundance of

OPEN ACCESS

Edited by:
Laura Grasa,
University of Zaragoza, Spain

Reviewed by:
Takeshi Susukida,
University of Toyama, Japan
Rodrigo M. Florentino,
University of Pittsburgh, United States

***Correspondence:**
Weiwei Jiang
wwjiang@njmu.edu.cn
Weibing Tang
twbcn@njmu.edu.cn

[†]These authors have contributed equally to this work and share first authorship

Specialty section:
This article was submitted to Gastrointestinal and Hepatic Pharmacology, a section of the journal Frontiers in Pharmacology

Received: 28 March 2022
Accepted: 18 May 2022
Published: 13 June 2022

Citation:
Yan M, Hou L, Cai Y, Wang H, Ma Y, Geng Q, Jiang W and Tang W (2022) Effects of Intestinal FXR-Related Molecules on Intestinal Mucosal Barriers in Biliary Tract Obstruction. Front. Pharmacol. 13:906452. doi: 10.3389/fphar.2022.906452

Abbreviations: FXR, farnesoid X receptor; OCA, Obeticholic acid; ALT, alanine aminotransferase; AST, aspartate aminotransferase; ALP, alkaline phosphatase; BDL, bile duct ligation; TNF-α, tumor necrosis factor-alpha; FGF15/19, fibroblast growth factor 15/19; SHP, small heterodimer partner; LPS, lipopolysaccharide; SHP, small heterodimer partner; PCNA, Proliferating Cell Nuclear Antigen; T-βMCA, taurine-β-muricholic acid; ASBT, Apical Sodium-BA transporter; I-BABP, Induction of intestinal BA-binding protein; OSTα, Organic Solute and Steroid Transporter Alpha; CYP7A1, Cholesterol 7-alpha Hydroxy-lase.

beneficial bacteria and reducing the relative abundance of harmful bacteria. Moreover, OCA reduced the apoptosis induced by LPS in Caco-2 cells.

Conclusion: The FXR agonist, OCA, activates the intestinal FXR signaling pathway and improves the composition and structure of the intestinal microbiota and intestinal barrier in BDL rats.

Keywords: FXR, biliary atresia, intestinal microbiota, obeticholic acid, bile duct ligation

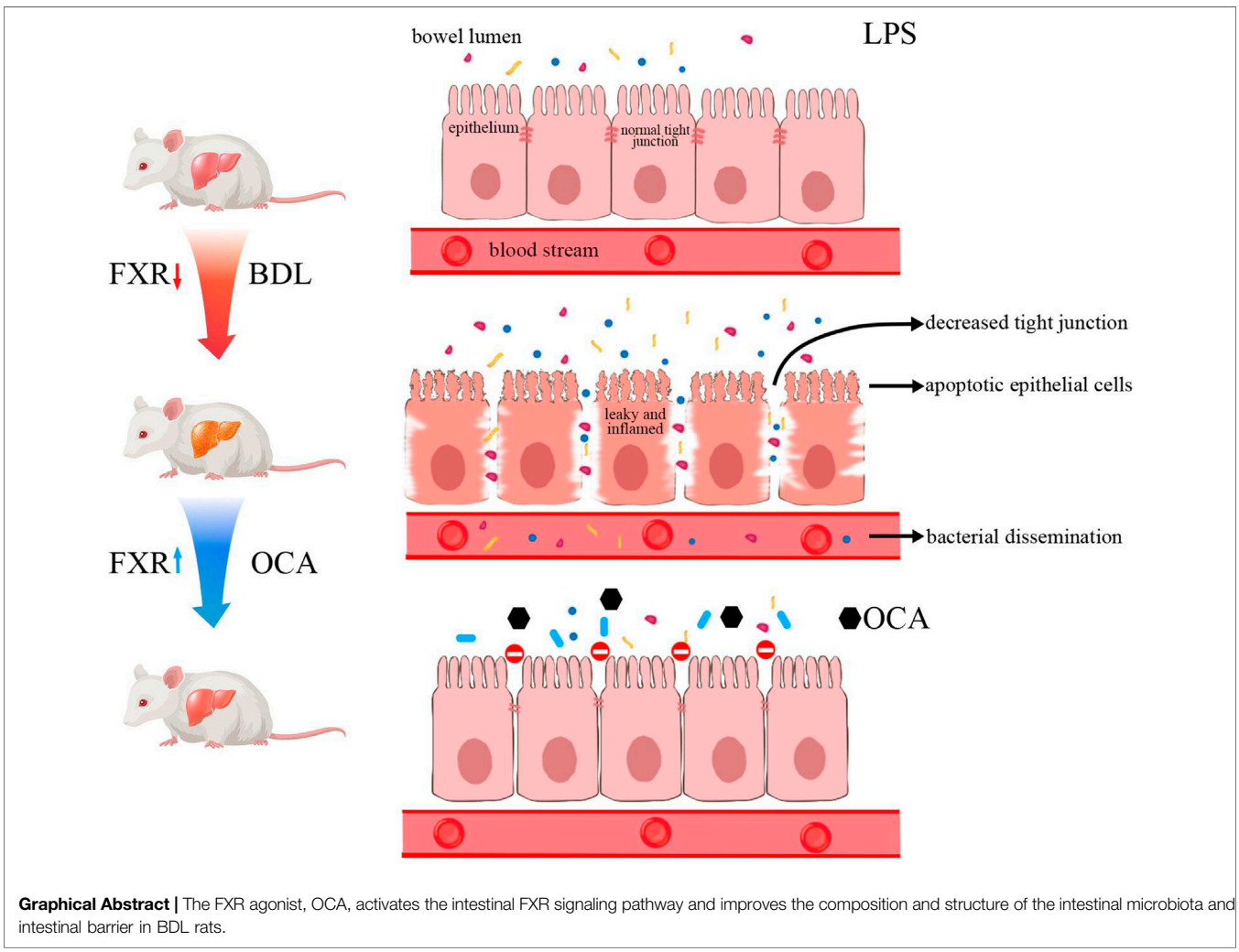

Graphical Abstract | The FXR agonist, OCA, activates the intestinal FXR signaling pathway and improves the composition and structure of the intestinal microbiota and intestinal barrier in BDL rats.

INTRODUCTION

Biliary obstruction is a pathologic condition of intrahepatic cholestasis caused by partial or complete obstruction of the intra- and extra-hepatic bile ducts that restricts bile flow into the intestinal tract. Biliary atresia (BA) is the most common cause of biliary obstruction in newborns. The most common cause of BA is inflammation and fibrosis of extrahepatic bile ducts, which reduces the passage of bile into the intestine (Asai et al., 2015; Wang et al., 2020). The reduction of bile acids in the intestine results in apoptosis of intestinal epithelial cells and atrophy of the intestinal mucous (Assimakopoulos et al., 2004). When the intestinal mucosal barrier is injured, the intestinal bacteria and endotoxin enter the blood, resulting in bacteremia and endotoxemia, respectively (Sorribas et al., 2019).

Bile acids are produced from cholesterol through oxidation reactions in hepatocytes, then conjugated with glycine and taurine. The bile acid enterohepatic circulation is strictly regulated by a large number of enzymes and transporters, of which the most important regulatory factor is the farnesoid X receptor (FXR) (Gonzalez et al., 2017). Bile acids in the body are natural ligands of the FXR (Cariello et al., 2018), including the

TABLE 1 | Primers for qRT-PCR evaluation of gene expression levels in human.

	Human primer sequence (5' to 3')
FXR	F: GGGACAGAACCTGGAAGTGG
	R:GCCAACATTCCCATCTCTTTGC
GAPDH	F: GCACCGTCAAGGCTGAGAAC
	R: GGATCTCGCTCCTGGAAGATG
SHP	F: CTCACTGGGTGCTGTGTGAA
	R: AAGAAGGCCAGCGATGTCAA
TNF-α	F : GATCGGTCCCAACAAGGAGG
	R : GCTTGGTGGTTTGCTACGAC
FGF19	F : TGTGTGGTGGTCCACGTATG
	R : CGGATCTCCTCCTCGAAAGC

TABLE 2 | Primers for qRT-PCR evaluation of gene expression levels in rats.

	Rat primer sequence (5' to 3')
fxr	F: GGGACAGAACCTGGAAGTGG
	R: GCCAACATTCCCATCTCTTTGC
gapdh	F: GCACCGTCAAGGCTGAGAAC
	R: GGATCTCGCTCCTGGAAGATG
shp	F: CTCACTGGGTGCTGTGTGAA
	R: AAGAAGGCCAGCGATGTCAA
tnf-α	F: GATCGGTCCCAACAAGGAGG
	R: GCTTGGTGGTTTGCTACGAC
fgf15	F: TGTGTGGTGGTCCACGTATG
	R: CGGATCTCCTCCTCGAAAGC
i-babp	F: TATGGCCTTCACCGGCAA
	R: TACGTCCCCTTTCAATCACA
ostα	F: GGGCAGATCGCTTGCTCACC
	R: TCAGGCTTTGAGCGTTGAGT
asbt	F: TGGGTTTCTTCCTGGCTAGACT
	R: TGTTCTGCATTCCAGTTTCCAA

primary bile acids [chenodeoxycholic acid (CDCA) and cholic acid (CA)], the secondary bile acids [deoxycholic acid (DCA) and lithocholic acid (LCA)], and their conjugates with taurine and glycine (Makishima et al., 1999; Trabelsi et al., 2017). The FXR also plays an important role in the reabsorption of bile acids by regulating the bile acid transporter in the ileum (Trauner and Fuchs, 2022). Activation of the FXR pathway in the ileum influences expression of the apical sodium-BA transporter (ASBT), intestinal BA-binding protein (I-BABP), and organic solute and steroid transporter alpha-beta (OSTα/β), thus, increasing bile acid reabsorption into the blood (Dawson, 2011). In addition, intestinal FXR increases the expression of FGF19, a hormone secreted into the portal blood and transported to the liver to suppress CYP7A1 expression (Kong et al., 2012; Liu et al., 2020). Therefore, the FXR has an important effect on regulating bile acid synthesis and enterohepatic circulation.

The intestinal microbiota is closely related to bile acid metabolism via interaction with bile acids (Fiorucci and Distrutti, 2015; Schneider et al., 2018). Accumulation of bile acids in the liver leads to hepatocyte apoptosis and changes in the diversity of the intestinal microbiota (Wang et al., 2020). Bile acids and bacteria have a two-way regulation relationship; specifically, bile acids affect the survival and growth of bacteria, while bacteria regulate the consistency of intestinal bile acids (Stojancevic et al., 2012). The mechanism underlying bile acid toxicity on bacteria is multifactorial, and includes membrane effects, DNA damage, RNA structure changes, and protein denaturation (Assimakopoulos et al., 2007). Patients with BA do not have normal bile acids in the intestinal tract, which has a significant impact on the intestinal microbiota (Song et al., 2021). In mice, the intestinal microbiota not only regulates secondary bile acid metabolism but also regulates bile acid metabolism by reducing the level of T-βMCA, which improves intestinal FGF15 production and reduces BA synthesis (Sayin et al., 2013). Gut microbial dysbiosis results in endotoxin translocation into the portal vein, where activation of the NLRP3 inflammasome contributes to increased liver injury (Keitel et al., 2019). Besides, transferring the intestinal microbiota of cholestatic mice to healthy mice leads to severe liver damage (Kwong and Puri, 2021). Therefore, regulation of the intestinal microbiota is a potential treatment for liver disease secondary to BA.

The regulatory function of hepatic and intestinal FXR on bile acid metabolism has been extensively studied, but the role of intestinal FXR on the intestine has not been established. The activation of FXR has been proved to increase the expression of the tight-junction proteins claudin-1 and occluding in bacterial translocation (Verbeke et al., 2015). The present study determined the influence of the FXR agonist, obeticholic acid (OCA), in protecting the intestinal barrier in rats with obstructive jaundice by blocking the entry of bile into the intestine, excluding the indirect effect of bile on the intestine, then determining the effect of intestinal FXR on the intestine. We showed that OCA partly restored the enterohepatic circulation by increasing FGF19 expression. In addition, we demonstrated that the FXR has a protective effect on cholestatic liver injury and improves intestinal epithelial cell apoptosis in BDL rats, thus providing a new potential target for clinical prevention of intestinal mucosal barrier injury in patients with obstructive jaundice.

MATERIALS AND METHODS

Tissues and Gut Microbial Collection

The current study involved 24 infants without hepatobiliary disease and 16 BA patients at the Children's Hospital of Nanjing Medical University from November 2017 to December 2020. All BA patients were diagnosed based on intraoperative cholangiograms and pathologic evaluation of liver biopsies at the Children's Hospital of Nanjing Medical University. Tissue samples were collected from BA patients undergoing the Kasai procedure. Matched controls were derived from patients without liver failure or malignancies, and were confirmed to not have BA or other congenital malformations. No study subjects were recently treated with antibiotics. All tissue samples were immediately frozen in liquid nitrogen and stored at −80°C. We acquired written informed consent from the subjects or their legal guardians.

TABLE 3 | Demographic clinical features of study subjects.

Information	Control (*n* = 24)	Biliary Atresia (*n* = 16)	*p* t
Age (days, mean SE)	70.81 (20.25)	55.63 (6.11)	0.5535 0.5979
Male (%)	15 (62.5)	8 (50)	
Female (%)	9 (37.5)	8 (50)	

TABLE 4 | Liver function.

Indicator	Control (*n* = 24)	Biliary Atresia (*n* = 16)	*p*	t
ALT (U/L)	35.25 ± 4.416	161.2 ± 18.34	<0.0001	7.579
AST (U/L)	40.75 ± 2.837	245.5 ± 34.61	<0.0001	7.020
ALP(U/L)	320 ± 21.06	577.6 ± 45.22	<0.0001	5.599
DBIL (μmol/L)	2.068 ± 0.1772	131.8 ± 8.741	<0.0001	17.21
TBIL (μmol/L)	5.599 ± 0.4707	167.6 ± 11.43	<0.0001	16.41

Ethics approval was given by the Research Ethics Committee of the Children's Hospital of Nanjing Medical University.

Animals Experiment Design

Animals were randomized into three groups and fed a regular diet. For the bile duct ligation (BDL) model, rats were anesthetized with chloral hydrate, then the bile duct was exposed and ligated with two non-resorbable surgical sutures. Rats that underwent BDL were divided into two groups ($n = 6–7$). After the procedure, rats received the treatment with vehicle (0.5% methylcellulose) or OCA (5 mg/kg/day dissolved in 0.5% methylcellulose) by daily gavage for 2 weeks. Two weeks later, all animals were sacrificed under anesthesia. Ileum content, the ileum, serum, and fecal samples were collected and immediately stored at −80°C.

Serum Measurements

Alanine aminotransferase (ALT) and aspartate aminotransferase (AST) were measured using an automated bioanalyzer (Thermo Scientific Indiko Plus, Wuhan, China). The serum lipopolysaccharide (LPS) levels were determined using enzyme-linked immunosorbent assay (ELISA) kits (RayBiotech, Inc., United States).

Intestinal Gene Expression

Ileum tissues (3–5 cm) were collected at 0.5–1.5 cm proximal to the ileocecal flap for gene expression studies. The process of tissue homogenates, RNA extraction and real-time quantitative polymerase chain reaction followed the protocol. The primer sequence is shown in **Table 1**, **2**.

Western Blot Analysis

The frozen tissues and cells were lysed on ice with RIPA buffer (Solarbio). The expression levels of target proteins in the ileum were detected by respective primary antibodies. For protein density, each band was determined and then quantified by using Image J software. Primary antibodies involved in this study includes: anti-cleaved caspase-3 (1:2000, Cell Signaling Technology), anti-PCNA (1: 1,000, Santa Cruz), anti-β-actin (1:1,000, Santa Cruz).

Gut Microbiota Sequencing and Microbial Analysis

Genomic DNA was extracted from fecal samples using a E. Z.N.A. ®Stool DNA Kit (D4015, Omega, Inc., United States) according to manufacturer's instructions. Amplicons of the V3–V4 region of the 16S rDNA gene were conducted by using a 341F/805R primer pair. Sequencing was carried out on a NovaSeq PE250 platform. Sequence data analyses were mainly conductd by using Quantitative Insights Into Microbial Ecology2 (QIIME2) and R packages (v3.5.2). For dereplication, feature table and feature sequence were obtained by DADA2. The raw data of 16Sr DNA gene sequencing and metabolomic sequencing quality control in each sample are provided in the supplementary materials. Bugbase was used for the predictions of the functional profile of a microbial community based on 16S rDNA sequence data. Based on Kyoto Encyclopedia of Genes and Genomes (KEGG) functional pathways, PICRUSt2 was used to analyze the metabolic networks of ileum microbiota, with an emphasis on the enriched pathways.

Cell Culture and Treatments

The human intestinal epithelial cell line, Caco-2, was cultured in RPMI-1640 medium supplemented with 10% fetal bovine serum (FBS), 0.1 mg/ml of streptomycin, 100 U/mL of penicillin, and 2 mmol/L L-glutamine. Caco-2 cells were incubated in a humid atmosphere (5% CO_2 and 95% air) at 37°C. Caco-2 cells were treated with LPS (100 μg/ml) for 24 h to induce intestinal epithelial injury followed with the FXR agonists, OCA (10 μM) an additional 24 h.

Cell Viability Assay

Cell viability was detected with a CCK8 kit (Beyotime, Nantong, China). After the above treatment, cells were cultivated in 96-well microplates at a concentration of 1 cells/well × 10^4 cells/well and incubated in medium containing 5% FBS for 12 h. CCK-8 (10 μl/well) was then added to the wells and 96-well microplates were incubated at 37°C for 1–4 h. The absorbance at 450 nm was measured using a Tecan Infinite M200 multimode microplate reader (Tecan, Mechelen, Belgium).

Cell Apoptosis Analysis

The TdT-mediated dUTP nick-end labeling (TUNEL) assay was used in rat ileum sections to measure apoptosis of intestinal epithelial cells according to the manufacturer's instructions (Beyotime, Shanghai, China). To detect Caco-2 cell apoptosis, cells were harvested and stained with the Annexin V-FITC/propidium iodide kit (KeyGen Biotech, Nanjing, China) following the manufacturer's instructions. Apoptosis rates were analyzed using FlowJo V7 software.

Statistical Analysis

All statistical analyses are conducted using GraphPad Prism (version 8; GraphPad Software Inc., San Diego, CA, United States). Data are presented as the mean ± SEM.

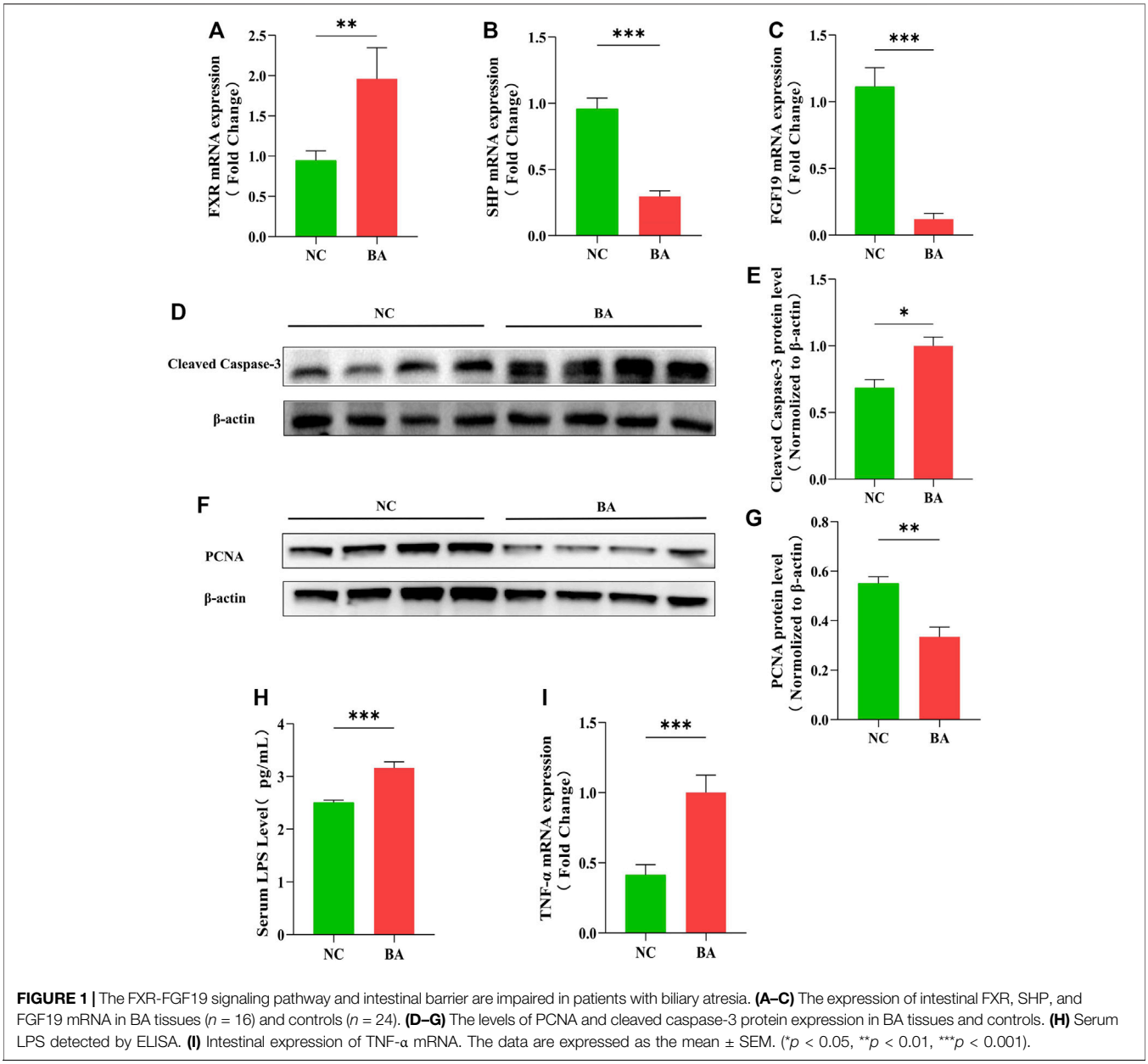

FIGURE 1 | The FXR-FGF19 signaling pathway and intestinal barrier are impaired in patients with biliary atresia. **(A–C)** The expression of intestinal FXR, SHP, and FGF19 mRNA in BA tissues (n = 16) and controls (n = 24). **(D–G)** The levels of PCNA and cleaved caspase-3 protein expression in BA tissues and controls. **(H)** Serum LPS detected by ELISA. **(I)** Intestinal expression of TNF-α mRNA. The data are expressed as the mean ± SEM. (*p < 0.05, **p < 0.01, ***p < 0.001).

Statistical comparisons were made using the one-way analysis of variance (ANOVA) with tukey's post hoc test or double-sided Student's t-test where appropriate. p value < 0.05 was considered significant. The qualitative data represent three independent experiments.

RESULTS

Clinical Information Analysis

Clinical information, including age, gender, and biochemical indicators, was obtained from 16 BA patients and 24 healthy controls. The mean ages of BA patients and controls were 55.63 ± 6.11 and 70.81 ± 20.25 days, respectively; there was no significant difference in mean age between the BA patients and healthy controls (**Table 3**). The serum alanine aminotransferase (ALT), aspartate aminotransferase (AST), alkaline phosphatase (ALP) direct bilirubin (DBIL), and total bilirubin (TBIL) levels were significantly increased in the BA group (**Table 4**).

The Farnesoid X Receptor-FGF19 Signaling Pathway and Intestinal Barrier Are Impaired in Patients With Biliary Atresia

First, FXR-related molecule expression in the 16 BA and 24 control samples was determined. The FXR was highly expressed in BA patients, while the small heterodimer partner

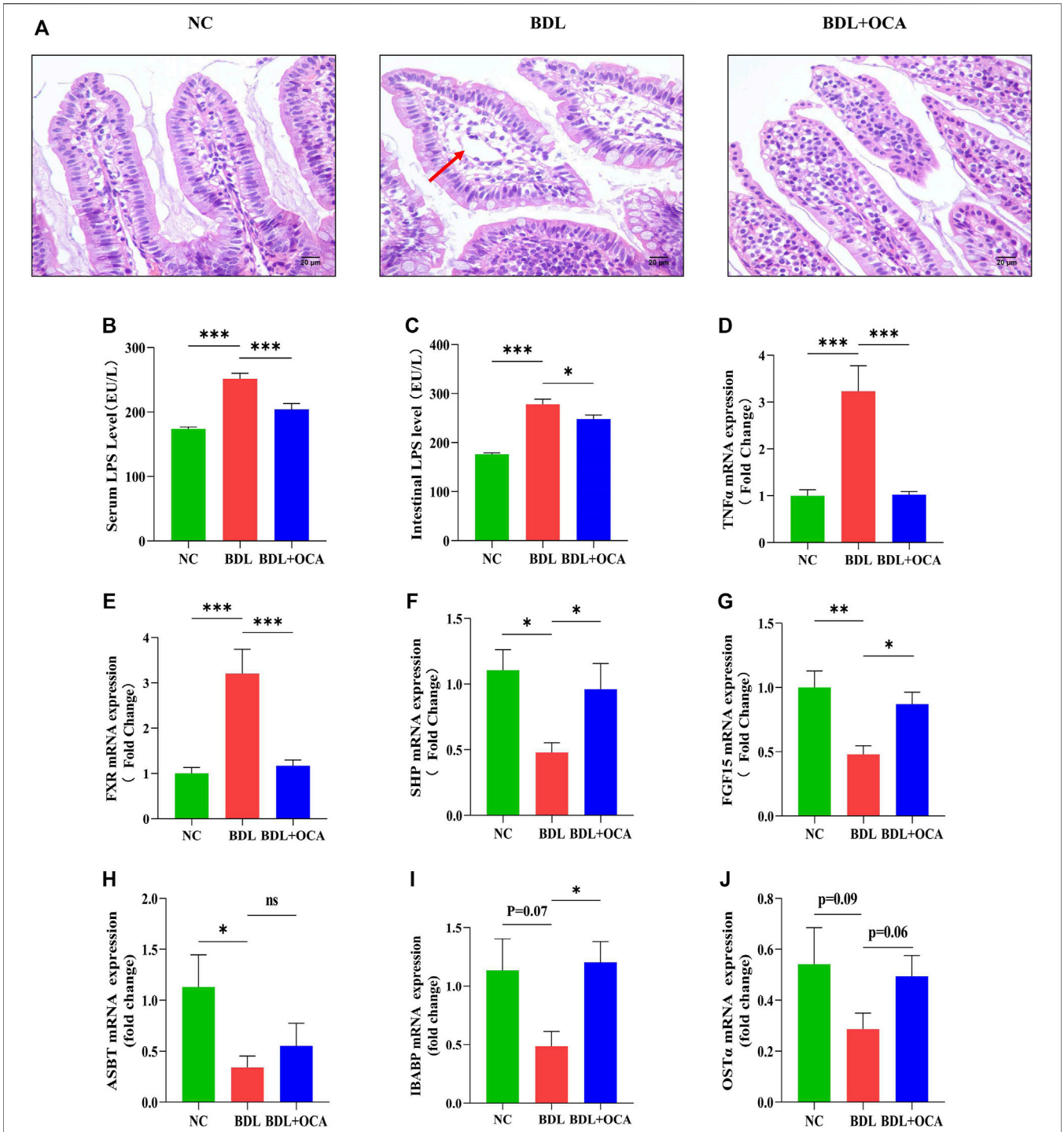

FIGURE 2 | OCA modulates the FXR signaling pathway and attenuates intestinal injury in BDL rats. **(A)** Representative images of intestinal sections stained with hematoxylin and eosin. **(B,C)** Serum and intestinal content of LPS detected by ELISA. **(D)** Intestinal mRNA expression of TNF-α. **(E–G)** Ileum expression of FXR, SHP, and FGF15 mRNA. **(H–J)** The bile acid transporter mRNA expression in ileum. The data are expressed as the mean ± SEM (n = 7–9). (OCA [5 mg/kg/day]) (*p < 0.05, **p < 0.01, ***p < 0.001)

(SHP) and FGF19 were significantly lower than in the control group (**Figures 1A–C**). The FXR-FGF19 signaling pathway was damaged in biliary obstruction, which might be involved in the development of BA. We also evaluated the apoptosis, proliferation and inflammatory response in intestinal tissues. The protein level of cleaved caspase-3 was greatly increased in

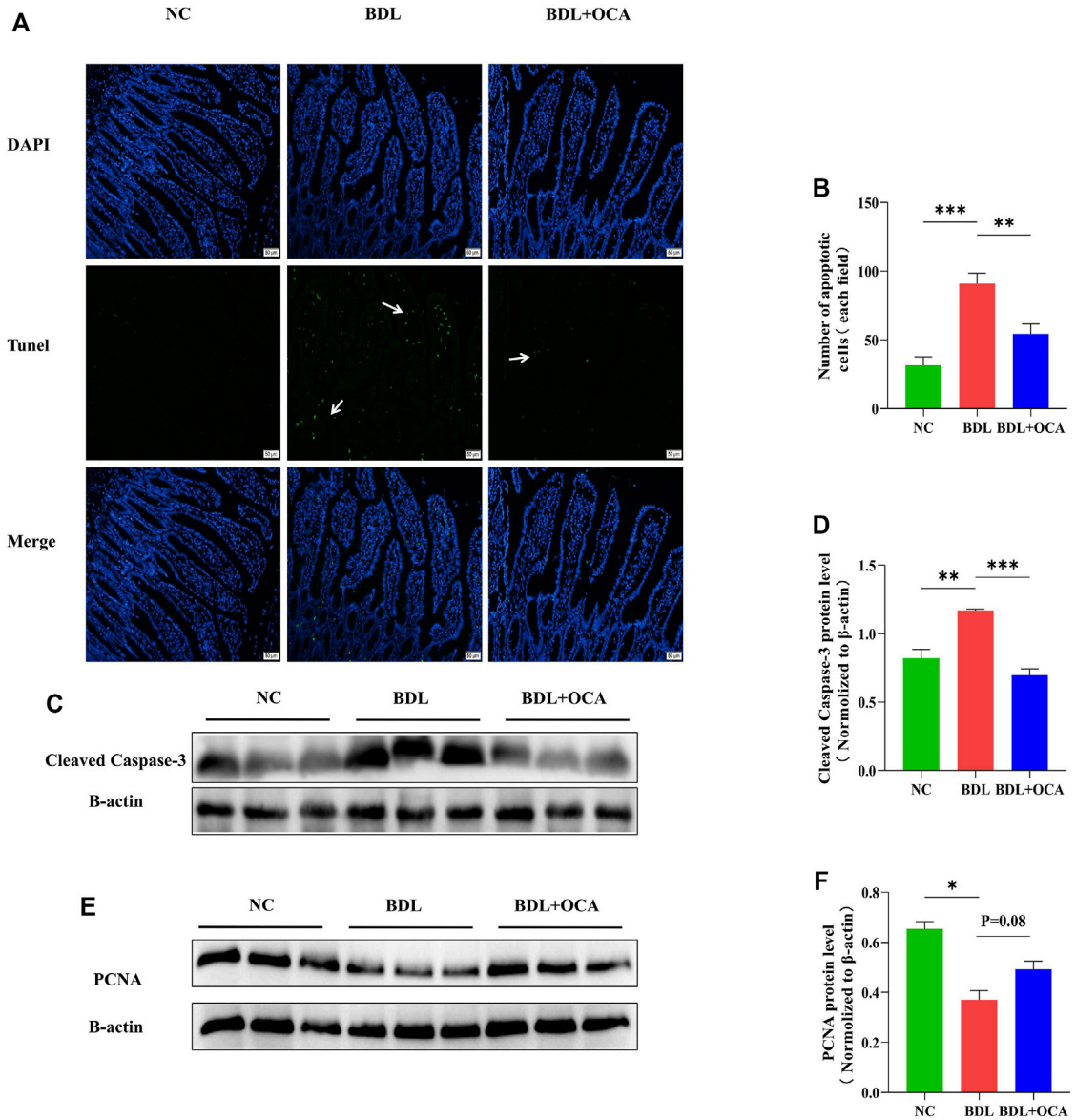

FIGURE 3 | OCA attenuates BDL-induced apoptosis of ileum epithelial cells. **(A)** TUNEL assay of small ileum sections. **(B)** The number of TUNEL-positive cells in the intestinal epithelium is shown. **(C,D)** Western blots of cleaved caspase-3 in ileum tissues from rats. **(E,F)** The protein expression level of PCNA in three groups. Bar graphs represent the mean ± SEM (n = 7–9). (OCA [5 mg/kg/day]) (*p < 0.05, **p < 0.01, ***p < 0.001)

BA samples (**Figures 1D,E**). Meanwhile, the expression levels of PCNA was significantly decreased in BA (**Figures 1F,G**). Serum LPS and intestinal TNF-α were significantly increased in BA patients (**Figures 1H,I**).

Obeticholic Acid Modulated Farnesoid X Receptor Signaling Pathway and Attenuated Intestinal Injury in Bile Duct Ligation Rats

To gain further insight into the effect of OCA, we determined the expression of FXR-related molecules and the impact on BDL rat intestines. HE staining revealed impaired intestinal mucosal architecture in BDL rats, in which intestinal villi were short, thick, and edematous, as shown by the red arrow. The mucosal injury was significantly decreased in BDL rats treated with OCA (**Figure 2A**). The serum and intestinal level of LPS were significantly increased in BDL rats compared with the control group, whereas OCA caused a marked decrease in the serum levels of these markers (**Figures 2B,C**). Intestinal TNF-α was also significantly increased in BDL rats, which was reduced by OCA (**Figure 2D**). Then, we examined the ileum FXR signaling pathway in the BDL rats and the changes produced by OCA. Expression of FXR in BDL rats ileum

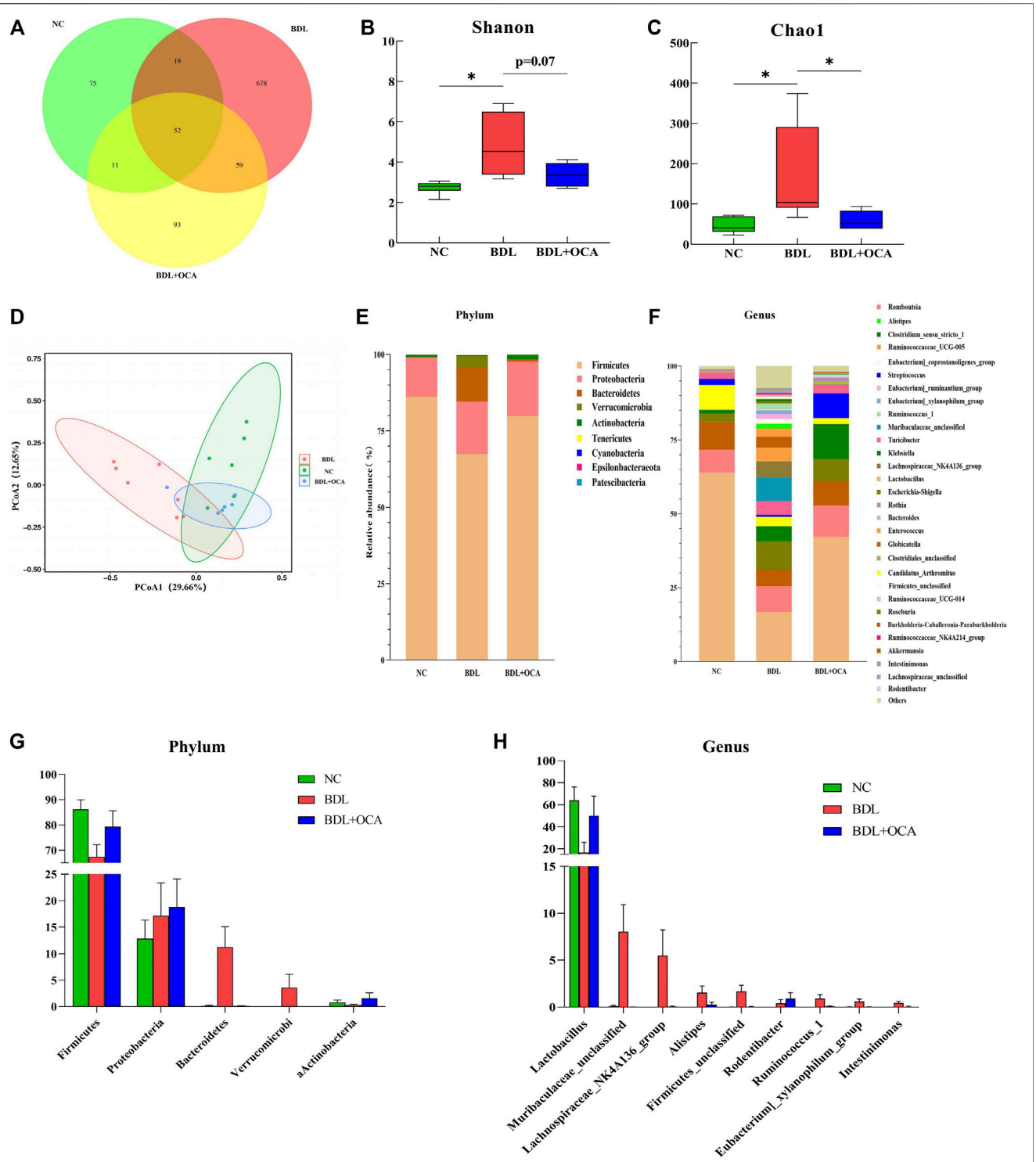

FIGURE 4 | OCA ameliorates dysbiosis of the ileum microbiota in BDL rats. **(A)** Venn diagram showing exclusive features per group. **(B,C)** Alpha-diversity analysis of ileum microbiota (Shannon and Chao1 index). **(D)** Differences of ileum microbial β-diversity. Beta-diversity was analyzed by principal coordinates using weighted Unifrac distances. **(E,F)** Composition of ileum microbiota at the phylum and genus levels. **(G,H)** Bacterial phyla and genera in ileum microbiota that were significantly changed in three groups and corresponding relative abundance. The data are expressed as the mean ± SEM ($n = 6–7$). (OCA [5 mg/kg/day]) (*$p < 0.05$, **$p < 0.01$, ***$p < 0.001$).

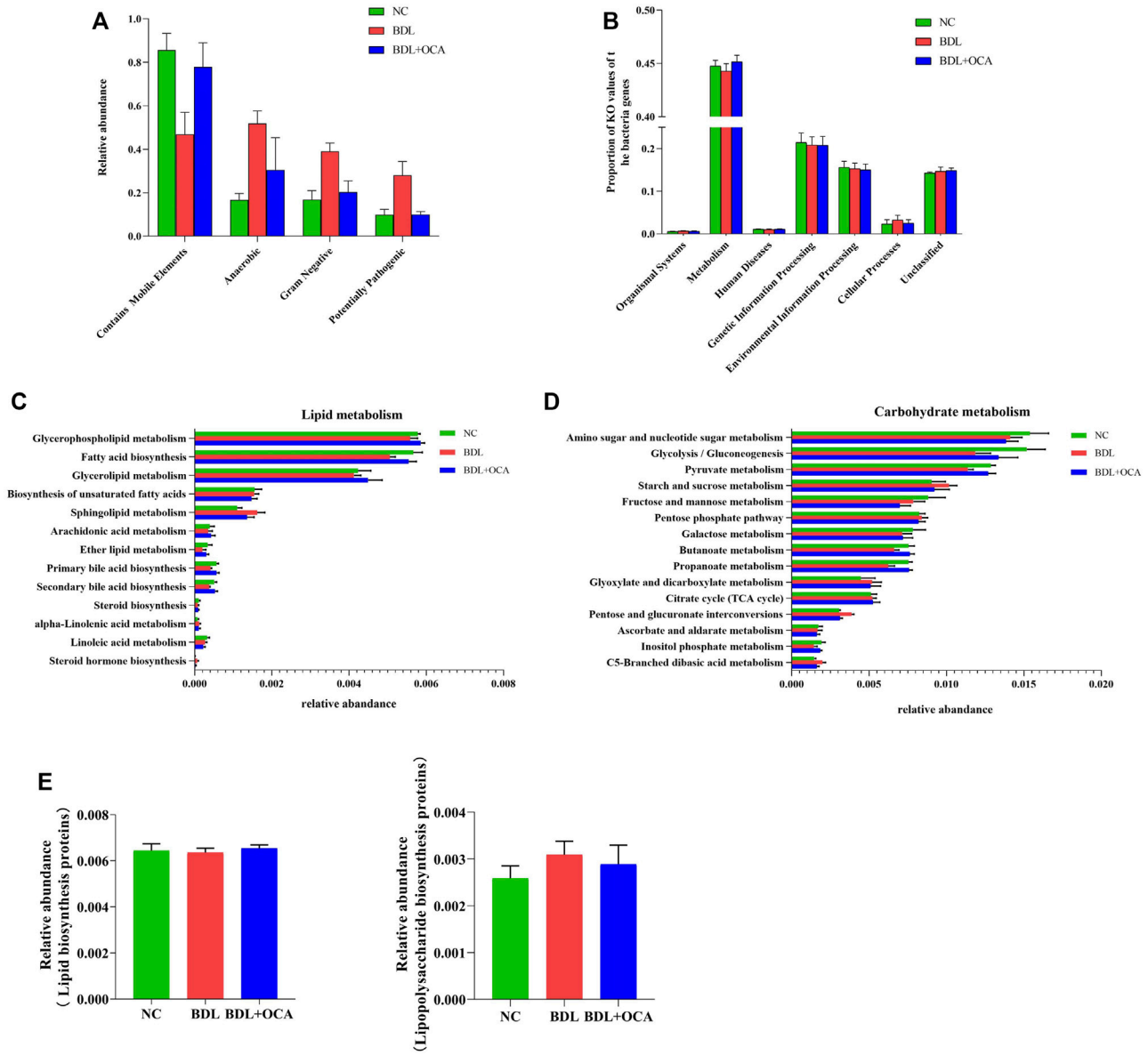

FIGURE 5 | Obeticholic acid ameliorated the dysbiosis of the ileum microbiota in bile duct ligation rats. **(A)** Relative abundances of four potential phenotypes predicted by BugBase. **(B)** Predicted functional profiles in all groups. **(C,D)** Relative abundance of the subordinate pathways of lipid and carbohydrate metabolism. **(E)** Comparison of gene sets associated with lipopolysaccharide biosynthesis and lipopolysaccharide biosynthesis proteins. The data are expressed as the mean ± SEM (n = 6–7). [OCA (5 mg/kg/day)].

was higher than controls (**Figure 2E**). However, the reduced activity of the FXR signaling pathway was indicated by the decreased ileum expression of the FXR target gene, such as SHP and FGF15. OCA effectively modulated the ileum FXR signaling pathway in BDL rats (**Figures 2F,G**). Furthermore, lack of bile acid in ileum contributde to the decreased trend of bile acid transporter mRNA expression, and FXR activation partially reversed this change (**Figures 2H–J**).

OCA attenuated BDL-induced apoptosis of ileum epithelial cells.

Previous studies have shown that bile acids stimulate intestinal epithelial proliferation (Yasuda et al., 2007). A lack of bile acid in the intestinal lumen is mainly attributed to impaired cell proliferation and increased apoptosis (Assimakopoulos et al., 2007). To determine whether the OCA-mediated protective effect against BDL-induced disruption of intestinal barrier function was due to an inhibition of cell apoptosis, we performed the TUNEL assay in ileum sections. Compared with controls, intestinal epithelial cell apoptosis was significantly increased in BDL rats, as shown

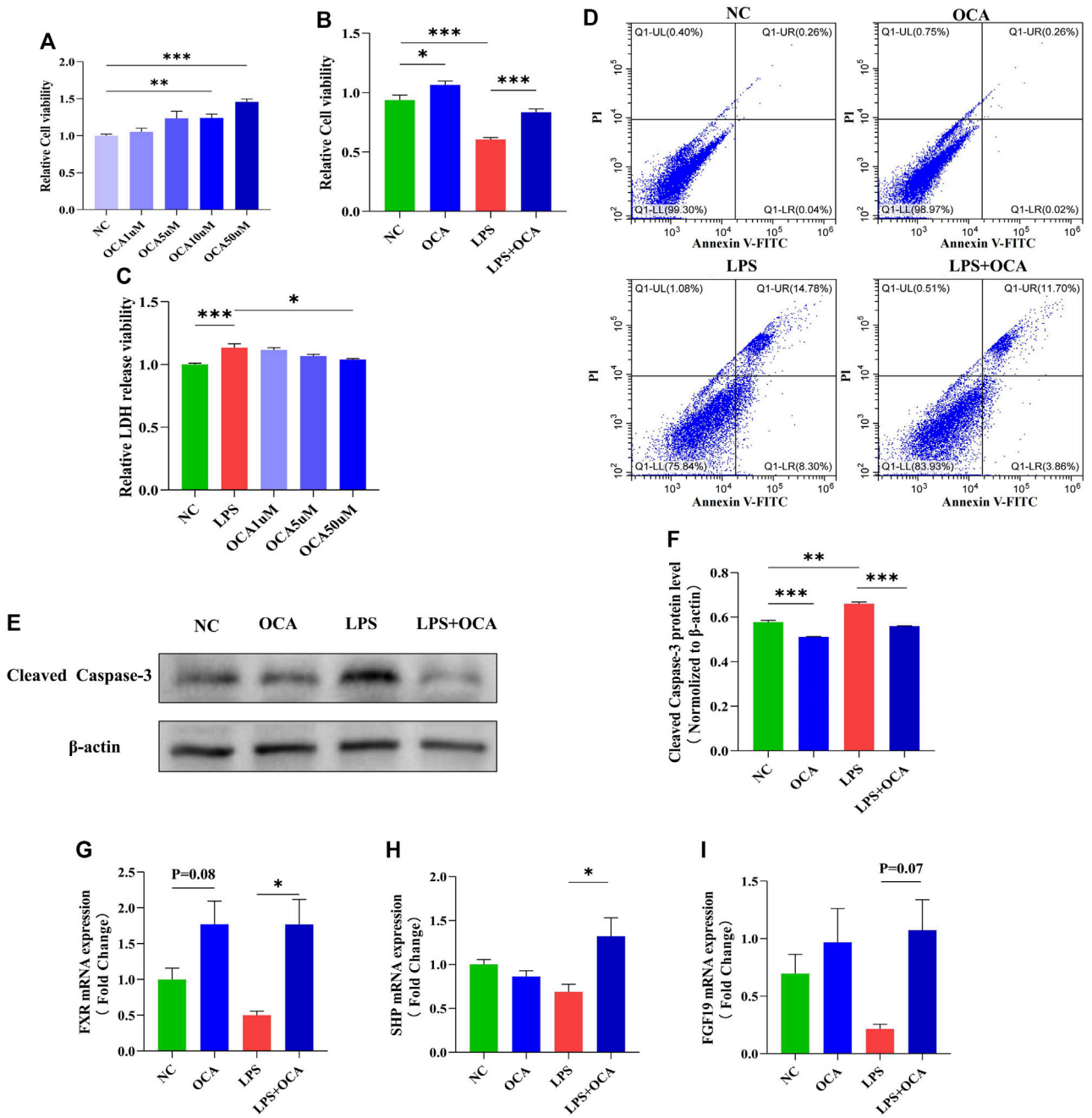

FIGURE 6 | OCA protected against LPS-induced apoptosis *in vitro*. **(A,B)** cell viability evaluated by CCK8 in the Caco-2 cell line. **(C)** LDH released in the supernatant of cultured cells was measured at the indicated time. **(D)** Cell apoptosis assay detected by flow cytometry in the Caco-2 cell line. **(E,F)** The level of cleaved caspase-3 protein expression in the Caco-2 cell line. **(G–I)** Real-time PCR analysis of FXR and its target genes FGF-19 and SHP. (OCA [10 μM], LPS [100 μg/ml]) (*p < 0.05, **p < 0.01, ***p < 0.001)

by the white arrow (**Figure 3A**). The number of apoptotic cells was clearly greater than controls (**Figure 3B**). As expected, intestinal epithelial cell apoptosis was markedly inhibited by OCA. Similar results were observed in a Western blot analysis, the levels of cleaved caspase-3 protein detected by western blot were increased in BDL rats compared with controls, and OCA attenuated BDL-induced upregulation of cleaved caspase-3 (**Figures 3C,D**). Consistent with these results, Treatment with OCA increased the expression of the PCNA in BDL rats (**Figures 3E,F**).

Obeticholic Acid Ameliorated the Dysbiosis of the Ileum Microbiota in Bile Duct Ligation Rats

To determine the mechanism involved in OCA-mediated protection against BDL-induced intestinal injury, we assessed the effects of BDL and OCA on microbiota composition in the ileum by amplifying and analyzing amplicons from the V3-V4 region of the 16S rDNA gene. A Venn diagram showed 75 features in the controls, 678 features in BDL rats, and 93 features in BDL rats treated with OCA (**Figure 4A**). The Shannon and Chao1 index was calculated to assess α-diversity in bacterial diversity. Significant differences existed between the controls and BDL rats, which were attenuated by OCA (**Figures 4B,C**). Principal coordinates analysis showed that microbial communities in BDL rats clustered separately from controls, and OCA treatment attenuated the distinction (**Figure 4D**). Differences in the microbiota community composition, ordered by relative abundance in the samples, were observed at the phylum and genus levels (**Figures 4E,F**).

As shown in **Figure 4G**, BDL rats had a reduced relative abundance of phylum Firmicutes that harbor bacteria with high bile salt hydrolase activity, which was increased by OCA treatment (Jones et al., 2008). In contrast, Bacteroidetes, a major bacterial phylum harboring bacteria with low bile salt hydrolase (BSH) activity, was significantly increased in BDL rats and attenuated by OCA treatment. At the genus level, the abundance of *Lactobacillus* was significantly decreased, and the abundance of the Lachnospiraceae NK4A136 group, Alistipes, Eubacterium_ruminantium_group, Intestinimonas, Ruminococcus_1, and Ruminococcaceae_NK4A214_group was significantly increased in BDL rats; however, OCA changed the unique enteric microbiome of BDL rats (**Figure 4H**). Compared with BDL rats, OCA-treated rats had fewer Lachnospiraceae_NK4A136_group, Eubacterium_ruminantium_group, Ruminococcus_1, and Intestinimonas, and more abundance of *Lactobacillus*.

Obeticholic Acid Altered the Functional Capacities of Ileum Microbiota in Bile Duct Ligation Rats

Four potential phenotypes (anaerobes, containing mobile elements, gram-negatives, and potentially pathogenic) were predicted to be significantly different in the three groups using BugBase. At the microbial community level, gene functions related to anaerobes, gram-negatives, and potentially pathogenic were increased in BDL rats. OCA treatment reduced the enrichment of gram-negatives and potentially pathogenic, possibly attributed to a decrease in the abundance of Bacteroidetes (**Figure 5A**). In addition, we gained functional prediction of the fecal bacteria through PICRUSt2 based on a KEGG database. The primary identified pathway of ileum microbiota was related to metabolism (**Figure 5B**), which was significantly decreased in BDL rats; however, OCA treatment improved enrichment of metabolism compared to BDL rats.

Furthermore, the relative abundances of ileum microbiota involved in primary and secondary bile acid biosynthesis-associated lipid metabolism were lower in BDL rats than controls, which may have been associated with lower bile acid levels (**Figure 5C**). Compared with BDL rats, OCA-treated BDL rats had an increased abundance of primary and secondary bile acid biosynthesis. The relative abundances of ileum microbiota related to sphingolipid metabolism and steroid hormone biosynthesis, which are involved in lipid metabolism, and were more significant in BDL rats than in other groups (**Figure 5C**). Subordinate pathways of carbohydrate metabolism were also analyzed and compared. Pyruvate metabolism, glycolysis/gluconeogenesis, an amino sugar, and nucleotide sugar metabolism were enriched in three groups of ileum microbiota (**Figure 5D**); however, there was an insignificant difference between the three cognitive groups in lipopolysaccharide biosynthesis and lipopolysaccharide biosynthesis proteins (**Figure 5E**).

Obeticholic Acid Protected Against Lipopolysaccharide-Induced Apoptosis *in Vitro*

The presence of bile acid in the intestine contributes to a normal gut barrier function by promoting intestinal epithelial cell proliferation. In biliary obstruction, intestinal mucosal injury is mainly due to more LPS caused by intestinal flora disorder (Assimakopoulos et al., 2007; Luo et al., 2022). To further confirm the effect of OCA on the proliferation and apoptosis of intestinal mucosal epithelial cells, Caco2 cells were incubated with LPS and OCA *in vitro*. OCA promoted the proliferation of Caco-2 cells based on concentration (**Figure 6A**). OCA improved the inhibitory effect of LPS on cell viability and cell proliferation rates (**Figure 6B**). OCA gradually reduced the released LDH in Caco-2 cells incubated with LPS as the OCA concentration increased (**Figure 6C**). Next, treatment of OCA significantly prevented apoptosis of Caco-2 cells incubated with LPS (**Figure 6D-F**). In addition, we determined whether OCA directly activates FXR by RT-PCR. OCA restored LPS-suppressed FXR expression in Caco-2 cells (**Figures 6G–I**).

DISCUSSION

Because biliary obstruction not only causes inflammation and fibrosis of the liver, biliary obstruction can also cause damage to the intestinal barrier, leading to endotoxemia. Therefore, protecting the intestinal mucosal barrier during biliary obstruction is an important treatment strategy. Indeed, our study showed that intestinal permeability, inflammation, and intestinal epithelial apoptosis was increased during biliary obstruction.

It is well-accepted that the FXR regulates the synthesis, transport, and enterohepatic circulation of bile acids by modulating the expression of related genes in the liver and small intestine (Liu et al., 2020). The main finding of this study showed that the relationship between the FXR pathway and the intestinal mucosal barrier during biliary obstruction. In BDL rats, the intestinal FXR signaling pathway was inhibited after

bile duct ligation, and the restoration of the FXR pathway improved intestinal barrier damage and intestinal microbiota imbalance. This finding provides new insight into the role of the FXR pathway in intestinal barrier injury.

Protection of the activated FXR pathway on intestinal barrier integrity was associated with reduced liver fibrogenesis. Hepatic accumulation of bile acid plays a pivotal role in the apoptosis of hepatocytes and bile duct hyperplasia, and eventually leads to liver fibrosis and cirrhosis in biliary obstruction (Fickert and Wagner, 2017). The decrease in intestinal bile leads to a deficiency in intestinal FXR activity, which weakens the inhibitory effect of CYP7A1 and leads to increased bile acid production and aggravation of liver fibrosis (Liu et al., 2020). In agreement with previous studies (Liu et al., 2020; Tsai et al., 2020; Modica et al., 2012), our results showed that OCA reduced liver fibrosis in rats with cholestasis by BDL (**Supplementary Figure S1**). The mechanisms underlying improved hepatic fibrosis by OCA remain unclear, although there are several explanations. Previous research has shown that bile acid activates intestinal FXR and elevates FGF15/19, which binds the FGF receptor and the β-Klotho complex on the surface of hepatocytes to inhibit CYP7A1 expression (Hartmann et al., 2018; Lee et al., 2018). In our study, biliary obstruction reduced intestinal bile acid concentration, leading to a significant reduction of SHP and FGF15 expression. Moreover, OCA significantly promoted the expression of SHP and FGF15, which inhibited CYP7A1 expression and decreased the production of bile acids. In addition, mitigation of liver fibrosis caused by OCA may be achieved by regulating the intestinal microbiota and restoring the intestinal barrier, thereby improving the "gut-liver axis" circulation, reducing liver inflammation, and ultimately alleviating liver fibrosis. Previous studies have shown that antibiotics which improve liver function in cholestatic patients indicate an active role of the microbiome in mediating liver injury during cholestasis (Tabibian et al., 2013). In previous study, decreased LPS production from the gut by OCA treatment activated TLR-4 and TLR-9, thus promoting inflammation, steatosis, and fibrosis, which might have contributed to reduced liver fibrosis (Lichtman et al., 1990).

The presence of bile in the intestine promotes intestinal epithelial cell proliferation and protects against apoptotic cell death, which contributes to the integrity of the intestinal barrier (Keitel and Häussinger, 2011). With the absence or reduction of bile in the intestine, the intestinal mucosal barrier is damaged, and the intestinal permeability is increased so that pathogenic bacteria and LPS translocate into the blood, causing bacteremia and endotoxemia (Iida et al., 2009; Wang et al., 2010). More LPS production facilitates liver and intestinal mucosal barrier damage through the LPS-TLR4 signaling pathway (An et al., 2022). Activation of the FXR pathway or the FXR agonists protects the mucosal integrity by regulating the expression of downstream genes related to mucosa protection and defense against inflammation in rodents (Vavassori et al., 2009; Gadaleta et al., 2011). Interestingly, in the case of bile duct obstruction, adding OCA can activate the FXR like bile acid, promoting the proliferation of intestinal epithelial cells and preventing cell apoptosis. Moreover, similar results were demonstrated *in vitro*, in which OCA attenuated LPS-induced apoptosis of Caco-2 cells. In the other hand, the increase of LPS disruptes bile acid metabolism (Xiong et al., 2017; Zhang et al., 2020), and contributes to the damage of liver and intestinal barrier. In the study of Sai Wang et al., LPS inhibited the expression of FXR signaling pathway in mouse primary hepatocytes (Wang et al., 2022), and we also found that OCA actived the FXR signaling pathway in lps-incubated Caco-2 cells, which may be involved in the mechanisms affecting the proliferation and apoptosis of Caco-2 cells. Our results extend the reparative effect of OCA on impaired intestinal barrier function; however, we only detected the expression of FXR-related genes, the mechanism by which the FXR promoted intestinal epithelial proliferation and inhibited apoptotic cell death warrants further study.

Microbiota and intestinal mucosal barrier are mutually influenced. Normal microbiota applies trophic effects on the intestinal mucosa, which display a significant role in mucosal protection and epithelial regeneration. Recently, the role of microbiota in maintaining the intestinal barrier has increasingly attracted more research attention. Probiotics and fecal microbiota transplantation are widely used in intestinal inflammatory diseases (Al-Sadi et al., 2021; Dou et al., 2021). The PICRUST2 analysis showed no difference in functional microbiota profiles of the LPS biosynthesis pathway among the three groups. These results implied that the elevation of plasma LPS in the BDL group and BA patients were primarily attributable to intestinal barrier dysfunction and microbiota dysbiosis, which has been associated with an increase in the levels of Gram-negative microbiota. Our results suggest that increased LPS produced by intestinal dysbiosis might damage intestinal barrier function, in which OCA treatment improved the intestinal barrier in biliary obstruction by modulating microbiota. In response to OCA, the increased bacterial load was normalized and intestinal dysbiosis improved in BDL rats, which showed that the beneficial effects of OCA on intestinal epithelial apoptosis in biliary obstruction are likely due to remodeling of intestinal microbiota. BSH is a principal enzyme that stimulates the "gateway" reaction in the bacterial metabolism of conjugated bile acid to produce deconjugated bile acid. OCA treatment rectifies the rising relative abundance of Bacteroidetes and the decreased relative richness of Firmicutes at the phylum level, which increases enrichment of the gut microbiota with BSH-containing phyla. Furthermore, *Lactobacillus* plays a key role in maintaining the intestinal mucosal barrier by increasing immunoglobulin secretion (Liu et al., 2021; Niu et al., 2021; Yang et al., 2021; Zhang et al., 2021). Our results showed that OCA treatment exhibited more abundance of *Lactobacillus*, thereby protecting against an impaired intestinal mucosal barrier in obstructive jaundice.

Intestinal microbiota displays various potential phenotypes and functions in response to changes in a different environment. Against colonization of potentially harmful bacteria in the intestine is a major function for normal intestinal microbiota (Dai and Walker, 1999). We observed that the OCA treatment significantly decreased the high abundance of potentially pathogenic and gram-negative microflora in the BDL group,

mostly attributed to the change in the abundance of Bacteroidetes. LPS derived from gram-negative bacteria can cause inflammatory responses and liver injuries (Rietschel et al., 1994; Machida et al., 2006; Aloman et al., 2007). This result is consistent with the level of LPS and TNF-α in the current study. In addition, analysis of KEGG pathway enrichment showed that OCA treatment greatly influences genes belonging to lipid metabolism pathways, including steroid hormone biosynthesis, sphingolipid metabolism, and primary and secondary bile acid biosynthesis.

Furthermore, it was concluded that the changed pathways in lipid metabolism were associated with biliary obstruction and OCA treatment. Biliary obstruction decreased bile acid metabolism-related genes, which were thought to be involved with inhibition of the FXR pathway. OCA treatment greatly stimulated activity of the FXR pathway, increasing the expression of bile acid metabolism-related genes. Recent studies have shown that intestinal FXR plays an indispensable role in glycolipid metabolism regulation, and intestinal-specific FXR agonists or antagonists participate in glucose and lipid metabolism regulation *in vivo* (Jiang et al., 2015a; Jiang et al., 2015b; Grundy, 2016). Our results also demonstrated that OCA attenuated the relative abundances of the genes involved in carbohydrate metabolism in biliary obstruction. The results of KEGG metabolic pathway analysis suggested that OCA had beneficial effects on BDL rats, which may be closely related to effective regulation of microbial metabolic pathways.

In general, OCA improved mucosal barrier function, down-regulated the concentrations of TNF-α and LPS, decreased the richness and diversity of the gut microbiota in the ileum, and reversed metabolic disorders.

CONCLUSION

Our study indicated that the active FXR pathway by OCA had beneficial effects on the intestinal barrier in BDL rats. Specifically, OCA changed the composition and structure of the intestinal microbiota and improved the metabolic function of the intestinal microbiota by increasing the relative abundance of beneficial bacteria and reducing the relative abundance of harmful bacteria. Moreover, OCA promoted the recovery of the intestinal barrier function of BDL rats by downregulating the levels of inflammatory cytokines and LPS. Therefore, this research provides a theoretical and application basis for developing the FXR pathway as a functional target to alleviate intestinal barrier injury in biliary obstruction.

DATA AVAILABILITY STATEMENT

The data presented in the study are deposited in the SRA of the NCBI (https://www.ncbi.nlm.nih.gov/sra), accession number SRR18791516-SRR18791534.

ETHICS STATEMENT

The studies involving human participants were reviewed and approved by the medical ethic committee of Nanjing Children's Hospital of Nanjing Medical University. Written informed consent to participate in this study was provided by the participants' legal guardian/next of kin. The animal study was reviewed and approved by Institutional Animal Care and Use Committee of NMU and Nanjing medical University.

AUTHOR CONTRIBUTIONS

All authors listed have made a substantial, direct, and intellectual contribution to the work and approved it for publication.

FUNDING

This study was funded by the Top Talents of Jiangsu Provincial Health Committee's Six One Project, China (LGY2020019); General Project of Nanjing Health Commission (YKK20121); the Jiangsu Provincial Key Research and Development Program, China (BE2017609); and Key Project of Science and Technology Development of Nanjing health committee, China (ZKX18037).

SUPPLEMENTARY MATERIAL

The Supplementary Material for this article can be found online at: https://www.frontiersin.org/articles/10.3389/fphar.2022.906452/full#supplementary-material

REFERENCES

Al-Sadi, R., Dharmaprakash, V., Nighot, P., Guo, S., Nighot, M., Do, T., et al. (2021). Bifidobacterium Bifidum Enhances the Intestinal Epithelial Tight Junction Barrier and Protects against Intestinal Inflammation by Targeting the Toll-like Receptor-2 Pathway in an NF-κb-independent Manner. *Int. J. Mol. Sci.* 22 (15), 8070. doi:10.3390/ijms22158070

Aloman, C., Gehring, S., Wintermeyer, P., Kuzushita, N., and Wands, J. R. (2007). Chronic Ethanol Consumption Impairs Cellular Immune Responses against HCV NS5 Protein Due to Dendritic Cell Dysfunction. *Gastroenterology* 132 (2), 698–708. doi:10.1053/j.gastro.2006.11.016

An, L., Wirth, U., Koch, D., Schirren, M., Drefs, M., Koliogiannis, D., et al. (2022). The Role of Gut-Derived Lipopolysaccharides and the Intestinal Barrier in Fatty Liver Diseases. *J. Gastrointest. Surg.* 26 (3), 671–683. doi:10.1007/s11605-021-05188-7

Asai, A., Miethke, A., and Bezerra, J. A. (2015). Pathogenesis of Biliary Atresia: Defining Biology to Understand Clinical Phenotypes. *Nat. Rev. Gastroenterol. Hepatol.* 12 (6), 342–352. doi:10.1038/nrgastro.2015.74

Assimakopoulos, S. F., Scopa, C. D., and Vagianos, C. E. (2007). Pathophysiology of Increased Intestinal Permeability in Obstructive Jaundice. *World J. Gastroenterol.* 13 (48), 6458–6464. doi:10.3748/wjg.v13.i48.6458

Assimakopoulos, S. F., Vagianos, C. E., Patsoukis, N., Georgiou, C., Nikolopoulou, V., and Scopa, C. D. (2004). Evidence for Intestinal Oxidative Stress in Obstructive Jaundice-Induced Gut Barrier Dysfunction

in Rats. *Acta Physiol. Scand.* 180 (2), 177–185. doi:10.1046/j.0001-6772.2003.01229.x

Cariello, M., Piccinin, E., Garcia-Irigoyen, O., Sabbà, C., and Moschetta, A. (2018). Nuclear Receptor FXR, Bile Acids and Liver Damage: Introducing the Progressive Familial Intrahepatic Cholestasis with FXR Mutations. *Biochim. Biophys. Acta Mol. Basis Dis.* 1864 (4 Pt B), 1308–1318. doi:10.1016/j.bbadis.2017.09.019

Dai, D., and Walker, W. A. (1999). Protective Nutrients and Bacterial Colonization in the Immature Human Gut. *Adv. Pediatr.* 46, 353–382.

Dawson, P. A. (2011). Role of the Intestinal Bile Acid Transporters in Bile Acid and Drug Disposition. *Handb. Exp. Pharmacol.* 201, 169–203. doi:10.1007/978-3-642-14541-4_4

Dou, X., Qiao, L., Chang, J., Yan, S., Song, X., Chen, Y., et al. (2021). Lactobacillus Casei ATCC 393 and It's Metabolites Alleviate Dextran Sulphate Sodium-Induced Ulcerative Colitis in Mice through the NLRP3-(Caspase-1)/IL-1β Pathway. *Food Funct.* 12 (23), 12022–12035. doi:10.1039/d1fo02405a

Fickert, P., and Wagner, M. (2017). Biliary Bile Acids in Hepatobiliary Injury - what Is the Link? *J. Hepatol.* 67 (3), 619–631. doi:10.1016/j.jhep.2017.04.026

Fiorucci, S., and Distrutti, E. (2015). Bile Acid-Activated Receptors, Intestinal Microbiota, and the Treatment of Metabolic Disorders. *Trends Mol. Med.* 21 (11), 702–714. doi:10.1016/j.molmed.2015.09.001

Gadaleta, R. M., Van Erpecum, K. J., Oldenburg, B., Willemsen, E. C., Renooij, W., Murzilli, S., et al. (2011). Farnesoid X Receptor Activation Inhibits Inflammation and Preserves the Intestinal Barrier in Inflammatory Bowel Disease. *Gut* 60 (4), 463–472. doi:10.1136/gut.2010.212159

Gonzalez, F. J., Jiang, C., Xie, C., and Patterson, A. D. (2017). Intestinal Farnesoid X Receptor Signaling Modulates Metabolic Disease. *Dig. Dis.* 35 (3), 178–184. doi:10.1159/000450908

Grundy, S. M. (2016). Metabolic Syndrome Update. *Trends Cardiovasc Med.* 26 (4), 364–373. doi:10.1016/j.tcm.2015.10.004

Hartmann, P., Hochrath, K., Horvath, A., Chen, P., Seebauer, C. T., Llorente, C., et al. (2018). Modulation of the Intestinal Bile Acid/farnesoid X Receptor/fibroblast Growth Factor 15 axis Improves Alcoholic Liver Disease in Mice. *Hepatology* 67 (6), 2150–2166. doi:10.1002/hep.29676

Iida, A., Yoshidome, H., Shida, T., Kimura, F., Shimizu, H., Ohtsuka, M., et al. (2009). Does Prolonged Biliary Obstructive Jaundice Sensitize the Liver to Endotoxemia? *Shock* 31 (4), 397–403. doi:10.1097/SHK.0b013e31818349ea

Jiang, C., Xie, C., Li, F., Zhang, L., Nichols, R. G., Krausz, K. W., et al. (2015a). Intestinal Farnesoid X Receptor Signaling Promotes Nonalcoholic Fatty Liver Disease. *J. Clin. Invest.* 125 (1), 386–402. doi:10.1172/JCI76738

Jiang, C., Xie, C., Lv, Y., Li, J., Krausz, K. W., Shi, J., et al. (2015b). Intestine-selective Farnesoid X Receptor Inhibition Improves Obesity-Related Metabolic Dysfunction. *Nat. Commun.* 6, 10166. doi:10.1038/ncomms10166

Jones, B. V., Begley, M., Hill, C., Gahan, C. G., and Marchesi, J. R. (2008). Functional and Comparative Metagenomic Analysis of Bile Salt Hydrolase Activity in the Human Gut Microbiome. *Proc. Natl. Acad. Sci. U. S. A.* 105 (36), 13580–13585. doi:10.1073/pnas.0804437105

Keitel, V., Dröge, C., and Häussinger, D. (2019). Targeting FXR in Cholestasis. *Handb. Exp. Pharmacol.* 256, 299–324. doi:10.1007/164_2019_231

Keitel, V., and Häussinger, D. (2011). TGR5 in the Biliary Tree. *Dig. Dis.* 29 (1), 45–47. doi:10.1159/000324127

Kong, B., Wang, L., Chiang, J. Y., Zhang, Y., Klaassen, C. D., and Guo, G. L. (2012). Mechanism of Tissue-specific Farnesoid X Receptor in Suppressing the Expression of Genes in Bile-Acid Synthesis in Mice. *Hepatology* 56 (3), 1034–1043. doi:10.1002/hep.25740

Kwong, E. K., and Puri, P. (2021). Gut Microbiome Changes in Nonalcoholic Fatty Liver Disease & Alcoholic Liver Disease. *Transl. Gastroenterol. Hepatol.* 6, 3. doi:10.21037/tgh.2020.02.18

Lee, S., Choi, J., Mohanty, J., Sousa, L. P., Tome, F., Pardon, E., et al. (2018). Structures of β-klotho Reveal a 'zip Code'-like Mechanism for Endocrine FGF Signalling. *Nature* 553 (7689), 501–505. doi:10.1038/nature25010

Lichtman, S. N., Sartor, R. B., Keku, J., and Schwab, J. H. (1990). Hepatic Inflammation in Rats with Experimental Small Intestinal Bacterial Overgrowth. *Gastroenterology* 98 (2), 414–423. doi:10.1016/0016-5085(90)90833-m

Liu, Y., Chen, K., Li, F., Gu, Z., Liu, Q., He, L., et al. (2020). Probiotic Lactobacillus Rhamnosus GG Prevents Liver Fibrosis through Inhibiting Hepatic Bile Acid Synthesis and Enhancing Bile Acid Excretion in Mice. *Hepatology* 71 (6), 2050–2066. doi:10.1002/hep.30975

Liu, Y., Zheng, S., Cui, J., Guo, T., Zhang, J., and Li, B. (2021). Alleviative Effects of Exopolysaccharide Produced by Lactobacillus Helveticus KLDS1.8701 on Dextran Sulfate Sodium-Induced Colitis in Mice. *Microorganisms* 9 (10), 2086. doi:10.3390/microorganisms9102086

Luo, Q., Shi, R., Liu, Y., Huang, L., Chen, W., and Wang, C. (2022). Histamine Causes Pyroptosis of Liver by Regulating Gut-Liver Axis in Mice. *Int. J. Mol. Sci.* 23 (7), 3710. doi:10.3390/ijms23073710

Machida, K., Cheng, K. T., Sung, V. M., Levine, A. M., Foung, S., and Lai, M. M. (2006). Hepatitis C Virus Induces Toll-like Receptor 4 Expression, Leading to Enhanced Production of Beta Interferon and Interleukin-6. *J. Virol.* 80 (2), 866–874. doi:10.1128/JVI.80.2.866-874.2006

Makishima, M., Okamoto, A. Y., Repa, J. J., Tu, H., Learned, R. M., Luk, A., et al. (1999). Identification of a Nuclear Receptor for Bile Acids. *Science* 284 (5418), 1362–1365. doi:10.1126/science.284.5418.1362

Modica, S., Petruzzelli, M., Bellafante, E., Murzilli, S., Salvatore, L., Celli, N., et al. (2012). Selective Activation of Nuclear Bile Acid Receptor FXR in the Intestine Protects Mice against Cholestasis. *Gastroenterology* 142 (2), 355–365. e1-4. doi:10.1053/j.gastro.2011.10.028

Niu, H., Zhou, X., Gong, P., Jiao, Y., Zhang, J., Wu, Y., et al. (2021). Effect of Lactobacillus Rhamnosus MN-431 Producing Indole Derivatives on Complementary Feeding-Induced Diarrhea Rat Pups through the Enhancement of the Intestinal Barrier Function[J]. *Mol. Nutr. Food Res.* 2021, e2100619. doi:10.1002/mnfr.202100619

Rietschel, E. T., Kirikae, T., Schade, F. U., Mamat, U., Schmidt, G., Loppnow, H., et al. (1994). Bacterial Endotoxin: Molecular Relationships of Structure to Activity and Function. *Faseb J.* 8 (2), 217–225. doi:10.1096/fasebj.8.2.8119492

Sayin, S. I., Wahlström, A., Felin, J., Jäntti, S., Marschall, H. U., Bamberg, K., et al. (2013). Gut Microbiota Regulates Bile Acid Metabolism by Reducing the Levels of Tauro-Beta-Muricholic Acid, a Naturally Occurring FXR Antagonist. *Cell Metab.* 17 (2), 225–235. doi:10.1016/j.cmet.2013.01.003

Schneider, K. M., Albers, S., and Trautwein, C. (2018). Role of Bile Acids in the Gut-Liver axis. *J. Hepatol.* 68 (5), 1083–1085. doi:10.1016/j.jhep.2017.11.025

Song, W., Sun, L. Y., Zhu, Z. J., Wei, L., Qu, W., Zeng, Z. G., et al. (2021). Association of Gut Microbiota and Metabolites with Disease Progression in Children with Biliary Atresia. *Front. Immunol.* 12, 698900. doi:10.3389/fimmu.2021.698900

Sorribas, M., Jakob, M. O., Yilmaz, B., Li, H., Stutz, D., Noser, Y., et al. (2019). FXR Modulates the Gut-Vascular Barrier by Regulating the Entry Sites for Bacterial Translocation in Experimental Cirrhosis. *J. Hepatol.* 71 (6), 1126–1140. doi:10.1016/j.jhep.2019.06.017

Stojancevic, M., Stankov, K., and Mikov, M. (2012). The Impact of Farnesoid X Receptor Activation on Intestinal Permeability in Inflammatory Bowel Disease. *Can. J. Gastroenterol.* 26 (9), 631–637. doi:10.1155/2012/538452

Tabibian, J. H., Talwalkar, J. A., and Lindor, K. D. (2013). Role of the Microbiota and Antibiotics in Primary Sclerosing Cholangitis. *Biomed. Res. Int.* 2013, 389537. doi:10.1155/2013/389537

Trabelsi, M. S., Lestavel, S., Staels, B., and Collet, X. (2017). Intestinal Bile Acid Receptors Are Key Regulators of Glucose Homeostasis. *Proc. Nutr. Soc.* 76 (3), 192–202. doi:10.1017/S0029665116002834

Trauner, M., and Fuchs, C. D. (2022). Novel Therapeutic Targets for Cholestatic and Fatty Liver Disease. *Gut* 71 (1), 194–209. doi:10.1136/gutjnl-2021-324305

Tsai, Y. L., Liu, C. W., Hsu, C. F., Huang, C. C., Lin, M. W., Huang, S. F., et al. (2020). Obeticholic Acid Ameliorates Hepatorenal Syndrome in Ascitic Cirrhotic Rats by Down-Regulating the Renal 8-Iso-Pgf2α-Activated COX-TXA2 Pathway. *Clin. Sci.* 134 (15), 2055–2073. doi:10.1042/CS20200452

Vavassori, P., Mencarelli, A., Renga, B., Distrutti, E., and Fiorucci, S. (2009). The Bile Acid Receptor FXR Is a Modulator of Intestinal Innate Immunity. *J. Immunol.* 183 (10), 6251–6261. doi:10.4049/jimmunol.0803978

Verbeke, L., Farre, R., Verbinnen, B., Covens, K., Vanuytsel, T., Verhaegen, J., et al. (2015). The FXR Agonist Obeticholic Acid Prevents Gut Barrier Dysfunction and Bacterial Translocation in Cholestatic Rats. *Am. J. Pathol.* 185 (2), 409–419. doi:10.1016/j.ajpath.2014.10.009

Wang, J., Qian, T., Jiang, J., Yang, Y., Shen, Z., Huang, Y., et al. (2020). Gut Microbial Profile in Biliary Atresia: a Case-Control Study. *J. Gastroenterol. Hepatol.* 35 (2), 334–342. doi:10.1111/jgh.14777

Wang, N., Yu, H., Ma, J., Wu, W., Zhao, D., Shi, X., et al. (2010). Evidence for Tight Junction Protein Disruption in Intestinal Mucosa of Malignant Obstructive Jaundice Patients. *Scand. J. Gastroenterol.* 45 (2), 191–199. doi:10.3109/00365520903406701

Wang, S., Feng, R., Wang, S. S., Liu, H., Shao, C., Li, Y., et al. (2022). *FOXA2 Prevents Hyperbilirubinaemia in Acute Liver Failure by Maintaining Apical MRP2 Expression Gut Published Online First*. doi:10.1136/gutjnl-2022-326987

Xiong, X., Ren, Y., Cui, Y., Li, R., Wang, C., and Zhang, Y. (2017). Obeticholic Acid Protects Mice against Lipopolysaccharide-Induced Liver Injury and Inflammation. *Biomed. Pharmacother.* 96, 1292–1298. doi:10.1016/j.biopha.2017.11.083

Yang, K. M., Zhu, C., Wang, L., Cao, S. T., Yang, X. F., Gao, K. G., et al. (2021). Early Supplementation with Lactobacillus Plantarum in Liquid Diet Modulates Intestinal Innate Immunity through Toll-like Receptor 4-mediated Mitogen-Activated Protein Kinase Signaling Pathways in Young Piglets Challenged with Escherichia coli K88. *J. Anim. Sci.* 99 (6), skab128. doi:10.1093/jas/skab128

Yasuda, H., Hirata, S., Inoue, K., Mashima, H., Ohnishi, H., and Yoshiba, M. (2007). Involvement of Membrane-type Bile Acid Receptor M-BAR/TGR5 in Bile Acid-Induced Activation of Epidermal Growth Factor Receptor and Mitogen-Activated Protein Kinases in Gastric Carcinoma Cells. *Biochem. Biophys. Res. Commun.* 354 (1), 154–159. doi:10.1016/j.bbrc.2006.12.168

Zhang, C., Gan, Y., Lv, J. W., Qin, M. Q., Hu, W. R., Liu, Z. B., et al. (2020). The Protective Effect of Obeticholic Acid on Lipopolysaccharide-Induced Disorder of Maternal Bile Acid Metabolism in Pregnant Mice. *Int. Immunopharmacol.* 83, 106442. doi:10.1016/j.intimp.2020.106442

Zhang, H., Qi, C., Zhao, Y., Lu, M., Li, X., Zhou, J., et al. (2021). Depletion of Gut Secretory Immunoglobulin A Coated Lactobacillus Reuteri Is Associated with Gestational Diabetes Mellitus-Related Intestinal Mucosal Barrier Damage. *Food Funct.* 12 (21), 10783–10794. doi:10.1039/d1fo02517a

Conflict of Interest: The authors declare that the research was conducted in the absence of any commercial or financial relationships that could be construed as a potential conflict of interest.

Publisher's Note: All claims expressed in this article are solely those of the authors and do not necessarily represent those of their affiliated organizations, or those of the publisher, the editors and the reviewers. Any product that may be evaluated in this article, or claim that may be made by its manufacturer, is not guaranteed or endorsed by the publisher.

frontiers | Frontiers in Pharmacology

ORIGINAL RESEARCH
published: 14 July 2022
doi: 10.3389/fphar.2022.904420

Nintedanib Alleviates Experimental Colitis by Inhibiting CEBPB/PCK1 and CEBPB/EFNA1 Pathways

Hailong Li[1†], Jinhe Li[1,2†], Ting Xiao[1†], Yayue Hu[1,2], Ying Yang[1], Xiaoting Gu[1], Ge Jin[3], Hailong Cao[3], Honggang Zhou[1,2]* and Cheng Yang[1,2]**

[1]The State Key Laboratory of Medicinal Chemical Biology, College of Pharmacy and Key Laboratory of Molecular Drug Research, Nankai University, Tianjin, China, [2]High-throughput Molecular Drug Screening Centre, Tianjin International Joint Academy of Biomedicine, Tianjin, China, [3]Department of Gastroenterology and Hepatology, General Hospital, Tianjin Medical University, Tianjin Institute of Digestive Diseases, Tianjin Key Laboratory of Digestive Diseases, Tianjin, China

OPEN ACCESS

Edited by:
Laura Grasa,
the University of Zaragoza, Spain

Reviewed by:
Enilton A Camargo,
Federal University of Sergipe, Brazil
Yongjun Xia,
the University of Shanghai for Science and Technology, China

***Correspondence:**
Hailong Cao
caohailong@tmu.edu.cn
Honggang Zhou
honggang.zhou@nankai.edu.cn
Cheng Yang
yangcheng@nankai.edu.cn

[†]These authors have contributed equally to this work

Specialty section:
This article was submitted to Gastrointestinal and Hepatic Pharmacology, a section of the journal Frontiers in Pharmacology

Received: 25 March 2022
Accepted: 13 June 2022
Published: 14 July 2022

Citation:
Li H, Li J, Xiao T, Hu Y, Yang Y, Gu X, Jin G, Cao H, Zhou H and Yang C (2022) Nintedanib Alleviates Experimental Colitis by Inhibiting CEBPB/PCK1 and CEBPB/EFNA1 Pathways. Front. Pharmacol. 13:904420. doi: 10.3389/fphar.2022.904420

The super-enhancer, a cluster of enhancers with strong transcriptional activity, has become one of the most interesting topics in recent years. This study aimed to investigate pathogenic super-enhancer–driven genes in IBD and screen therapeutic drugs based on the results. In this study, through the analysis of differentially expressed genes in colitis patients from the GEO database and the analysis of the super-enhancer–associated database, we found that the super-enhancer pathogenic genes PCK1 and EFNA1 were simultaneously regulated by transcription factor CEBPB through two super-enhancers (sc-CHR20-57528535 and sc-CHR1-155093980). Silencing CEBPB could significantly inhibit the expression of PCK1 and EFNA1 and enhance the expression of epithelial barrier proteins claudin-1, occludin, and ZO-1. In LPS-induced Caco-2 cells, drugs commonly used in clinical colitis including tofacitinib, oxalazine, mesalazine, and sulfasalazine inhibited mRNA levels of CEBPB, PCK1, and EFNA1. In the drug screening, we found that nintedanib significantly inhibited the mRNA and protein levels of CEBPB, PCK1, and EFNA1. *In vivo* experiments, nintedanib significantly alleviated DSS-induced colitis in mice by inhibiting CEBPB/PCK1 and CEBPB/EFNA1 signaling pathways. At the genus level, nintedanib improved the composition of the gut microbiota in mice with DSS-induced experimental colitis. In conclusion, we found that PCK1 and EFNA1 are highly expressed in colitis and they are regulated by CEBPB through two super-enhancers, and we further demonstrate their role *in vivo* and *in vitro*. Nintedanib may be a potential treatment for IBD. Super-enhancers may be a new way to explore the pathogenesis of colitis.

Keywords: super-enhancer, inflammatory bowel disease, nintedanib, CEBPB/PCK1, CEBPB/EFNA1

INTRODUCTION

Inflammatory bowel disease (IBD), a chronic nonspecific inflammatory bowel disease common in North America and Europe, includes ulcerative colitis and Crohn's disease (Kaplan, 2015; Ng, 2015). In recent decades, IBD incidence has rapidly increased in newly industrialized regions such as Asia and has evolved into a global disease (Ng et al., 2013; Park et al., 2014). These conditions and high incidence rates have heavily burdened patients and the healthcare system (Kappelman et al., 2008; Kappelman et al., 2013). The cause of IBD is not clear. Environmental, infectious, immune, and

genetic factors are closely related to the pathogenesis of IBD (Ramos and Papadakis, 2019). The traditional therapeutic drugs for IBD are mainly salicylic acid, steroid hormones, and immunosuppressant drugs, which have a limited remission rate and can cause serious side effects, including potential liver and kidney damage (Zoubek et al., 2019). Therefore, it is necessary to explore a more effective molecular mechanism and find suitable alternative drugs to treat IBD.

Enhancers, DNA sequences on the genome, precisely regulate the spatiotemporal expression of target genes through cis-interactions during cell development and differentiation (Witte et al., 2015; Li et al., 2021a). It is an important cis-regulatory element in the cell identity and the development process of multicellular organisms (Agrawal and Rao, 2021). Super-enhancers (SEs), a class of transcription enhancers newly discovered in recent years, usually contain the same components associated with enhancer activity, including transcription factors and cofactors (Hnisz et al., 2013; Whyte et al., 2013; Xi Wang et al., 2019). Compared with enhancers, super-enhancers can bind transcription factors at a higher density (Hnisz et al., 2013; Higashijima and Kanki, 2021). Therefore, super-enhancers can regulate higher levels of gene transcription.

It was found that super-enhancers not only determine the cell fate in the process of stem cell differentiation and development, but also play a key role in the occurrence and development of tumors, autoimmune diseases, and other diseases (Hnisz et al., 2013; Loven et al., 2013; Brown et al., 2014). For example, there are active super-enhancers near the oncogene c-MYC in pancreatic cancer and colorectal cancer, while no corresponding super-enhancers are found in the corresponding normal tissues (Hnisz et al., 2013). In common complex diseases such as systemic lupus erythematosus, rheumatoid arthritis, multiple sclerosis, and other immune-related diseases, it was found that the expression of pathogenic genes is highly correlated with the abnormal activation of some super-enhancers (Costa-Reis and Sullivan, 2013). Among the 72 single-nucleotide polymorphisms (SNPs) in systemic lupus erythematosus, 22 SNPs occurred in the super-enhancer region (Deng and Tsao, 2010).

Because super-enhancers play a key role in determining cell identity and development, we believe that super-enhancers are involved in the occurrence and development of IBD diseases. However, the role of pathogenic super-enhancers in the pathological process of IBD has not been reported. The purpose of this study is to predict the potential pathogenic super-enhancers of IBD. The study of the role of super-enhancers in the development of IBD will help us to further explore the pathogenesis of this refractory disease and find new therapeutic targets and candidate drugs.

MATERIALS AND METHOD

Identification of Differentially Expressed Genes

The GEO database is a database for storing chips, second-generation sequencing, and other high-throughput sequencing data. The GEO database was searched to find the datasets (GSE107499, GSE75214, and GSE59071) containing differential genes in colon tissues of normal people and IBD patients. The differentially expressed genes were analyzed and found by the GEO2R tool.

Prediction of Pathogenic Genes Driven by Super-enhancers

SEA version 3.0 is an online database that can provide information about super-enhancers. By collecting and analyzing the public Chip-Seq data, the SEA website contains information on the super-enhancers and their related genes found in different cells and tissues. In SEA, we identified the super-enhancers in the human sigmoid colon using H3k27ac Chip-sequencing and collected the information on the super-enhancer, including super-enhancer ID, genomic site, length, related genes, and transcription factors. Then, the super-enhancer–related genes and differentially expressed genes were cross-linked to obtain the differentially expressed genes driven by the super-enhancers. The interaction network between transcription factors, super-enhancers, and related genes was constructed using Cytoscape software.

KEGG Pathway Analysis

The overlapping genes were analyzed by the KEGG pathway. The KEGG pathway data were uploaded to the Hiplot website to form a bubble chart.

LPS-Infected Caco-2 Cells

The Caco-2 cell line was purchased from Wuhan Procell Life Technology Co., Ltd (Wuhan, China) and cultured in DMEM high-glucose medium (Solarbio, China) supplemented with 20% fetal bovine serum (FBS, Yeasen, China). All of the media contained 50 U/mL penicillin and 50 U/mL streptomycin. All cells were incubated with 5% CO_2 at 37°C. After pre-protecting the cells for 2 h by adding the drug or an equal volume of vehicle, cells were treated with 1 μg/ml LPS to stimulate Caco-2 cells for 24 h, and the protein and mRNA expression levels were detected.

RNA Extraction and Quantitative Real-Time Polymerase Chain Reaction (qRT-PCR)

Total RNA was extracted from Caco-2 cells and colon tissues by TRIzol reagent (Tiangen, Beijing, China) and quantified by using a NanoDrop 8000 spectrophotometer (Thermo Fisher Scientific Inc., Waltham, MA, United States). RNA was reverse transcribed into cDNA with the first-strand cDNA synthesis Supermix kit (Yeasen, Shanghai, China), and the PCR system was prepared with the Yeasen qRT-PCR kit to amplify cDNA and performed with CFX96 touch (BIORAD, United States) according to the protocol of the manufacturer. The reaction conditions were as follows: predenaturation at 95°C for 30 s, denatured at 95°C for 10 s, annealed at 60°C for 20 s, extended at 70°C for 20 s, and repeated 40 cycles. GAPDH was used as the standard control. The forward and reverse primer sequences of CEBPB, PCK1, EFNA1, and GAPDH are as follows. The cycle threshold was

automatically generated, and the relative expressions of CEBPB, PCK1, and EFNA1 mRNA were calculated by the $2^{-\triangle\triangle Ct}$ method.

For humans:

CEBPB forward primer: ACGGGCCGCCCTTATAAAT; CEBPB reverse primer: CAGGCCACCAGGCGTTG; PCK1 forward primer: CGGAAAGAAACCTGTGGATCTC; PCK1 reverse primer: CAGATGTGGATGTGATCAGGCT; EFNA1 forward primer: GCTATGGAGTTCCTCTGGGC; EFNA1 reverse primer: ACGTAGTCATTCAGCTGCACA; GAPDH forward primer: GACAGTCAGCCGCATCTTCT; GAPDH reverse primer: GCGCCCAATACGACCAAATC;

For mice:

CEBPB forward primer: TTATAAACCTCCCGCTCGGC; CEBPB reverse primer: TTCCATGGGTCTAAAGGCGG; PCK1 forward primer: ACACACGCAAACTACCAAGC; PCK1 reverse primer: GTCCTCGTAATGTGGGCAGA; EFNA1 forward primer: GGAAGAACAAGGAGTGGAGAC; EFNA1 reverse primer: CAGGCAGGGTCAATAATGGG; GAPDH forward primer: GGAGAGTGTTTCCTCGTCCC; GAPDH reverse primer: CCGTTGAATTTGCCGTGAGT;

Western Blot

After grouping Caco-2 cells and colon tissues, the RIPA lysate was used to extract the protein in the cells and tissues, and the protein content was measured using the BCA kit (Beyotime, Beijing), and 30 μg protein was taken for detection. The protein samples were added into polyacrylamide gel (8–15%) and then electrophoretic gel, then transferred to the PVDF membrane (Millipore, MA, United States), sealed for 2 h with 5% skim milk powder, and incubated overnight with 1–1,000 diluted antibody at 4°C. Subsequently, PVDF membranes were incubated with rabbit antibodies diluted 1:1 000 for 2 h, and protein bands were obtained after development using a biospectral gel imaging system (UVP, CA, United States). Finally, Image J software was used for gray analysis.

Animal Experiment

Male C57BL/6J mice (SPF grade) aged 6–8 weeks, weighing 18–22 g, came from the animal experiment center of the Jinnan campus of Nankai University. Fifty SPF mice were randomly divided into normal group, dextran sodium sulfate (DSS) group, sulfasalazine (SASP) group, nintedanib low-dose group (Nin, 50 mg/kg), and nintedanib high-dose group (100 mg/kg), with 10 mice in each group. After adaptive feeding for 1 week, the mice in the normal group were free to eat and drink water, and for the mice in other groups, the daily drinking water volume of each mouse was calculated to be 6 ml, and the DSS solution was added to the daily drinking water volume for 8 consecutive days to establish the model of IBD in mice. While drinking 5% DSS solution daily, SASP (200 $mg{\cdot}kg^{-1}{\cdot}Day^{-1}$) and nintedanib (50 and 100 $mg{\cdot}kg^{-1}{\cdot}Day^{-1}$) were administered by gavage at 1–7 days, respectively. 0.5% CMC-Na was administered by gavage in the normal group and the DSS group for 7 days. The body weight, stool consistency (degree of diarrhea), and blood in stool were recorded every day. On the 8th day, after fasting for 12 h, 10% chloral hydrate was injected intraperitoneally. The colon and rectum of mice were washed with the PBS solution. 1 cm tissue from the anus was selected and placed in 10% formalin. The remaining intestinal tissue was put into a cryopreservation tube and stored at −80°C. The intestinal tissue was fixed in formalin for 24 h, dehydrated, embedded, sliced, stained with hematoxylin-eosin and Alcian blue (PH = 2.5, Beyotime, Beijing), and observed under the microscope.

The Disease Activity Index Score

The characteristics of feces were observed, and the situation of fecal occult blood was determined and scored accordingly. DAI scoring criteria are as follows (Peng et al., 2019):

1) Body mass score: no change or increase, 0 point; reduce 1%–5%, 1 point; reduce 5%–10%, 2 points; reduce 10%–15%, 3 points; the reduction is greater than 15%, 4 points.
2) Fecal character score: normal, 0; soft stool and spherical stool, 1 point; paste or hemispherical stool and no anal attachment, 2 points; paste stool and anal adhesion, 3 points; loose stool, 4 points.
3) Fecal occult blood score: negative, 0; weak positive, 1 point; positive, 2 points; strong positive, 3 points; gross bloody stool, 4 points. DAI score = (body mass score + fecal character score + fecal occult blood score)/3.

Pathological Staining

The sections were stained with hematoxylin-eosin and observed under the microscope. The histopathological evaluation criteria are as follows (Stillie and Stadnyk, 2009):

1) Degree of inflammation: none, mild, moderate, and severe;
2) Depth of lesion involvement: no lesion, mucosa, submucosa and transmural;
3) Recess destruction: no destruction, basal 1/3 destruction, basal 2/3 destruction, basal destruction, and only epithelial integrity;
4) The range of lesions involved: 1–25%, 26–50%, 51–75%, and 76–100%.

Clinical Samples

A total of 3 ulcerative colitis tissues and 3 colonic ulcer distal control tissues were collected from healthy volunteers (1 male and 2 females, aged 49–63 years) and UC patients (2 males and 1 female, aged 37–58 years) during endoscopy at the Department of Digestive Diseases, Tianjin Medical University General Hospital (Tianjin, China). Patients with ulcerative colitis were untreated preoperatively. Samples were independently identified by two pathologists. These tissues were obtained from patients who underwent colonoscopy at Tianjin Medical University General Hospital after signing informed consent. The entire study was approved by the ethics committee of Tianjin Medical University General Hospital.

Immunohistochemistry

The tissue sections were dewaxed, hydrated, and antigen repaired. After incubation with endogenous peroxidase blocker and immune serum (rabbit) with the immunohistochemical kit (Maixin, Fuzhou, China), the CEBPB Rabbit antibody (1: 50 dilution; Affinity) was incubated overnight at 4°C. The next

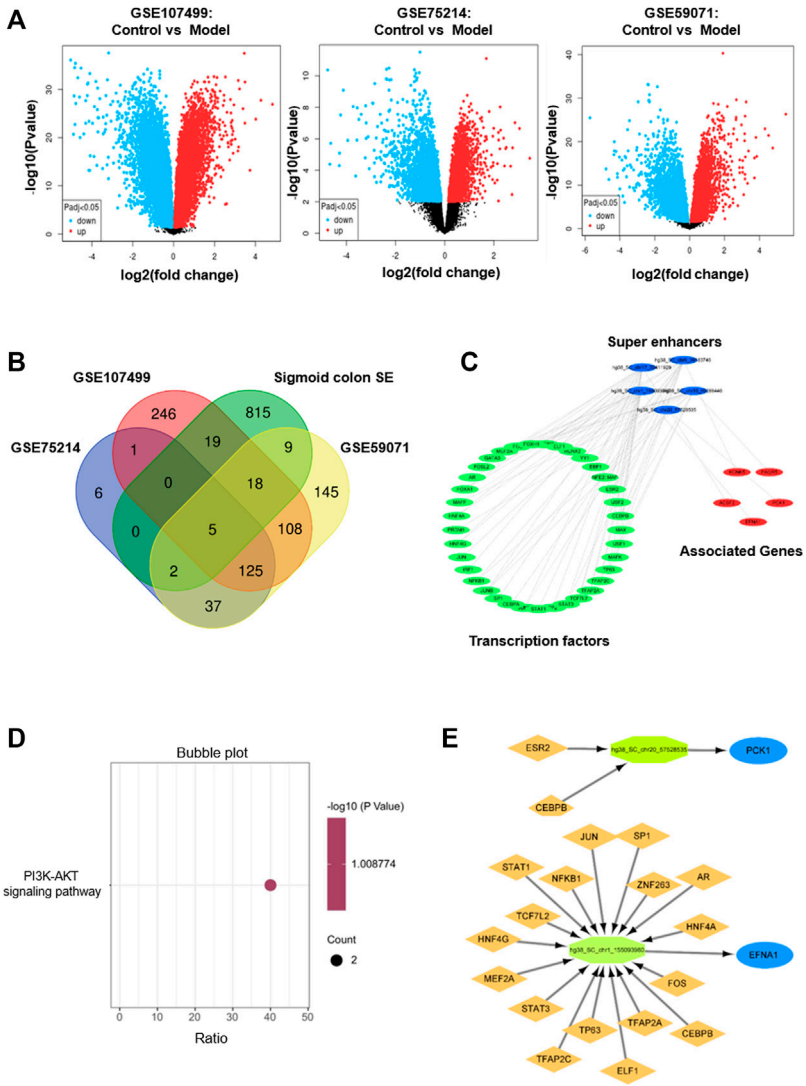

FIGURE 1 | Identification of potential pathogenic super-enhancer–driver genes in IBD. **(A)** Volcano diagram of differentially expressed genes between IBD patients and normal people in datasets GSE107499, GSE75214, and GSE59071 in the GEO database. **(B)** Venn diagram formed by cross-linking of super-enhancer–associated genes and differentially expressed genes in dataset in inflammatory bowel disease. **(C)** Interaction network of TF, super-enhancer, and related genes in inflammatory bowel disease. **(D)** The KEGG pathway analysis. **(E)** TFs binding PCK1 and EFNA1 super-enhancers.

day, nonspecific secondary antibody and streptavidin peroxidase were used for incubation, DAB (Maixin, Fuzhou, China) color development, hematoxylin staining, and the slices were sealed after dehydration. Finally Image J software was used for IHC scoring.

Transfection siRNA

Caco-2 cells were inoculated into 96-well plates and cultured in a 5% CO_2 incubator at 37°C for 24 h. When the cell density reached 50–70%, si-CEBPB (Gene Pharma, shanghai) and the negative control group (NC) were transfected into the cell line according to the instructions of the lipo 8000 reagents (Beyotime, Beijing). 48 h after transfection, the cells were collected for the Western blot analysis. CEBPB siRNA sequences were sense 5′-CGCCUGCUUUAAAUCCOUTT-3′ and antisense 5′- AUG GAUUUUAAAGGCAGCGTT-3’. The CEBPB negative control sequences were sense 5′-UUCUCCGAACGUGUCACGGUTT-3′ and antisense 5′-ACGUGACACGUUCGGAGAATT-3’.

Microbial Community Analysis

The feces of mice in the normal group, the DSS group, and the nintedanib (100 mg/kg) group were collected and stored at −80°C. For 16S rDNA gene sequencing, fecal samples were sent to the gene and genome analysis center (Microread gene, Beijing, China) for sequencing under dry ice conditions. Primers corresponding to the bacterial 16S rRNA hypervariable region (V3–V4) were selected for amplification. The sequencing results of all samples and the statistical results of

TABLE 1 | DEGs in colon tissue or mucosa of IBD from GEO datasets.

No.	Datasets	Control group	Model group	Sample number	Upregulated DEGs	Downregulated DEGs
				C/M	M vs. C	M vs. C
1	GSE107499	Human colon tissue biospy_Non-lesional	Human colon tissue biospy_lesional	44/75	825	1684
2	GSE75214	Biopsy from normal colonic mucosa of control individual	Biopsy from inflamed colonic mucosa of active CD patient	11/8	180	572
3	GSE59071	Biopsy from normal colonic mucosa of control individual	Biopsy from inflamed colonic mucosa of active UC patient	11/74	461	841

C, control group; M, model group.

TABLE 2 | Information of potential pathogenic super-enhancers in IBD.

SEID	Loci	Length	Associated gene	Tissue type
1527529	chr17:5041192950459994	48,065	ACSF2	Sigmoid_Colon
1526949	chr1:155093980155132239	38,259	EFNA1	Sigmoid_Colon
1527572	chr20:5752853557546613	18,078	PCK1	Sigmoid_Colon
1526704	chr15:6928844669329461	41,015	PAQR5	Sigmoid_Colon
1526811	chr6:39183746–39223978	40,232	KCNK5	Sigmoid_Colon

SEID: ID of super-enhancer in SEA.

sequence data are based on sequencing reads and operational taxonomic units (OTUs).

Statistical Analysis

All the data were analyzed using GraphPad Prism 8.4.2 (GraphPad Software, Inc., San Diego, CA) and expressed as mean ± SD. Two and multiple groups were compared using the independent sample t-test and ANOVA, respectively. $p < 0.05$ was considered statistically significant.

RESULTS

Identification of CEBPB/PCK1 and CEBPB/EFNA1 Pathways Driven by Potentially Pathogenic Super-Enhancers in Inflammatory Bowel Disease

We first analyzed the GEO database (GSE107499\GSE75214\GSE59071), and the DEGs volcano is shown in **Figure 1A**. Super-enhancers usually positively regulate gene expression, so we analyzed the upregulated DEGs in the database. A total of 1,366 upregulated DEGs in IBD patients were found using three different GEO datasets (**Table 1**). 863 super-enhancer–related genes were identified in the human sigmoid colon by the SEA website. We cross-linked these super-enhancer–related genes with upregulated DEGs to predict potential super-enhancer–driven pathogenic genes in IBD. The Venn diagram shows that there are 5 gene overlaps (**Figure 1B**), which are considered potential super-enhancer–driven IBD pathogenic genes. The information on potential pathogenic SEs of IBD is shown in **Table 2**. Cytoscape software was used to construct the interaction network of transcription factors, super-enhancers, and related genes (**Figure 1C**). Subsequently, we performed KEGG network analysis of these five potential super-enhancer–driven pathogenic genes and found that PCK1 and EFNA1 genes were enriched in the PI3K–Akt pathway (**Table 3**, **Figure 1D**). Subsequently, we constructed the interaction networks of these two genes with super-enhancers and TFs. Surprisingly, we found that the transcription factor CEBPB existed in the relationship between the two interaction networks at the same time (**Figure 1E**). Therefore, we believe that CEBPB/PCK1 and CEBPB/EFNA1 may be the key pathways for the potential treatment of IBD.

Silencing Transcription Factor CEBPB Significantly Inhibits the Expression of PCK1 and EFNA1 and Increases the Expression of Intestinal Epithelial Barrier Protein

To verify whether CEBPB regulates PCK1 and EFNA1 to improve colitis, we designed the interfering RNA of CEBPB. As shown in **Figure 2A**, after silencing the transcription factor CEBPB, the protein expression levels of PCK1 and EFNA1 decreased significantly. This indicates that PCK1 and EFNA1 are regulated by the transcription factor CEBPB. At the same time, silencing the transcription factor CEBPB also found that the intestinal barrier proteins ZO-1, occludin, and claudin-1 increased (**Figure 2B**), indicating that inhibiting

TABLE 3 | The result of the KEGG pathway enrichment analysis.

Term	Genes	Count	Gene ratio	*p*-value (E)
PI3K–Akt signaling pathway	EFNA1\PCK1	2	40	9.8–2

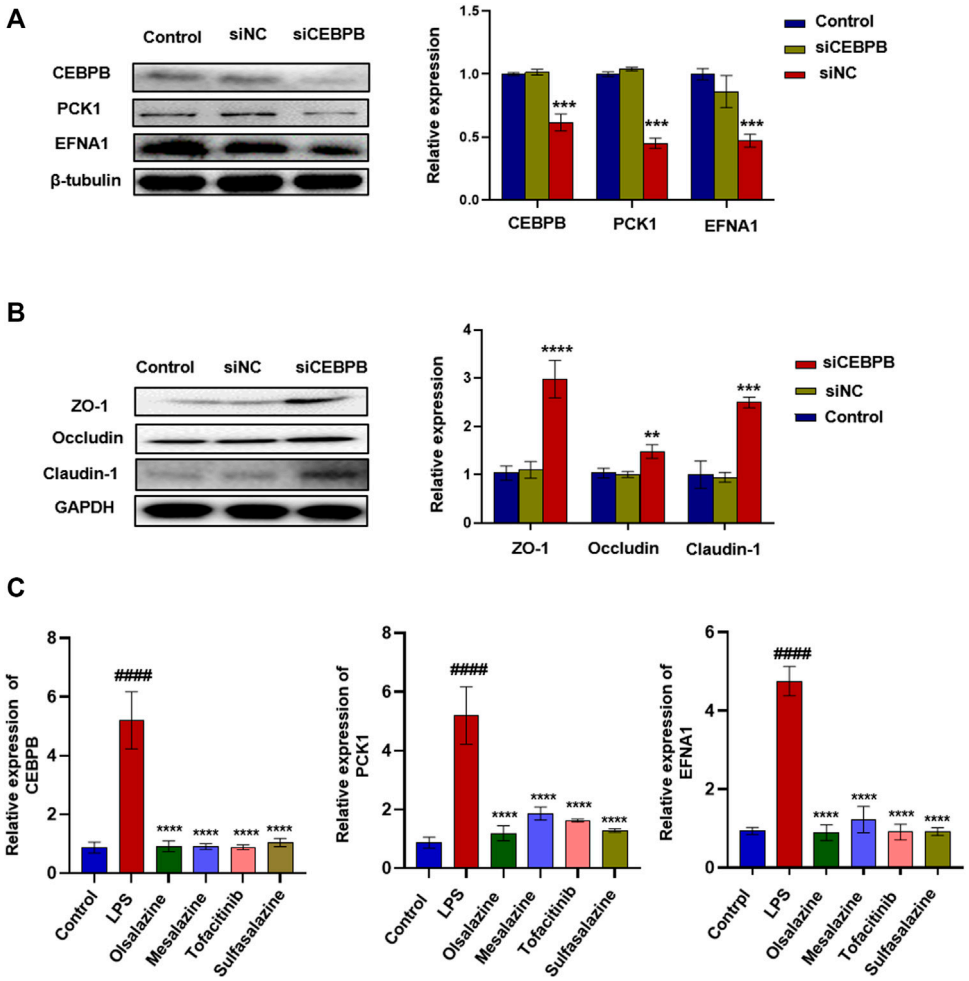

FIGURE 2 | Silencing transcription factor CEBPB significantly inhibited the expression of PCK1\EFNA1 and increased the expression of intestinal epithelial barrier protein. The protein expression of super-enhancer–associated gene PCK1\EFNA1 **(A)** and intestinal barrier proteins ZO-1, occludin, and claudin-1 **(B)** after transfection of siCEBPB. Data are presented as the mean ± SD ($n = 3$). $^{*}p < 0.01$ and $^{**}p < 0.05$ significantly different from the control group. **(C)** Inhibitory effect of IBD marketed drugs (olsalazine, mesalazine, tofacitinib, and sulfasalazine) on CEBPB, PCK1, and CEBPB mRNA. Data are presented as the mean ± SD ($n = 3$). $^{\#\#\#\#}p < 0.001$ significantly different from the control group; $^{*}p < 0.1$, $^{***}p < 0.001$ and $^{****}p < 0.0001$, significantly different from LPS groups.

CEBPB can restore the damaged intestinal barrier proteins. The aforementioned results indicate that PCK1 and EFNA1 pathways regulated by CEBPB may participate in the pathogenesis of IBD through epithelial barrier proteins. Subsequently, we detected the mRNA levels of CEBPB, PCK1, and EFNA1 in LPS-stimulated Caco-2 cells after being treated with the marketed drugs commonly used for the treatment of IBD (sulfasalazine, mesalazine, olsalazine, and tofacitinib). The results showed that LPS significantly promoted the expression of CEBPB, PCK1, and EFNA1 mRNA in Caco-2 cells, while sulfasalazine, mesalazine, olsalazine, and tofacitinib significantly inhibited the expression of CEBPB, PCK1, and EFNA1 mRNA stimulated by LPS (**Figure 2C**).

Nintedanib Significantly Inhibits the CEBPB/PCK1 and CEBPB/EFNA1 Pathways

The aforementioned four marketed drugs have different degrees of side effects, so it is necessary to develop new safe and effective drugs. Some small-molecule drugs of tyrosine kinase inhibitors

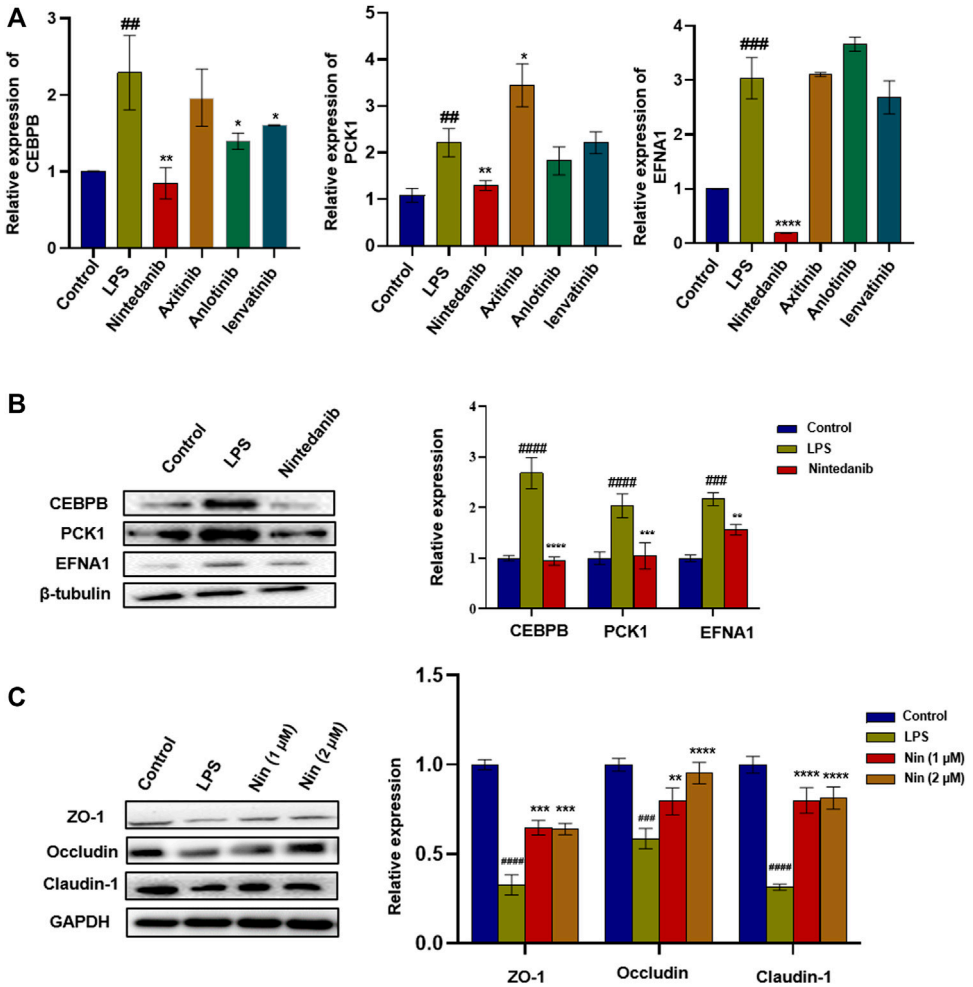

FIGURE 3 | Screening of tyrosine kinase inhibitors and the effect of nintedanib on barrier protein in Caco-2 cells. **(A)** Screening of tyrosine kinase inhibitors in LPS-induced Caco-2 cells. **(B)** Nintedanib significantly inhibited the protein expression levels of CEBPB, PCK1, and EFNA1. **(C)** Nintedanib improves the injury of intestinal epithelial barrier protein *in vitro*. Data are presented as the mean ± SD ($n = 3$). $^{\#}p < 0.05$, $^{\#\#}p < 0.01$, $^{\#\#\#}p < 0.001$ and $^{\#\#\#\#}p < 0.0001$ significantly different from the control group; $^{*}p < 0.05$, $^{**}p < 0.01$, $^{***}p < 0.001$, and $^{****}p < 0.0001$, significantly different from LPS groups.

(such as nintedanib and anlotinib) have been proved to have certain anti-inflammatory effects (Wollin et al., 2014). We wanted to determine the efficacy of tyrosine kinase inhibitors such as anlotinib, lenvatinib, axitinib, and nintedanib in treating IBD. As shown in **Figure 3A**, compared with the normal group, the mRNA levels of CEBPB, PCK1, and EFNA1 in the LPS group increased significantly. Similar to tofacitinib, sulfasalazine, oxalazine, and mesalazine, mRNA levels of CEBPB, PCK1, and EFNA1 in the nintedanib group were significantly reduced after administration, while the mRNA levels in anlotinib, lenvatinib, and axitinib groups did not change significantly after administration. After treating LPS-induced Caco-2 cells with nintedanib, it was found that the nintedanib group could significantly reduce the protein expression levels of CEBPB, PCK1, and EFNA1. At the same time, nintedanib can repair the damage to intestinal barrier protein caused by LPS (**Figure 3B,C**). These results suggest that nintedanib may alleviate IBD by inhibiting CEBPB/PCK1 and CEBPB/EFNA1 pathways.

Nintedanib Improves DSS-Induced Experimental Colitis in Mice

To further verify the therapeutic effect of nintedanib on colitis, we used 5% DSS to induce colitis in mice. As shown in **Figure 4A**, the murine experimental colitis animal model was established. Compared with the control group, DSS-treated mice significantly reduced body weight, increased DAI, and shortened colon weight length (**Figure 4B,C,D**). Significant tissue damage was found in the histological examination of the colon of DSS-treated mice, with a high microdamage score (**Figure 4E**). The positive control SASP (100 mg/kg) and nintedanib (50, 100 mg/kg) could significantly recover the experimental colitis-related

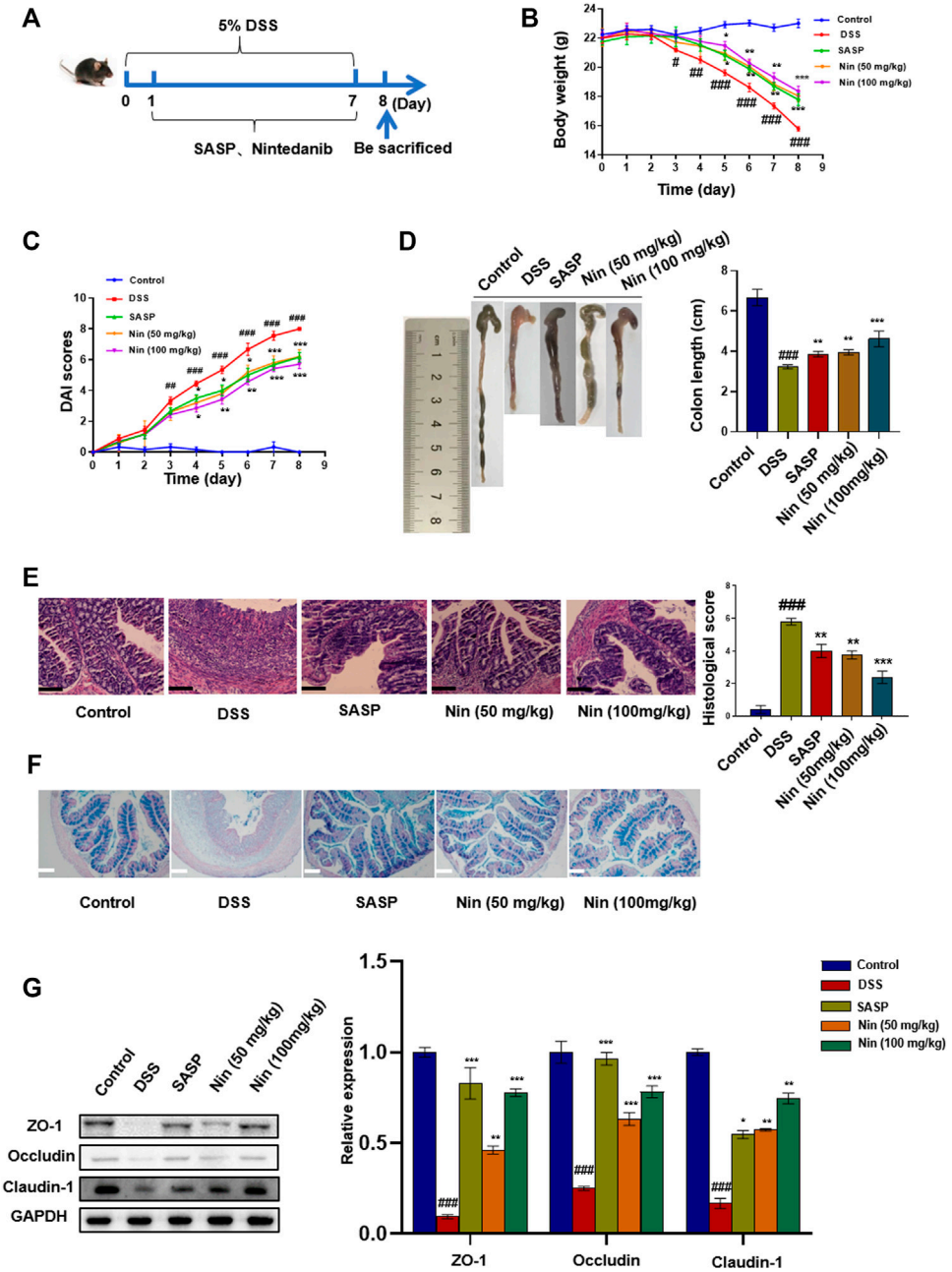

FIGURE 4 | Effect of nintedanib on DSS-induced experimental colitis in mice. **(A)** 5% DSS-induced experimental colitis in mice. Effects of nintedanib on weight change **(B)**, the DAI score **(C)**, and colon length change **(D)** in experimental colitis mice. **(E)** Histological sections of colonic tissue stained with hematoxylin and eosin are shown using a microscope. Scale bars represent 50 μm. **(F)** Representative images of Alcian blue-stained inner mucus layer of colonic sections. Scale bars represent 50 μm. **(G)** The effect of nintedanib on the expression of intestinal epithelial barrier proteins ZO-1, occludin, and claudin-1. Data are presented as the mean ± SD (n = 5). $^{\#\#}p < 0.01$, $^{\#\#\#}p < 0.001$, significantly different from the control group; $^{*}p < 0.05$, $^{**}p < 0.01$, $^{***}p < 0.001$, significantly different from DSS groups.

symptoms of mice caused by DSS, such as weight loss, increased DAI, shortened colon length, and colonic tissue injury.

Alcian blue staining was used to observe the expression of intestinal mucins. Intestinal mucin is stained blue by Alcian blue, and nuclei are stained red by nuclear fast red fuel. As shown in **Figure 4F**, DSS caused damage to the intestinal mucosa, with a significant decrease in the mucin expression. The intestinal mucosal injury caused by DSS was alleviated by intragastric administration [SASP, nintedanib (50, 100 mg/kg)].

We conducted the Western blot test on colonic tissue and found that the intestinal barrier protein in the DSS group was seriously damaged. The positive drug group and low- and high-dose groups (50 and 100 mg/kg) of nintedanib could significantly

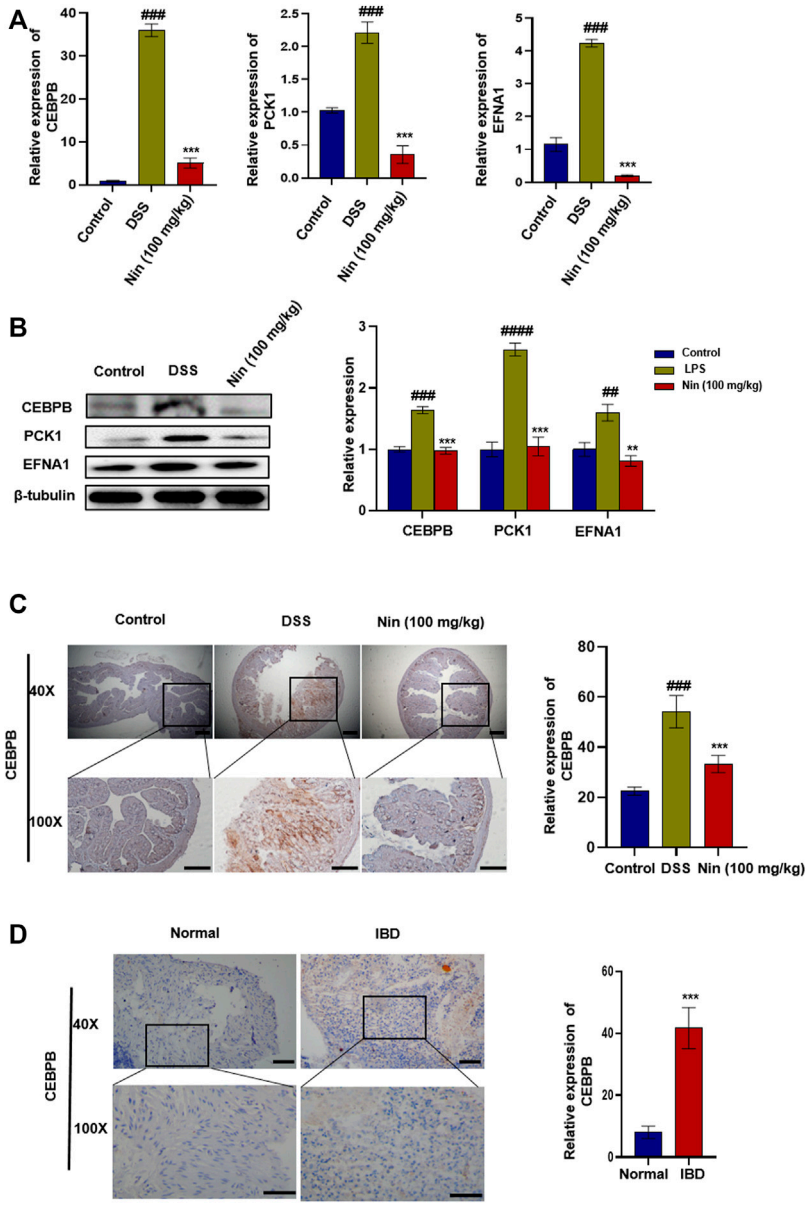

FIGURE 5 | Inhibition of CEBPB/PCK1 and CEBPB/EFNA1 pathways by nintedanib *in vivo*. **(A)** Effect of nintedanib on the level of CEBPB, PCK1, and EFNA1 mRNA in the colon tissue. **(B)** Effect of nintedanib on the expression of CEBPB, PCK1, and EFNA1 proteins in the colon tissue. The IHC staining analysis of CEBPB in mouse **(C)** and human **(D)** colon tissues. Scale bars represent 50 μm. Data are presented as the mean ± SD ($n = 5$). $^{\#}p < 0.05$, $^{\#\#}p < 0.01$, $^{\#\#\#}p < 0.001$ and $^{\#\#\#\#}p < 0.0001$, significantly different from the control group; $^{*}p < 0.05$, $^{**}p < 0.01$, $^{***}p < 0.001$ and $^{****}p < 0.0001$, significantly different from DSS groups.

recover the damaged intestinal barrier protein, and the high-dose group of nintedanib had a better effect (**Figure 4G**).

Nintedanib Improves DSS-Induced Experimental Colitis in Mice by Inhibiting CEBPB/PCK1 and CEBPB/EFNA1 Pathways

As shown in **Figure 5A,B**, the mRNA and protein expression of CEBPB, PCK1, and EFNA1 in the DSS group increased significantly, and the mRNA and protein expression of CEBPB, PCK1, and EFNA1 decreased significantly after nintedanib administration. IHC results showed that CEBPB increased significantly after DSS treatment, while CEBPB immunostaining decreased significantly after nintedanib treatment (**Figure 5C**). These results suggested that nintedanib may inhibit DSS-induced experimental colitis in mice by inhibiting CEBPB/PCK1 and CEBPB/EFNA1 pathways. IHC of tissue sections from healthy individuals and IBD patients similarly demonstrated a significant increase in CEBPB in tissue sections from IBD patients (**Figure 5D**). The patient information is shown in **Table 4**.

TABLE 4 | Basic information of patients.

Pathology number	Gender	Age
1414251	Female	58
1314397	Male	37
1730153	Female	63
1704203	Female	49
1310072	Male	35
1702166	Male	54

Effects of Nintedanib on Gut Microbiota of Experimental Colitis Mice

Since the gut microbiota is an important factor contributing to IBD, we utilized bacterial 16S rRNA sequencing to investigate the modulation of gut microbiota composition by nintedanib in mice. As shown in **Figure 6A**, we first used the Venn diagram to visualize the results of OTU cluster analysis between different groups. In total, 2931 OTUs were obtained from the feces of control, DSS-, and nintedanib-treated mice, 802 of which were shared by all three groups. The number of unique OTUs in the control, DSS, and nintedanib groups was 651, 302, and 182, respectively. Next, as shown in **Figure 6B**, we used linear discriminant analysis effect size (lefse) to identify differentially expressed OTUs between the feces of different groups of mice. Principal coordinate analysis (PCOA) was used to analyze the community structure of the mouse gut microbiota in the three groups (**Figure 6C**). On the PCOA plot, each symbol represents one gut microbiota. The more similar the abundance and composition of species, the closer the distance between samples. The results showed that the gut microbiota was significantly different between the different groups. The relationship between the gut microbiota from the three groups of fecal samples was investigated using a gut microbiota tree generated by the UPGMA algorithm. The dendrogram (**Figure 6D**) described and compared the similarity and difference relationship between the three samples intuitively through the dendritic structure. **Figure 6E** showed that the composition of the gut microbiota in different groups was significantly different at the genus level. After DSS treatment, the relative abundances of *Lachnospiraceae*, *Rikenellaceae*, and *Oscillospira* significantly decreased and that of *Sutterella* significantly increased compared with those of the control group (**Figure 6F**). After nintedanib administration, the gut microbiota of the mice was significantly altered compared with the DSS group (**Figure 6G**). The relative abundances of *Sutterella* and *S24-7* decreased, and those of *Bacteroides*, *Bilophila*, and *Parabacteroides* increased significantly, with *Bacteroides* becoming the dominant genus. Collectively, the gut microbiota of the control, DSS, and nintedanib groups were significantly different, and nintedanib significantly changed the composition of the intestinal microbiota in mice with DSS-induced experimental colitis.

DISCUSSION

IBD is an autoimmune disease. The destruction of the intestinal epithelial barrier and the increase of mucosal permeability activate the immune response, resulting in tissue injury, pathological changes, and clinical manifestations of IBD (Wendelsdorf et al., 2010). Super-enhancers regulate gene transcription by aggregating TFs, such as abnormal transcription driven by super-enhancers in most cancer cells (Sengupta and George, 2017). It has been reported that the genetic changes of super-enhancers can cause gene transcription imbalance (Sengupta and George, 2017). At present, it has been found that SNPs often appear in the super-enhancer region in a variety of autoimmune diseases such as systemic lupus erythematosus (Vahedi et al., 2015). In one study, 13 of the 76 SNPs in type 1 diabetes patients were located in the super-enhancers region (Hnisz et al., 2013). Because super-enhancers are closely related to the occurrence and development of autoimmune diseases, we have reason to believe that super-enhancers and their driving genes are related to the pathogenesis of IBD. This study studied the role of TFs, super-enhancers and their regulatory genes in IBD, and screened some existing drugs in the market. The results show that CEBPB/PCK1 and CEBPB/EFNA1 pathways can be used to study the pathogenesis of IBD, and nintedanib can effectively alleviate IBD.

Super-enhancer is an ultralong cis-acting element that controls gene transcription (Cheng et al., 2016). It controls gene expression by enriching transcription factors and binding to specific DNA sequences. We analyzed the data in the GEO database, found the upregulated DEGs (PCK1 and EFNA1) in IBD patients compared with normal people, and constructed CEBPB/PCK1 and CEBPB/EFNA1 pathways composed of TFs, super-enhancers, and their related genes. Such pathways are considered to play an important role in the occurrence of IBD.

The function of super-enhancers is reflected by their associated genes (Li et al., 2021a). KEGG pathway gene enrichment analysis is helpful to find out the possible roles of these super-enhancer–associated genes in the development and progression of IBD. Interestingly, the PI3K–Akt signaling pathway was the most important one. It is well known that PI3K–Akt has a close relationship with the occurrence and development of intestinal inflammation (Gao et al., 2021).

CEBPB is an important transcription factor that belongs to the CCAAT enhancer-binding proteins family. It is mainly involved in important life activities such as cell proliferation and differentiation, tumorigenesis and apoptosis, body inflammatory response, and so on through the regulation of gene transcription of target cells (Ramji and Foka, 2002). PCK1 and EFNA1 have been found to be involved in important life activities such as cell proliferation and apoptosis, tumor angiogenesis, malignant cell events, and invasiveness (Sadasivam et al., 2014), and their expression is upregulated in a variety of tumors [such as colorectal cancer (Shi et al., 2012)]. However, whether there is a link between transcription factors and super-enhancer–driven genes is still unknown. Therefore, we designed the simulant of CEBPB to inhibit the activity of transcription factors. Surprisingly, after silencing transcription factor CEBPB, the expression of super-enhancer–related genes decreased, which proved that transcription factor CEBPB affected the expression of super-enhancer–driving genes PCK1 and EFNA1.

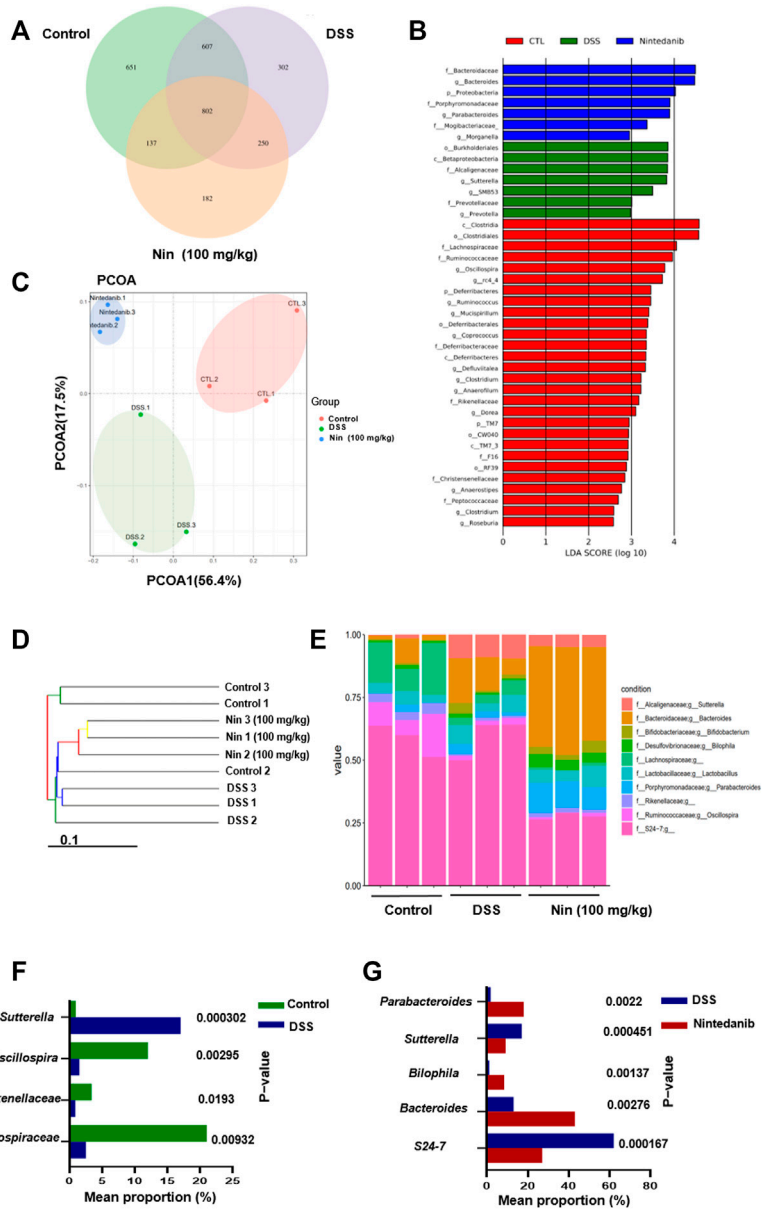

FIGURE 6 | Nintedanib regulates the gut microbiota composition of DSS-induced experimental colitis. **(A)** The Venn diagram showing the unique and shared OTUs from control, DSS, and nintedanib groups. **(B)** The difference of OTUs among the control group, the DSS group, and the nintedanib group was determined by linear discriminant analysis combined with effect size (lefse). **(C)** PCOA of gut microbiota communities based on the OTU level. **(D)** The clustering analysis of the evolution of the gut microbiotas between control, DSS, and nintedanib groups. Based on the distance matrix, the gut microbiota tree was constructed using the UPGMA (unweighted pair group method with arithmetic mean) clustering method for analysis. **(E)** Histograms of relative abundance of grouped species at the genus level. **(F)** Gut microbiota differentially expressed at genus level between control and DSS groups. **(G)** Gut microbiota differentially expressed at genus level between DSS and nintedanib groups.

The destruction of intestinal epithelial barrier protein is an important manifestation of colitis. The destruction of intestinal epithelial barrier function will lead to the immune response of the body and produce the clinicopathological manifestations of IBD (Su et al., 2009; Novak and Mollen, 2015). ZO-1 (Furuse et al., 1994), occludin (Furuse et al., 1998), and claudin-1 are intestinal epithelial barrier proteins, which are very important for the stability of epithelial barrier function. Previous studies have shown that geniposide and diosmetin can improve colitis by significantly increasing the damaged intestinal barrier protein (Xu et al., 2017; Li et al., 2021b). In the experiment, we found that the expression of related barrier proteins ZO-1, occludin, and claudin-1 increased significantly after silencing the transcription factor CEBPB. This indicates that CEBPB/PCK1 and CEBPB/EFNA1 pathways affect the expression of intestinal barrier protein. Sulfasalazine, mesalazine, olsalazine, and tofacitinib

are the first-line drugs in the treatment of IBD (Tursi et al., 2008; Song et al., 2017; Sayoc-Becerra et al., 2020). In order to further prove the role of CEBPB/PCK1 and CEBPB/EFNA1 pathways in IBD, we selected positive drugs for verification. The results were as expected, the listed drugs could significantly inhibit the mRNA expression levels of CEBPB, PCK1, and EFNA1.

As we all know, the safety of listed drugs is known and the development of new indications can greatly save development time and cost. Tyrosine kinase inhibitors are most often developed as cancer targets (van Vollenhoven et al., 2012; Huang et al., 2020). Later, it was found that some of them have anti-inflammatory properties (Roskoski, 2016; McInnes and Schett, 2017). Previous studies by us and others have found that some tyrosine kinase inhibitors have anti-inflammatory effects in pulmonary fibrosis, but none have investigated this in enteritis (Varone et al., 2018; Ruan et al., 2020). Therefore, we used these two pathways to screen some existing tyrosine kinase inhibitors (anlotinib, lenvatinib, axitinib, and nintedanib) to study whether they have a certain role in the treatment of IBD. Our data showed that nintedanib can significantly inhibit the mRNA expression levels of CEBPB, PCK1, and EFNA1 at the same time. Therefore, we chose nintedanib for further verification. Consistent with the aforementioned results, in Caco-2 cells, nintedanib could significantly inhibit the protein expression levels of CEBPB, PCK1, and EFNA1, and aid the destruction of intestinal barrier protein induced by LPS.

Studies have shown that gut microbiota plays a key role in the pathogenesis of IBD (Hernández-Chirlaque et al., 2016). The study by Shuang Jin et al. found that significant changes in gut microbiota can lead to IBD (Jin et al., 2017). Here, we studied the effects of DSS and nintedanib on the changes in gut microbiota in mice. We analyzed the effect of nintedanib on the composition of the gut microbial community. At the genus level, there are fundamental changes in the compositional structure of the gut microbial community. In the nintedanib group, the *Bacteroidetes* substitution *S24-7* became the most abundant strain. *Bacteroidetes* is an important keystone bacterium (Wilson et al., 1997; Franks et al., 1998; Hayashi et al., 2002), which has a significant impact on human health, especially in sugar fermentation and polysaccharide (Xu et al., 2003). *Sutterella* is commonly associated with human diseases, such as autism (Dan et al., 2020) and inflammatory bowel disease (Kaakoush, 2020), but the health effects of these bacteria remain unclear and are considered harmful in several studies (Cai et al., 2019). Nevertheless, there is no doubt that nintedanib reversed the trend of increased *sutterella* abundance compared with the DSS group. *Parabacteroides*, one of the core microbiota in humans, is a potential, novel antimetabolic syndrome probiotic, and here, we could find a significant increase in the abundance of *Parabacteroides* (Kai Wang et al., 2019). The results showed that the composition of gut microbiota in mice with experimental colitis was improved by nintedanib at the genus level, which may account for the therapeutic efficacy of nintedanib in experimental colitis.

CONCLUSION

In summary, this study shows that inhibition of super-enhancer–driven CEBPB/PCK1 and CEBPB/EFNA1 signaling pathways can reduce LPS-induced barrier dysfunction *in vitro* and improve DSS-induced experimental colitis *in vivo*. Nintedanib has a certain role in the treatment of IBD. However, there are still many deficiencies in this study. For example, there are few studies on the transcriptional enhancement effect of super-enhancers (SC-CHR20-57528535 and SC-CHR1-155093980) on the transcription factor CEBPB, which is the focus of our next study. In conclusion, this study provides a new idea for the pathogenesis of enteritis and the exploration of candidate drugs.

DATA AVAILABILITY STATEMENT

The datasets presented in this study can be found in online repositories. The names of the repository/repositories and accession number(s) can be found in the article/Supplementary Material.

ETHICS STATEMENT

The studies involving human participants were reviewed and approved by the Department of Gastroenterology and Hepatology, General Hospital. The patients/participants provided their written informed consent to participate in this study. The animal study was reviewed and approved by the Institutional Animal Care and Use Committee (IACUC) of Nankai University.

AUTHOR CONTRIBUTIONS

XG, HZ, and HC supervised the project, designed experiments, and wrote the manuscript. HL and JL performed experiments and analyzed data. YH, YY, and GJ performed experimental colitis modeling experiments in mice. TX provided technical assistance in pharmacology. All authors read and approved the final manuscript.

FUNDING

This work received financial support from the National Natural Science Foundation of China [Grant 81871972], Tianjin Science and Technology Project [Grant No. 19YFZCSY00160], and the Foundation of Organ Fibrosis Druggability Joint Research Centre of Nankai and Guokaixingcheng [Grant 735-F1040051].

REFERENCES

Agrawal, P., and Rao, S. (2021). Super-Enhancers and CTCF in Early Embryonic Cell Fate Decisions. *Front. Cell Dev. Biol.* 9, 653669. doi:10.3389/fcell.2021.653669

Brown, J. D., Lin, C. Y., Duan, Q., Griffin, G., Federation, A., Paranal, R. M., et al. (2014). NF-κB Directs Dynamic Super Enhancer Formation in Inflammation and Atherogenesis. *Mol. Cell* 56 (2), 219–231. doi:10.1016/j.molcel.2014.08.024

Cai, X., Han, Y., Gu, M., Song, M., Wu, X., Li, Z., et al. (2019). Dietary Cranberry Suppressed Colonic Inflammation and Alleviated Gut Microbiota Dysbiosis in Dextran Sodium Sulfate-Treated Mice. *Food Funct.* 10 (10), 6331–6341. doi:10.1039/c9fo01537j

Cheng, H., Dou, X., and Han, J. D. (2016). Understanding Super-enhancers. *Sci. China Life Sci.* 59 (3), 277–280. doi:10.1007/s11427-016-5028-3

Costa-Reis, P., and Sullivan, K. E. (2013). Genetics and Epigenetics of Systemic Lupus Erythematosus. *Curr. Rheumatol. Rep.* 15 (9), 369. doi:10.1007/s11926-013-0369-4

Dan, Z., Mao, X., Liu, Q., Guo, M., Zhuang, Y., Liu, Z., et al. (2020). Altered Gut Microbial Profile Is Associated with Abnormal Metabolism Activity of Autism Spectrum Disorder. *Gut Microbes* 11 (5), 1246–1267. doi:10.1080/19490976.2020.1747329

Deng, Y., and Tsao, B. P. (2010). Genetic Susceptibility to Systemic Lupus Erythematosus in the Genomic Era. *Nat. Rev. Rheumatol.* 6 (12), 683–692. doi:10.1038/nrrheum.2010.176

Franks, A. H., Harmsen, H. J., Raangs, G. C., Jansen, G. J., Schut, F., and Welling, G. W. (1998). Variations of Bacterial Populations in Human Feces Measured by Fluorescent *In Situ* Hybridization with Group-specific 16S rRNA-Targeted Oligonucleotide Probes. *Appl. Environ. Microbiol.* 64 (9), 3336–3345. doi:10.1128/AEM.64.9.3336-3345.1998

Furuse, M., Itoh, M., Hirase, T., Nagafuchi, A., Yonemura, S., Tsukita, S., et al. (1994). Direct Association of Occludin with ZO-1 and its Possible Involvement in the Localization of Occludin at Tight Junctions. *J. Cell Biol.* 127 (6 Pt 1), 1617–1626. doi:10.1083/jcb.127.6.1617

Furuse, M., Fujita, K., Hiiragi, T., Fujimoto, K., and Tsukita, S. (1998). Claudin-1 and -2: Novel Integral Membrane Proteins Localizing at Tight Junctions with No Sequence Similarity to Occludin. *J. Cell Biol.* 141 (7), 1539–1550. doi:10.1083/jcb.141.7.1539

Gao, T., Wang, T., Wang, Z., Cao, J., Dong, Y., and Chen, Y. (2021). Melatonin-mediated MT2 Attenuates Colitis Induced by Dextran Sodium Sulfate via PI3K/AKT/Nrf2/SIRT1/RORα/NF-κB Signaling Pathways. *Int. Immunopharmacol.* 96, 107779. doi:10.1016/j.intimp.2021.107779

Hayashi, H., Sakamoto, M., and Benno, Y. (2002). Phylogenetic Analysis of the Human Gut Microbiota Using 16S rDNA Clone Libraries and Strictly Anaerobic Culture-Based Methods. *Microbiol. Immunol.* 46 (8), 535–548. doi:10.1111/j.1348-0421.2002.tb02731.x

Hernández-Chirlaque, C., Aranda, C. J., Ocón, B., Capitán-Cañadas, F., Ortega-González, M., Carrero, J. J., et al. (2016). Germ-free and Antibiotic-Treated Mice Are Highly Susceptible to Epithelial Injury in DSS Colitis. *J. Crohns Colitis* 10 (11), 1324–1335. doi:10.1093/ecco-jcc/jjw096

Higashijima, Y., and Kanki, Y. (2021). Potential Roles of Super Enhancers in Inflammatory Gene Transcription. *Febs. J.* doi:10.1111/febs.16089

Hnisz, D., Abraham, B. J., Lee, T. I., Lau, A., Saint-André, V., Sigova, A. A., et al. (2013). Super-enhancers in the Control of Cell Identity and Disease. *Cell* 155 (4), 934–947. doi:10.1016/j.cell.2013.09.053

Huang, L., Jiang, S., and Shi, Y. (2020). Tyrosine Kinase Inhibitors for Solid Tumors in the Past 20 Years (2001-2020). *J. Hematol. Oncol.* 13 (1), 143. doi:10.1186/s13045-020-00977-0

Jin, S., Zhao, D., Cai, C., Song, D., Shen, J., Xu, A., et al. (2017). Low-dose Penicillin Exposure in Early Life Decreases Th17 and the Susceptibility to DSS Colitis in Mice through Gut Microbiota Modification. *Sci. Rep.* 7 (1), 43662. doi:10.1038/srep43662

Kaakoush, N. O. (2020). Sutterella Species, IgA-Degrading Bacteria in Ulcerative Colitis. *Trends Microbiol.* 28 (7), 519–522. doi:10.1016/j.tim.2020.02.018

Kai Wang, K., Liao, M., Zhou, N., Bao, L., Ma, K., Zheng, Z., et al. (2019). Parabacteroides Distasonis Alleviates Obesity and Metabolic Dysfunctions via Production of Succinate and Secondary Bile Acids. *Cell Rep.* 26 (1), 222–e5. e225. doi:10.1016/j.celrep.2018.12.028

Kaplan, G. G. (2015). The Global Burden of IBD: from 2015 to 2025. *Nat. Rev. Gastroenterol. Hepatol.* 12 (12), 720–727. doi:10.1038/nrgastro.2015.150

Kappelman, M. D., Rifas-Shiman, S. L., Porter, C. Q., Ollendorf, D. A., Sandler, R. S., Galanko, J. A., et al. (2008). Direct Health Care Costs of Crohn's Disease and Ulcerative Colitis in US Children and Adults. *Gastroenterology* 135 (6), 1907–1913. doi:10.1053/j.gastro.2008.09.012

Kappelman, M. D., Moore, K. R., Allen, J. K., and Cook, S. F. (2013). Recent Trends in the Prevalence of Crohn's Disease and Ulcerative Colitis in a Commercially Insured US Population. *Dig. Dis. Sci.* 58 (2), 519–525. doi:10.1007/s10620-012-2371-5

Li, H., Zhao, C., Li, Z., Yao, K., Zhang, J., Si, W., et al. (2021a). Identification of Potential Pathogenic Super-enhancers-driven Genes in Pulmonary Fibrosis. *Front. Genet.* 12, 644143. doi:10.3389/fgene.2021.644143

Li, H.-l., Wei, Y.-y., Li, X.-h., Zhang, S.-s., Zhang, R.-t., Li, J.-h., et al. (2021b). Diosmetin Has Therapeutic Efficacy in Colitis Regulating Gut Microbiota, Inflammation, and Oxidative Stress via the Circ-Sirt1/Sirt1 axis. *Acta Pharmacol. Sin.* 43, 919–932. doi:10.1038/s41401-021-00726-0

Lovén, J., Hoke, H. A., Lin, C. Y., Lau, A., Orlando, D. A., Vakoc, C. R., et al. (2013). Selective Inhibition of Tumor Oncogenes by Disruption of Super-enhancers. *Cell* 153 (2), 320–334. doi:10.1016/j.cell.2013.03.036

McInnes, I. B., and Schett, G. (2017). Pathogenetic Insights from the Treatment of Rheumatoid Arthritis. *Lancet* 389 (10086), 2328–2337. doi:10.1016/s0140-6736(17)31472-1

Ng, S. C. (2015). Emerging Leadership Lecture: Inflammatory Bowel Disease in Asia: Emergence of a "Western" Disease. *J. Gastroenterol. Hepatol.* 30 (3), 440–445. doi:10.1111/jgh.12859

Ng, S. C., Tang, W., Ching, J. Y., Wong, M., Chow, C. M., Hui, A. J., et al. (2013). Incidence and Phenotype of Inflammatory Bowel Disease Based on Results from the Asia-Pacific Crohn's and Colitis Epidemiology Study. *Gastroenterology* 145 (1), 158–e2. doi:10.1053/j.gastro.2013.04.007

Novak, E. A., and Mollen, K. P. (2015). Mitochondrial Dysfunction in Inflammatory Bowel Disease. *Front. Cell Dev. Biol.* 3, 62. doi:10.3389/fcell.2015.00062

Park, S. J., Kim, W. H., and Cheon, J. H. (2014). Clinical Characteristics and Treatment of Inflammatory Bowel Disease: a Comparison of Eastern and Western Perspectives. *World J. Gastroenterol.* 20 (33), 11525–11537. doi:10.3748/wjg.v20.i33.11525

Peng, Y., Yan, Y., Wan, P., Chen, D., Ding, Y., Ran, L., et al. (2019). Gut Microbiota Modulation and Anti-inflammatory Properties of Anthocyanins from the Fruits of Lycium Ruthenicum Murray in Dextran Sodium Sulfate-Induced Colitis in Mice. *Free Radic. Biol. Med.* 136, 96–108. doi:10.1016/j.freeradbiomed.2019.04.005

Ramji, D. P., and Foka, P. (2002). CCAAT/enhancer-binding Proteins: Structure, Function and Regulation. *Biochem. J.* 365 (Pt 3), 561–575. doi:10.1042/BJ20020508

Ramos, G. P., and Papadakis, K. A. (2019). Mechanisms of Disease: Inflammatory Bowel Diseases. *Mayo. Clin. Proc.* 94 (1), 155–165. doi:10.1016/j.mayocp.2018.09.013

Roskoski, R., Jr. (2016). Janus Kinase (JAK) Inhibitors in the Treatment of Inflammatory and Neoplastic Diseases. *Pharmacol. Res.* 111, 784–803. doi:10.1016/j.phrs.2016.07.038

Ruan, H., Lv, Z., Liu, S., Zhang, L., Huang, K., Gao, S., et al. (2020). Anlotinib Attenuated Bleomycin-Induced Pulmonary Fibrosis via the TGF-B1 Signalling Pathway. *J. Pharm. Pharmacol.* 72 (1), 44–55. doi:10.1111/jphp.13183

Sadasivam, M., Ramatchandirin, B., Balakrishnan, S., Selvaraj, K., and Prahalathan, C. (2014). The Role of Phosphoenolpyruvate Carboxykinase in Neuronal Steroidogenesis under Acute Inflammation. *Gene* 552 (2), 249–254. doi:10.1016/j.gene.2014.09.043

Sayoc-Becerra, A., Krishnan, M., Fan, S., Jimenez, J., Hernandez, R., Gibson, K., et al. (2020). The JAK-Inhibitor Tofacitinib Rescues Human Intestinal Epithelial Cells and Colonoids from Cytokine-Induced Barrier Dysfunction. *Inflamm. Bowel. Dis.* 26 (3), 407–422. doi:10.1093/ibd/izz266

Sengupta, S., and George, R. E. (2017). Super-Enhancer-Driven Transcriptional Dependencies in Cancer. *Trends Cancer* 3 (4), 269–281. doi:10.1016/j.trecan.2017.03.006

Shi, Z. Z., Zhang, Y. M., Shang, L., Hao, J. J., Zhang, T. T., Wang, B. S., et al. (2012). Genomic Profiling of Rectal Adenoma and Carcinoma by Array-Based

Comparative Genomic Hybridization. *BMC Med. Genomics* 5, 52. doi:10.1186/1755-8794-5-52

Song, Y., Jang, J., Shin, T. H., Bae, S. M., Kim, J. S., Kim, K. M., et al. (2017). Sulfasalazine Attenuates Evading Anticancer Response of CD133-Positive Hepatocellular Carcinoma Cells. *J. Exp. Clin. Cancer Res.* 36 (1), 38. doi:10.1186/s13046-017-0511-7

Stillie, R., and Stadnyk, A. W. (2009). Role of TNF Receptors, TNFR1 and TNFR2, in Dextran Sodium Sulfate-Induced Colitis. *Inflamm. Bowel Dis.* 15 (10), 1515–1525. doi:10.1002/ibd.20951

Su, L., Shen, L., Clayburgh, D. R., Nalle, S. C., Sullivan, E. A., Meddings, J. B., et al. (2009). Targeted Epithelial Tight Junction Dysfunction Causes Immune Activation and Contributes to Development of Experimental Colitis. *Gastroenterology* 136 (2), 551–563. doi:10.1053/j.gastro.2008.10.081

Tursi, A., Brandimarte, G., Elisei, W., Giorgetti, G. M., Inchingolo, C. D., and Aiello, F. (2008). Effect of Mesalazine on Epithelial Cell Proliferation in Colonic Diverticular Disease. *Dig. Liver. Dis.* 40 (9), 737–742. doi:10.1016/j.dld.2008.02.022

Vahedi, G., Kanno, Y., Furumoto, Y., Jiang, K., Parker, S. C., Erdos, M. R., et al. (2015). Super-enhancers Delineate Disease-Associated Regulatory Nodes in T Cells. *Nature* 520 (7548), 558–562. doi:10.1038/nature14154

van Vollenhoven, R. F., Fleischmann, R., Cohen, S., Lee, E. B., García Meijide, J. A., Wagner, S., et al. (2012). Tofacitinib or Adalimumab versus Placebo in Rheumatoid Arthritis. *N. Engl. J. Med.* 367 (6), 508–519. doi:10.1056/NEJMoa1112072

Varone, F., Sgalla, G., Iovene, B., Bruni, T., and Richeldi, L. (2018). Nintedanib for the Treatment of Idiopathic Pulmonary Fibrosis. *Expert. Opin. Pharmacother.* 19 (2), 167–175. doi:10.1080/14656566.2018.1425681

Wendelsdorf, K., Bassaganya-Riera, J., Hontecillas, R., and Eubank, S. (2010). Model of Colonic Inflammation: Immune Modulatory Mechanisms in Inflammatory Bowel Disease. *J. Theor. Biol.* 264 (4), 1225–1239. doi:10.1016/j.jtbi.2010.03.027

Whyte, W. A., Orlando, D. A., Hnisz, D., Abraham, B. J., Lin, C. Y., Kagey, M. H., et al. (2013). Master Transcription Factors and Mediator Establish Super-enhancers at Key Cell Identity Genes. *Cell* 153 (2), 307–319. doi:10.1016/j.cell.2013.03.035

Wilson, K. H., Ikeda, J. S., and Blitchington, R. B. (1997). Phylogenetic Placement of Community Members of Human Colonic Biota. *Clin. Infect. Dis.* 25 Suppl 2 (Suppl. 2), S114–S116. doi:10.1086/516230

Witte, S., O'Shea, J. J., and Vahedi, G. (2015). Super-enhancers: Asset Management in Immune Cell Genomes. *Trends Immunol.* 36 (9), 519–526. doi:10.1016/j.it.2015.07.005

Wollin, L., Maillet, I., Quesniaux, V., Holweg, A., and Ryffel, B. (2014). Antifibrotic and Anti-inflammatory Activity of the Tyrosine Kinase Inhibitor Nintedanib in Experimental Models of Lung Fibrosis. *J. Pharmacol. Exp. Ther.* 349 (2), 209–220. doi:10.1124/jpet.113.208223

Xi Wang, X., Cairns, M. J., and Yan, J. (2019). Super-enhancers in Transcriptional Regulation and Genome Organization. *Nucleic Acids Res.* 47 (22), 11481–11496. doi:10.1093/nar/gkz1038

Xu, J., Bjursell, M. K., Himrod, J., Deng, S., Carmichael, L. K., Chiang, H. C., et al. (2003). A Genomic View of the Human-Bacteroides Thetaiotaomicron Symbiosis. *Science* 299 (5615), 2074–2076. doi:10.1126/science.1080029

Xu, B., Li, Y. L., Xu, M., Yu, C. C., Lian, M. Q., Tang, Z. Y., et al. (2017). Geniposide Ameliorates TNBS-Induced Experimental Colitis in Rats via Reducing Inflammatory Cytokine Release and Restoring Impaired Intestinal Barrier Function. *Acta Pharmacol. Sin.* 38 (5), 688–698. doi:10.1038/aps.2016.168

Zoubek, M. E., Pinazo-Bandera, J., Ortega-Alonso, A., Hernández, N., Crespo, J., Contreras, F., et al. (2019). Liver Injury after Methylprednisolone Pulses: A Disputable Cause of Hepatotoxicity. A Case Series and Literature Review. *United Eur. Gastroenterol. J.* 7 (6), 825–837. doi:10.1177/2050640619840147

Conflict of Interest: The authors declare that the research was conducted in the absence of any commercial or financial relationships that could be construed as a potential conflict of interest.

Publisher's Note: All claims expressed in this article are solely those of the authors and do not necessarily represent those of their affiliated organizations, or those of the publisher, the editors, and the reviewers. Any product that may be evaluated in this article, or claim that may be made by its manufacturer, is not guaranteed or endorsed by the publisher.

frontiers | Frontiers in Pharmacology

BRIEF RESEARCH REPORT
published: 15 July 2022
doi: 10.3389/fphar.2022.913124

Cisplatin-Induced Anorexia and Pica Behavior in Rats Enhanced by Chronic Stress Pretreatment

Zhijun Guo[1,2†], Jingjing Duan[2†], Yitian Chen[1,2], Weijia Cai[1,2], Chenghua Yang[2], Zhen Yang[2], Xiufeng Liu[2] and Feng Xu[1,2]*

[1]School of Pharmaceutical Sciences, Southern Medical University, Guangzhou, China, [2]Fengxian Hospital, Southern Medical University, Shanghai, China

Background: Chemotherapy-induced nausea and vomiting severely impairs the treatment and prognosis of cancer patients. Depressive mood disorder might aggravate nausea and vomiting in cancer patients; however, the role of neurotransmitters and receptors involved in the mediation of emesis and nausea is still not well elaborated.

Methods: The study was carried out based on the chronic unpredictable mild stress–induced depression-like phenotype rat model and cisplatin-induced pica rat model establishment. Forty male Sprague–Dawley rats were randomized into the non-treated control group and the chronic stress group, which were exposed to 8 weeks of stress. Each group was then sub-divided into vehicle subgroups (n = 10) and cisplatin subgroups (n = 10) which were given cisplatin to induce pica behavior. Kaolin and food intake were recorded after administration. The medulla oblongata and ileum tissues were obtained. Neurotransmitters involved in the mediation of emesis and nausea (5-HT, DA, SP, and AEA) were detected using an ELISA kit. Vomit-related receptors (5-HT_3R, DA_2R, NK_1R, and CB_1R) in tissues were assayed for mRNA and protein expression by RT-qPCR and Western blotting.

Results: Behavioral test and sucrose preference validated that depression-like phenotype rat models were established successfully. The kaolin consumption test confirmed that chronic stress pretreatment aggravated anorexia and pica behavior. Vomiting-related molecules' data showed that chronic stress exposure increased 5-HT and SP levels in the medulla oblongata. Vomiting-related receptor expression data showed that chronic stress pretreatment upregulated 5-HT_3R, DA_2R, and NK_1R expressions and downregulated the CB_1R expression in the medulla oblongata. However, chronic stress pretreatment downregulated 5-HT_3R, DA_2R, and NK_1R expressions and upregulated the CB_1R expression in the ileum.

Conclusion: Chronic stress pretreatment aggravates anorexia and vomiting progress, which might be *via* altering neurotransmitters and receptors involved in the mediation of emesis and the nausea level and expression in the central nervous system.

Keywords: chronic unpredictable mild stress, anorexia, pica, cisplatin, chemotherapy-induced nausea and vomiting

OPEN ACCESS

Edited by:
Thomas Brzozowski, Jagiellonian University Medical College, Poland

Reviewed by:
Feifei Guo, Qingdao University, China
Nguyen Minh Duc, Pham Ngoc Thach University of Medicine, Vietnam
Tito Borner, University of Pennsylvania, United States

***Correspondence:**
Feng Xu
xuf@smu.edu.cn

[†]*These authors have contributed equally to this work*

Specialty section:
This article was submitted to Gastrointestinal and Hepatic Pharmacology, a section of the journal Frontiers in Pharmacology

Received: *05 April 2022*
Accepted: *14 June 2022*
Published: *15 July 2022*

Citation:
Guo Z, Duan J, Chen Y, Cai W, Yang C, Yang Z, Liu X and Xu F (2022) Cisplatin-Induced Anorexia and Pica Behavior in Rats Enhanced by Chronic Stress Pretreatment. Front. Pharmacol. 13:913124. doi: 10.3389/fphar.2022.913124

INTRODUCTION

Chemotherapy-induced nausea and vomiting (CINV) is a critically adverse drug reaction in cancer patients (Aapro, 2018), which severely disturbs treatment decision and impairs overall quality of life and therapeutic outcome (Hawkins and Grunberg, 2009; Bray et al., 2018; Natale, 2018).

Serotonin (5-HT) and substance P (SP) are key factors involved in the vomiting process (Darmani and Ray, 2009). When 5-HT or/and SP combines with the corresponding receptors, the vomiting center in the medulla oblongata is triggered and thus results in vomiting. Although new therapeutics have been developed for nausea and vomiting control, CINV is still very challenging for cancer chemotherapy patients (Jordan et al., 2015; Warr, 2018). Up to now, CINV has remained a thorny issue in cancer chemotherapy (Dranitsaris et al., 2017). Approximately 9–30% of cancer patients still suffer from serious vomiting despite current anti-emetic medications (Mersiades et al., 2018). A further complication is that many risk factors are identified to aggravate CINV, including history of nausea/vomiting, expectancy of CINV, alcohol intake, and anxiety/depression (Mosa et al., 2020).

In our previous work, we found that the frequency and extent of subjectively experienced adverse drug reactions (anorexia, nausea, and fatigue) in cancer chemotherapy patients seemed to be well in line with the severity of their depression (Zhou et al., 2010). Chronic stress pretreatment might aggravate the vomiting process; however, the underlying mechanism is still not clear. In addition, many documents indicated that the gastrointestinal function was affected by a specific psychological mood disorder status such as depression and anxiety (Peng and Liang, 1999; Liu et al., 2015), further indicating that chronic stress pretreatment is related to changes in the gastrointestinal function.

In this study, we hypothesized that chronic stress pretreatment might aggravate nausea and vomiting. Due to the special physiological and anatomical structure, rats are lacking a vomiting response. Non-nutritive substance consumption, such as kaolin consumption (pica behavior), can indirectly reflect the degree of vomiting in rats (Borner et al., 2020). We examined the kaolin consumption in this study to explore the vomiting response in rats. As the vomiting process involves many molecules and receptors (Li and Xu, 2020), this study focused on neurotransmitters involved in the mediation of emesis and nausea 5-HT, DA, SP and AEA level, 5-HT_3R, DA_2R, NK_1R, and CB_1R expressions in the central nervous system and aimed to explore the relevant molecule profile of chronic stress aggravating CINV based on chronic unpredictable mild stress (CUMS) and/or the pica rat model.

MATERIALS AND METHODS

Animals

Male Sprague–Dawley rats weighing 120–150 g were purchased from Shanghai Jiesijie Laboratory Animal Technology Co., Ltd. (Animal Quality Certificate: 20180004058940). Rats were housed in a specific pathogen-free (SPF) laboratory with a regular 12-h light (06:00–18:00)-dark (18:00–06:00) cycle, at the Laboratory Animal Center, East China Normal University, Shanghai. All rats were allowed to adapt to the new environment for 1 week before CUMS model establishment. The body weight of rats was measured biweekly. Animal procedures complied with the ARRIVE guidelines. This study was reviewed and approved by the Animal Research Ethics Committee in Fengxian Hospital, Southern Medical University (No. 201920143).

Behavioral Testing—Open Field Test

The OFT was used to evaluate the locomotion activity and exploratory behavior of rats. Each rat was individually placed at the center of a box (100 cm × 100 cm × 40 cm) divided into 25 cm × 25 cm^2 squares and observed for 5 min. The crossing numbers of squares (locomotion activity) and the rearing times (exploratory behavior) were monitored using a ZSZFT Video Analysis System (ZSZRDC Science and Technology Co., Ltd., China). The OFT was only conducted before and after 8 weeks of modeling to maintain a relatively unfamiliar environment for rats.

Sucrose Preference Test

The SPT was used to detect the anhedonia status in depression-like phenotype rats (Liu et al., 2018). Rats were individually housed in cages for isolation adaption. Sucrose training for 48 h helped the rats adapt to the sucrose solution. At the first 24 h, two bottles of 1% sucrose solution (Sigma, St. Louis, MO, United States) were given to the rats. At the second 24 h, a bottle of water and a bottle of 1% sucrose solution were given to the rats. After 23 h of deprivation of water and food, a bottle of water and a bottle of 1% sucrose solution were given to the rats, and the intake of water and sucrose solution for 1 h was recorded. The positions of the two bottles were exchanged every 6 h to eliminate unilateral preference during the whole test.

$$\text{Sucrose preference}\% = (\text{sucrose solution consumption}/(\text{sucrose solution} + \text{water consumption})) \times 100\%.$$

Chronic Stress Model

After OFT and SPT primary screening, rats with normal behavior were divided into the non-treated control group ($n = 20$) and the chronic stress group ($n = 20$) with a random number table. Rats in the chronic stress group were individually housed in cages and exposed to the following stressors in a random order once a day for 8 weeks: restraint (activity restriction in a 30 cm × 6 cm plastic bottle, 1 h), hot water swimming (45°C, 5 min), cold water swimming (4°C, 5 min), clip tail (clip 1 cm from the end of the tail, 1 min), cage tilting (45°, 24 h), horizontal shaking (30 min), damp padding (24 h), noise interference (industrial noise from a media player, 2 h), and day/night inversion (24 h) (Antoniuk et al., 2019; Li et al., 2019; Zhao et al., 2020). The use of the same stress for two consecutive days was avoided for the purpose of unpredictability. Rats in the non-treated control group were grouped in cages and fed normally without any stress during this period.

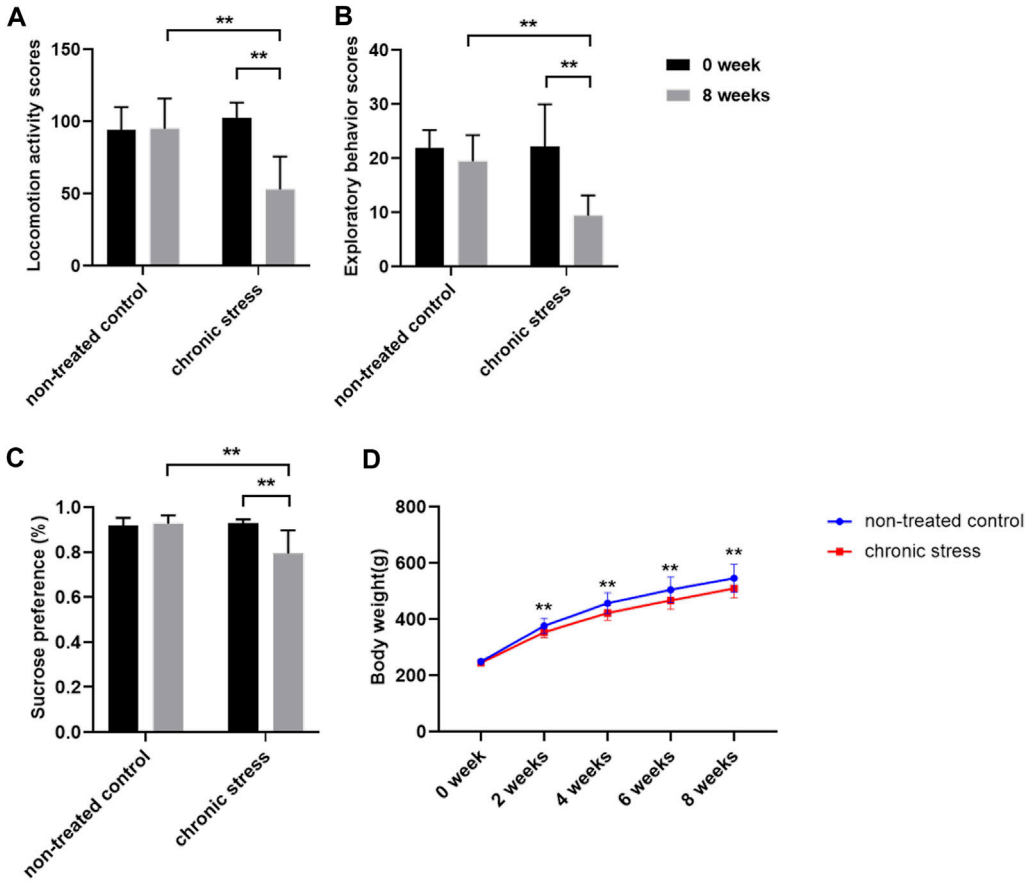

FIGURE 1 | Chronic stress model was established successfully (n = 20/group). **(A)** Locomotion activity scores. **(B)** Exploratory behavior scores. **(C)** Sucrose preference. **(D)** Body weight. Data were expressed as mean ± SD. $^{**}p < 0.01$ (statistical comparisons between the two groups were performed using the two independent sample t-test, and the same group was performed with the paired sample t-test. Repeated measurement data was performed using two-way repeated measures ANOVA.).

Cisplatin-Induced Pica Model

Here, 2% Arabic gum solution was prepared by stirring Arabic gum powder (Shanghai Macklin Biochemical Co., Ltd.) in distilled water at room temperature until it was completely dissolved. Then, 500 g kaolin (Shanghai Yuanye Biological Technology Co., Ltd.) and 200 ml of 2% Arabic gum solution were mixed to make a thick paste. The paste was dried at room temperature and molded into chow food in the shape of pellets. After 8 weeks of chronic stress, rats in both the non-treated control group and the chronic stress group were further subdivided into the vehicle subgroup (normal saline) and the cisplatin subgroup (cisplatin administration), respectively, as follows: non-treated/saline group (n = 10), non-treated/cisplatin group (n = 10), CUMS/cisplatin group (n = 10), and CUMS group (n = 10). Rats in the non-treated/saline group, non-treated/cisplatin group, and CUMS/cisplatin group were individually housed in cages and given kaolin pellets for 1 week of adaptation. Food was provided simultaneously during the cisplatin-induced pica model. Non-treated/cisplatin group and CUMS/cisplatin group rats were then given 6 mg/kg cisplatin (Qilu Pharmaceutical Co., Ltd.) intraperitoneally; meanwhile, rats in the non-treated/saline group were given normal saline intraperitoneally. The intake of kaolin and food was recorded at 24 h after administration. For the cisplatin-induced pica behavior model, rats were not given any stress to avoid affecting kaolin and food intake.

Measurement of Neurotransmitters and Receptors Involved in the Mediation of Emesis and Nausea

To further investigate the effect of chronic stress pretreatment on vomit-related molecules, we examined the vomit-related neurotransmitters' levels and vomit-related receptors' expression in the non-treated/saline group and CUMS group. Then, 24 h after cisplatin administration, the medulla oblongata and ileum tissues of rats in the non-treated/saline group and CUMS group were collected. Portions of tissues were homogenized at 4°C. The levels of 5-HT, DA, SP, and AEA in the tissue homogenate were detected using the ELISA kit (Jiangsu Jianglai Biotechnology Co., Ltd.), according to the manufacturer's protocol. Portions of tissues were preserved in

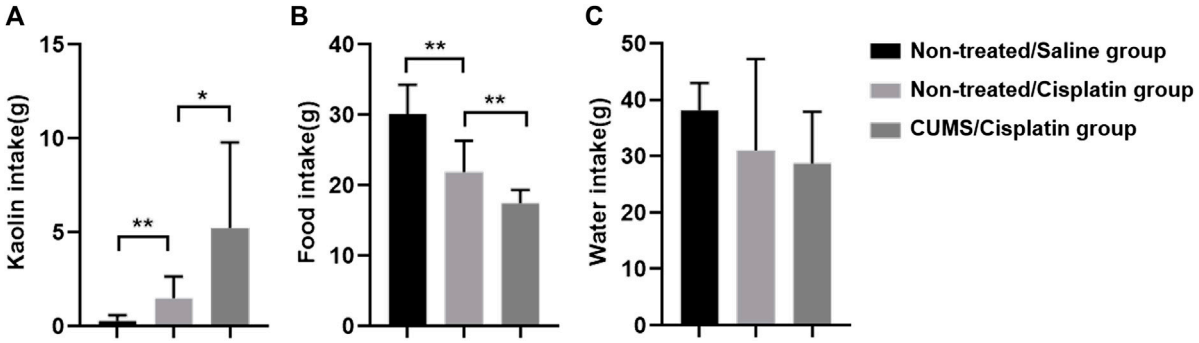

FIGURE 2 | Chronic stress pretreatment enhanced cisplatin (6 mg/kg)-induced anorexia and pica behavior in rats (n = 10/group). **(A)** Kaolin intake. **(B)** Food intake. **(C)** Water intake. *p < 0.05 and **p < 0.01(statistical comparisons in the inter-groups were performed using one-way analysis of variance (ANOVA).).

liquid nitrogen for receptor mRNA and protein expression measurement.

For RT-qPCR measurement, briefly, total RNA of the medulla oblongata and ileum tissues were extracted with TRIzol (Invitrogen™, Carlsbad, United States), according to the protocol, and the RNA concentration was measured using a NanoDrop ND-100 spectrophotometer (Thermo Scientific, Wilmington, DE, United States). Tli RNaseH Plus was used according to the manufacturer's protocol. The $2^{-\Delta\Delta CT}$ method was used to normalize the fold change in the gene expression. The primer sequences are as follows:

GADPH forward primer, 5′-CAAGAAGGTGGTGAAGCAG-3′ and reverse primer, 5′-CAAAGGTGGAAGAATGGG-3'; *5-HT_3R* forward primer, 5′-CTGTCCTCCATCCGCCACTCC-3′ and reverse primer, 5′- CAGCAGCCTGTCCAGCACATATC-3'; *DA_2R* forward primer, 5′- CACACGCTACAGCTCCAAG-3′ and reverse primer, 5′- GAAGGACAGGACCCAGACA-3'; *NK_1R* forward primer, 5′- CCGCTACCATGAGCAAGT-3′ and reverse primer, 5′- AGGGCAGGAGGAAGAAGA-3'; and *CB_1R* forward primer, 5′- GGACCCAGAAGAGCATCA-3′ and reverse primer, 5′- ATCAACACCACCAGGATCA-3'. The gene expression was normalized with the following: experimental group: target gene/housekeeping gene; control group: target gene/housekeeping gene).

For Western blot, briefly, the medulla oblongata and ileum tissues were individually ground and sonicated in RIPA buffer (Beyotime, China) for 30 min and centrifuged at 14,000 g for 20 min at 4°C. The supernatant was quantified using the BCA protein assay kit (Beyotime, China), analyzed by 10% SDS-PAGE (Beyotime, China), and transferred onto a nitrocellulose filter membrane (Pall, America). After 1 h of blocking, the membranes were incubated with the primary antibody (5-HT_3R antibody, CB_1R antibody, and β-actin antibody were purchased from Proteintech, NK_1R antibody was purchased from Immunoway, and DA_2R antibody was purchased from Bioss; dilution rate: 5-HT_3R, CB_1R, NK_1R, and DA_2R were 1:1000, and β-actin was 1: 5000) overnight at 4°C, followed by incubation with secondary antibodies (Goat anti-rabbit antibody and goat anti-mouse antibody were purchased from Proteintech; dilution rate: goat anti-rabbit and goat anti-mouse were 1:5000), and detected with an ECL buffer (NCM Biotech, China). The intensity of each band was determined by ImageJ software. The protein expression was normalized with the following: experimental group: target protein/housekeeping protein; control group: target protein/housekeeping protein).

Statistical Analysis

All analysis was performed using SPSS 19.0. Data were expressed as mean ± SD. Statistical comparisons between the two groups were performed using the two independent sample t-tests, and the same group was performed with paired samples' t-test. The inter-groups were performed using one-way analysis of variance (ANOVA). Repeated measurement data were performed using two-way repeated measures ANOVA. LSD and Dunnett's T3 were used for *post hoc* multiple comparisons. $p < 0.05$ was considered to be statistically significant.

RESULTS

Chronic Stress Model Validation

After 8 weeks of CUMS model establishment, the locomotion activity scores, exploratory behavior scores, and sucrose preference were decreased in chronic stress group rats compared to baseline ($p < 0.01$). However, there was little change in the non-treated control rats over time (**Figures 1A–C**). The results showed that depression-like behavior was successfully induced in rats in the chronic stress group compared with rats in the non-treated control group. Compared to the non-treated control group, a moderate reduction in the body weight in chronic stress group rats was observed from the second week of CUMS model establishment (**Figure 1D**). Behavioral test and sucrose preference test results indicated that the chronic stress–induced depression-like phenotype rat model was successfully established.

Chronic Stress Pretreatment Aggravates Cisplatin-Induced Anorexia and Pica Behavior

Kaolin pellets were given to rats in the non-treated/saline group, non-treated/cisplatin group, and CUMS/cisplatin group for

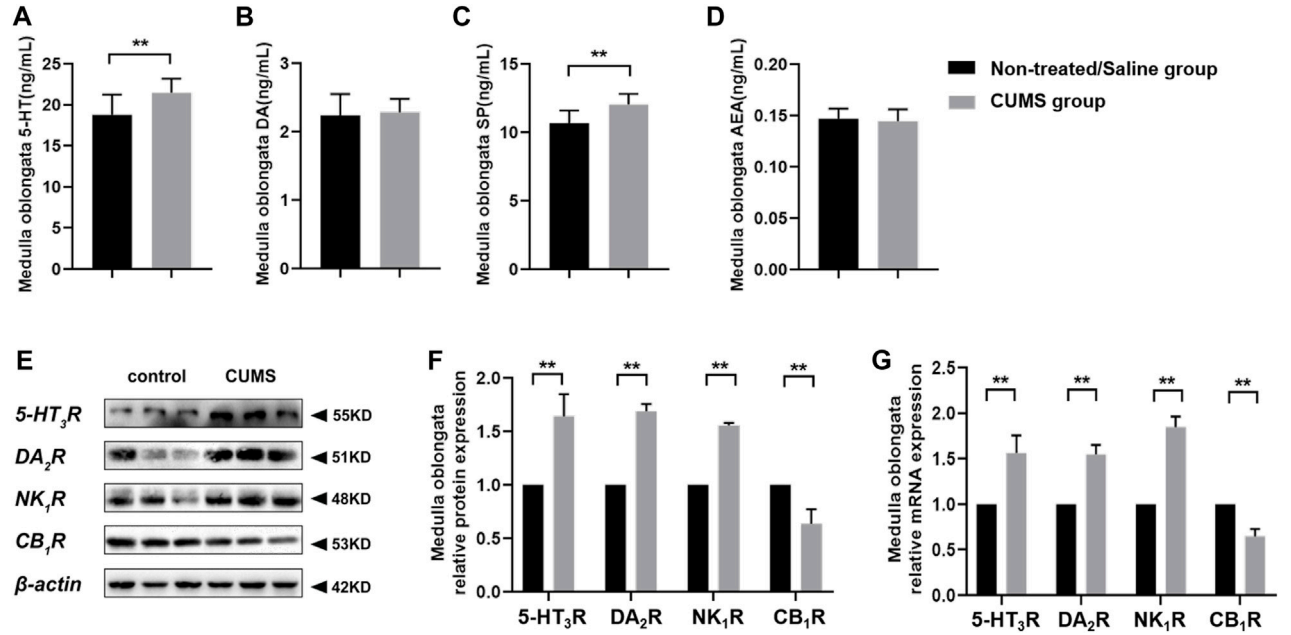

FIGURE 3 | Chronic stress increased 5-HT and SP levels, upregulated 5-HT_3R, DA_2R, and NK_1R expressions, and downregulated the CB_1R expression in the CNS (n = 10/group). **(A–D)** Vomit-related neurotransmitter levels in the medulla oblongata. **(E)** Representative Western blotting bands of vomit-related receptors. **(F)** Relative protein expression of vomit-related receptors in the medulla oblongata (normalization: experimental group (target protein/housekeeping protein)/control group (target protein/housekeeping protein)). **(G)** Relative mRNA expression of vomit-related receptors in the medulla oblongata (normalization: experimental group (target gene/housekeeping gene)/control group (target gene/housekeeping gene)). Data were expressed as mean ± SD. $^{**}p < 0.01$ (statistical comparisons between the two groups were performed using the two independent sample t-test).

1 week of adaptation. 24 h after administration, kaolin consumption was significantly increased both in the non-treated/cisplatin group and CUMS/cisplatin group compared to that in the non-treated/saline group (**Figure 2A**). Furthermore, the kaolin consumption in the CUMS/cisplatin group increased more significantly than that in the non-treated/cisplatin group ($p < 0.01$), suggesting that chronic stress aggravated vomit-like behavior (increased kaolin consumption). In addition, food intake was decreased in the non-treated/cisplatin group and CUMS/cisplatin group (**Figure 2B**). Chronic stress pretreatment enhanced the reduction of food in the CUMS/cisplatin group. However, there was no significant change in water consumption among the three groups (**Figure 2C**). Data revealed that cisplatin administration increased the kaolin consumption, and chronic stress pretreatment enhanced this effect in rats.

Chronic Stress Increases 5-HT and SP Levels, Upregulates 5-HT_3R, DA_2R, and NK_1R, and Downregulates the CB_1R Expression in the Medulla Oblongata

We further investigated the neurotransmitters and receptors involved in the mediation of emesis and the nausea level and receptor expression in the central nervous system (CNS) of the non-treated/saline group and CUMS group. Compared with the non-treated/saline group, chronic stress significantly increased 5-HT and SP levels in the CUMS group ($p < 0.01$). However, little change occurred in DA and AEA levels between the non-treated/saline group and CUMS group (**Figures 3A–D**). The immunoblotting and RT-qPCR assay results showed that chronic stress obviously upregulated 5-HT_3R, DA_2R, and NK_1R expressions but downregulated the CB_1R expression in the medulla oblongata in the CUMS group ($p < 0.01$) compared to those in the non-treated/saline group (**Figures 3E–G**). Results showed that chronic stress increased the levels of vomit-related neurotransmitters 5-HT and SP and altered vomit-related receptors' expression in the medulla oblongata, which means that more vomit-related neurotransmitters could combine with the corresponding vomit-related receptors and then affect the vomiting process.

Chronic Stress Does Not Alter 5-HT, DA, SP, and AEA Levels, but Downregulates 5-HT_3R, DA_2R, and NK_1R Expressions, and Upregulates the CB_1R Expression in Ileum Tissue

To figure out the effect of chronic stress on neurotransmitters involved in the mediation of emesis and nausea in ileum tissue, we measured the 5-HT, DA, SP, and AEA levels and 5-HT_3R, DA_2R, NK_1R, and CB_1R expressions. ELISA assay revealed that there was no significant change for relevant molecule levels between the non-treated/saline group and CUMS group (**Figures 4A–D**). In addition, the Western blot assay and RT-qPCR results displayed that chronic stress downregulated 5-

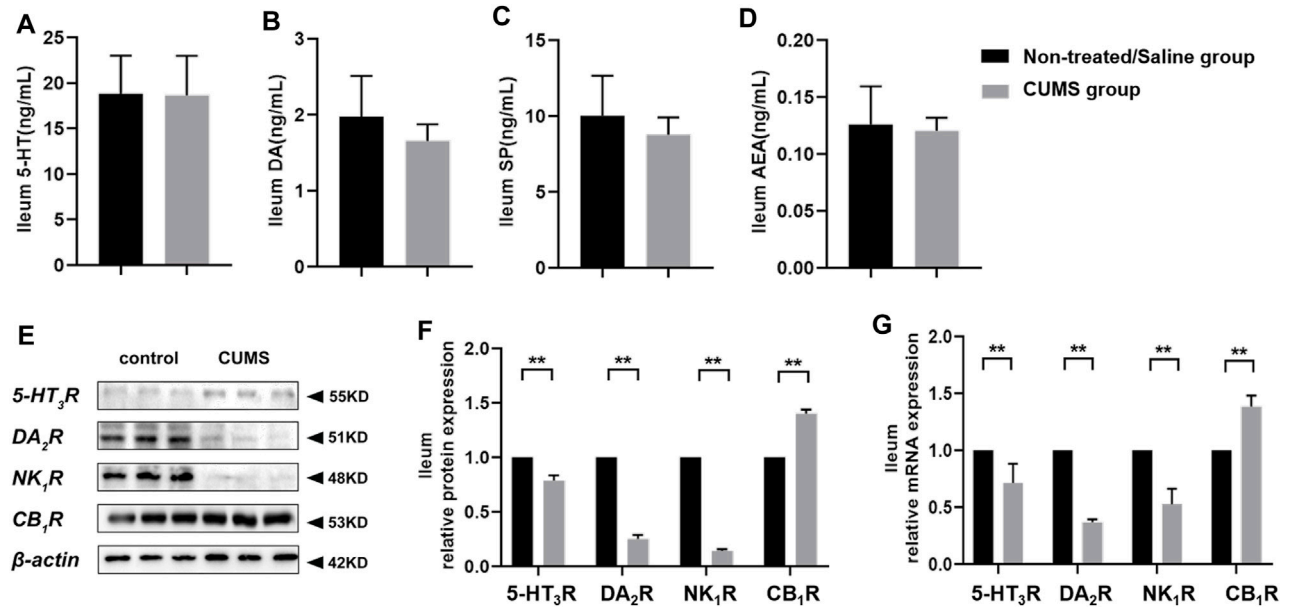

FIGURE 4 | Chronic stress did not alter 5-HT, DA, SP, and AEA levels, downregulated 5-HT_3R, DA_2R, and NK_1R expressions, and upregulated the CB_1R expression in the peripheral system (n = 10/group). **(A–D)** Vomit-related neurotransmitter levels in the ileum. **(E,F)** Representative Western blotting bands and relative protein expressions of vomit-related receptors in the ileum [normalization: experimental group (target protein/housekeeping protein)/control group (target protein/housekeeping protein)]. **(G)** Relative mRNA expression of vomit-related receptors in the ileum [normalization: experimental group (target gene/housekeeping gene)/control group (target gene/housekeeping gene)]. Data were expressed as mean ± SD. $^{**}p < 0.01$ (statistical comparisons between the two groups were performed using the two independent sample t-test).

HT_3R, DA_2R, and NK_1R expressions and upregulated the CB_1R expression in the ileum in the CUMS group ($p < 0.01$) compared to the non-treated/saline group (**Figures 4E–G**). We noticed that chronic stress did not significantly change the vomit-related neurotransmitters' level in the ileum, and the alteration of vomit-related receptors in the ileum was inconsistent with that in the CNS.

DISCUSSION

In this study, we established a chronic stress–induced depression-like behavior and cisplatin–induced pica rat model. Chronic stress pretreatment decreases food intake and significantly increases kaolin consumption after cisplatin injection, which suggest that chronic stress pretreatment induces anorexia and aggravates cisplatin-induced pica behavior. We explored the relevant molecule profile in this process and found for the first time that chronic stress might aggravate the vomiting progress *via* altering the level of neurotransmitters and the expression of receptors involved in the mediation of emesis and nausea in the central nervous system of rats.

Clinical evidences indicated that anorexia nervosa often occurs in individuals with stress, anxiety-like, or depression-like behavior (Lian et al., 2017; Lloyd et al., 2019), suggesting the possible association between mood disorder and anorexia. Similar to this finding, our previous work also noted that cancer chemotherapy patients with severe depression seemed more likely to have frequent and severe adverse drug reactions including anorexia, nausea, and fatigue (Zhou et al., 2010). Nausea and vomiting, one of the most terrible adverse reactions experienced by cancer patients, is associated with multiple risk factors including gender, age, anticancer drug dose, history of morning sickness, and alcohol intake. More and more researchers believe that depression and the anxiety mood disorder play a great role in chemotherapy-induced nausea and vomiting (Navari and Aapro, 2016; Kawazoe et al., 2018; Tsuji et al., 2019; Guo and Xu, 2020; Nasu et al., 2020). In addition, expectancy psychology of nausea and vomiting promote vomiting progress for cancer patients (Mosa et al., 2020).

Due to the special physiological structure, rodent animals like rats lack vomiting reflex. Therefore, vomiting in rats is assessed by pica behavior (Takeda et al., 1993). Cisplatin is a classic anticancer drug with high emetogenicity (Bamias et al., 2019), which causes severe nausea and vomiting, especially acute vomiting in cancer patients (Zhang et al., 2018). The cisplatin-induced pica rat model is a widely used animal model for antiemetic screening. Based on this pica model, we further confirmed that chronic stress–induced depression-like phenotype rats are more prone to displaying pica behavior (vomit-like behavior).

As the nausea and vomiting process involves various neurotransmitters and receptors (Di Maio et al., 2018), we studied the 5-HT, DA, SP, and AEA levels and 5-HT_3R, DA_2R, NK_1R, and CB_1R expressions in tissue and explored their possible change during the chronic stress process. The results suggested that 5-HT and SP elevation, as 5-HT_3R and

NK_1R expressions increase in the CNS, might play a crucial role in the chronic stress aggravating vomit. As elevated levels of 5-HT and SP are bound with highly expressed 5-HT_3R/NK_1R, vomiting response is triggered easily, frequently, and severely (Phillips et al., 2016). Why there is no change in 5-HT and SP levels in the ileum is worthy of further in-depth research.

In this study, we mainly focused on the effect of chronic stress on vomit-related molecules' level while not considering the antiemetic drug efficacy of rats. It would be beneficial to investigate the efficacy for the cisplatin-induced pica behavior in our chronic stress experimental condition in rats in future. In addition, recently, data have shown that different bedding in the cages may influence food intake (Lovasz et al., 2020); bedding change in our CUMS model establishment process might interfere with the results, and it might be an important limitation to the present study.

CONCLUSION

In this study, chronic stress aggravates cisplatin-induced anorexia and vomiting progress in rats which might be increasing the level of neurotransmitters 5-HT and SP, upregulating the expressions of receptors 5-HT_3R, DA_2R, and NK_1R, and downregulating the CB_1R expression in the central nervous system.

DATA AVAILABILITY STATEMENT

The raw data supporting the conclusions of this article will be made available by the authors, without undue reservation.

ETHICS STATEMENT

The animal study was reviewed and approved by The Animal Research Ethics Committee in Fengxian Hospital, Southern Medical University.

AUTHOR CONTRIBUTIONS

Experimental conception and design: FX. Experimental operation: ZG, JD, YC, WC, CY, ZY, and XL. Writing and revising the manuscript: ZG and FX. All authors reviewed the manuscript.

FUNDING

This work was supported by the Shanghai Municipal Science Commission [grant number 19411971700].

REFERENCES

Aapro, M. (2018). CINV: Still Troubling Patients after All These Years. *Support Care Cancer* 26, 5–9. doi:10.1007/s00520-018-4131-3

Antoniuk, S., Bijata, M., Ponimaskin, E., and Wlodarczyk, J. (2019). Chronic Unpredictable Mild Stress for Modeling Depression in Rodents: Meta-Analysis of Model Reliability. *Neurosci. Biobehav Rev.* 99, 101–116. doi:10.1016/j.neubiorev.2018.12.002

Bamias, A., Tzannis, K., Bamia, C., Harshman, L. C., Crabb, S., Plimack, E. R., et al. (2019). The Impact of Cisplatin- or Non-cisplatin-containing Chemotherapy on Long-Term and Conditional Survival of Patients with Advanced Urinary Tract Cancer. *Oncologist* 24, 1348–1355. doi:10.1634/theoncologist.2018-0739

Borner, T., Shaulson, E. D., Ghidewon, M. Y., Barnett, A. B., Horn, C. C., Doyle, R. P., et al. (2020). GDF15 Induces Anorexia through Nausea and Emesis. *Cell Metab.* 31, 351–362. e5. doi:10.1016/j.cmet.2019.12.004

Bray, F., Ferlay, J., Soerjomataram, I., Siegel, R. L., Torre, L. A., and Jemal, A. (2018). Global Cancer Statistics 2018: GLOBOCAN Estimates of Incidence and Mortality Worldwide for 36 Cancers in 185 Countries. *CA Cancer J. Clin.* 68, 1–31. doi:10.3322/caac.21492

Darmani, N. A., and Ray, A. P. (2009). Evidence for a Re-evaluation of the Neurochemical and Anatomical Bases of Chemotherapy-Induced Vomiting. *Chem. Rev.* 109, 3158–3199. doi:10.1021/cr900117p

Di Maio, M., Baratelli, C., Bironzo, P., Vignani, F., Bria, E., Sperti, E., et al. (2018). Efficacy of Neurokinin-1 Receptor Antagonists in the Prevention of Chemotherapy-Induced Nausea and Vomiting in Patients Receiving Carboplatin-Based Chemotherapy: A Systematic Review and Meta-Analysis. *Crit. Rev. Oncol. Hematol.* 124, 21–28. doi:10.1016/j.critrevonc.2018.02.001

Dranitsaris, G., Molassiotis, A., Clemons, M., Roeland, E., Schwartzberg, L., Dielenseger, P., et al. (2017). The Development of a Prediction Tool to Identify Cancer Patients at High Risk for Chemotherapy-Induced Nausea and Vomiting. *Ann. Oncol.* 28, 1260–1267. doi:10.1093/annonc/mdx100

Guo, Z., and Xu, F. (2020). Research Progress on Classification and Drug Therapy of Chemotherapy-Induced Nausea and Vomiting. *China Pharm.* 29, 1–6. doi:10.3969/j.issn.1006-4931.2020.22.001

Hawkins, R., and Grunberg, S. (2009). Chemotherapy-Induced Nausea and Vomiting: Challenges and Opportunities for Improved Patient Outcomes. *Clin. J. Oncol. Nurs.* 13, 54–64. doi:10.1188/09.CJON.54-64

Jordan, K., Jahn, F., and Aapro, M. (2015). Recent Developments in the Prevention of Chemotherapy-Induced Nausea and Vomiting (CINV): a Comprehensive Review. *Ann. Oncol.* 26, 1081–1090. doi:10.1093/annonc/mdv138

Kawazoe, H., Murakami, A., Yamashita, M., Nishiyama, K., Kobayashi-Taguchi, K., Komatsu, S., et al. (2018). Patient-related Risk Factors for Nausea and Vomiting with Standard Antiemetics in Patients with Breast Cancer Receiving Anthracycline-Based Chemotherapy: A Retrospective Observational Study. *Clin. Ther.* 40, 2170–2179. doi:10.1016/j.clinthera.2018.10.004

Li, N., Wang, Q., Wang, Y., Sun, A., Lin, Y., Jin, Y., et al. (2019). Fecal Microbiota Transplantation from Chronic Unpredictable Mild Stress Mice Donors Affects Anxiety-like and Depression-like Behavior in Recipient Mice via the Gut Microbiota-Inflammation-Brain axis. *Stress* 22, 592–602. doi:10.1080/10253890.2019.1617267

Li, Z., and Xu, F. (2020). Chronic Stress Alters Expression of Vomiting-related Receptors in CNS in SD Rats. *FASEB J.* 34, 06802. doi:10.1096/fasebj.2020.34.s1.06802

Lian, Q., Zuo, X., Mao, Y., Luo, S., Zhang, S., Tu, X., et al. (2017). Anorexia Nervosa, Depression and Suicidal Thoughts Among Chinese Adolescents: a National School-Based Cross-Sectional Study. *Environ. Health Prev. Med.* 22, 30. doi:10.1186/s12199-017-0639-2

Liu, M. Y., Yin, C. Y., Zhu, L. J., Zhu, X. H., Xu, C., Luo, C. X., et al. (2018). Sucrose Preference Test for Measurement of Stress-Induced Anhedonia in Mice. *Nat. Protoc.* 13, 1686–1698. doi:10.1038/s41596-018-0011-z

Liu, Y., Bai, S., Ma, J., Wu, F., Liu, J., Wu, Z., et al. (2015). Research Progress of Functional Diarrea Treated with Chinese Medicine. *J. Liaoning Univ. TCM* 17, 78–80. doi:10.13194/j.issn.1673-842x.2015.02.028

Lloyd, E. C., Haase, A. M., Foster, C. E., and Verplanken, B. (2019). A Systematic Review of Studies Probing Longitudinal Associations between Anxiety and Anorexia Nervosa. *Psychiatry Res.* 276, 175–185. doi:10.1016/j.psychres.2019.05.010

Lovasz, R. M., Marks, D. L., Chan, B. K., and Saunders, K. E. (2020). Effects on Mouse Food Consumption after Exposure to Bedding from Sick Mice or

Healthy Mice. *J. Am. Assoc. Lab. Anim. Sci.* 59, 687–694. doi:10.30802/AALAS-JAALAS-19-000154

Mersiades, A. J., Tognela, A., Haber, P. S., Stockler, M., Lintzeris, N., Simes, J., et al. (2018). Oral Cannabinoid-Rich THC/CBD Cannabis Extract for Secondary Prevention of Chemotherapy-Induced Nausea and Vomiting: a Study Protocol for a Pilot and Definitive Randomised Double-Blind Placebo-Controlled Trial (CannabisCINV). *BMJ Open* 8, e020745. doi:10.1136/bmjopen-2017-020745

Mosa, A. S. M., Hossain, A. M., Lavoie, B. J., and Yoo, I. (2020). Patient-Related Risk Factors for Chemotherapy-Induced Nausea and Vomiting: A Systematic Review. *Front. Pharmacol.* 11, 329. doi:10.3389/fphar.2020.00329

Nasu, I., Shimano, R., Kawazoe, H., Nakamura, T., Miura, Y., Takano, T., et al. (2020). Patient-related Risk Factors for Nausea and Vomiting with Standard Antiemetics in Patients with Cancer Receiving Carboplatin: A Retrospective Study. *Clin. Ther.* 42, 1975–1982. doi:10.1016/j.clinthera.2020.08.007

Natale, J. J. (2018). Overview of the Prevention and Management of CINV. *Am. J. Manag. Care* 24, S391–S397.

Navari, R. M., and Aapro, M. (2016). Antiemetic Prophylaxis for Chemotherapy-Induced Nausea and Vomiting. *New Engl. J. Med.* 374, 1356–1357. doi:10.1056/NEJMra1515442

Peng, L., and Liang, H. (1999). Depression and Functional Diseases of the Digestive Tract. *Shijie Huaren Xiaohua Zazhi* 7 (7), 601–602.

Phillips, R. S., Friend, A. J., Gibson, F., and Pizer, B. (2016). Antiemetic Medication for Prevention and Treatment of Chemotherapy-Induced Nausea and Vomiting in Childhood. *Cochrane Database Syst. Rev.* 2 (2), CD007786. doi:10.1002/14651858.CD007786.pub3

Takeda, N., Hasegawa, S., Morita, M., and Matsunaga, T. (1993). Pica in Rats Is Analogous to Emesis: an Animal Model in Emesis Research. *Pharmacol. Biochem. Be* 45, 817. doi:10.1016/0091-3057(93)90126-e

Tsuji, D., Suzuki, K., Kawasaki, Y., Goto, K., Matsui, R., Seki, N., et al. (2019). Risk Factors Associated with Chemotherapy-Induced Nausea and Vomiting in the Triplet Antiemetic Regimen Including Palonosetron or Granisetron for Cisplatin-Based Chemotherapy: Analysis of a Randomized, Double-Blind Controlled Trial. *Support Care Cancer* 27, 1139–1147. doi:10.1007/s00520-018-4403-y

Warr, D. (2018). Bringing it All Together in the Treatment of CINV: Application of Current Knowledge into Routine Clinical Practice. *Support Care Cancer* 26, 29–33. doi:10.1007/s00520-018-4117-1

Zhang, L., Lu, S., Feng, J., Dechaphunkul, A., Chang, J., Wang, D., et al. (2018). A Randomized Phase III Study Evaluating the Efficacy of Single-Dose NEPA, a Fixed Antiemetic Combination of Netupitant and Palonosetron, versus an Aprepitant Regimen for Prevention of Chemotherapy-Induced Nausea and Vomiting (CINV) in Patients Receiving Highly Emetogenic Chemotherapy (HEC). *Ann. Oncol.* 29, 452–458. doi:10.1093/annonc/mdx698

Zhao, Q., Wang, A., Gao, X., Li, L., and Zhao, J. (2020). Research Progress in Depression-like Rat Model Induced by Chronic Unpredictable Mild Stress. *Laboratory Animal Comp. Med.* 40, 344–353. doi:10.3969/j.issn.1674-5817.2020.04.012

Zhou, T., Duan, J. J., Zhou, G. P., Cai, J. Y., Huang, Z. H., Zeng, Y. T., et al. (2010). Impact of Depression Mood Disorder on the Adverse Drug Reaction Incidence Rate of Anticancer Drugs in Cancer Patients. *J. Int. Med. Res.* 38, 2153–2159. doi:10.1177/147323001003800631

Conflict of Interest: The authors declare that the research was conducted in the absence of any commercial or financial relationships that could be construed as a potential conflict of interest.

Publisher's Note: All claims expressed in this article are solely those of the authors and do not necessarily represent those of their affiliated organizations, or those of the publisher, the editors, and the reviewers. Any product that may be evaluated in this article, or claim that may be made by its manufacturer, is not guaranteed or endorsed by the publisher.

frontiers | Frontiers in Pharmacology

ORIGINAL RESEARCH
published: 22 July 2022
doi: 10.3389/fphar.2022.934467

Alanine Aminotransferase and Bilirubin Dynamic Evolution Pattern as a Novel Model for the Prediction of Acute Liver Failure in Drug-Induced Liver Injury

*Ruiyuan Yang[1†], Kexin Li[1†], Cailun Zou[1†], Aileen Wee[2], Jimin Liu[3], Liwei Liu[4], Min Li[5], Ting Wu[1], Yu Wang[1], Zikun Ma[1], Yan Wang[1], Jingyi Liu[6], Ang Huang[7], Ying Sun[7], Binxia Chang[7], Qingsheng Liang[7], Jidong Jia[1], Zhengsheng Zou[7] and Xinyan Zhao[1]**

[1]Liver Research Center, Beijing Friendship Hospital, Capital Medical University, National Clinical Research Center for Digestive Diseases, Beijing, China, [2]Department of Pathology, Yong Loo Lin School of Medicine, National University of Singapore, Singapore, Singapore, [3]Department of Pathology and Molecular Medicine, Faculty of Health Sciences, McMaster University, Hamilton, ON, Canada, [4]Fourth Department of Liver Disease (Difficult and Complicated Liver Diseases and Artificial Liver Center), Beijing You'an Hospital, Capital Medical University, Beijing, China, [5]Clinical Epidemiology and Evidence Base Medicine Unit, Beijing Friendship Hospital, Capital Medical University, Beijing, China, [6]Department of Critical Liver Diseases, Liver Research Center, Beijing Friendship Hospital, Capital Medical University, National Clinical Research Center for Digestive Diseases, Beijing, China, [7]Senior Department of Hepatology, The Fifth Medical Center of PLA General Hospital, Beijing, China

Aims: To develop, optimize, and validate a novel model using alanine aminotransferase (ALT) and total bilirubin (TB) dynamic evolution patterns in predicting acute liver failure (ALF) in drug-induced liver injury (DILI) patients.

Methods: The demographics, clinical data, liver biopsy, and outcomes of DILI patients were collected from two hospitals. According to the dynamic evolution of ALT and TB after DILI onset, the enrolled patients were divided into ALT-mono-peak, TB-mono-peak, double-overlap-peak, and double-separate-peak (DSP) patterns and compared. Logistic regression was used to develop this predictive model in both discovery and validation cohorts.

Results: The proportion of ALF was significantly higher in patients with the DSP pattern than in the ALT-mono-peak pattern and DOP pattern (10.0 vs. 0.0% vs. 1.8%,$p < 0.05$). The area under receiver operating characteristic curve (AUROC) of the DSP pattern model was 0.720 (95% CI: 0.682–0.756) in the discovery cohort and 0.828 (95% CI: 0.788–0.864) in the validation cohort in predicting ALF, being further improved by combining with international normalized ratio (INR) and alkaline phosphatase (ALP) (AUROC in the discovery cohort: 0.899; validation cohort: 0.958). Histopathologically, patients with the DSP pattern exhibited a predominantly cholestatic hepatitis pattern (75.0%, $p < 0.05$) with a higher degree of necrosis (29.2%, $p = 0.084$).

Conclusion: DILI patients with the DSP pattern are more likely to progress to ALF. The predictive potency of the model for ALF can be improved by incorporating INR and ALP.

OPEN ACCESS

Edited by:
Laura Grasa,
University of Zaragoza, Spain

Reviewed by:
Hartmut Jaeschke,
University of Kansas Medical Center Research Institute, United States
Ming-Hua Zheng,
First Affiliated Hospital of Wenzhou Medical University, China

***Correspondence:**
Xinyan Zhao
zhao_xinyan@ccmu.edu.cn

†These authors share first authorship

Specialty section:
This article was submitted to Gastrointestinal and Hepatic Pharmacology, a section of the journal Frontiers in Pharmacology

Received: 02 May 2022
Accepted: 08 June 2022
Published: 22 July 2022

Citation:
Yang R, Li K, Zou C, Wee A, Liu J, Liu L, Li M, Wu T, Wang Y, Ma Z, Wang Y, Liu J, Huang A, Sun Y, Chang B, Liang Q, Jia J, Zou Z and Zhao X (2022) Alanine Aminotransferase and Bilirubin Dynamic Evolution Pattern as a Novel Model for the Prediction of Acute Liver Failure in Drug-Induced Liver Injury. Front. Pharmacol. 13:934467. doi: 10.3389/fphar.2022.934467

This novel model allows for better identification of high-risk DILI patients, enabling timely measures to be instituted for better outcome.

Keywords: drug toxicity, predictive model, dynamic evolution pattern, clinical characteristic, clinical outcome

INTRODUCTION

There have been dramatic changes in recent decades in the spectrum of liver diseases with a far-reaching impact on healthcare systems worldwide. The majority of chronic hepatitis C patients can be cured (Dennis et al., 2021), and chronic hepatitis B can be effectively controlled (European Association for the Study of the Liver, 2017). Drug-induced liver injury (DILI) has gradually emerged as a relatively common clinical liver disease with significant derangement of liver biochemical tests. Epidemiological data suggest that the annual incidence of DILI is 2.7–13.9 per 100,000 in Europe and North America (Vega et al., 2017; Sgro et al., 2002); it is even higher in the Asia-Pacific region (Suk et al., 2012; Shen et al., 2019) with an annual incidence of 13.9–23.8 per 100,000.

DILI is the most common cause of acute liver failure (ALF) in Europe and North America (Khandelwal et al., 2011; Reuben et al., 2016; Stravitz and Lee, 2019), and the mortality associated with DILI-induced ALF is as high as 80% if liver transplantation had not been performed (Stravitz and Lee, 2019). A recent prospective study from the Drug-Induced Liver Injury Network (DILIN) found that 10% of patients died or required liver transplantation within 2 years of DILI onset, in 80% of which DILI played a major or contributory role. (Hayashi et al., 2017).

Early identification of DILI-induced ALF is critical in clinical practice so that timely measures can be adopted to improve the final outcome. Various predictive models of ALF have been established. Hyman Zimmerman's model (Hy's Law), the most impactful, was used for early prediction of ALF during drug development and in clinical settings. It was validated by the Spanish DILI registry (Andrade et al., 2005) Swedish Adverse Drug Reactions Advisory Committee (SADRAC) database (Björnsson and Olsson, 2005) and the US DILIN (Chalasani et al., 2008; Andrade and Robles-Díaz, 2020). Subsequently, Spanish scholars updated Hy's law and proposed a novel independent prognostic algorithm (named Robles-Diaz Model in our study) for DILI-induced ALF to achieve a better balance between sensitivity and specificity (Robles-Diaz et al., 2014; Lo Re et al., 2015). However, these models are based on specific values of liver biochemical parameter(s) at a single time point (onset/peak), and their predictive capability can certainly be improved. Whether the dynamic evolution patterns of ALT and TB in patients with DILI can be used as a new model to predict DILI-induced ALF has not been studied yet.

In this study, a novel model based on the dynamic evolution of ALT and TB in predicting DILI-induced ALF was established, optimized, and validated. The significance was to assist in early and accurate identification of high-risk DILI patients for timely intervention to improve clinical outcome.

PATIENTS AND METHODS

Study Subjects

The study population was divided into the discovery cohort and the validation cohort. From January 2016 to December 2018, the medical records of patients with DILI were retrieved as the discovery cohort at the Senior Department of Hepatology, the Fifth Medical Center of PLA General Hospital, Beijing, China. Additionally, patients between January 2013 and December 2020 at the Liver Research Center, Beijing Friendship Hospital, Capital Medical University, Beijing, China, were included in the external validation cohort.

1.1 Inclusion criteria: 1) Age ≥ 18 years; 2) the chronological sequence between drug and liver injury was clear; 3) the Roussel–Uclaf Causality Assessment Method (RUCAM) score is ≥6.

1.2 Exclusion criteria: 1) Acute viral hepatitis A to E, Epstein-Barr virus or cytomegalovirus infection, autoimmune liver diseases (autoimmune hepatitis, primary biliary cholangitis, and primary sclerosing cholangitis), non-alcoholic steatohepatitis, alcoholic liver disease, hereditary and metabolic liver diseases, biliary obstruction, and ischemic hepatitis; 2) systemic infections (such as sepsis); 3) organ transplantation; and 4) malignant tumor of the liver, bile duct, or pancreas.

Study Methods

Retrieval of Onset Data and Hospitalization Data

Demographic, clinical, and laboratory data at the onset and hospital admission were retrieved, including blood routine, liver biochemical tests, lipid profiles, international normalized ratio (INR), viral hepatitis, and autoimmune markers. The dynamic evolution of ALT and TB during the course of the disease was recorded, and the corresponding patterns were established.

Clinical Classification, Causality, and Severity of Drug-Induced Liver Injury

Clinical classification of DILI was based on the Council for International Organizations of Medical Sciences (CIOMS) criteria: hepatocellular injury type: $R \geq 5$, cholestatic: $R \leq 2$, and mixed: $2 < R < 5$ (Aithal et al., 2011).

The causality of the drug to liver injury was assessed using the Roussel Ucalaf causality assessment (RUCAM) (Danan and Teschke, 2015).

Severity of cases was graded as mild, moderate, severe, acute liver failure, and fatal according to the Chinese 2015 DILI guidelines (Yu et al., 2017).

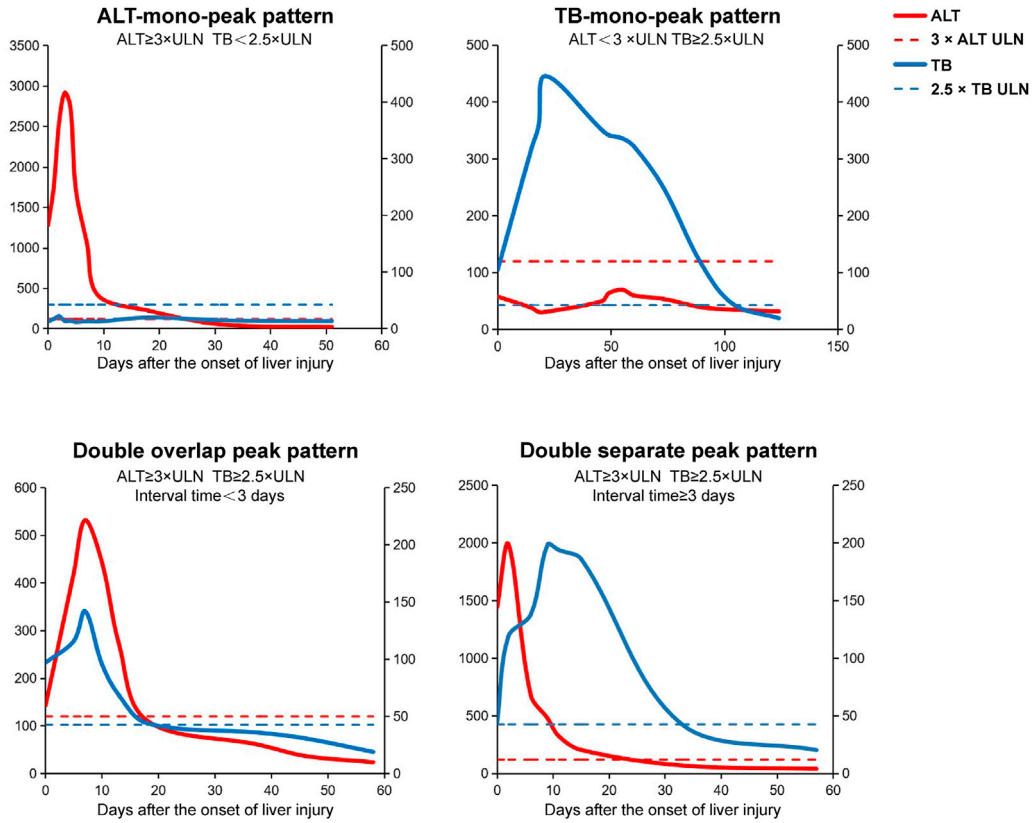

FIGURE 1 | Schematic diagram of the four different dynamic evolution patterns of ALT and TB in DILI. The ALT-TB dynamic evolution pattern is defined as the following four patterns: (1) ALT-mono-peak pattern, ALT ≥ 3×ULN, and TB < 2.5×ULN; (2) TB-mono-peak pattern, ALT < 3×ULN and TB ≥ 2.5×ULN; (3) ALT and TB double overlap peak pattern, ALT ≥ 3×ULN and TB ≥ 2.5×ULN, and the time interval between ALT and TB peak <3 days; (4) ALT and TB double separate peak pattern, ALT ≥ 3×ULN and TB ≥ 2.5×ULN, and the time interval between ALT and TB peaks ≥3 days. Abbreviations: DILI, drug-induced liver injury; ALT, alanine aminotransferase; TB, total bilirubin.

Criteria for Prediction Models of Drug-Induced Liver Injury-Induced Acute Liver Failure

The current prediction models are as follows:

(i) Hy's law: ALT or AST >3×ULN and TB > 2×ULN, ALP <2×ULN (Temple, 2006);
(ii) New Hy's law (nHy's law): TB > 2×ULN, nR ≥ 5 [nR value defined as (measured highest ALT or AST/their ULN)/(measured ALP/ALP ULN)] (Robles-Diaz et al., 2014); and
(iii) Robles-Diaz Model (Robles-Diaz et al., 2014): AST >17.3×ULN and TB > 6.6×ULN, or AST ≤17.3×ULN, but AST/ALT >1.5 (Björnsson and Olsson, 2005).

Definition of Alanine Aminotransferase-Total Bilirubin Dynamic Evolution Patterns

In order to establish a new prediction model for predicting ALF after the onset of DILI, the ALT-TB dynamic evolution patterns are defined as the following four patterns (**Figure 1**): 1) ALT-mono-peak pattern: ALT ≥3×ULN and TB < 2.5×ULN; 2) TB-mono-peak pattern: ALT <3×ULN and TB ≥ 2.5×ULN; 3) ALT and TB double overlap peak (DOP) pattern: ALT ≥3×ULN and TB ≥ 2.5×ULN, with the time interval between ALT and TB peaks being <3 days; and 4) ALT and TB double separate peak (DSP) pattern: ALT ≥3×ULN and TB ≥ 2.5×ULN, with the time interval between ALT and TB peaks being ≥3 days.

Assessment of Liver Pathology

The liver biopsies were stained with hematoxylin and eosin (H&E), reticulin, Masson trichrome, periodic acid-Schiff with diastase (PAS-D), cytokeratin 7 (CK7), and CK19. Liver biopsies of enrolled patients (if any) were reviewed and classified by a clinical liver pathologist (XYZ) according to the pathological classification of DILI by Kleiner et al. (2014) and Wang et al. (2019).

Follow-Up and Definition of Clinical Outcomes for Drug-Induced Liver Injury

Follow-up within 1 year of DILI onset was achieved by means of a hospital management system (HIS) query, telephone consultation, and post-discharge laboratory test records. The clinical outcomes included ALF or death/liver transplantation.

The definition of ALF is according to the American Association for the Study of Liver Diseases (AASLD) guideline

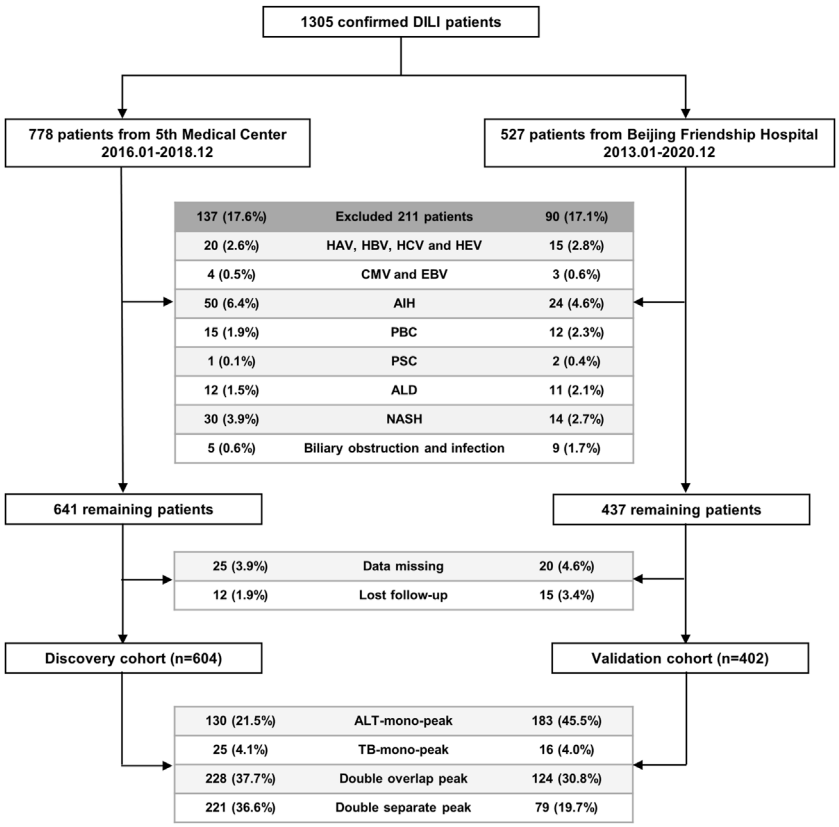

FIGURE 2 | Flowchart of the enrolled patients with DILI in the discovery and validation cohorts. Abbreviations: DILI, drug-induced liver injury; HAV, hepatitis A virus; HBV, hepatitis B virus; HCV, hepatitis C virus; HEV, hepatitis E virus; CMV, cytomegalovirus; EBV, Epstein-Barr virus; AIH, autoimmune hepatitis; PBC, primary biliary cholangitis; PSC, primary sclerosing cholangitis; ALD, alcoholic liver disease; NASH, non-alcoholic steatohepatitis; ALT, alanine aminotransferase; TB, Total bilirubin.

for the management of ALF (Polson and Lee, 2005). Liver-related deaths include (Hayashi et al., 2017) 1) DILI directly causing death and 2) aggravation of DILI or induction of another fatal disease (e.g., sepsis, multiorgan failure, and others).

Statistical Analysis

All data were analyzed using R version 3.3.3 and SPSS software (version 21.0; IBM Corp., Armonk, NY). Differences between groups were analyzed by ANOVA analysis for normally distributed variables, the Kruskal–Wallis H-test for non-normally distributed continuous variables, and the Chi-square test for categorical data. Mann–Whitney *U* tests were performed for multiple comparisons. Bilateral $p < 0.05$ was regarded as statistical difference.

The receiver operating characteristic (ROC) curves were used to analyze the prognostic performance of the previously published models and our novel model, and the area under ROC curve (AUROC) of the different models was compared by the Delong method. Logistic regression and the bootstrap method were used to develop and validate the optimized model in discovery and validation cohorts. In logistic regression, variables with $p < 0.05$ in the univariate analysis were screened as input variables and independent variables were screened using a likelihood ratio-based forward method to establish a logistic regression model.

This study has been approved by the Medical Ethics Committee of Beijing Friendship Hospital, Capital Medical University (Approval No.: 2020-P2-071-01), and the informed consent form has been waived.

RESULTS

Demographic and Clinical Characteristics According to Alanine Aminotransferase-Total Bilirubin Dynamic Evolution Patterns

Patients diagnosed with DILI at the Fifth Medical Center of PLA General Hospital were enrolled in the discovery cohort (604 cases) from January 2016 to December 2018, and patients diagnosed with DILI at the Beijing Friendship Hospital, Capital Medical University, were enrolled in the external validation cohort (402 cases) from January 2013 to December 2020 (**Figure 2**).

In the discovery cohort, 372 out of 604 cases (61.6%) were female, with a median age of 49 years. The common clinical symptoms were jaundice (78.6%), fatigue (74.2%), and poor appetite (70.5%). Hepatocellular injury was predominant

TABLE 1 | Comparison of the demographic data and liver biochemical parameters among the four ALT-TB dynamic evolution patterns in DILI.

Discovery cohort	Total (*n* = 604)	ALT-mono-peak (*n* = 130)	TB-mono-peak (*n* = 25)	ALT and TB double overlap peak (*n* = 228)	ALT and TB double separate peak (*n* = 221)	*p* value
Female (n, %)	372 (61.6)	90 (69.2)	14 (56.0)	137 (60.1)	131 (59.3)	0.235
Age (years)	49.0 (40.0, 57.0)	50.0 (39.0, 58.0)	54.0 (49.00, 62.0)	48.5 (40.0, 56.0)	48.0 (40.0, 57.0)	0.111
BMI (kg/m^2)	23.3 (21.3, 25.4)	23.9 (22.1, 25.4)	22.1 (19.0, 24.9)	23.1 (21.4, 25.3)	23.3 (21.2, 25.4)	0.209
Latency (days)	27.0 (10.0, 50.0)	30.0 (12.0, 60.0)	30.0 (14.0, 90.0)	30.0 (10.0, 60.0)	20.0 (10.0, 40.0)	0.404
R-value at onset	17.0 (6.9, 31.2)	15.2 (9.4, 29.5)	0.9 (0.5, 1.8)	20.1 (9.5, 32.7)	16.4 (5.7, 32.1)	**<0.001**◆▲▼
Selected liver biochemical tests at DILI onset						
ALT (U/L)	809.5 (321.8, 1262.8)	570.0 (324.0, 954.0)	67.0 (41.0, 85.0)	950.5 (506.0, 1307.5)	843.0 (338.0, 1422.0)	**<0.001**◆●★▲▼
AST (U/L)	546.5 (203.8, 931.0)	352.0 (187.0, 692.0)	60.0 (47.0, 86.0)	668.5 (335.0, 956.5)	605.0 (223.0, 1026.0)	**<0.001**◆●★▲▼
ALP (U/L)	166.0 (127.0, 226.0)	131.0 (94.0, 180.0)	235.0 (196.0, 348.0)	168.5 (130.5, 215.0)	178.0 (140.0, 246.0)	**<0.001**◆●★▲▼
GGT (U/L)	179.0 (100.3, 311.8)	137.0 (72.0, 250.0)	114.0 (62.0, 431.0)	183.0 (117.5, 328.5)	206.0 (118.0, 308.0)	**<0.001**●★
TB (μmol/L)	113.5 (40.5, 200.1)	19.9 (14.7, 26.5)	131.0 (114.5, 311.9)	140.7 (88.9, 232.0)	150.0 (90.2, 207.5)	**<0.001**◆●★
DB (μmol/L)	79.8 (22.6, 148.5)	8.0 (5.5, 13.8)	104.9 (65.8, 254.0)	100.1 (60.2, 175.1)	105.7 (64.0, 153.3)	**<0.001**◆●★
ALB (g/L)	36.0 (32.0, 38.0)	38.0 (36.0, 41.0)	33.0 (30.0, 36.0)	36.0 (32.0, 38.0)	34.0 (31.0, 37.0)	**<0.001**◆●★▲†
CHE (KU/L)	5439.0 (4367.0, 6480.0)	6602.0 (5677.0, 7685.0)	4681.0 (2586.0, 5280.0)	5458.0 (4502.0, 6429.0)	4823.0 (3900.0, 5870.0)	**<0.001**◆●★▲†
TBA (μmol/L)	80.5 (15.0, 219.8)	8.0 (4.0, 15.0)	94.0 (33.0, 247.0)	62.0 (18.0, 179.5)	204.0 (115.0, 283.0)	**<0.001**◆●★†
Cr (μmol/L)	64.0 (52.0, 76.0)	61.0 (52.0, 73.3)	57.0 (47.0, 76.0)	63.0 (52.0, 75.0)	67.0 (55.0, 81.5)	**0.009**★
CHOL (mmol/L)	3.9 (3.2, 4.8)	4.2 (3.5, 4.9)	4.2 (3.5, 4.9)	4.0 (3.4, 4.7)	3.6 (2.9, 4.7)	**0.003**★
TG (mmol/L)	2.1 (1.4, 3.2)	1.2 (1.0, 1.6)	3.2 (2.5, 4.2)	2.0 (1.4, 2.7)	2.9 (2.2, 4.0)	**<0.001**◆●★▲†
INR	1.0 (0.9, 1.1)	1.0 (0.9, 1.0)	1.0 (0.9, 1.0)	1.0 (0.9, 1.1)	1.0 (1.0, 1.2)	**<0.001**●★▼†
Selected liver biochemical tests at their peak time						
ALT (U/L)	829.5 (365.5, 1276.3)	603.0 (386.0, 1080.0)	81.0 (61.0, 97.0)	961.5 (518.0, 1334.0)	855.0 (405.0, 1455.0)	**<0.001**◆●▲▼
AST (U/L)	583.5 (247.3, 965.8)	378.0 (222.0, 703.0)	82.0 (58.0, 109.0)	675.5 (372.0, 963.5)	657.0 (272.0, 1095.0)	**<0.001**◆●★▲▼
ALP (U/L)	185.5 (139.3, 244.0)	142.0 (106.0, 202.0)	294.0 (210.0, 401.0)	180.0 (138.0, 232.5)	206.0 (157.0, 281.0)	**<0.001**◆●★▲▼†
GGT (U/L)	202.0 (117.0, 365.0)	170.0 (79.0, 311.0)	133.0 (92.0, 494.0)	206.5 (129.0, 386.5)	230.0 (137.0, 353.0)	**<0.001**●★
TB (μmol/L)	145.9 (53.9, 281.6)	21.2 (15.7, 29.3)	307.8 (145.1, 386.8)	142.4 (89.5, 235.35)	260.9 (159.1, 361.5)	**<0.001**◆●★†

Abbreviations: DILI, drug-induced liver injury; BMI, body mass index; ALT, alanine aminotransferase; AST, aspartate aminotransferase; ALP, alkaline phosphatase; GGT, glutamyltransferase; TB, total bilirubin; DB, direct bilirubin; ALB, albumin; CHE, cholinesterase; TBA, total bile acid; Cr, creatinine; CHOL, cholesterol; TG, triglycerides; INR, International normalized ratio. Data were presented as median (quartile). ◆*There is a statistical difference between ALT-mono-peak and TB-mono-peak.* ●*There is a statistical difference between ALT-mono-peak and double overlap peak.* ★*There is a statistical difference between ALT-mono-peak and double separate peak.* ▲*There is a statistical difference between TB-mono-peak and double overlap peak.* ▼*There is a statistical difference between TB-mono-peak and double separate peak.* †*There is a statistical difference between double overlap peak and double separate peak.*

(80.0%). There was no significant difference in age, sex, latency, and BMI among the four dynamic evolution patterns ($p > 0.05$) (**Table 1**). The median hospitalization time was significantly longer (23.0 days) in patients with the DSP pattern.

At DILI onset, ALT, AST, ALP, GGT, TB, DB, and INR were significantly higher in the two double-peak patterns than in the ALT-mono-peak pattern ($p < 0.05$) (**Table 1**). Furthermore, INR levels were significantly higher in the DSP pattern than in the DOP pattern. Total bile acid (TBA) levels were significantly higher in the DSP pattern than in the ALT-mono-peak pattern and DOP pattern ($p < 0.05$), and its median values were 20 times higher than the upper limit of normal. Albumin (ALB) and cholinesterase (CHE) levels were significantly lower in the DSP pattern than that in the ALT-mono-peak pattern and DOP pattern ($p < 0.05$). At the peak level of biochemical tests, TB and ALP were significantly higher in the DSP pattern than in the ALT-mono-peak pattern and DOP pattern ($p < 0.05$). The proportion of ALF was significantly higher in patients with the DSP pattern than in the ALT-mono-peak pattern and DOP pattern (10.0 vs. 0.0% vs. 1.8%, $p < 0.05$) (**Table 2**).

Comparison of Clinical Characteristics and Laboratory Data at Drug-Induced Liver Injury Onset Between the ALF/non-ALF Group and Drug-Induced Liver Injury With/Without Non-Alcoholic Fatty Liver Disease Group

The laboratory tests at DILI onset showed that INR, TB, and TBAs were significantly higher, while ALB was significantly lower in the ALF group than in the non-ALF group ($p < 0.05$) (**Supplementary Table S4**). No significant difference in ALT, AST, ALP, and GGT was found between the two groups (**Supplementary Table S4**). In the discovery cohort, 99 of 604 cases (16.3%) had underline NAFLD. No significant difference was found in the outcomes of ALF and liver-related death/LT between the two groups (**Supplementary Table S5**). There was no significant difference between the

TABLE 2 | Comparison of clinical classification, severity, and outcomes among the four ALT-TB dynamic evolution patterns in DILI.

Discovery cohort	Total (*n* = 604)	ALT-mono-peak (*n* = 130)	TB-mono-peak (*n* = 25)	ALT and TB double overlap peak (*n* = 228)	ALT and TB double separate peak (*n* = 221)	*p* value
Injury pattern, n (%)						**<0.001**
Hepatocellular	483 (80.0)	116 (89.2)	0 (0.0)	197 (86.4)	170 (76.9)	◆★▲▼
Cholestatic	43 (7.1)	2 (1.5)	20 (80.0)	9 (3.9)	12 (5.4)	◆▲▼
Mixed	78 (12.9)	12 (9.2)	5 (20.0)	22 (9.6)	39 (17.6)	
Culprit drug(s), n (%)						**0.017**
HDS	302 (50.0)	48 (36.9)	12 (48.0)	121 (53.1)	121 (53.1)	●★
Drugs	119 (19.7)	34 (26.2)	7 (28.0)	35 (15.4)	43 (19.5)	
HDS + Drugs	183 (30.3)	48 (36.9)	6 (24.0)	72 (31.6)	57 (25.8)	
Severity, n (%)						**<0.001**
Mild	155 (25.7)	130 (100.0)	2 (8.0)	0 (0.0)	23 (10.4)	◆●★▲†
Moderate	79 (13.1)	0 (0.0)	3 (12.0)	52 (22.8)	24 (10.9)	◆●★†
Severe	339 (56.1)	0 (0.0)	17 (68.0)	172 (75.4)	150 (67.9)	◆●★
ALF/Fatal	31 (5.1)	0 (0.0)	3 (12.0)	4 (1.8)	24 (10.9)	◆★▲†
Outcomes, n (%)						
Acute liver failure	28 (4.6)	0 (0.0)	2 (8.0)	4 (1.8)	22 (10.0)	**<0.001**◆★†
Liver-related Death/LT	13 (2.2)	0 (0.0)	2 (8.0)	0 (0.0)	11 (5.0)	**<0.001**◆▲†
Duration of hospitalization (days), n (%)	15.0 (11.0–23.0)	11.0 (7.0–15.0)	15.0 (10.0–29.0)	13.5 (9.0–19.0)	23.0 (15.0–32.0)	**<0.001**◆●★†

Abbreviations: DILI, drug-induced liver injury; HDS, herbal and dietary supplements; ALT, alanine aminotransferase; TB, total bilirubin; ALF, acute liver failure; LT, liver transplantation. Data were presented as median (quartile). ◆*There is a statistical difference between ALT-mono-peak and TB-mono-peak.* ●*There is a statistical difference between ALT-mono-peak and double overlap peak.* ★*There is a statistical difference between ALT-mono-peak and double separate peak.* ▲*There is a statistical difference between TB-mono-peak and double overlap peak.* ▼*There is a statistical difference between TB-mono-peak and double separate peak.* †*There is a statistical difference between double overlap peak and double separate peak.*

DILI with NAFLD and DILI without the NAFLD group except for BMI, GGT, and the proportion of females (**Supplementary Table S5**).

Prediction of Acute Liver Failure According to Alanine Aminotransferase-Total Bilirubin Dynamic Evolution Patterns

As shown in **Table 2**, the two double-peak pattern groups had a significantly higher proportion of ALF than the two mono-peak pattern groups: 22 cases (10.0%) in the DSP and four (1.8%) in the DOP patterns but none in the ALT-mono-peak pattern ($p < 0.001$). The DSP pattern had the worst outcomes—22 patients (10.0%) developed ALF and 11 (5%) developed liver-related death.

As a novel model for the prediction of ALF, the sensitivity and specificity of the DSP pattern were 78.6 and 65.5%, respectively. The AUROC of the DSP model was 0.720 (95% CI: 0.682–0.756), whereas the AUROCs of Hy's law, nHy's law, and Robles-Diaz Model were 0.515 (95% CI: 0.474–0.555), 0.583 (95% CI: 0.543–0.623), and 0.635 (95% CI: 0.595–0.673), respectively (**Table 3**). The AUROC of the DSP model was significantly superior to the Hy's law and nHy's law models (**Figure 3**) ($Z = 3.386$, $p < 0.001$ or $Z = 2.757$, $p = 0.006$), comparable with the Robles-Diaz Model ($Z = 1.296$, $p = 0.195$).

The AUROC of the DSP pattern in DILI with NAFLD patients was 0.859 (95% CI: 0.775–0.921), with a sensitivity of 100.0% and a specificity of 71.9%.

Verification of Alanine Aminotransferase-Total Bilirubin Dynamic Evolution Patterns in the Prediction of Acute Liver Failure

We conducted both internal and external verification on the potency of the DSP model in predicting DILI-induced ALF. A validity evaluation of the DSP model using internal validation was performed by bootstrap methods. The AUROC of the DSP model was 0.720 (95% CI:0.682–0.756), and the Brier score used to assess the calibration of the model was 0.044.

An additional independent 402 patients were enrolled in the external validation cohort. The patients were also mainly females (70.1%), the median age of onset was 57.0 years, and the main clinical type was hepatocellular injury (60.9%) (**Supplementary Table S1**). The median hospitalization time was significantly longer (14.0 days) in patients with the DSP pattern. The rates of ALF (12.7%) and DILI-induced deaths or liver transplantation (3.8%) in the DSP group were higher than that in other groups but without significance (**Supplementary Table S2**). The AUROC of the DSP model for predicting ALF in the validation cohort was 0.828 (95% CI: 0.788–0.864) with a Brier score of 0.027 (**Table 3**).

TABLE 3 | Comparison of the double separate peak model with existing prediction models.

	Discovery cohort				Validation cohort	
	AUROC (95% CI)	***p* Value**	**Sensitivity (%)**	**Specificity (%)**	**AUROC (95% CI)**	***p* Value**
Hy's Law	0.515 (0.474–0.555)	<0.001	67.86	35.07	0.723 (0.677–0.766)	<0.001
nHy's Law	0.583 (0.543–0.623)	<0.001	82.14	34.55	0.696 (0.648–0.740)	<0.001
Robles-Diaz Model	0.635 (0.595–0.673)	<0.001	57.14	69.79	0.838 (0.799–0.873)	0.038
Double separate peak model	0.720 (0.682–0.756)	<0.001	78.57	65.45	0.828 (0.788–0.864)	0.034
Optimized double separate peak model	0.899 (0.872–0.922)	Ref	75.00	90.45	0.958 (0.933–0.975)	Ref

Abbreviations: AUROC, area under receiver operating characteristic; CI, confidence interval; nHy's law, new Hy's law. AUROC of Hy's law, nHy's law, Robles-Diaz Model, and ALT and TB double separate peak models were all compared with the optimized double separate peak model.

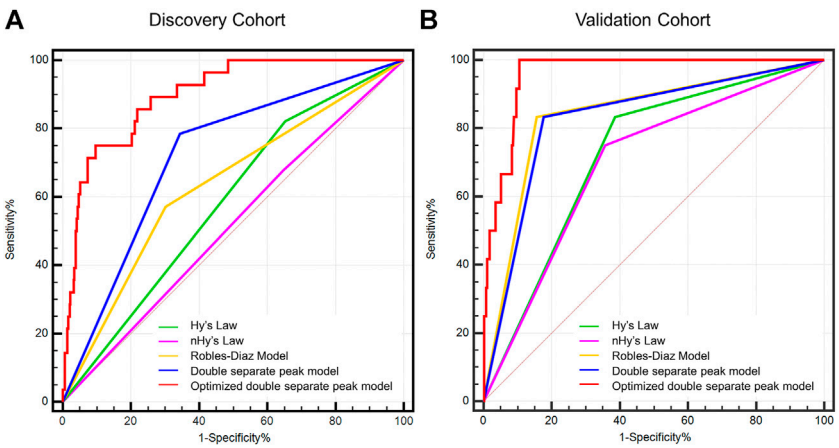

FIGURE 3 | Potency comparison among different models in predicting DILI-induced ALF. The AUROC of the DSP model was significantly superior to that of Hy's law and nHy's law models and comparable with the Robles-Diaz Model. The prediction potency of ALF was further improved when incorporated with INR and ALP at DILI onset, which was significantly better than the three previous models with an AUROC for predicting DILI-induced ALF of 0.899 (95% CI: 0.87–0.921) in the discovery cohort and 0.958 (95% CI: 0.933–0.975) in the validation cohort, respectively [Figure **(A)** and **(B)**]. Abbreviations: AUROC, area under receiver operating characteristic; DSP, ALT, and TB double separate peak patterns; nHy's Law, new Hy's Law; DILI, drug-induced liver injury; ALT, alanine aminotransferase; TB, total bilirubin.

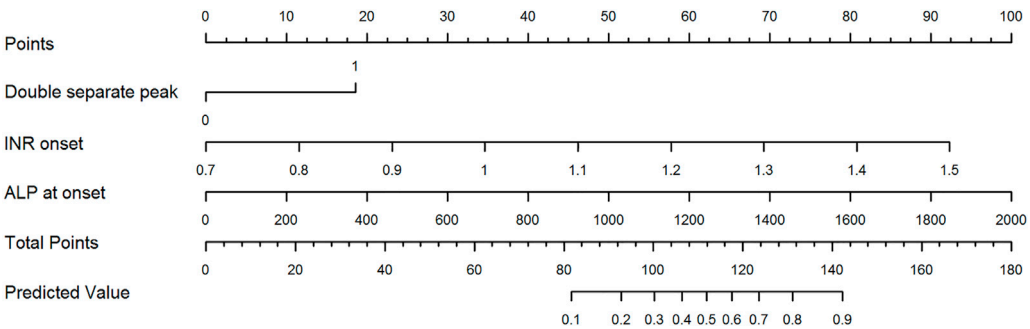

FIGURE 4 | Optimized double separate peak model with INR and ALP at DILI onset. Points are assigned for double separate peak, INR, and ALP at DILI onset using the linear points scale at the top of the figure. The risk of acute liver failure correlating with the total points is on the two linear scales at the bottom of the figure. Abbreviations: ALP, alkaline phosphatase; INR, international normalized ratio.

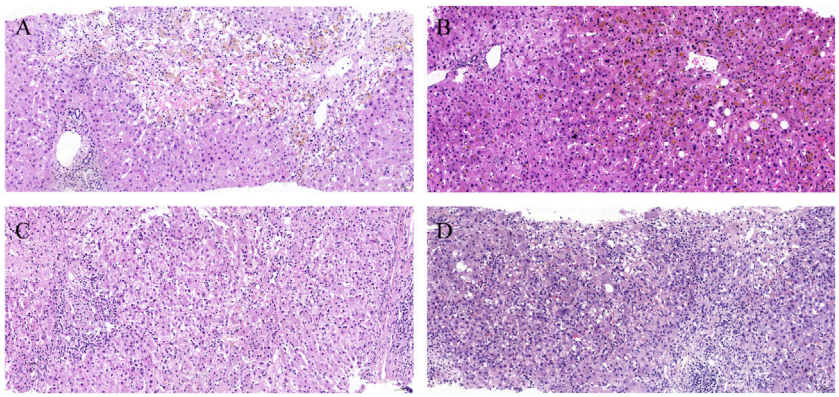

FIGURE 5 | Histological injury patterns. **(A)** Histological acute hepatitis pattern (lobular necroinflammation with cholestasis) mainly correlated with the ALT-mono-peak pattern. **(B)** Histological acute cholestasis pattern (hepatocellular and canalicular cholestasis without obvious necroinflammation) mainly correlated with the TB-mono-peak pattern. **(C)** Histological cholestatic hepatitis pattern (mild to moderate lobular necroinflammation with mild cholestasis) mainly correlated with the ALT and TB double overlap peak pattern. **(D)** Histological cholestatic hepatitis pattern (moderate to severe lobular necroinflammation with moderate cholestasis) mainly correlated with ALT and TB double separate peak patterns. Abbreviations: ALT, alanine aminotransferase; TB, total bilirubin.

Optimization of the Double Separate Peak Model by Incorporation of International Normalized Ratio and Alkaline Phosphatase at Drug-Induced Liver Injury Onset

In light of the role of laboratory parameters other than ALT and TB in the prognostic assessment of DILI, the logistic regression model was used to screen for risk factors for the development of ALF in patients with DILI. When the variables with p value <0.05 were included in the multivariate analysis, it was found that INR (OR = 11.8, $p < 0.001$) and ALP at DILI onset (OR = 1.004, $p = 0.002$), complementary with the DSP model (OR = 3.906, $p = 0.007$), were independent risk factors for the development of ALF in patients with DILI, and the logistic regression model was as follows: Logistic (p) = 1.347 × DSP pattern + 8.363 × INR + 0.004 × ALP (**Figure 4**).

Then, we investigated the predictive potency for ALF of the incorporated DSP model with INR and ALP at DILI onset. In the discovery cohort, the AUROC of the optimized model was found to be 0.899 (95% CI: 0.872–0.922), with a sensitivity of 75.0% and a specificity of 90.5%, which was superior to the DSP model alone and the three previous models (**Figure 3**; **Table 3**). Internal validation by bootstrap shows that the AUROC was 0.892 with a Brier score of 0.038. The AUROC and Brier scores in the independent validation cohort were 0.958 (95% CI: 0.933–0.975) and 0.022, respectively. Additionally, the AUROC in DILI with NAFLD patients of the optimized model was 0.896 (95% CI: 0.818–0.948), with a sensitivity of 100.0% and a specificity of 81.3%. The value of this new model in the subgroup of DILI with NAFLD has similar predictive potency compared to all DILI patients in terms of ALF.

Comparison of Pathological Classification According to Alanine Aminotransferase-Total Bilirubin Dynamic Evolution Patterns

A total of 227 patients enrolled in the discovery cohort underwent liver biopsy during hospitalization. Histological injury patterns were shown in **Figure 5**. The patients with the DSP pattern had predominantly cholestatic hepatitis (75.0%), which was significantly higher than that in the ALT-mono-peak pattern ($p < 0.05$) (**Supplementary Table S3**). The histological degree of moderate or severe and severe necrosis trended higher in the DSP pattern (29.2%) than in the ALT-mono-peak (11.8), TB-mono-peak (20.0), and DOP (23.2%) patterns.

DISCUSSION

DILI is the leading cause of ALF in Europe and North America (Stravitz and Lee, 2019) and the third leading cause in China (You et al., 2013; Medina-Caliz et al., 2016). Timely and accurate identification of DILI-induced ALF is the prerequisite for improving the prognosis. Currently, the prognostic models of DILI, such as Hy's law, nHy's law, and Robles-Diaz Model, are based on single-point biochemical markers at onset or peak time. In this study, we categorized the dynamic evolution patterns of ALT-TB after DILI onset into four patterns: ALT-mono-peak pattern, TB-mono-peak pattern, DOP pattern, and DSP pattern. The patients with the DSP pattern had significantly more severe disease with a significantly longer hospital stay than other patterns, with an AUROC for predicting DILI-induced ALF of 0.720 (95% CI: 0.682–0.756), a sensitivity of 0.79, and a specificity of 0.66. When we incorporated ALP and INR at DILI onset to the new dynamic model, the AUROC of the optimized model was 0.899 (95% CI: 0.872–0.922) with improvement in both sensitivity and specificity. Furthermore, our results had been validated by an independent external DILI cohort.

The advantages of the new model are the following: first, the most common liver biochemical parameters, namely, ALT and TB, were used—this was simple, not restricted by region, and especially useful in developing countries. The prediction potency can be further improved if incorporated with INR and ALP at DILI onset. Second, we defined the criteria for the dynamic biochemical patterns. DILI patients would usually have the results of a set of their liver biochemical tests before admission. According to these

biochemical data, we can easily determine whether ALT or TB is solely or doubly elevated, that is, the mono-peak or double peak patterns. When the liver biochemical tests are checked again during hospitalization, any further increase in TB would implicate the DSP pattern. In the enrolled patients, 86.0% of the DSP pattern was confirmed within 1 week of admission thus implying timely determination of the dynamic patterns without any delay.

In comparison with other predictive models, the DSP model had significantly higher predictive capability of ALF. This is due to it being based not only on the key parameters at onset or peak level but also on the changes within a short period of time, depicting the whole picture along with the natural course of DILI. The kinetics of liver biochemical markers have been used in prediction of treatment response in alcoholic hepatitis, (Rachakonda et al., 2020), chronic hepatitis C (pegylated interferon and ribavirin) (Lee et al., 1998), and acute severe autoimmune hepatitis (Rahim et al., 2020). In the study, we employed them in the prediction of ALF in DILI.

Furthermore, our data showed that DILI patients with or without underlying NAFLD had similar clinical outcomes in terms of ALF and liver-related death/LT. However, the recent guideline suggested that the patients with NASH rather than NAFLD may have an increased risk of severe liver injury and adverse outcome (Regev et al., 2019). Since it is not possible to biopsy all patients with underlying NAFLD to discriminate between NAFL and NASH, the well-accepted non-invasive markers for this discrimination are highly warranted in the field.

Liver pathology determines the severity of liver injury by the lesion characteristic, injury degree, and the regeneration mode, which determines the clinical severity of DILI[22] (Kleiner, 2018; Kleiner, 2017). Comparison of the histological patterns of DILI according to the various peak patterns revealed that the DSP pattern was associated with more instances of acute cholestatic hepatitis with a higher degree of necrosis and greater cholestasis. The results from the SADRAC database (Robles-Diaz et al., 2014) have shown that the extent of necrosis predicts low survival. Similarly, liver failure and death are associated with more severe necrosis (Robles-Diaz et al., 2014). This histologically accounts for why the DSP pattern is associated with more severe liver injury and hence more likely to be predictive of poorer outcome.

In the study, we proposed, optimized, and validated a novel model which can predict acute ALF after DILI onset with fairly good potency. However, enrolled cases of this study are all hospitalized patients, which are not representative of the entire DILI population. In order to overcome this limitation, we are planning to enroll a prospective DILI cohort to validate the model in a future study as well as the subgroup of DILI with NAFLD (Zhou et al., 2021).

CONCLUSION

The dynamic evolution patterns of ALT and TB are correlated with the prognosis of DILI. Patients with the DSP pattern (ALT $\geq$ 3 $\times$ ULN, TB $\geq$ 2.5 $\times$ ULN, with the peak time interval between ALT and TB being $\geq$3 days) are more likely to progress to ALF. The prediction potency of the model can be further improved by incorporating with INR and ALP at DILI onset so that extra care can be implemented in time for improving the outcomes in patients with DILI.

DATA AVAILABILITY STATEMENT

The datasets presented in this article are not readily available because the datasets generated and/or analyzed during the current study are not publicly available due to the local policy but are available from the corresponding author on reasonable request. Requests to access the datasets should be directed to zhao_xinyan@ccmu.edu.cn.

ETHICS STATEMENT

The studies involving human participants were reviewed and approved by the Medical Ethics Committee of Beijing Friendship Hospital, Capital Medical University (Approval No. 2020-P2-071-01). The informed consent form has been waived.

AUTHOR CONTRIBUTIONS

Study concept and design: XZ. Acquisition of data: RY, CZ, KL, YW, LL, YW, ZM, TW, JL, AH, YS, BC, and QL. Statistical Analysis and interpretation of data: CZ, KL, RY, and ML. Drafting of the manuscript: KL, CZ, and RY. Critical revision of the manuscript for important intellectual content: XZ, ZZ, JJ, AW, and JL. Obtained funding and study supervision: ML, YW, ZZ, and XZ.

FUNDING

This work was funded by grants from the National Natural Science Foundation of China-Youth Science Fund (No. 82103902; 81900526) and the China Hepatitis Prevention and Treatment Foundation of Wang Baoen Liver Fibrosis Research Fund (No. 2021060).

SUPPLEMENTARY MATERIAL

The Supplementary Material for this article can be found online at: https://www.frontiersin.org/articles/10.3389/fphar.2022.934467/full#supplementary-material

REFERENCES

Aithal, G. P., Watkins, P. B., Andrade, R. J., Larrey, D., Molokhia, M., Takikawa, H., et al. (2011). Case Definition and Phenotype Standardization in Drug-Induced Liver Injury. *Clin. Pharmacol. Ther.* 89, 806–815. doi:10.1038/clpt.2011.58

Andrade, R. J., Lucena, M. I., Fernández, M. C., Pelaez, G., Pachkoria, K., García-Ruiz, E., et al. (2005). Drug-induced Liver Injury: an Analysis of 461 Incidences Submitted to the Spanish Registry over a 10-year Period. *Gastroenterology* 129, 512–521. doi:10.1016/j.gastro.2005.05.006

Andrade, R. J., and Robles-Díaz, M. (2020). Diagnostic and Prognostic Assessment of Suspected Drug-Induced Liver Injury in Clinical Practice. *Liver Int.* 40, 6–17. doi:10.1111/liv.14271

Björnsson, E., and Olsson, R. (2005). Outcome and Prognostic Markers in Severe Drug-Induced Liver Disease. *Hepatology* 42, 481–489. doi:10.1002/hep.20800

Chalasani, N., Fontana, R. J., Bonkovsky, H. L., Watkins, P. B., Davern, T., Serrano, J., et al. (2008). Causes, Clinical Features, and Outcomes from a Prospective Study of Drug-Induced Liver Injury in the United States. *Gastroenterology* 135, 1924–1934. e1-4. doi:10.1053/j.gastro.2008.09.011

Danan, G., and Teschke, R. (2015). RUCAM in Drug and Herb Induced Liver Injury: The Update. *Int. J. Mol. Sci.* 17, 14. doi:10.3390/ijms17010014

Dennis, B. B., Naji, L., Jajarmi, Y., Ahmed, A., and Kim, D. (2021). New Hope for Hepatitis C Virus: Summary of Global Epidemiologic Changes and Novel Innovations over 20 Years. *World J. Gastroenterol.* 27, 4818–4830. doi:10.3748/wjg.v27.i29.4818

European Association for the Study of the Liver (2017). EASL 2017 Clinical Practice Guidelines on the Management of Hepatitis B Virus Infection. *J. Hepatol.* 67:370–398.doi:10.1016/j.jhep.2017.03.021

Hayashi, P. H., Rockey, D. C., Fontana, R. J., Tillmann, H. L., Kaplowitz, N., Barnhart, H. X., et al. (2017). Death and Liver Transplantation within 2 Years of Onset of Drug-Induced Liver Injury. *Hepatology* 66, 1275–1285. doi:10.1002/hep.29283

Khandelwal, N., James, L. P., Sanders, C., Larson, A. M., and Lee, W. M. (2011). Unrecognized Acetaminophen Toxicity as a Cause of Indeterminate Acute Liver Failure. *Hepatology* 53, 567–576. doi:10.1002/hep.24060

Kleiner, D. E., Chalasani, N. P., Lee, W. M., Fontana, R. J., Bonkovsky, H. L., Watkins, P. B., et al. (2014). Hepatic Histological Findings in Suspected Drug-Induced Liver Injury: Systematic Evaluation and Clinical Associations. *Hepatology* 59, 661–670. doi:10.1002/hep.26709

Kleiner, D. E. (2017). Drug-induced Liver Injury: The Hepatic Pathologist's Approach. *Gastroenterol. Clin. North Am.* 46, 273–296. doi:10.1016/j.gtc.2017.01.004

Kleiner, D. E. (2018). Histopathological Challenges in Suspected Drug-Induced Liver Injury. *Liver Int.* 38, 198–209. doi:10.1111/liv.13584

Lee, W. M., Reddy, K. R., Tong, M. J., Black, M., van Leeuwen, D. J., Hollinger, F. B., et al. (1998). Early Hepatitis C Virus-RNA Responses Predict Interferon Treatment Outcomes in Chronic Hepatitis C. *Hepatology* 28, 1411–1415. doi:10.1002/hep.510280533

Lo Re, V., 3rd, Haynes, K., Forde, K. A., Goldberg, D. S., Lewis, J. D., Carbonari, D. M., et al. (2015). Risk of Acute Liver Failure in Patients with Drug-Induced Liver Injury: Evaluation of Hy's Law and a New Prognostic Model. *Clin. Gastroenterol. Hepatol.* 13, 2360–2368. doi:10.1016/j.cgh.2015.06.020

Medina-Caliz, I., Robles-Diaz, M., Garcia-Muñoz, B., Stephens, C., Ortega-Alonso, A., Garcia-Cortes, M., et al. (2016). Definition and Risk Factors for Chronicity Following Acute Idiosyncratic Drug-Induced Liver Injury. *J. Hepatol.* 65, 532–542. doi:10.1016/j.jhep.2016.05.003

Polson, J., and Lee, W. M. (2005). AASLD Position Paper: the Management of Acute Liver Failure. *Hepatology* 41, 1179–1197. doi:10.1002/hep.20703

Rachakonda, V., Bataller, R., and Duarte-Rojo, A. (2020). Recent Advances in Alcoholic Hepatitis. *F1000Res* 9, F1000. doi:10.12688/f1000research.20394.1

Rahim, M. N., Miquel, R., and Heneghan, M. A. (2020). Approach to the Patient with Acute Severe Autoimmune Hepatitis. *JHEP Rep.* 2, 100149. doi:10.1016/j.jhepr.2020.100149

Regev, A., Palmer, M., Avigan, M. I., Dimick-Santos, L., Treem, W. R., Marcinak, J. F., et al. (2019). Consensus: Guidelines: Best Practices for Detection, Assessment and Management of Suspected Acute Drug-Induced Liver Injury during Clinical Trials in Patients with Nonalcoholic Steatohepatitis. *Aliment. Pharmacol. Ther.* 49, 702–713. doi:10.1111/apt.15153

Reuben, A., Tillman, H., Fontana, R. J., Davern, T., McGuire, B., Stravitz, R. T., et al. (2016). Outcomes in Adults with Acute Liver Failure between 1998 and 2013: An Observational Cohort Study. *Ann. Intern Med.* 164, 724–732. doi:10.7326/M15-2211

Robles-Diaz, M., Lucena, M. I., Kaplowitz, N., Stephens, C., Medina-Cáliz, I., González-Jimenez, A., et al. (2014). Use of Hy's Law and a New Composite Algorithm to Predict Acute Liver Failure in Patients with Drug-Induced Liver Injury. *Gastroenterology* 147, 109–118. e5. doi:10.1053/j.gastro.2014.03.050

Sgro, C., Clinard, F., Ouazir, K., Chanay, H., Allard, C., Guilleminet, C., et al. (2002). Incidence of Drug-Induced Hepatic Injuries: a French Population-Based Study. *Hepatology* 36, 451–455. doi:10.1053/jhep.2002.34857

Shen, T., Liu, Y., Shang, J., Xie, Q., Li, J., Yan, M., et al. (2019). Incidence and Etiology of Drug-Induced Liver Injury in Mainland China. *Gastroenterology* 156, 2230. e11. doi:10.1053/j.gastro.2019.02.002

Stravitz, R. T., and Lee, W. M. (2019). Acute Liver Failure. *Lancet* 394, 869–881. doi:10.1016/S0140-6736(19)31894-X

Suk, K. T., Kim, D. J., Kim, C. H., Park, S. H., Yoon, J. H., Kim, Y. S., et al. (2012). A Prospective Nationwide Study of Drug-Induced Liver Injury in Korea. *Am. J. Gastroenterol.* 107, 1380–1387. doi:10.1038/ajg.2012.138

Temple, R. (2006). Hy's Law: Predicting Serious Hepatotoxicity. *Pharmacoepidemiol Drug Saf.* 15, 241–243. doi:10.1002/pds.1211

Vega, M., Verma, M., Beswick, D., Bey, S., Hossack, J., Merriman, N., et al. (2017). The Incidence of Drug- and Herbal and Dietary Supplement-Induced Liver Injury: Preliminary Findings from Gastroenterologist-Based Surveillance in the Population of the State of Delaware. *Drug Saf.* 40, 783–787. doi:10.1007/s40264-017-0547-9

Wang, T., Zhao, X., Shao, C., Ye, L., Guo, J., Peng, N., et al. (2019). A Proposed Pathologic Sub-classification of Drug-Induced Liver Injury. *Hepatol. Int.* 13, 339–351. doi:10.1007/s12072-019-09940-9

You, S., Rong, Y., Zhu, B., Zhang, A., Zang, H., Liu, H., et al. (2013). Changing Etiology of Liver Failure in 3,916 Patients from Northern China: a 10-year Survey. *Hepatol. Int.* 7, 714–720. doi:10.1007/s12072-013-9424-5

Yu, Y. C., Mao, Y. M., Chen, C. W., Chen, J. J., Chen, J., Cong, W. M., et al. (2017). CSH Guidelines for the Diagnosis and Treatment of Drug-Induced Liver Injury. *Hepatol. Int.* 11, 221–241. doi:10.1007/s12072-017-9793-2

Zhou, Y. J., Wong, V. W., and Zheng, M. H. (2021). Consensus Scoring Systems for Nonalcoholic Fatty Liver Disease: an Unmet Clinical Need. *Hepatobiliary Surg. Nutr.* 10, 388–390. doi:10.21037/hbsn-21-80

Conflict of Interest: The authors declare that the research was conducted in the absence of any commercial or financial relationships that could be construed as a potential conflict of interest.

GLOSSARY

AASLD American Association for the Study of Liver Diseases
ALB albumin
ALF acute liver failure
ALP alkaline phosphatase
ALT alanine aminotransferase
AST aspartate aminotransferase
AUROC area under receiver operating characteristic
BMI body mass index
CHE cholinesterase
CK7 cytokeratin 7
CIOMS Council for International Organizations of Medical Sciences
CI confidence interval
Cr creatinine
DILI drug-induced liver injury
DILIN drug-induced liver injury network
DOP ALT and TB double overlap peak pattern
DSP ALT and TB double separate peak pattern
GGT gamma glutamyltransferase
HDS herbal and dietary supplements
H&E hematoxylin and eosin
HGB hemoglobin
HIS hospital management system
INR international normalized ratio
LT liver transplantation
NAFLD non-alcoholic fatty liver disease
nHy's Law new Hy's Law
NSAIDs non-steroidal anti-inflammatory drugs
PAS-D periodic acid-Schiff with diastase
PLT platelets
ROC receiver operating characteristic
RUCAM Roussel Uclaf causality assessment method
SADRAC Swedish Adverse Drug Reactions Advisory Committee
TBA total bile acid
TB total bilirubin
ULN upper limit of normal
WBC white blood cell

frontiers | Frontiers in Pharmacology

TYPE Original Research
PUBLISHED 26 August 2022
DOI 10.3389/fphar.2022.905564

OPEN ACCESS

EDITED BY
Thomas Brzozowski,
Jagiellonian University Medical College, Poland

REVIEWED BY
Dan Lucian Dumitrascu,
Iuliu Haţieganu University of Medicine and Pharmacy, Romania
Qasim Aziz,
Queen Mary University of London, United Kingdom

*CORRESPONDENCE
Qunhong Wu,
wuqunhong@163.com
Yanhua Hao,
hyhyjw@126.com

†These authors have contributed equally to this work and share first authorship

SPECIALTY SECTION
This article was submitted to Gastrointestinal and Hepatic Pharmacology, a section of the journal Frontiers in Pharmacology

RECEIVED 09 April 2022
ACCEPTED 18 July 2022
PUBLISHED 26 August 2022

CITATION
Wang K, Liu H, Liu J, Han L, Kang Z, Liang L, Jiang S, Meng N, Chen P, Xu Q, Wu Q and Hao Y (2022), Factors related to irritable bowel syndrome and differences among subtypes: A cross-sectional study in the UK Biobank. *Front. Pharmacol.* 13:905564. doi: 10.3389/fphar.2022.905564

Factors related to irritable bowel syndrome and differences among subtypes: A cross-sectional study in the UK Biobank

Kexin Wang[1,2,3†], Huan Liu[1,2†], Jingjing Liu[1,2], Liyuan Han[4], Zheng Kang[1,2], Libo Liang[1,2], Shengchao Jiang[1,2], Nan Meng[1,2], Peiwen Chen[1,2], Qiao Xu[1,2], Qunhong Wu[1,2*] and Yanhua Hao[1,2*]

[1]Department of Health Policy, School of Health Management, Harbin Medical University, Harbin, Heilongjiang, China, [2]Department of Social Medicine, School of Public Health, Harbin Medical University, Harbin, Heilongjiang, China, [3]Department of Epidemiology, School of Public Health, Harbin Medical University, Harbin, Heilongjiang, China, [4]Department of Global Health, Ningbo Institute of Life and Health Industry, University of Chinese Academy of Sciences, Ningbo, Zhejiang, China

Background: Irritable bowel syndrome (IBS) reduces patients' quality of life and causes great burdens due to its unclear pathogenesis and criteria for diagnosis. This study aimed to explore the differences in prevalence and the influencing factors for IBS and its subtypes.

Methods: The UK Biobank surveyed 174,771 adult participants who completed the Digestive Health Questionnaire (DHQ) through emails and websites. DHQ included the Rome III criteria, IBS symptom severity score, and Patient Health Questionnaire 12 Somatic Symptom score. The UK Biobank also asked regarding previous IBS diagnosis, diagnosis for post-infectious IBS (PI-IBS), and environmental exposures and associated conditions (including anxiety or depression, based on treatment sought or offered). Pearson's Chi-squared test or Wilcoxon's rank-sum test was used for potential associations. Binary logic regression based on sex stratification was used to examine associations between selected factors and IBS and its subtypes.

Results: This study included 31,918 participants who met the Rome III criteria for IBS. The pooled prevalence of IBS in the UK Biobank was 18.3%, with mixed IBS as the predominant subtype (59.0%), followed by diarrhea-predominant IBS (25.1%), constipation-predominant IBS (14.7%), and untyped IBS (1.1%). IBS was significantly associated with somatization (male: OR = 5.326, 95% CI = 4.863–5.832; female: OR = 4.738, 95% CI = 4.498–4.992) and coeliac disease (male: OR = 4.107, 95% CI = 3.132–5.385; female: OR = 3.783, 95% CI = 3.310–4.323). Differences in antibiotics and mental status were presented among subtypes and sex. Furthermore, 1,787 individuals were diagnosed with PI-IBS in the group of patients with IBS. The prevalence of PI-IBS in IBS was 16.6% in the UK Biobank, and it was characterized by diarrhea, fever, bloody diarrhea, and vomiting.

Conclusion: Somatization and coeliac disease are primary risk factors for IBS. Distinguishing differential risk factors is critical for the precise diagnosis and treatment of IBS subtypes, particularly sex-specific differences in mental health status. General practitioners should focus on the treatment according to IBS subtypes.

KEYWORDS

disorders of gut–brain interaction, irritable bowel syndrome, Rome III, prevalence, risk factors, gender, subtypes

1 Introduction

Irritable bowel syndrome (IBS), defined as the disorder of gut–brain interaction (DGBI), had pooled prevalence rates of 10.1% in countries based on an internet survey and 3.5% in countries based on a household survey, which used Rome III diagnostic criteria (Sperber et al., 2021). Its characteristic symptoms include abdominal pain and altered bowel habits, including stool consistency and frequency (Drossman, 2006). Although the pain and disturbing symptoms caused by IBS are not life-threatening, they severely impair the quality of life of patients and result in tremendous economic burden (Wong and Drossman, 2010; Canavan et al., 2014a; Tack et al., 2019).

The obscure pathophysiology and lack of specific biomarkers for IBS make its diagnosis difficult (Fichna and Storr, 2012). In addition, many overlapping symptoms between IBS and other comorbidities, such as coeliac disease, increase the difficulty of the diagnosis of IBS (Aziz and Simrén, 2021). To date, the diagnosis of IBS is based on symptoms according to Rome criteria, in which the positive diagnosis for IBS was updated from Rome III to Rome IV in 2016. The Rome IV criteria are more restrictive than the Rome III criteria. For example, the global prevalence of IBS was 3.8% with the Rome IV criteria and 9.2% with Rome III criteria (Oka et al., 2020). Aziz et al. (2018) showed a lack of major implications in the diagnosis of IBS from Rome III to Rome IV, and patients with IBS diagnosed by Rome IV had more severe clinical symptoms.

Based on the current research, the diagnosis of IBS remains unelucidated; therefore, it is important to gain a fundamental understanding of the potential factors influencing IBS for better diagnosis and treatment. The female sex, younger age, and lower income were recognized as IBS risk factors (Drossman et al., 1993; Talley et al., 1995; Jiang et al., 2019). However, a recent study showed that the pooled prevalence of IBS was 11.5% between 18 and 39 years of age, 9.7% between 40 and 64 years of age, and 7.5% over 65 years of age (Sperber et al., 2021). This implies that patients with IBS aged over 40 years should be more concerned. Heredity may also be an important risk factor for IBS, with an incidence of approximately 33% (Whorwell et al., 1986). A cohort study showed that patients with IBS reported antibiotic use of 29.2%, with a 1.8-fold risk of IBS (Krogsgaard et al., 2018). Another study explored the possible cumulative effects of psychological changes on the severity of the gastrointestinal symptoms of IBS (Midenfjord et al., 2020). Symptoms of IBS included not only gastrointestinal symptoms but also extraintestinal symptoms (Whitehead et al., 2002; Patel et al., 2015). Therefore, some influencing factors related to symptoms of IBS caused general concern (Black et al., 2020). In the UK, Black et al. (2020) reported that somatization measured by the Patient Health Questionnaire 12 (PHQ-12) was independently associated with the severity of IBS symptoms. They proposed a process whereby gastrointestinal symptoms and discomfort caused severe IBS symptoms, which prompted patients to pay further attention to the symptoms of IBS. Moreover, some diseases with similar symptoms to IBS, such as coeliac disease, should be explored in the future (Ford et al., 2009). Common foods, including wheat, barley, and rye, (Baydoun et al., 2012), contain certain ingredients that may also trigger discomfort and symptoms, such as food intolerance, in patients with IBS (Eswaran et al., 2011; Böhn et al., 2013).

Based on the Rome III bowel habit subclassification (Longstreth et al., 2006), IBS was classified into four subtypes: constipation-predominant IBS (IBS-C), diarrhea-predominant IBS (IBS-D), mixed IBS (IBS-M), and untyped IBS (IBS-U). However, only a few studies comprehensively focused on the differences among these IBS subtypes. Using psychological factors as an example, single-subtype IBS-M presented a higher level of depression and anxiety (Hu et al., 2021). Comparing IBS-C with IBS-D, the prevalence of anxiety and depression were markedly different (Fond et al., 2014). Overall, research works exploring the differences of potential risk factors among subtypes were limited.

Post-infectious irritable bowel syndrome (PI-IBS) may appear after acute gastroenteritis or following an episode of infective gastroenteritis as a special subtype of IBS (Dunlop et al., 2003), with a pooled prevalence varying from 7% to more than one-third of all IBS cases (Schwille-Kiuntke et al., 2011). Some studies reported the influencing factors for PI-IBS; however, differences in influencing factors for PI-IBS and general IBS subtypes remain unclear.

This cross-sectional study aims to examine the differences in the prevalence of IBS and the influencing factors associated with IBS and its subtypes based on the Rome III criteria using UK Biobank's extensive sample data of adults aged 40–69 years in the United Kingdom. It also aims to provide guidance for better

diagnosis and treatment of IBS in the United Kingdom and other nations.

2 Materials and methods

2.1 Participants

The UK Biobank was a large-scale multiple cohort study consisting of approximately 500,000 individuals (aged 40–69 years) recruited from across the United Kingdom between 2006 and 2010 (Collins, 2012). At the end of 2015, a team led by a group of gastroenterologists and the UK Biobank jointly planned and designed a survey on an extremely common abdominal disease, IBS, which was performed in 2017. Participants in the study were from the baseline survey and were invited mainly by email and on the participant website. As of 18 July 2018, about 174,771 participants completed the web-based questionnaire, including the participants' self-reported socioeconomic information and the Rome III criteria, IBS symptom severity score (IBS-SSS), and PHQ-12 questionnaires. The UK Biobank received ethical approval from the National Health Service National Research Ethics Service 11/NW/0382 and was part of the UK Biobank project 52632.

2.2 Inclusion and exclusion criteria

In this study, IBS was diagnosed based on the Rome III questionnaire, and participants with missing data in the Rome III questionnaire were excluded. A total of 174,217 participants completed the Rome III questionnaire, including 31,918 participants with IBS and 142,299 participants with non-IBS; this data was used to calculate the prevalence of IBS in the UK Biobank. To further analyze the factors associated with IBS and its subtypes, this study included participants with moderate to severe IBS symptoms based on an IBS-SSS score of ≥ 175 (Bonfiglio et al., 2018). The exclusion criteria were as follows: 1) participants with IBS who had missing data in IBS-SSS, 2) participants with IBS who had no symptoms or with mild symptoms (IBS-SSS score of <175), and 3) participants who could not confirm a history of IBS. The exclusion criteria eliminated the effect of IBS history on factors associated with IBS and its subtypes. Finally, 147,336 participants were included in this study, in which 17,695 had IBS and 129,641 were without IBS (non-IBS).

The UK Biobank used all IBS respondents who met the diagnosis of the Rome III criteria (n = 31,918) to identify PI-IBS further. In the UK Biobank database, only those who had been diagnosed with IBS (with IBS history) answered questions regarding the onset symptoms of IBS in the questionnaire. Therefore, only participants with a history of IBS diagnosis were included to define PI-IBS. Finally, a sample size of 10,760 participants were included, in which 1,787 were with PI-IBS and 8,973 were without PI-IBS but with IBS (non-PI-IBS), which was used to estimate the prevalence of PI-IBS among IBS patients in the UK Biobank. Moreover, this study also excluded the data with IBS-SSS score of < 175 to analyze the associations between PI-IBS and non-PI-IBS, which determined a sample size of 8,256 patients (Figure 1).

2.3 Study measurements

2.3.1 Diagnosis of irritable bowel syndrome and its subtypes

The Rome III criteria were used to diagnose IBS based on symptoms such as chronic abdominal pain or discomfort at least 3 days per month in the last 3 months associated with two or more following symptoms: 1) improvement with defecation, 2) the onset of a change in the frequency of stool, and 3) the onset of a change in the form or appearance of stool. Moreover, the criteria included the last 3 months with symptom onset at least 6 months prior to diagnosis. The IBS subtypes were defined in terms of stool forms (hard/lumpy and loose/watery in at least 25% of evaluations).

2.3.2 Diagnosis of post-infectious irritable bowel syndrome

Our study defined PI-IBS based on the criteria set in previous studies (Dunlop et al., 2003; Johnsen et al., 2018) as follows: 1) patients with a confirmed diagnosis of IBS, 2) patients with a sudden onset of IBS and also diagnosed with an infectious disease when the IBS symptoms first appeared (or 2 weeks prior), and 3) patients with two or more symptoms, including fever, diarrhea, bloody diarrhea, and vomiting.

2.3.3 Irritable bowel syndrome symptoms

IBS-SSS was used to determine the severity of IBS symptoms experienced within the previous 3 months, including abdominal pain, distension, satisfaction with bowel habits, and interference with the participants' life in general. IBS-SSS yielded a total score ranging from 0 to 500, and the scores were divided into four categories: remission of IBS symptoms (0–74), mild IBS (75–174), moderate IBS (175–299), and severe IBS (300–500) (Card et al., 2018).

2.3.4 Extraintestinal somatic symptoms

The PHQ-12 is a modified version of the commonly used PHQ-15, which is a validated questionnaire that assesses the severity of somatic symptoms (Francis et al., 1997). Participants were asked to rate the severity of 12 symptoms over the previous 3 months. These symptoms, one of which was only applicable to women, were rated from 0 (not bothered at all) to 2 (extremely bothered). Therefore, the total PHQ-12 score ranged from 0 to 24 for women and from 0 to

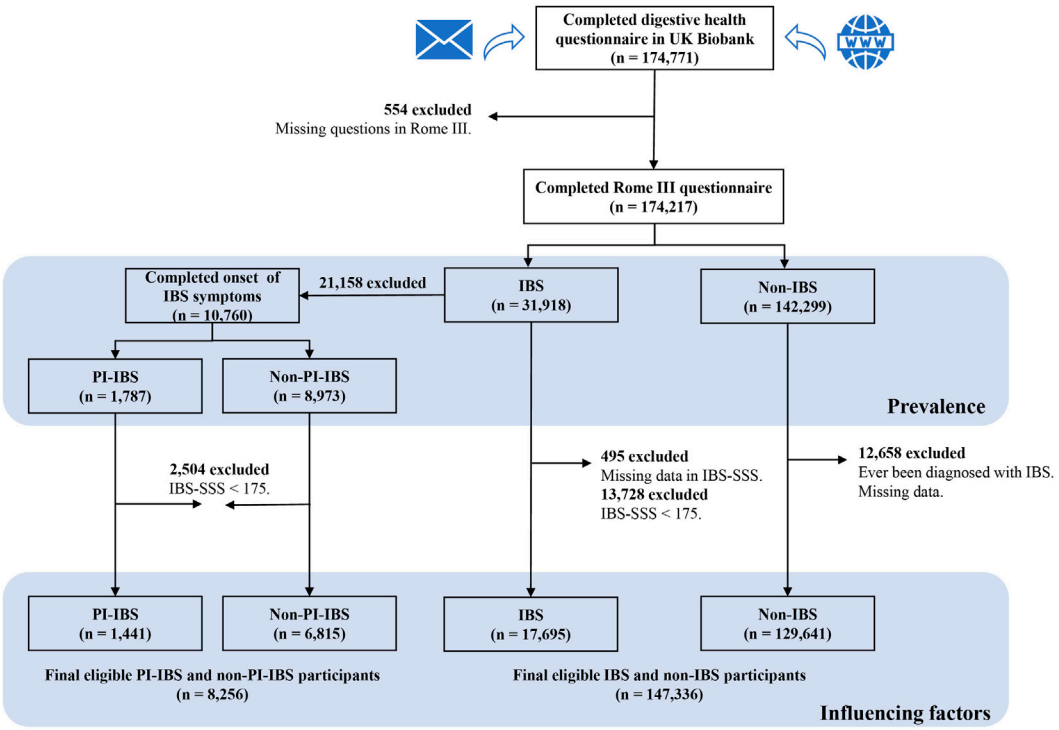

FIGURE 1
Flowchart of participant inclusion and exclusion. IBS, irritable bowel syndrome; non-IBS, participants without IBS; PI-IBS, post-infectious IBS; non-PI-IBS, participants without PI-IBS but with IBS; and IBS-SSS, IBS symptom severity score.

22 for men. In this study, the PHQ-12 score was used to identify whether participants experience somatization symptoms (Polster et al., 2018). A PHQ-12 score of > 6 was defined as high somatization, whereas a PHQ-12 score of ≤ 6 was defined as low somatization.

2.3.5 Anxiety, depression, and other potential factors

Regarding mental health, the two main variables included anxiety and depression. Participants were asked the following questions: "Have you ever been offered or sought treatment for anxiety?" and "Have you ever been offered or sought treatment for depression?" Participants' mode of birth was also asked as follows: "Were you born by caesarean section?" Furthermore, participants' IBS family history was examined with the following question: "Do you have a family history of IBS in your parents/siblings/children?" We also considered previous antibiotic misuse, which was assessed with the question: "During childhood or as a teenager, did you receive long-term or recurrent courses (3 or more per year) of antibiotics (for example, for tonsillitis or acne)?" Other health issues that may affect IBS were also assessed. Participants were asked whether they had been diagnosed with coeliac disease or gluten sensitivity. After participants who selected "prefer not to answer" or "do not know" or "missing" were considered as "missing data," the final response categories were included, with 1 = yes, 0 = no, and missing data.

2.3.6 Demographic and socioeconomic variables

In this study, potential demographic and socioeconomic variables, including age, sex, and socioeconomic status (Townsend Deprivation Score), were analyzed. Age was determined by the baseline age and time when participants completed the Digestive Health Questionnaire. The Townsend Deprivation Score was calculated immediately prior to the participant joining the UK Biobank. Participants were assigned a score corresponding to the output area in which their postcode was located. The Townsend Deprivation Score was derived from the participants' postcode, with negative scores reflecting relatively greater affluence (Spiller et al., 2010).

2.4 Statistical analysis

Descriptive statistics were calculated, including frequencies and percentages for binary categorical variables, and median and interquartile ranges were presented for continuous variables that were not normally distributed. A univariate analysis was

TABLE 1 Participants' characteristics.

Variable	All (n = 147,336)		p-value	Men (n = 66,089)		p-value	Women (n = 81,247)		p-value
	IBS n = 17,695	Non-IBS n = 129,641		IBS n = 4,151	Non-IBS n = 61,938		IBS n = 13,544	Non-IBS n = 67,703	
Sex									
Female	13,544 (76.5%)	67,703 (52.2%)	<0.001	NA	NA		NA	NA	
Male	4,151 (23.5%)	61,938 (47.8%)		NA	NA		NA	NA	
Age (years)									
Mean (SD)	54.37 (7.795)	56.14 (7.684)	<0.001	55.02 (7.993)	56.61 (7.760)	<0.001	54.17 (7.722)	55.71 (7.589)	<0.001
Median (IQR)	55 (48, 61)	57 (50, 62)		56 (48, 62)	58 (51, 63)		54 (48.61)	56 (50.62)	
Townsend Deprivation Score									
Mean (SD)	−1.42 (3.007)	−1.73 (2.821)	<0.001	−1.29 (3.156)	−1.78 (2.827)	<0.001	−1.45 (2.959)	−1.69 (2.814)	<0.001
Median (IQR)	−2.24 (−3.70, 0.36)	−2.45 (−3.81, −0.19)		−2.18 (−3.72, 0.57)	−2.51 (−3.85, −0.27)		−2.25 (−3.69, 0.28)	−2.4 (−3.78, −0.12)	
Missing data	30 (0.2%)	149 (0.1%)		10 (0.2%)	67 (0.1%)		20 (0.1%)	82 (0.1%)	
Ever been offered/sought treatment for anxiety									
Yes	6,692 (37.8%)	23,698 (18.3%)	<0.001	1,368 (33.0%)	9,067 (14.6%)	<0.001	5,324 (39.3%)	14,631 (21.6%)	<0.001
No	10,935 (61.8%)	105656 (81.5%)		2,772 (66.8%)	52,759 (85.2%)		8,163 (60.3%)	52,897 (78.1%)	
Missing data	68 (0.4%)	287 (0.2%)		11 (0.3%)	112 (0.2%)		57 (0.4%)	175 (0.3%)	
Ever been offered/sought treatment for depression									
Yes	7,228 (40.8%)	26,498 (20.4%)	<0.001	1,404 (33.8%)	9,849 (15.9%)	<0.001	5,824 (43.0%)	16,649 (24.6%)	<0.001
No	10,391 (58.7%)	102794 (79.3%)		2,732 (65.8%)	51,968 (83.9%)		7,659 (56.5%)	50,826 (75.1%)	
Missing data	76 (0.4%)	349 (0.3%)		15 (0.4%)	121 (0.2%)		61 (0.5%)	228 (0.3%)	
Family history of IBS									
Yes	4,993 (28.2%)	13,985 (10.8%)	<0.001	941 (22.7%)	4,982 (8.0%)	<0.001	4,052 (29.9%)	9,003 (13.3%)	<0.001
No	7,859 (44.4%)	102,225 (78.9%)		1848 (44.5%)	49,500 (79.9%)		6,011 (44.4%)	52,725 (77.9%)	
Missing data	4,843 (27.4%)	13,431 (10.4%)		1,362 (32.8%)	7,456 (12.0%)		3,481 (25.7%)	5,975 (8.8%)	
Born by caesarean section									
Yes	447 (2.5%)	3,298 (2.5%)	0.811	111 (2.7%)	1,598 (2.6%)	0.498	336 (2.5%)	1,700 (2.5%)	0.924
No	16,313 (92.2%)	118899 (91.7%)		3,552 (85.6%)	54,707 (88.3%)		12,761 (94.2%)	64,192 (94.8%)	
Missing data	935 (5.3%)	7,444 (5.7%)		488 (11.8%)	5,633 (9.1%)		447 (3.3%)	1,811 (2.7%)	
Long-term/recurrent antibiotics as child or teenager									
Yes	4,163 (23.5%)	13,997 (10.8%)	<0.001	715 (17.2%)	4,906 (7.9%)	<0.001	3,448 (25.5%)	9,091 (13.4%)	<0.001
No	11,003 (62.2%)	105232 (81.2%)		2,771 (66.8%)	52,078 (84.1%)		8,232 (60.8%)	53,154 (78.5%)	
Missing data	2,529 (14.3%)	10,412 (8.0%)		665 (16.0%)	4,954 (8.0%)		1,864 (13.8%)	5,458 (8.1%)	
Diagnosed with coeliac disease or gluten sensitivity									
Yes	890 (5.0%)	1,462 (1.1%)	<0.001	146 (3.5%)	510 (0.8%)	<0.001	744 (5.5%)	952 (1.4%)	<0.001
No	16,351 (92.4%)	127,701 (98.5%)		3,827 (92.2%)	61,139 (98.7%)		12,524 (92.5%)	66,562 (98.3%)	
Missing data	454 (2.6%)	478 (0.4%)		178 (4.3%)	289 (0.5%)		276 (2.0%)	189 (0.3%)	
PHQ-12 Score									
≤6	5,748 (32.5%)	98,940 (76.3%)	<0.001	1,698 (40.9%)	50,667 (81.8%)	<0.001	8,918 (65.8%)	17,636 (26.0%)	<0.001
>6	11,174 (63.1%)	27,668 (21.3%)		2,256 (54.3%)	10,032 (16.2%)		4,050 (29.9%)	48,273 (71.3%)	
Missing data	773 (4.4%)	3,033 (2.3%)		197 (4.7%)	1,239 (2.0%)		576 (4.3%)	1794 (2.6%)	

Data were mean (SD) or n (%) unless noted otherwise. The distribution of age and the Townsend Deprivation Score is non-normal; therefore, the mean (SD) and median (P25, P75) are used to describe. The p-value was calculated by the chi-square test and Wilcoxon's rank-sum test where applicable. In this analysis, "Do not know," "Prefer not to answer," and "missing" were coded as missing data.

performed using Pearson's chi-squared test or Wilcoxon's rank-sum test. Binary logic regression was used to examine associations between IBS and its associated factors. Multinomial logistic regression models were used to study the relationship between the independent variables and IBS subtypes (i.e., taking non-IBS patients as the reference standard). Data were stratified by sex to

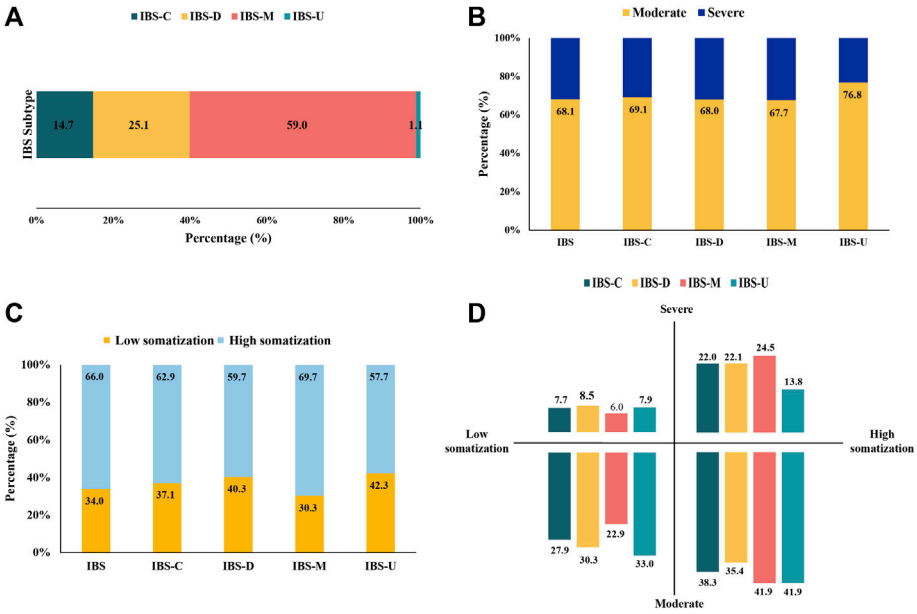

FIGURE 2
Distribution of IBS subtypes and somatization symptoms. (n = 17,695). **(A)** Proportions of participants defined as IBS subtypes. **(B)** Proportions of IBS and its subtypes with moderate and severe symptoms. **(C)** Proportions of IBS and its subtypes with somatization. **(D)** Distribution of IBS subtypes in the field of somatization and symptom severity.

identify the differences in influencing factors of IBS. We adjusted for demographic and socioeconomic factors in Models 2 and 4, respectively. All data were analyzed by SAS V.9.4 (SAS Institute), and statistical significance was set at $p < 0.05$.

3 Results

3.1 Participants' characteristics

There were 31,918 participants diagnosed with IBS by the Rome III criteria out of the 174,217 participants who completed the Rome III questionnaire; therefore, the estimated prevalence of IBS based on the Rome III criteria in the UK Biobank was 18.3%. Furthermore, this study used the data comprising 17,695 IBS and 129,641 non-IBS (n = 147,336) participants to analyze the associations between IBS and its factors. The general characteristics of participants are presented in Table 1. There were 17,695 patients with IBS, and 76.5% of them were women. Over 60% of patients with IBS had high somatization (PHQ-12 score of >6). Sex, age, socioeconomic status, family history of IBS, somatization, antibiotics misuse, coeliac disease, anxiety, and depression were all associated with IBS (p <0.001).

As illustrated in Figure 2 and Supplementary Table S1, IBS-M was predominant, accounting for 59.0% of the cases, followed by IBS-D (25.1%), IBS-C (14.7%), and IBS-U (1.1%). Over 30% of patients with IBS had severe symptoms, including patients with IBS-M (32.3%) having the most and those with IBS-U (23.2%) having the least symptoms. Patients with IBS-M (69.7%) had high somatization, higher than the overall level of IBS (66.0%). IBS-M and IBS-U patients had moderate symptoms and the highest somatization (41.9%).

"Continuously feeling tired or having low energy;" "pain in the arms, legs, or joints;" "trouble sleeping;" and "back pain" were the four major somatic symptoms. Sex-specific differences and subtypes of other somatic symptoms are summarized in Figure 3 and Supplementary Tables S2–S4. A majority of women with IBS suffered from these four major somatic symptoms than men with IBS. A majority of men with IBS-C suffered from back pain and had trouble sleeping than men with IBS-M. Men with IBS-U suffered from low energy and had relatively low sleep problems. In women with IBS-C and IBS-U, having trouble sleeping was more severe than pain in the arms, legs, or joints.

3.2 Logistic regression analysis of factors associated with irritable bowel syndrome, stratified by sex

Independent variables that were significant predictors of IBS in the chi-squared tests or Wilcoxon's rank-sum test were entered into the logistic regression analysis model (Figure 4; Supplementary Table S5). After adjustment for age and the Townsend Score (Model 2), younger participants were more

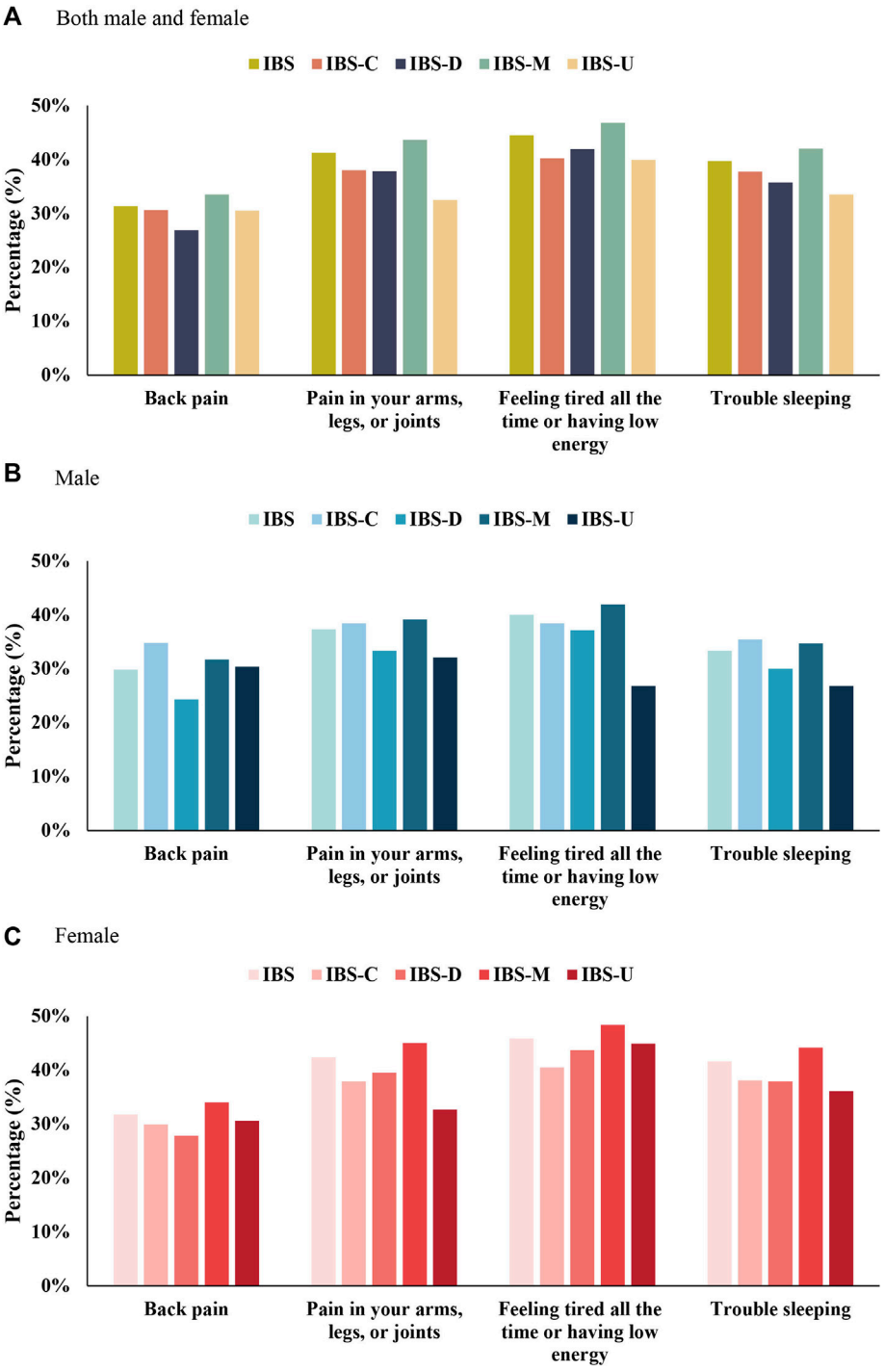

FIGURE 3
Top four extraintestinal somatic symptoms in IBS and its subtypes. **(A)** Both male and female. **(B)** Male. **(C)** Female.

likely to develop IBS for both men and women. Men with a lower economic level were more likely to have IBS (OR = 1.028, 95% CI = 1.013–1.044). High somatization was the most important influencing factor; people experiencing this symptom were four times more likely to have IBS (male: odds ratio [OR] = 4.786, 95% confidence interval [CI] = 4.544–5.041; female: OR = 5.326, 95% CI = 4.863–5.832). Coeliac disease (male: OR = 4.107, 95% CI =

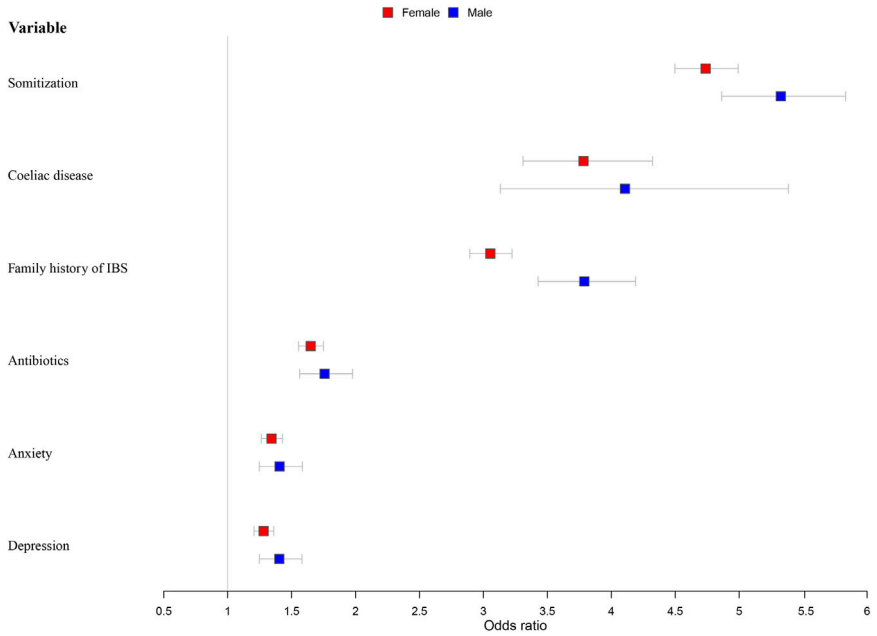

FIGURE 4
Models of factors associated with IBS stratified by sex and adjusted for age and socioeconomic status.

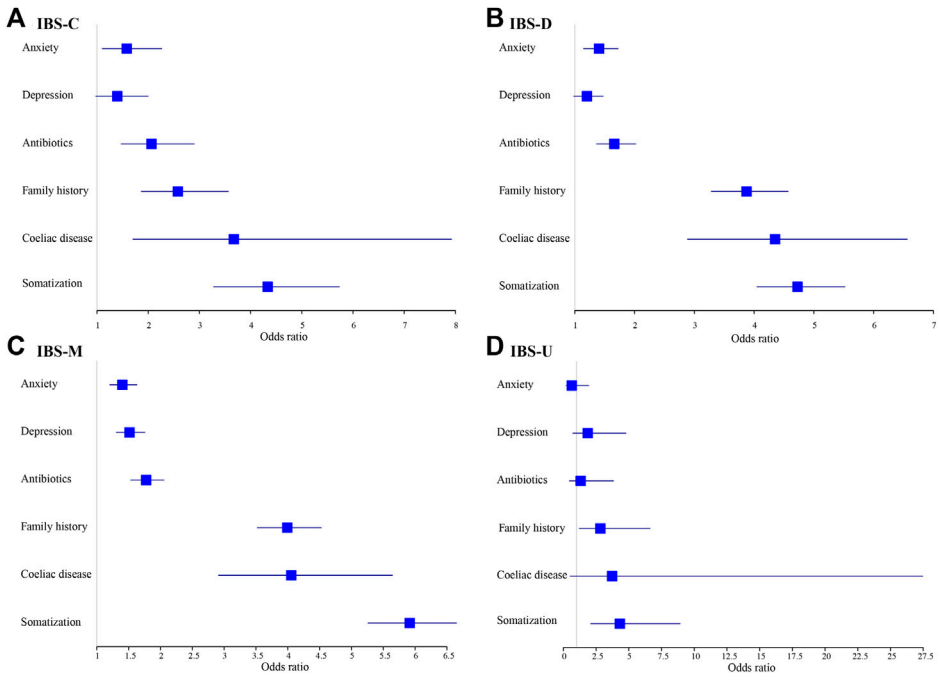

FIGURE 5
Models of factors associated with IBS subtypes for males and adjusted for age and socioeconomic status. **(A)** IBS-C. **(B)** IBS-D. **(C)** IBS-M. **(D)** IBS-U.

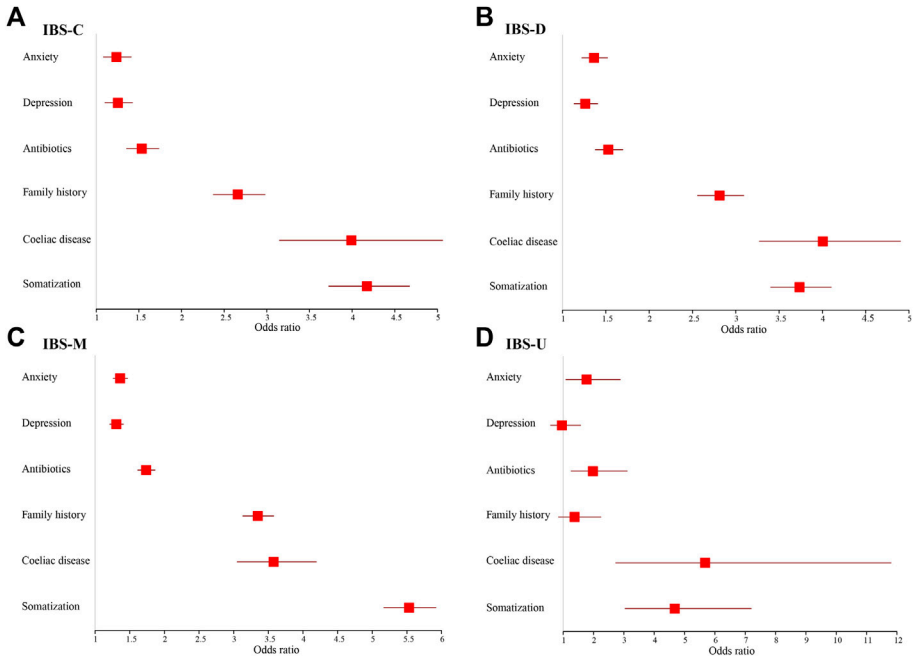

FIGURE 6
Models of factors associated with IBS subtypes for females and adjusted for age and socioeconomic status. **(A)** IBS-C. **(B)** IBS-D. **(C)** IBS-M. **(D)** IBS-U.

3.132–5.385; female: OR = 3.783, 95% CI = 3.310–4.323) and family history of IBS (male: OR = 3.789, 95% CI = 3.427–4.190; female: OR = 3.054, 95% CI = 2.893–3.224) were the second important influencing factors; participants with these were about three to four times more susceptible to IBS. Other significant factors included antibiotics abuse (male: OR = 1.758, 95% CI = 1.563–1.977; female: OR = 1.649, 95% CI = 1.555–1.749), anxiety (male: OR = 1.406, 95% CI = 1.247–1.585; female: OR = 1.343, 95% CI = 1.263–1.429), and depression (male: OR = 1.404, 95% CI = 1.248–1.581; female: OR = 1.281, 95% CI = 1.206–1.361).

3.3 Multinominal logistic regression analysis of potential influencing factors of different irritable bowel syndrome subtypes, stratified by sex

Figures 5, 6 show adjusted OR values (Model 4) of multiple IBS influencing factors for each IBS subtype in men and women (see details in Supplementary Table S6). Somatization and coeliac disease were the top two influencing factors of each IBS subtype for both men and women. Men with high somatization and coeliac disease were most likely to develop IBS-M and IBS-D, up to 5.915 and 4.351 times than men with low somatization and without coeliac disease, respectively. In addition, coeliac disease, antibiotics, and anxiety significantly affected patients with IBS-C, IBS-D, and IBS-M, whereas depression affected only patients with IBS-M ($p < 0.05$).

In women, high somatization ranked first in patients with IBS-C, IBS-M, and IBS-U cases, but coeliac disease ranked first in IBS-D. Women with high somatization suffered up to 5.531, 4.676, and 4.173 times more from IBS-M, IBS-U, and IBS-C, respectively, than women with low somatization. Women with coeliac disease were 4.005 times more likely to develop IBS-D compared to women with high somatization. In addition, women on antibiotics and those with anxiety and depression were significantly more prone to suffer from each IBS subtype ($p < 0.05$), except for women with depression to IBS-U.

3.4 Chi-squared analysis of differences in influencing factors among irritable bowel syndrome subtypes

As shown in Table 2, somatization, antibiotics, anxiety, and depression significantly differed among the four IBS subtypes (p <0.05). Patients with IBS-M had the highest symptoms, including somatization, anxiety, and depression, with the highest rate being up to 66.4% with high somatization (see Supplementary Tables S7, S8 for sex differences).

TABLE 2 Chi-square analysis of differences in influencing factors among different subtypes (n = 17,695).

	IBS-C n = 2,608	IBS-D n = 4,448	IBS-M n = 10,436	IBS-U n = 203	p-value
Sex					<0.001
Female	2,246 (86.1%)	3,239 (72.8%)	7,912 (75.8%)	147 (72.4%)	
Male	362 (13.9%)	1,209 (27.2%)	2,524 (24.2%)	56 (27.6%)	
Age (years)					<0.001
Mean (SD)	54.41 (7.858)	54.26 (7.766)	54.35 (7.788)	57.22 (7.483)	
Median (IQR)	55 (48, 61)	54 (48, 61)	55 (48, 61)	58 (52, 63)	
Townsend Deprivation Score					0.009
Mean (SD)	−1.57 (2.902)	−1.47 (2.944)	−1.35 (3.063)	−1.81 (2.704)	
Median (IQR)	−2.33 (−3.76, 0.01)	−2.26 (−3.71, 0.30)	−2.18 (−3.67, 0.50)	−2.45 (−3.85, −0.53)	
Missing data	4 (0.2%)	7 (0.2%)	17 (0.2%)	2 (1.0%)	
Ever been offered/sought treatment for anxiety					0.003
Yes	931 (35.7%)	1,628 (36.6%)	4,059 (38.9%)	74 (36.5%)	
No	1,667 (63.9%)	2,813 (63.2%)	6,326 (60.6%)	129 (63.5%)	
Missing data	10 (0.4%)	7 (0.2%)	51 (0.5%)	0 (0.0%)	
Ever been offered/sought treatment for depression					<0.001
Yes	1,026 (39.3%)	1713 (38.5%)	4,421 (42.4%)	68 (33.5%)	
No	1,568 (60.1%)	2,721 (61.2%)	5,969 (57.2%)	133 (65.5%)	
Missing data	14 (0.5%)	14 (0.3%)	46 (0.4%)	2 (1.0%)	
Family history of IBS					<0.001
Yes	686 (26.3%)	1,223 (27.5%)	3,048 (29.2%)	36 (17.7%)	
No	1,269 (48.7%)	2082 (46.8%)	4,397 (42.1%)	111 (54.7%)	
Missing data	653 (25.0%)	1,143 (25.7%)	2,991 (28.7%)	56 (27.6%)	
Long-term/recurrent antibiotics as child or teenager					<0.001
Yes	587 (22.5%)	968 (21.8%)	2,562 (24.5%)	46 (22.7%)	
No	1,652 (63.3%)	2,902 (65.2%)	6,316 (60.5%)	133 (65.5%)	
Missing data	369 (14.1%)	578 (13.0%)	1,558 (14.9%)	24 (11.8%)	
Diagnosed with coeliac disease or gluten sensitivity					0.959
Yes	133 (5.1%)	222 (5.0%)	523 (5.0%)	12 (5.9%)	
No	2,408 (92.3%)	4,123 (92.7%)	9,630 (92.3%)	190 (93.6%)	
Missing data	67 (2.6%)	103 (2.3%)	283 (2.7%)	1 (0.5%)	
PHQ-12 Score					<0.001
≤6	928 (35.6%)	1,725 (38.8%)	3,012 (28.9%)	83 (40.9%)	
>6	1,573 (60.3%)	2,555 (57.4%)	6,933 (66.4%)	113 (55.7%)	
Missing data	107 (4.1%)	168 (3.8%)	491 (4.7%)	7 (3.4%)	

Data were mean (SD) or n (%) unless noted otherwise. The distribution of age and the Townsend Deprivation Score is non-normal; therefore, the mean (SD) and median (P25 and P75) are used to describe. The p-value was calculated by the chi-square test and Wilcoxon's rank-sum test where applicable. In this analysis, "Do not know," "Prefer not to answer," and "missing" were coded as missing data.

3.5 Prevalence and influencing factors of post-infectious irritable bowel syndrome

A total of 1,787 individuals met our definition of PI-IBS, and the proportion of PI-IBS in IBS was 1,787/10,760 (16.6%). To further analyze the differences between PI-IBS and non-PI-IBS, eligible participants, including 1,441 PI-IBS and 6,815 non-PI-IBS, were included (n = 8,256). A univariate analysis (Table 3) showed statistical differences in anxiety, depression, family history of IBS, antibiotics abuse, coeliac disease, and somatization between PI-IBS and non-PI-IBS groups (p <0.05). Figure 7 shows the severity of the initial symptoms in both PI-IBS and non-PI-IBS groups. This study found that all the patients with PI-IBS had diarrhea, whereas almost all non-PI-IBS patients had no bloody diarrhea, vomiting, and fever. In the PI-IBS group, the symptoms of fever, bloody diarrhea, and vomiting were more severe than those in the non-PI-IBS group.

TABLE 3 Differences between PI-IBS and non-PI-IBS.

Variable	All (n = 8,256)		p-value
	PI-IBS n = 1,441 (%)	Non-PI-IBS n = 6,815 (%)	
Sex			0.011
Female	1,117 (77.5)	5,484 (80.5)	
Male	324 (22.5)	1,331 (19.5)	
Age (years)			<0.001
Mean (SD)	53.27 (7.614)	54.76 (7.722)	
Median (IQR)	53 (47, 59.5)	55 (49, 61)	
Townsend Deprivation Score			<0.001
Mean (SD)	−0.98 (3.168)	−1.56 (2.918)	
Median (IQR)	−1.76 (−3.48, 0.96)	−2.35 (−3.73, 0.13)	
Missing data	2 (0.1)	11 (0.2)	
Ever been offered/sought treatment for anxiety			<0.001
Yes	698 (48.4)	2,916 (42.8)	
No	741 (51.4)	3,867 (56.7)	
Missing data	2 (0.1)	32 (0.5)	
Ever been offered/sought treatment for depression			<0.001
Yes	726 (50.4)	3,017 (44.3)	
No	711 (49.3)	3,767 (55.3)	
Missing data	4 (0.3)	31 (0.5)	
Family history of IBS			0.002
Yes	574 (39.8)	2,382 (35.0)	
No	509 (35.3)	2,629 (38.6)	
Missing data	358 (24.8)	1,804 (26.5)	
Long-term/recurrent antibiotics as child or teenager			<0.001
Yes	496 (34.4)	1,619 (23.8)	
No	712 (49.4)	4,162 (61.1)	
Missing data	233 (16.2)	1,034 (15.2)	
Diagnosed with coeliac disease or gluten sensitivity			<0.001
Yes	139 (9.6)	395 (5.8)	
No	1,246 (86.5)	6,264 (91.9)	
Missing data	56 (3.9)	156 (2.3)	
PHQ-12 Score			<0.001
≤6	271 (18.8)	2,043 (30.0)	
>6	1,097 (76.1)	4,433 (65.0)	
Missing data	73 (5.1)	339 (5.0)	

Data were mean (SD) or n (%) unless noted otherwise. The distribution of age and the Townsend Deprivation Score is non-normal; therefore, the mean (SD) and median (P25 and P75) are used to describe. The p-value was calculated by the chi-square test and Wilcoxon's rank-sum test where applicable. In this analysis, "Do not know," "Prefer not to answer," and "missing" were coded as missing data.

4 Discussion

To the best of our knowledge, this is the first study to estimate risk factors for IBS and its subtypes using the UK Biobank database. The prevalence of IBS reported in this study was relatively high at 18.3%, which was similar to the estimate found in western countries (3%–22%) (Lovell and Ford, 2012). Somatization and coeliac disease were the top two prominent potential influencing factors associated with IBS for both men and women. Meanwhile, the differences between both subtypes and sexes were mainly focused on psychological factors, especially depression. The proportion of PI-IBS in the UK Biobank was 16.6%, and patients with PI-IBS were afflicted by diarrhea compared with non-PI-IBS patients.

The prevalence of IBS in the UK Biobank was 18.3%, which was rational and acceptable. According to the published literatures,

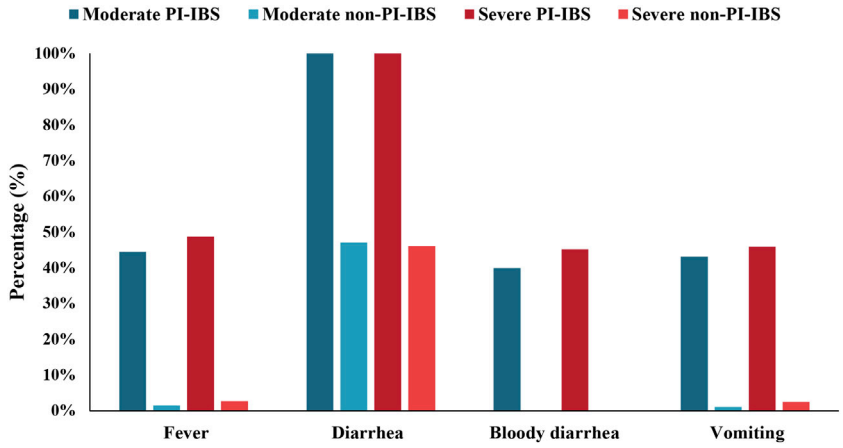

FIGURE 7
Initial symptoms of participants with PI-IBS and non-PI-IBS stratified by moderate and severe symptoms.

the prevalence of IBS in the UK Biobank was still within the scope of UK prevalence ranging from 6.1% to 21.6% (Kennedy and Jones, 2000). Possible reasons for the relatively high prevalence in the UK Biobank were as follows: 1) the UK Biobank attracted healthier volunteers (Fry et al., 2017); however, DHQ decreased "the healthy effect" and amplified the prevalence of IBS in this study. Moreover, 52.1% of participants in the UK Biobank fully completed DHQ after the initial email invitation. Therefore, we considered that DHQ attracted those who were more concerned about digestive health or confused about digestive diseases. 2) Different diagnosis criteria, questionnaires, and methods of questionnaire administration may give rise to differences in the prevalence of IBS (Oka et al., 2020; Sperber et al., 2021). 3) When estimating the prevalence of IBS in the UK Biobank, this study did not restrict a pain/discomfort frequency of at least 2 days a week, similar to that in pathophysiology research and clinical trials (Guthrie et al., 2003). The study followed the general principles to put 2 or 3 days a month, 1 day a week, or more than 1 day a week and comfort or pain on each day as one of the criteria to diagnose IBS.

Somatization was a high-risk factor and ranked first in IBS for both males and females. It reflected patient's sensitivity to pain and other non-gastrointestinal physical stimuli. This study found that more than 63% of patients with IBS had high somatization, especially for the IBS-M subtype (66.4%), with the feeling of exhaustion all the time or having low energy as the most disturbing somatic symptom (Patel et al., 2015). Somatization was considered a criterion for the diagnosis and treatment of IBS for the instructive understanding of its mechanism. High somatization was caused by visceral hypersensitivity, whereas low somatization was caused by gastrointestinal symptoms (Whitehead et al., 2002; Camilleri and Ford, 2017). Also, high somatization in IBS-M, compared with IBS-C and IBS-D, may be partly explained by more frequency of bloating or abdominal distension and increased levels of anxiety and depression (Patel et al., 2015). This study also found that IBS with severe symptoms had a higher level of somatization than IBS with moderate symptoms (73.4% vs. 58.3%). Somatic symptoms can predict the severity of IBS symptoms, although the tools used were Diagnostic Criteria for Psychosomatic Research-Revised and Somatic Symptom Disorder (PHQ-12 and 7-item Whiteley Index) (Schneider et al., 2017). Therefore, we recommend that doctors should be aware of the connection between somatization and IBS during diagnosis, particularly in patients with IBS-M. Antispasmodics are the most commonly prescribed drugs for IBS and help relieve symptoms of abdominal pain and colic (Volta et al., 2016). However, it is not advisable to blindly use such drugs. Instead, direct treatment of IBS is the more effective method. For example, providing problem-oriented and patient-centered self-management guidelines formulated according to the needs of patients improved the symptoms and patients' quality of life (Atkinson et al., 2004).

Coeliac disease was another high-risk factor and ranked second in IBS-C, IBS-D, and IBS-M, except in IBS-U in both men and women. Food and diet were the main factors to cause discomfort, and over 80% of IBS respondents reported gastrointestinal symptoms caused by food intolerance (Böhn et al., 2013). For person with coeliac disease, consuming protein gluten found in some whole grains (wheat, rye, and barley) can cause the body's immune system to attack the small intestine and trigger IBS symptoms (Simrén et al., 2001; Faresjö et al., 2010). Other "trigger foods" of IBS, such as fatty foods, dairy products, coffee, and alcohol, can exacerbate gastrointestinal reactions and increase discomfort; therefore,

patients with IBS tend to exhibit visceral hypersensitivity after eating (Hammer et al., 2008; Irvine et al., 2017). For example, capsaicin can provoke visceral pain and hypersensitivity in patients (McKenzie et al., 2016). We observed that 5.0% of patients with IBS had coeliac disease higher than the previous study with 3.3% (National Institute for Health and Care Excellence, 2018). Interestingly, we found that patients with IBS had a higher risk of coeliac disease, with an OR of approximately 3–5 compared with that in non-IBS patients, although there were no differences regarding this factor among IBS subtypes. We may conclude that clinicians can evaluate the possibility of suffering from IBS through coeliac disease, but this factor cannot assist in diagnosing IBS subtypes.

Clinically, doctors are likely to start with a complete disease history, physical exam, and some tests to rule out other conditions in the absence of effective inspection tools. However, an excessive inspection may take place. In view of the close relationship with diet, doctors should carefully inquire about the patient's dietary habits and discomfort of the digestive system for the diagnosis to provide individualized treatment in accordance with the appropriate IBS subtypes, such as IBS-U and IBS-D for women and IBS-M and IBS-D for men. For the treatment of IBS, clinicians may consider recommending that patients undertake dietary therapy based on guidance provided by the National Institute for Health and Care Excellence and the British Dietetic Association (Maxwell et al., 2002; Staudacher et al., 2012). In addition, a low or free fermentable oligosaccharides, disaccharides, monosaccharides, and polyols (FODMAPs) diet was an effective therapy (Pimentel et al., 2011); however, clinicians should emphasize a balanced diet instead of a single diet.

Long-term/recurrent use of antibiotics in children or adolescents was a relatively new variable to assess the influencing factors for IBS and its subtypes, except for IBS-U. We found that 12.3% of patients had a history of antibiotic exposure, and IBS-M was the most affected, which aligns with the results of a previous study (Krogsgaard et al., 2018). Antibiotics could affect the gut microbiota, which plays an important role in the occurrence and development of IBS. First, consistent alterations in the gut microbiota of patients with IBS may remind a significant association between gut microbiota and IBS pathophysiology (Sharpe et al., 1992). Second, the gut microbiota may involve and alter the construction of the gut epithelial barrier (Kennedy et al., 2014). Third, the gut microbiota is involved in the brain–gut axis and has effects on the pathogenesis of depression and anxiety (Drossman and Hasler, 2016). Antibiotics can modulate anxious and depressive behavior by modulating the gut microbiota (Tait and Sayuk, 2021). However, antibiotics not only modulated the gut microbiota but also disrupted the normal gut microbiota. They also triggered the alterations of the gut microbiota and gastrointestinal motility and led to chronic gastrointestinal symptoms (Thiwan and Drossman, 2006; Kinsinger, 2017). Therefore, antibiotics may not only exacerbate but also improve the symptoms of IBS (Klem et al., 2017; Berumen et al., 2020). To conclude, the use of antibiotics may be considered a "double-edged sword", and problem-oriented and patient-centered guidelines should be formulated. Clinicians could use antibiotics for short-term therapeutic effects, although they need to be carefully considered for long-term use. To some extent, this study has confirmed that antibiotic abuse in children was a potential risk factor for IBS. However, the inherent link between the long-term use of antibiotics and the mechanism of IBS remains unproven. Therefore, greater emphasis and attention should be placed on proving the impacts of different kinds and duration of use of antibiotics on IBS and its subtypes.

Mental disorders were recognized risk factors for IBS. Patients with IBS exhibited higher anxious and depressive tendencies (Cremonini and Talley, 2005), and about 40% of women with IBS had mental problems in this study. Furthermore, over 20% of people with mental disabilities had IBS, which may indicate a potential interaction between psychological factors and IBS. The brain–gut axis, the bidirectional communication mechanism between the gut and the central nervous system, is usually used to explain this phenomenon (Corsetti and Linaclotide, 2013; Canavan et al., 2014b). Pain perception, emotional arousal, and cognitive response formed by the brain-affected bowel movement and secretion provided a top-down communication conduction method. In contrast, intestinal function regulated the central nervous system and promoted intestinal responses to emotions and cognition, which provided bottom-up communication (Porcelli et al., 2020). Based on the model of IBS pathogenesis, non-pharmacological treatments have also been proposed; commonly used psychological therapies are cognitive behavioral therapy and hypnotherapy (Duan et al., 2019). It is important that antidepressants are considered as treatment options for IBS and are prioritized or recommended to patients with both IBS and depression as a safe, long-term drug treatment method (Piche et al., 2009).

In this study, the prevalence of PI-IBS in the UK Biobank was 16.6% among patients with IBS, which was a logical reference to other literature (Schwille-Kiuntke et al., 2011; Johnsen et al., 2018). Some patients with PI-IBS (about 10%) eventually develop IBS (Heenan et al., 2020). This may indicate that PI-IBS does not have long-term stability and ultimately transits to IBS. This study found that patients with PI-IBS suffered from diarrhea, although this could not determine the differences between PI-IBS and non-PI-IBS. Instead, bloody diarrhea may be considered in the diagnosis of PI-IBS. Once diagnosed with PI-IBS, the patient's prognosis is likely to improve rather than worsen (Bercik et al., 2011); therefore, attention should be paid to the severity of symptoms in patients with PI-IBS. This study believed that more attention should be paid to the effects of antibiotics on patients with PI-IBS. A previous study reported that the patients who were given antibiotics following infection were more likely to develop longer-lasting IBS symptoms

(Mearin et al., 2005; Spiller and Garsed, 2009; Ghoshal et al., 2012; Ringel and Maharshak, 2013).

This study used high-quality large sample data with 174,217 participants from the UK Biobank to explore and analyze the differences in influencing factors of IBS in terms of sexes and subtypes. This study found that the pooled prevalence of IBS in the UK Biobank was approximately 18.3%, of which the prevalence of PI-IBS was 16.6%. This study reveals that somatization and coeliac disease are the most prominent influencing factors of IBS and its subtypes. Considerable differences associated with sex and subtypes are reflected in psychological factors and coeliac disease. The main results of this study were to comprehensively demonstrate the differences of influencing factors based on sex and subtypes. This research could provide guidance for clinicians and suggest that special attention is required regarding sex-specific differences. Moreover, this study emphasizes the importance of psychological treatment and adoption of particular treatment according to each subtype. However, there were several limitations in the UK Biobank database that should be considered. First, this study was a cross-sectional study using the UK Biobank database. Therefore, this study could not establish causal relationships based on the results. Second, the UK Biobank may attract participants who are more concerned with digestive health and their self-reported exposures and outcomes may cause reporting bias. This study may not represent the full picture of the UK; however, we still put emphasis on the advantages and use of the UK Biobank database because this study aimed to explore the differences of factors associated with IBS subtypes rather than the epidemiological features of IBS. Third, the DHQ was designed by a group of experts in 2015, when Rome III was still the common standard for diagnosing IBS. Sadly, at the time of the 2017 study, the questionnaire had not been updated, which posed some limitations to the study. Future studies should use the latest IBS diagnostic tools to explore and compare the relationships between various influencing factors and to identify the mediators and moderators that affect IBS. Moreover, longitudinal research exploring the causal relationship between various risk factors and IBS is required.

Data availability statement

The datasets presented in this study can be found in online repositories. The names of the repository/repositories and accession number(s) can be found at: https://www.ukbiobank.ac.uk/; application number 56320.

Ethics statement

The studies involving human participants were reviewed and approved. This research was conducted using the UK Biobank resource under application number 56320. The UK Biobank received ethical approval from the National Health Service National Research Ethics Service (REC reference 11/NW/0382), and this study complies with the Declaration of Helsinki ethical principles for medical research. The patients/participants provided their written informed consent to participate in this study.

Author contributions

KW and HL conducted the calculations, analyzed the results, and drafted the manuscript. QW and YH agreed to the final approval of the version to be published. JL and LH made substantial contributions to the acquisition of data. ZK and LL revised the manuscript critically for important intellectual content. SJ, NM, PC, and QX participated in the collection of part data.

Funding

This work was funded by QW of the National Natural Science Foundation of China (Grant No. 71333003) and the National Office for Philosophy and Social Sciences (Grant No. 19AZD013). The funding body supported the design of the study, data analysis, proofreading, and fine-tuning of the manuscript.

Acknowledgments

We would like to thank the UK Biobank and Editage (www.editage.cn) for English language editing.

Conflict of interest

The authors declare that the research was conducted in the absence of any commercial or financial relationships that could be construed as a potential conflict of interest.

Publisher's note

Supplementary material

The Supplementary Material for this article can be found online at: https://www.frontiersin.org/articles/10.3389/fphar.2022.905564/full#supplementary-material

References

Atkinson, W., Sheldon, T. A., Shaath, N., and Whorwell, P. J. (2004). Food elimination based on IgG antibodies in irritable bowel syndrome: A randomised controlled trial. *Gut* 53 (10), 1459–1464. doi:10.1136/gut.2003.037697

Aziz, I., and Simrén, M. (2021). The overlap between irritable bowel syndrome and organic gastrointestinal diseases. *Lancet Gastroenterol. Hepatol.* 6 (2), 139–148. doi:10.1016/s2468-1253(20)30212-0

Aziz, I., Törnblom, H., Palsson, O. S., Whitehead, W. E., and Simrén, M. (2018). How the change in IBS criteria from Rome III to Rome IV impacts on clinical characteristics and key pathophysiological factors. *Am. J. Gastroenterol.* 113 (7), 1017–1025. doi:10.1038/s41395-018-0074-z

Baydoun, A., Maakaron, J. E., Halawi, H., Abou Rahal, J., and Taher, A. T. (2012). Hematological manifestations of celiac disease. *Scand. J. Gastroenterol.* 47 (12), 1401–1411. doi:10.3109/00365521.2012.706828

Bercik, P., Denou, E., Collins, J., Jackson, W., Lu, J., Jury, J., et al. (2011). The intestinal microbiota affect central levels of brain-derived neurotropic factor and behavior in mice. *Gastroenterology* 141 (2), 599–609. doi:10.1053/j.gastro.2011.04.052

Berumen, A., Lennon, R., Breen-Lyles, M., Griffith, J., Patel, R., Boxrud, D., et al. (2020). Characteristics and risk factors of post-infection irritable bowel syndrome after Campylobacter enteritis. *Clin. Gastroenterol. Hepatol.* 23, 1855–1863e1. doi:10.1016/j.cgh.2020.07.033

Black, C. J., Yiannakou, Y., Houghton, L. A., Shuweihdi, F., West, R., Guthrie, E., et al. (2020). Anxiety-related factors associated with symptom severity in irritable bowel syndrome. *Neurogastroenterol. Motil.* 32 (8), e13872. doi:10.1111/nmo.13872

Böhn, L., Störsrud, S., Törnblom, H., Bengtsson, U., and Simrén, M. (2013). Self-reported food-related gastrointestinal symptoms in IBS are common and associated with more severe symptoms and reduced quality of life. *Am. J. Gastroenterol.* 108 (5), 634–641. doi:10.1038/ajg.2013.105

Bonfiglio, F., Zheng, T., Garcia-Etxebarria, K., Hadizadeh, F., D'Amato, M., Bresso, F., et al. (2018). Female-specific association between variants on chromosome 9 and self-reported diagnosis of irritable bowel syndrome. *Gastroenterology* 155 (1), 168–179. doi:10.1053/j.gastro.2018.03.064

Camilleri, M., and Ford, A. C. (2017). Pharmacotherapy for irritable bowel syndrome. *J. Clin. Med.* 27 (11), E101. doi:10.3390/jcm6110101

Canavan, C., West, J., and Card, T. (2014a). Review article: The economic impact of the irritable bowel syndrome. *Aliment. Pharmacol. Ther.* 40 (9), 1023–1034. doi:10.1111/apt.12938

Canavan, C., West, J., and Card, T. (2014b). The epidemiology of irritable bowel syndrome. *Clin. Epidemiol.* 6, 71–80. doi:10.2147/clep.S40245

Card, T., Enck, P., Barbara, G., Boeckxstaens, G. E., Santos, J., Azpiroz, F., et al. (2018). Post-infectious IBS: Defining its clinical features and prognosis using an internet-based survey. *United Eur. Gastroenterol. J.* 6 (8), 1245–1253. doi:10.1177/2050640618779923

Collins, R. (2012). What makes UK Biobank special? *Lancet* 379 (9822), 1173–1174. doi:10.1016/S0140-6736(12)60404-8

Corsetti, M., and Linaclotide, T. J. (2013). A new drug for the treatment of chronic constipation and irritable bowel syndrome with constipation. *United Eur. Gastroenterol. J.* 1 (1), 7–20. doi:10.1177/2050640612474446

Cremonini, F., and Talley, N. J. (2005). Irritable bowel syndrome: Epidemiology, natural history, health care seeking and emerging risk factors. *Gastroenterol. Clin. North Am.* 34 (2), 189–204. doi:10.1016/j.gtc.2005.02.008

Drossman, D. A., and Hasler, W. L. (2016). Rome IV-functional GI disorders: Disorders of gut-brain interaction. *Gastroenterology* 150 (6), 1257–1261. doi:10.1053/j.gastro.2016.03.035

Drossman, D. A., Li, Z., Andruzzi, E., Temple, R. D., Talley, N. J., Thompson, W. G., et al. (1993). U.S. householder survey of functional gastrointestinal disorders. Prevalence, sociodemography, and health impact. *Dig. Dis. Sci.* 38 (9), 1569–1580. doi:10.1007/bf01303162

Drossman, D. A. (2006). The functional gastrointestinal disorders and the Rome III process. *Gastroenterology* 130 (5), 1377–1390. doi:10.1053/j.gastro.2006.03.008

Duan, R., Zhu, S., Wang, B., and Duan, L. (2019). Alterations of gut microbiota in patients with irritable bowel syndrome based on 16S rRNA-targeted sequencing: A systematic review. *Clin. Transl. Gastroenterol.* 10 (2), e00012. doi:10.14309/ctg.0000000000000012

Dunlop, S. P., Jenkins, D., and Spiller, R. C. (2003). Distinctive clinical, psychological, and histological features of postinfective irritable bowel syndrome. *Am. J. Gastroenterol.* 98 (7), 1578–1583. doi:10.1111/j.1572-0241.2003.07542.x

Eswaran, S., Tack, J., and Chey, W. D. (2011). Food: The forgotten factor in the irritable bowel syndrome. *Gastroenterol. Clin. North Am.* 40 (1), 141–162. doi:10.1016/j.gtc.2010.12.012

Faresjö, A., Johansson, S., Faresjö, T., Roos, S., and Hallert, C. (2010). Sex differences in dietary coping with gastrointestinal symptoms. *Eur. J. Gastroenterol. Hepatol.* 22 (3), 327–333. doi:10.1097/meg.0b013e32832b9c53

Fichna, J., and Storr, M. A. (2012). Brain-gut interactions in IBS. *Front. Pharmacol.* 3, 127. doi:10.3389/fphar.2012.00127

Fond, G., Loundou, A., Hamdani, N., Boukouaci, W., Dargel, A., Oliveira, J., et al. (2014). Anxiety and depression comorbidities in irritable bowel syndrome (IBS): A systematic review and meta-analysis. *Eur. Arch. Psychiatry Clin. Neurosci.* 264 (8), 651–660. doi:10.1007/s00406-014-0502-z

Ford, A. C., Chey, W. D., Talley, N. J., Malhotra, A., Spiegel, B. M., and Moayyedi, P. (2009). Yield of diagnostic tests for celiac disease in individuals with symptoms suggestive of irritable bowel syndrome: Systematic review and meta-analysis. *Arch. Intern. Med.* 169 (7), 651–658. doi:10.1001/archinternmed.2009.22

Francis, C. Y., Morris, J. A., and Whorwell, P. J. (1997). The irritable bowel severity scoring system: A simple method of monitoring irritable bowel syndrome and its progress. *Aliment. Pharmacol. Ther.* 11 (2), 395–402. doi:10.1046/j.1365-2036.1997.142318000.x

Fry, A., Littlejohns, T. J., Sudlow, C., Doherty, N., Adamska, L., Sprosen, T., et al. (2017). Comparison of sociodemographic and health-related characteristics of UK Biobank participants with those of the general population. *Am. J. Epidemiol.* 186 (9), 1026–1034. doi:10.1093/aje/kwx246

Ghoshal, U. C., Shukla, R., Ghoshal, U., Gwee, K. A., Ng, S. C., and Quigley, E. M. (2012). The gut microbiota and irritable bowel syndrome: Friend or foe? *Int. J. Inflamm.* 2012, 151085. doi:10.1155/2012/151085

Guthrie, E., Creed, F., Fernandes, L., Ratcliffe, J., Van Der Jagt, J., Martin, J., et al. (2003). Cluster analysis of symptoms and health seeking behaviour differentiates subgroups of patients with severe irritable bowel syndrome. *Gut* 52 (11), 1616–1622. doi:10.1136/gut.52.11.1616

Hammer, J., Führer, M., Pipal, L., and Matiasek, J. (2008). Hypersensitivity for capsaicin in patients with functional dyspepsia. *Neurogastroenterol. Motil.* 20 (2), 125–133. doi:10.1111/j.1365-2982.2007.00997.x

Heenan, P. E., Keenan, J. I., Bayer, S., Simon, M., and Gearry, R. B. (2020). Irritable bowel syndrome and the gut microbiota [Review]. *J. R. Soc. N. Z.* 50 (3), 470–490. doi:10.1080/03036758.2019.1695635

Hu, Z., Li, M., Yao, L., Wang, Y., Wang, E., Yuan, J., et al. (2021). The level and prevalence of depression and anxiety among patients with different subtypes of irritable bowel syndrome: A network meta-analysis. *BMC Gastroenterol.* 21 (1), 23. doi:10.1186/s12876-020-01593-5

Irvine, A. J., Chey, W. D., and Ford, A. C. (2017). Screening for celiac disease in irritable bowel syndrome: An updated systematic review and meta-analysis. *Am. J. Gastroenterol.* 112 (1), 65–76. doi:10.1038/ajg.2016.466

Jiang, C., Xu, Y., Sharma, S., Zhang, L., Wang, H., Song, J., et al. (2019). Psychosocial factors associated with irritable bowel syndrome development in Chinese College freshmen. *J. Neurogastroenterol. Motil.* 25 (2), 233–240. doi:10.5056/jnm18028

Johnsen, P. H., Hilpüsch, F., Cavanagh, J. P., Leikanger, I. S., Kolstad, C., Valle, P. C., et al. (2018). Faecal microbiota transplantation versus placebo for moderate-to-severe irritable bowel syndrome: A double-blind, randomised, placebo-controlled, parallel-group, single-centre trial. *Lancet. Gastroenterol. Hepatol.* 3 (1), 17–24. doi:10.1016/s2468-1253(17)30338-2

Kennedy, P. J., Cryan, J. F., Dinan, T. G., and Clarke, G. (2014). Irritable bowel syndrome: A microbiome-gut-brain axis disorder? *World J. Gastroenterol.* 20 (39), 14105–14125. doi:10.3748/wjg.v20.i39.14105

Kennedy, T. M., and Jones, R. H. (2000). Epidemiology of cholecystectomy and irritable bowel syndrome in a UK population. *Br. J. Surg.* 87 (12), 1658–1663. doi:10.1046/j.1365-2168.2000.01596.x

Kinsinger, S. W. (2017). Cognitive behavioral therapy for patients with irritable bowel syndrome: Current insights. *Psychol. Res. Behav. Manag.* 10, 231–237. doi:10.2147/prbm.S120817

Klem, F., Wadhwa, A., Prokop, L. J., Sundt, W. J., Farrugia, G., Camilleri, M., et al. (2017). Prevalence, risk factors, and outcomes of irritable bowel syndrome after infectious enteritis: A systematic review and meta-analysis. *Gastroenterology* 152 (5), 1042–1054. doi:10.1053/j.gastro.2016.12.039

Krogsgaard, L. R., Engsbro, A. L., and Bytzer, P. (2018). Antibiotics: A risk factor for irritable bowel syndrome in a population-based cohort. *Scand. J. Gastroenterol.* 53 (9), 1027–1030. doi:10.1080/00365521.2018.1500638

Longstreth, G. F., Thompson, W. G., Chey, W. D., Houghton, L. A., Mearin, F., and Spiller, R. C. (2006). Functional bowel disorders. *Gastroenterology* 130 (5), 1480–1491. doi:10.1053/j.gastro.2005.11.061

Lovell, R. M., and Ford, A. C. (2012). Global prevalence of and risk factors for irritable bowel syndrome: A meta-analysis. *Clin. Gastroenterol. Hepatol.* 10 (7), 712–721. doi:10.1016/j.cgh.2012.02.029

Maxwell, P. R., Rink, E., Kumar, D., and Mendall, M. A. (2002). Antibiotics increase functional abdominal symptoms. *Am. J. Gastroenterol.* 97 (1), 104–108. doi:10.1111/j.1572-0241.2002.05428.x

McKenzie, Y. A., Bowyer, R. K., Leach, H., Gulia, P., Horobin, J., O'Sullivan, N. A., et al. (2016). British Dietetic Association systematic review and evidence-based practice guidelines for the dietary management of irritable bowel syndrome in adults (2016 update). *J. Hum. Nutr. Diet.* 29 (5), 549–575. doi:10.1111/jhn.12385

Mearin, F., Pérez-Oliveras, M., Perelló, A., Vinyet, J., Ibañez, A., Coderch, J., et al. (2005). Dyspepsia and irritable bowel syndrome after a Salmonella gastroenteritis outbreak: One-year follow-up cohort study. *Gastroenterology* 129 (1), 98–104. doi:10.1053/j.gastro.2005.04.012

Midenfjord, I., Borg, A., Törnblom, H., and Simrén, M. (2020). Cumulative effect of psychological alterations on gastrointestinal symptom severity in irritable bowel syndrome. *Am. J. Gastroenterol.* 116, 769–779. doi:10.14309/ajg.0000000000001038

National Institute for Health and Care Excellence (2018). *Clinical guidelines. Irritable bowel syndrome in adults: Diagnosis and management*. London: National Institute for Health and Care Excellence (UK)Copyright © NICE.

Oka, P., Parr, H., Barberio, B., Black, C. J., Savarino, E. V., and Ford, A. C. (2020). Global prevalence of irritable bowel syndrome according to Rome III or IV criteria: A systematic review and meta-analysis. *Lancet. Gastroenterol. Hepatol.* 5 (10), 908–917. doi:10.1016/s2468-1253(20)30217-x

Patel, P., Bercik, P., Morgan, D. G., Bolino, C., Pintos-Sanchez, M. I., Moayyedi, P., et al. (2015). Irritable bowel syndrome is significantly associated with somatisation in 840 patients, which may drive bloating. *Aliment. Pharmacol. Ther.* 41 (5), 449–458. doi:10.1111/apt.13074

Piche, T., Barbara, G., Aubert, P., Bruley des Varannes, S., Dainese, R., Nano, J. L., et al. (2009). Impaired intestinal barrier integrity in the colon of patients with irritable bowel syndrome: Involvement of soluble mediators. *Gut* 58 (2), 196–201. doi:10.1136/gut.2007.140806

Pimentel, M., Lembo, A., Chey, W. D., Zakko, S., Ringel, Y., Yu, J., et al. (2011). Rifaximin therapy for patients with irritable bowel syndrome without constipation. *N. Engl. J. Med.* 364 (1), 22–32. doi:10.1056/NEJMoa1004409

Polster, A. V., Palsson, O. S., Törnblom, H., Öhman, L., Sperber, A. D., Whitehead, W. E., et al. (2018). Subgroups of IBS patients are characterized by specific, reproducible profiles of GI and non-GI symptoms and report differences in healthcare utilization: A population-based study. *Neurogastroenterol. Motil.* 31 (1), e13483. doi:10.1111/nmo.13483

Porcelli, P., De Carne, M., and Leandro, G. (2020). Distinct associations of DSM-5 somatic symptom disorder, the diagnostic criteria for psychosomatic ResearchRevised (DCPR-R) and symptom severity in patients with irritable bowel syndrome [article]. *Gen. Hosp. Psychiatry* 64, 56–62. doi:10.1016/j.genhosppsych.2020.03.004

Ringel, Y., and Maharshak, N. (2013). Intestinal microbiota and immune function in the pathogenesis of irritable bowel syndrome. *Am. J. physiology Gastrointest. liver physiology* 305 (8), G529–G541. doi:10.1152/ajpgi.00207.2012

Schneider, A., Rosenberger, S., Bobardt, J., Bungartz-Catak, J., Atmann, O., Haller, B., et al. (2017). Self-help guidebook improved quality of life for patients with irritable bowel syndrome. *PLoS One* 12 (7), e0181764. doi:10.1371/journal.pone.0181764

Schwille-Kiuntke, J., Frick, J. S., Zanger, P., and Enck, P. (2011). Post-infectious irritable bowel syndrome--a review of the literature. *Z. Gastroenterol.* 49 (8), 997–1003. doi:10.1055/s-0031-1281581

Sharpe, M., Peveler, R., and Mayou, R. (1992). The psychological treatment of patients with functional somatic symptoms: A practical guide. *J. Psychosom. Res.* 36 (6), 515–529. doi:10.1016/0022-3999(92)90037-3

Simrén, M., Abrahamsson, H., and Björnsson, E. S. (2001). An exaggerated sensory component of the gastrocolonic response in patients with irritable bowel syndrome. *Gut* 48 (1), 20–27. doi:10.1136/gut.48.1.20

Sperber, A. D., Bangdiwala, S. I., Drossman, D. A., Ghoshal, U. C., Simren, M., Tack, J., et al. (2021). Worldwide prevalence and burden of functional gastrointestinal disorders, results of Rome foundation global study. *Gastroenterology* 160 (1), 99–114.e3. doi:10.1053/j.gastro.2020.04.014

Spiller, R., and Garsed, K. (2009). Postinfectious irritable bowel syndrome. *Gastroenterology* 136 (6), 1979–1988. doi:10.1053/j.gastro.2009.02.074

Spiller, R. C., Humes, D. J., Campbell, E., Hastings, M., Neal, K. R., Dukes, G. E., et al. (2010). The Patient Health Questionnaire 12 Somatic Symptom scale as a predictor of symptom severity and consulting behaviour in patients with irritable bowel syndrome and symptomatic diverticular disease. *Aliment. Pharmacol. Ther.* 32, 811–820. doi:10.1111/j.1365-2036.2010.04402.x

Staudacher, H. M., Lomer, M. C., Anderson, J. L., Barrett, J. S., Muir, J. G., Irving, P. M., et al. (2012). Fermentable carbohydrate restriction reduces luminal bifidobacteria and gastrointestinal symptoms in patients with irritable bowel syndrome. *J. Nutr.* 142 (8), 1510–1518. doi:10.3945/jn.112.159285

Tack, J., Stanghellini, V., Mearin, F., Yiannakou, Y., Layer, P., Coffin, B., et al. (2019). Economic burden of moderate to severe irritable bowel syndrome with constipation in six European countries. *BMC Gastroenterol.* 19 (1), 69. doi:10.1186/s12876-019-0985-1

Tait, C., and Sayuk, G. S. (2021). The brain-gut-microbiotal Axis: A framework for understanding functional gi illness and their therapeutic interventions. *Eur. J. Intern. Med.* 84, 1–9. doi:10.1016/j.ejim.2020.12.023

Talley, N. J., Zinsmeister, A. R., and Melton, L. J. (1995). Irritable bowel syndrome in a community: Symptom subgroups, risk factors, and health care utilization. *Am. J. Epidemiol.* 142 (1), 76–83. doi:10.1093/oxfordjournals.aje.a117548

Thiwan, S. I., and Drossman, D. A. (2006). Treatment of functional gi disorders with psychotropic medicines: A review of evidence with a practical approach. *Gastroenterol. Hepatol.* 2 (9), 678–688.

Volta, U., Pinto-Sanchez, M. I., Boschetti, E., Caio, G., De Giorgio, R., and Verdu, E. F. (2016). Dietary triggers in irritable bowel syndrome: Is there a role for gluten? *J. Neurogastroenterol. Motil.* 22 (4), 547–557. doi:10.5056/jnm16069

Whitehead, W. E., Palsson, O., and Jones, K. R. (2002). Systematic review of the comorbidity of irritable bowel syndrome with other disorders: What are the causes and implications? *Gastroenterology* 122 (4), 1140–1156. doi:10.1053/gast.2002.32392

Whorwell, P. J., McCallum, M., Creed, F. H., and Roberts, C. T. (1986). Non-colonic features of irritable bowel syndrome. *Gut* 27 (1), 37–40. doi:10.1136/gut.27.1.37

Wong, R. K., and Drossman, D. A. (2010). Quality of life measures in irritable bowel syndrome. *Expert Rev. Gastroenterol. Hepatol.* 4 (3), 277–284. doi:10.1586/egh.10.19

frontiers | Frontiers in Pharmacology

TYPE Original Research
PUBLISHED 05 September 2022
DOI 10.3389/fphar.2022.944886

OPEN ACCESS

EDITED BY
Marilia Seelaender,
University of São Paulo, Brazil

REVIEWED BY
Carlos Ernesto Fernández-García,
Princess University Hospital, Spain
Morgan D. Fullerton,
University of Ottawa, Canada

*CORRESPONDENCE
Chengxia Kan,
fykanchengxia@wfmc.edu.cn
Xiaodong Sun,
xiaodong.sun@wfmc.edu.cn

†These authors have contributed equally to this work and share first authorship

SPECIALTY SECTION
This article was submitted to Gastrointestinal and Hepatic Pharmacology, a section of the journal Frontiers in Pharmacology

RECEIVED 16 May 2022
ACCEPTED 11 August 2022
PUBLISHED 05 September 2022

CITATION
Ma Y, Zhang G, Kuang Z, Xu Q, Ye T, Li X, Qu N, Han F, Kan C and Sun X (2022), Empagliflozin activates Sestrin2-mediated AMPK/mTOR pathway and ameliorates lipid accumulation in obesity-related nonalcoholic fatty liver disease.
Front. Pharmacol. 13:944886.
doi: 10.3389/fphar.2022.944886

Empagliflozin activates Sestrin2-mediated AMPK/mTOR pathway and ameliorates lipid accumulation in obesity-related nonalcoholic fatty liver disease

Yuting Ma[1,2†], Guangdong Zhang[1,2†], Zenggguang Kuang[1,2], Qian Xu[1,2], Tongtong Ye[1,2], Xue Li[2,3], Na Qu[2,3], Fang Han[2,3], Chengxia Kan[1,2*] and Xiaodong Sun[1,2*]

[1]Department of Endocrinology and Metabolism, Affiliated Hospital of Weifang Medical University, Weifang, China, [2]Clinical Research Center, Affiliated Hospital of Weifang Medical University, Weifang, China, [3]Department of Pathology, Affiliated Hospital of Weifang Medical University, Weifang, China

Empagliflozin (EMPA) therapy has led to improvements in patients with non-alcoholic fatty liver disease (NAFLD). Sestrin2 is a stress-inducible protein that controls the AMPK-mTOR pathway and inhibits oxidative damage in cells. This study investigated the functional implications of EMPA on the multifactorial pathogenesis of NAFLD and potential underlying molecular mechanisms of pathogenesis. An *in vitro* model of NAFLD was established by treating HepG2 cells with palmitic acid (PA); an *in vivo* model of NAFLD was generated by feeding C57BL/6 mice a high-fat diet. Investigations of morphology and lipid deposition in liver tissue were performed. Expression patterns of Sestrin2 and genes related to lipogenesis and inflammation were assessed by reverse transcription polymerase chain reaction. Protein levels of Sestrin2 and AMPK/mTOR pathway components were detected by Western blotting. NAFLD liver tissues and PA-stimulated HepG2 cells exhibited excessive lipid production and triglyceride secretion, along with upregulation of Sestrin2 and increased expression of lipogenesis-related genes. EMPA treatment reversed liver damage by upregulating Sestrin2 and activating the AMPK-mTOR pathway. Knockdown of Sestrin2 effectively increased lipogenesis and enhanced the mRNA expression levels of lipogenic and pro-inflammatory genes in PA-stimulated HepG2 cells; EMPA treatment did not affect these changes. Furthermore, Sestrin2 knockdown inhibited AMPK-mTOR signaling pathway activity. The upregulation of Sestrin2 after treatment with EMPA protects against lipid deposition-related metabolic disorders; it also inhibits lipogenesis and inflammation through activation of the AMPK-mTOR signaling pathway. These results suggest that Sestrin2 can be targeted by EMPA therapy to alleviate lipogenesis and inflammation in obesity-related NAFLD.

KEYWORDS

nonalcoholic fatty liver disease, free fatty acids, empagliflozin, inflammation, AMPK-mTOR

Introduction

Non-alcoholic fatty liver disease (NAFLD) is a chronic metabolic disease characterized by excessive triglycerides accumulation without heavy alcohol consumption (Neuschwander-Tetri, 2017; Younossi, 2019). The increased prevalence of obesity worldwide is associated with an increase in global NAFLD risk. Triglycerides accumulated in liver labeling with single steatosis, followed by hepatic steatosis, steatohepatitis, cirrhosis, and even hepatocellular carcinoma (Viganò et al., 2018). Obesity-related increases in free fatty acids (FFAs) lead to enhanced lipotoxic metabolite production, thus resulting in a pro-inflammatory phenotype accompanied by increased expression of pro-inflammatory cytokines (Haukeland et al., 2006; Lucero et al., 2011; Marra and Lotersztajn, 2013). FFAs can also increase intracellular lipid accumulation, leading to hepatic lipotoxicity through its effects on the regulatory patterns of various genes (Chu et al., 2013). Additionally, FFAs impair endoplasmic reticulum function and initiate the unfolded protein response (Liu et al., 2010). This FFA-induced lipotoxicity causes lipid oxidation and eventually progresses to excessive lipid peroxidation, which is associated with enhanced risk of NAFLD pathogenesis (Zámbó et al., 2013; Mota et al., 2016).

Sodium-glucose cotransporter-2 inhibitors (SGLT-2is) are novel hypoglycemic medications used to treat diabetes (Kramer and Zinman, 2019). SGLT-2is decrease blood glucose levels by enhancing glycosuria and diuresis; these changes produce additional benefits, including body weight reduction (Kramer and Zinman, 2019). Previous clinical trials and meta-analyses have shown that SGLT-2is [e.g., empagliflozin (EMPA), canagliflozin, and dapagliflozin] have protective functions in patients with heart failure, cardiovascular diseases, and/or diabetic nephropathy (Fitchett et al., 2019; Li et al., 2021; Tuttle et al., 2021). Additionally, SGLT-2is can maintain liver structure and function in patients with NAFLD (Coelho et al., 2020; Mantovani et al., 2020). Moreover, the use of SGLT-2is has led to improvements in histologic steatosis, lobular inflammation, hepatocyte ballooning, and fibrosis in patients with liver steatosis (Hsiang and Wong, 2020). Thus, SGLT-2i therapy appears to be a promising strategy for management of NAFLD.

Sestrin2 (Sesn2) is a highly conserved stress-inducible protein expressed in multiple tissues (e.g., liver, muscles, heart, and kidneys); it acts as a critical regulator of obesity-associated pathologies (Gong et al., 2021). As a stress-inducible metabolic protein, Sesn2 participates in the maintenance of metabolic homeostasis by regulating responses to various stresses, including oxidative stress and metabolic pathologies (Sun W. et al., 2020). Consistent with this function, sestrin2 knockout mice demonstrated increased fibrosis and the enhancement of inflammatory responses, apoptosis, and reactive oxygen species production (Hwang et al., 2017). Previous studies showed that Sesn2 prevents NAFLD and protects against hepatic fibrosis induced by various drugs (Yang et al., 2019; Han et al., 2020). Increased Sesn2 expression reportedly protects against hepatic steatosis, attenuates hepatic endoplasmic reticulum stress, and alleviates fibrosis in obese mice (Park et al., 2014; Jegal et al., 2020). Moreover, Sesn2 can activate the AMPK pathway and suppress mTOR signaling to attenuate various metabolic disorders, including insulin resistance, mitochondrial dysfunction, and cardiac dysfunction (Sun X. et al., 2020; Kishimoto et al., 2021). Based on the previous literature summarized above, we hypothesized that Sesn2 could serve as a novel therapeutic target for various aging- and obesity-associated diseases.

While SGLT2is are regarded as key regulators of lipid metabolism in NAFLD therapy, the underlying mechanisms have not been fully elucidated. Here, we aimed to explore the potential mechanism by which EMPA protects against lipogenesis and inflammation through assessment of Sesn2-mediated AMPK-mTOR signaling and cellular antioxidant signaling in a model of high-fat diet (HFD)-induced NAFLD.

Materials and methods

Materials

A detailed list of materials is provided in Supplementary Table S1.

Animals

Six-week-old male C57BL/6J mice (Shandong Jinan Pengyue Animal Breeding Co., Ltd.) were housed in ventilated cages (five mice per cage). All mice were randomly assigned to one of the following three groups: the normal control group was fed normal chow (10% fat, 320 kcal per 100 g); the HFD and EMPA groups were fed an HFD (54% fat, 529.8 kcal per 100 g) for 12 weeks to establish the NAFLD model. Then, the EMPA group was received EMPA (10 mg/kg/d diluted in saline) by oral gavage) for another 8 weeks, whereas the other two groups received saline. Body fat in mice was measured using the Mouse-Body Composition Analyzer (Bruker, Germany). All mice were housed under standard laboratory conditions (temperature, 22 ± 1°C; humidity, 55%–60%; 12-h/12-h light and dark cycles). All animal experiments were approved by the Animal Ethics Committee of Weifang Medical University.

Cell culture

The HepG2 human hepatocyte cell line was grown in Dulbecco's modified Eagle medium supplemented with 10%

fetal bovine serum. All cells were maintained at 37°C in a humidified incubator. For *in vitro* experiments, cells were seeded and then cultured to a density of 70%–80%; subsequently, they were supplemented with 0.5 mM palmitic acid (PA) for 24 h, then treated with 1 μM EMPA for 24 h (Sun X. et al., 2020). Finally, the cells were collected for future analysis.

Biochemical analyses

Mice were anesthetized with 2% sodium pentobarbital via intraperitoneal injection. Blood samples were obtained, and the liver was collected and weighed. Serum alanine aminotransferase, aspartate aminotransferase, FFA, lipid peroxidation, malondialdehyde (MDA), and triglyceride levels were determined using commercial kits. Total liver or cellular lipids were extracted; hepatic triglyceride, lipid peroxidation, and MDA contents were quantified according to the manufacturer's instructions.

Hematoxylin and eosin and Oil Red O staining

Liver tissues were fixed overnight with 4% paraformaldehyde. In accordance with standard protocols, the tissue sections were subjected to H&E staining and ORO staining. HepG2 cells were subjected to ORO staining using an ORO Stain Kit (Solarbio, Beijing, China). After treatment, cells were washed and then fixed with ORO Fixative. Subsequently, the cells were briefly washed and soaked in ORO reagent for 30 min, then washed with distilled water and subjected to nuclear staining with Mayer's hematoxylin for 1 min. Finally, red-stained lipid droplets of the cells were visualized via microscopy. ORO contents were quantified by the addition of 100% isopropanol to each well and measurement of sample absorbance at 495 nm using a microplate reader.

Cell transfection

siRNA directed against Sesn2 (siSESN2; sequences are listed in Supplementary Table S2) and negative control siRNA (siNC) were purchased from Qingke Co., Ltd. (Beijing, China). Cell transfection was performed using Lipofectamine 3000. HepG2 cells were seeded in six-well plates at 2.5×10^5 cells/well. Lipofectamine-3000 reagent was diluted in 125 μl of OPTI-MEM (Invitrogen); siSESN2 or siNC (7.5 μl) was diluted in the same volume of OPTI-MEM in a separate tube. The diluted siRNA and Lipofectamine-3000 were then mixed and incubated for 15 min. Before subsequent experiments, the cells were cultured for 6 h; the medium was then replaced with fresh Dulbecco's modified Eagle medium for 48 h siSESN2 knockdown efficiency was examined by reverse transcription polymerase chain reaction (RT-PCR) and Western blotting. Before harvest, the transfected cells were stimulated with 0.5 mM PA or treated with or without 1 μM EMPA for 24 h.

Western blot analysis

Equal amounts of total protein were resolved via 10% sodium dodecyl sulfate–polyacrylamide gel electrophoresis, then transferred to polyvinylidene fluoride membranes. The membranes were incubated with anti-Sesn2, anti-Nrf2, anti-PGC1α, anti-p-mTOR, anti-p-AMPK (Thr172), anti-AMPK, anti-mTOR, or anti-HO-1 antibodies (1:1000) and anti-β-actin (1:5000) at 4°C overnight. The membranes were then incubated with the secondary antibody for 1 h. Blots were then developed by enhanced chemiluminescence and analyzed using ImageJ software (NIH, Bethesda, MD, United States).

Quantitative PCR analysis

Total RNA was isolated from cell lines or liver tissues using TRIzol. RNA was reverse transcribed to cDNA using the PrimeScript RT reagent Kit with gDNA Eraser. qPCR was performed with TB Green premix Ex Taq II. β-actin was used as an internal control to calculate relative expression. PCR primer sequences are shown in Supplementary Tables S2, S3.

Statistical analysis

The results were analyzed by GraphPad Prism 9.0; all data are expressed as means ± standard errors of the mean (SEM) and assessed for normality. Comparisons between two groups were assessed using unpaired Student's t-tests; comparisons among three or more groups were conducted using one-way ANOVA followed by Turkey's test. Differences with $p < 0.05$ were considered statistically significant.

Results

EMPA reduced body weight and fat mass, while improving lipid metabolism, in HFD mice

We established an HFD model in C57BL/6J mice. After 12 weeks, the HFD mice displayed significantly increased body weight and fat mass ($p < 0.05$). Eight-week

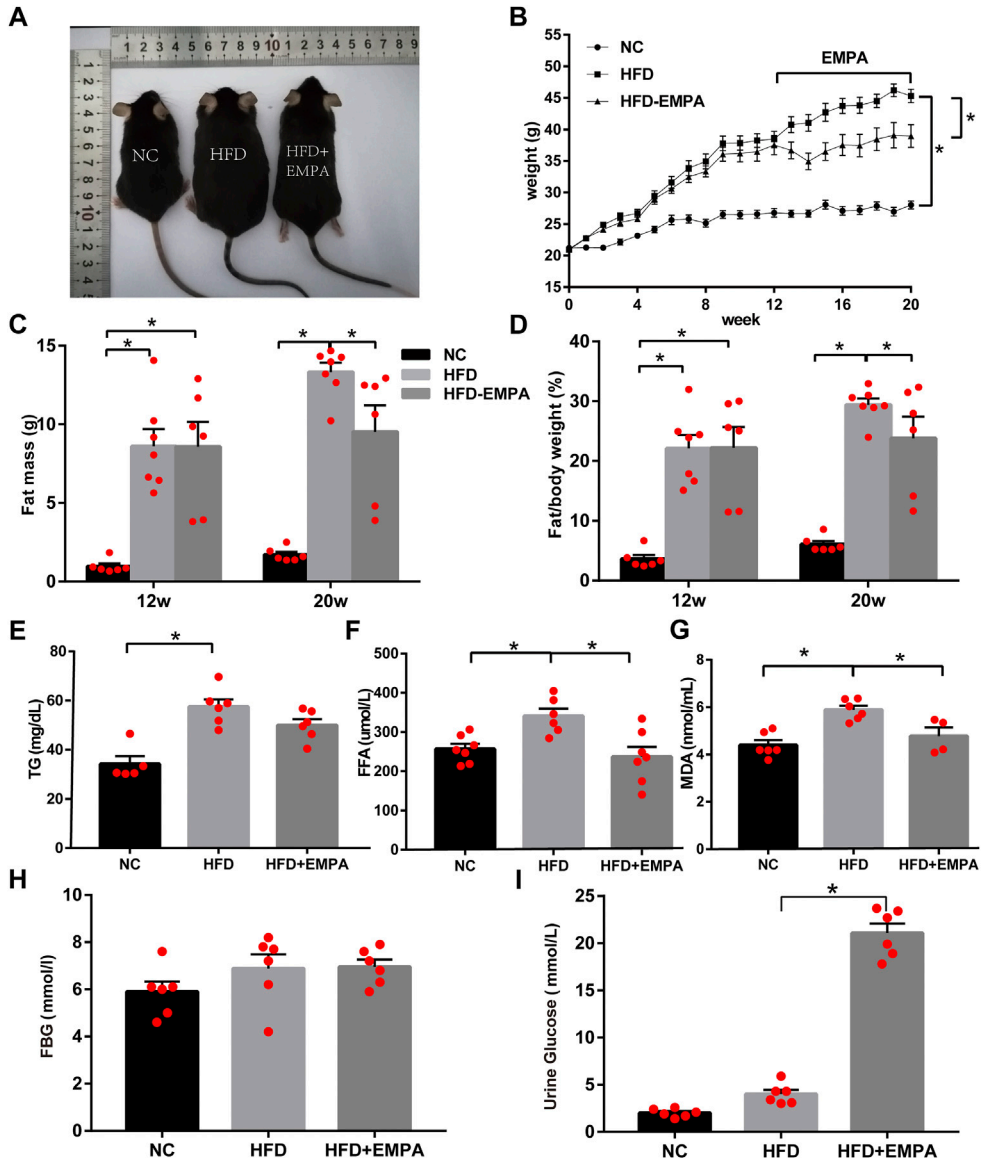

FIGURE 1
Body weight, fat mass and biochemical parameters in HFD mice with or without empagliflozin. **(A)** Morphology of mice. **(B)** Weekly body weights. **(C)** Body fat mass of the mice. **(D)** Body fat/body weight. **(E)** Plasma triglycerides levels. **(F)** Plasma free fatty acid levels. **(G)** Lipid peroxidation MDA levels. **(H)** Fasting glucose levels. **(I)** Urine glucose. Data are presented as means ± SEM (n = 4-6/group); *p < 0.05.

administration of EMPA by oral gavage significantly suppressed both weight gain and fat mass (p < 0.05; Figures 1A–D). Additionally, circulating triglyceride, FFA, and lipid peroxidation (MDA) levels increased in HFD mice; these changes were alleviated after EMPA treatment (Figures 1E–G). Fasting blood glucose did not significantly differ among groups (p > 0.05; Figure 1H), but urine glucose was significantly increased after EMPA treatment (p < 0.05; Figure 1I). These results showed that EMPA alleviated metabolic alterations.

EMPA improved hepatic function and alleviated hepatic lipid accumulation in HFD mice

Compared with control mice, HFD mice exhibited significantly greater liver mass, serum transaminase levels, and liver MDA content, indicating apparent hepatic injury after HFD induction (p < 0.05). EMPA treatment significantly reduced liver mass, liver MDA content, and serum transaminase levels, including both alanine

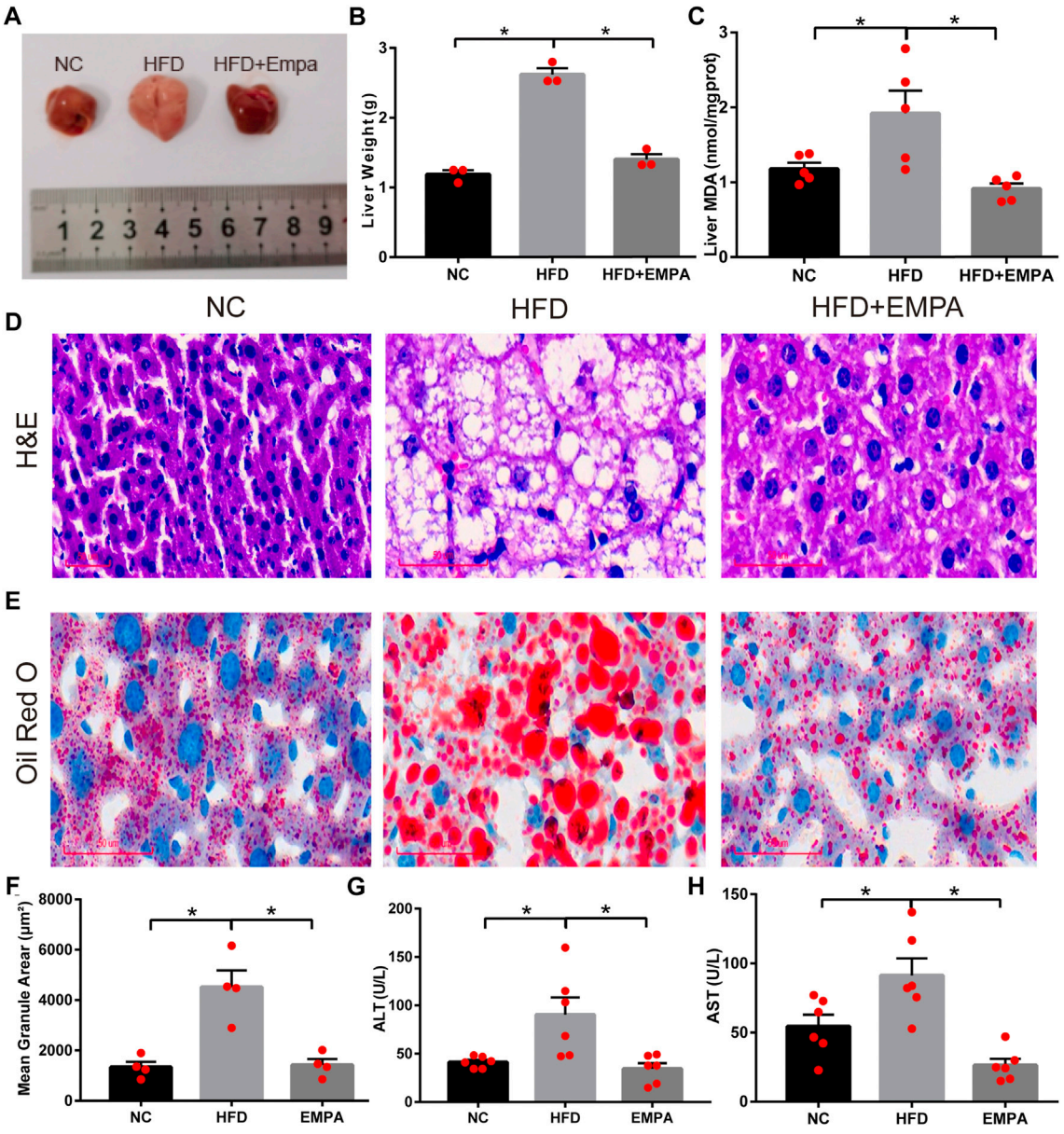

FIGURE 2
Empagliflozin alleviated hepatic function and lipid accumulation in HFD mice. **(A)** Liver morphology of mice. **(B)** Liver weight. **(C)** Liver MDA. **(D)** H&E staining. Scale bar, 50 μm. **(E)** Oil Red O staining. Scale bar, 50 μm. **(F)** quantification of Oil Red O. **(G)** Serum ALT levels. **(H)** Serum AST levels. Data are means ± SEM (n = 3–6/group). *$p < 0.05$.

aminotransferase and aspartate aminotransferase ($p < 0.05$; Figures 2A–H). Additionally, H&E and ORO staining showed noticeable histopathological changes, including increased hepatocyte volumes, more dispersed lipid vacuoles, and greater accumulation of lipid droplet deposition in HFD mice; these effects were alleviated by EMPA treatment (Figures 2D–F). These findings indicated that EMPA significantly reduced hepatic injury in HFD mice.

EMPA upregulated Sesn2-mediated signaling in HFD mice

To explore whether EMPA could activate Sesn2, we first evaluated the expression of liver Sesn2 via Western blotting. We found that HFD administration tended to enhance Sesn2 expression, but this difference was not statistically significant ($p > 0.05$); however, EMPA treatment upregulated Sesn2 expression ($p < 0.05$; Figure 3A). Consistent with the

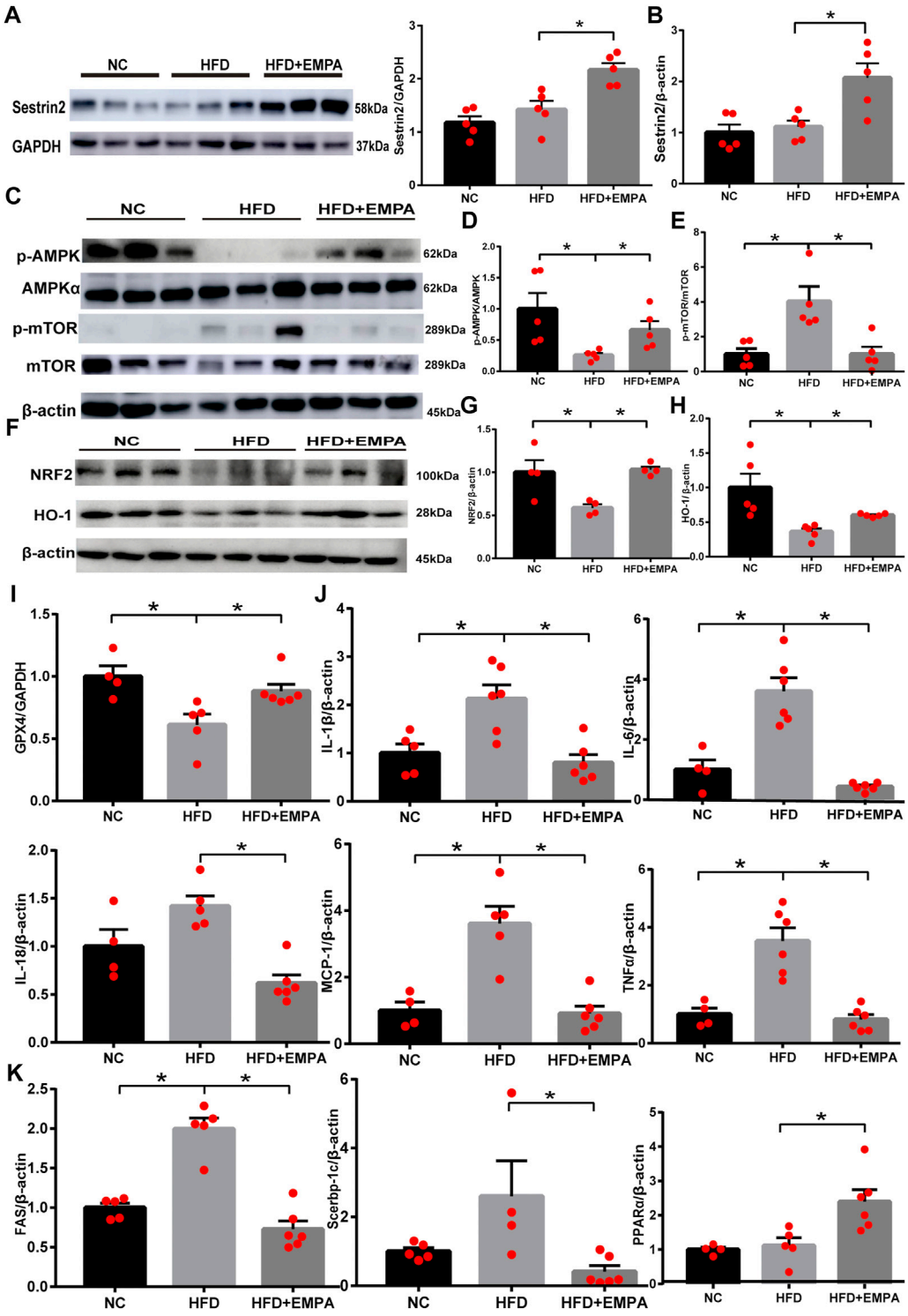

FIGURE 3
Empagliflozin upregulated the Sestrin2-mediated signaling pathway and protected HFD mice from hepatic inflammation and steatosis. **(A)** Western blotting analyses for Sestrin2. **(B)** mRNA expression of Sestrin2. **(C–H)** Western blotting analyses were conducted to detect the expression levels of p-AMPK, p-mTOR, and Nrf2/HO-1. **(I)** GPX4 mRNA. **(J)** mRNA expression of inflammatory cytokines. **(K)** qPCR results for genes associated with fatty acid synthesis and β-oxidation. Data are means ± SEM (n = 4-6/group). *$p < 0.05$.

Western blotting results, RT-PCR analysis indicated that EMPA treatment upregulated Sesn2 mRNA expression ($p < 0.05$; Figure 3B). Because Sesn2 controls the AMPK-mTOR and oxidative stress pathways, we examined whether EMPA affected these pathways. EMPA treatment significantly increased AMPK phosphorylation and decreased mTOR phosphorylation ($p < 0.05$; Figures 3C–E). Additionally, HFD administration inhibited the expression of anti-oxidative stress pathway components Nrf2; the expression levels of Nrf2 and its target genes (GCLC and HMOX1) were enhanced after EMPA treatment ($p < 0.05$; Figures 3F–H, Supplementary Figure S1). Finally, HFD administration downregulated the lipid peroxide gene (*GPX4*), while EMPA treatment upregulated the expression of *GPX4* ($p < 0.05$; Figure 3I). These findings showed that EMPA upregulated the Sesn2-mediated signaling pathway and the anti-oxidative system to alleviate the onset of NAFLD.

EMPA protected HFD mice from hepatic inflammation and steatosis

Next, we evaluated the effects of EMPA on NAFLD-related inflammation. Compared with control mice, HFD mice exhibited greater inflammation in the liver, as demonstrated by significant increases in the mRNA expression levels of *IL-6, IL-1β, IL-18, MCP-1*, and *TNF-α*. However, this HFD-related inflammation was suppressed by EMPA treatment ($p < 0.05$; Figure 3J). To more fully explore the molecular mechanism underlying the effects EMPA on lipid generation and metabolism, lipogenic and fatty acid β-oxidation genes were evaluated. As expected, HFD-induced disordered fatty acid oxidation in mice was significantly mitigated by EMPA treatment, as demonstrated by improvements in lipogenic and fatty acid β-oxidation genes (*FAS, Srebp-1c,* and *PPARα*) ($p < 0.05$; Figure 3K). These results illustrated that EMPA suppressed inflammation and steatosis during NAFLD development.

EMPA activated Sesn2 and inhibited AMPK-mTOR signaling in PA-stimulated HepG2 cells

As expected, the relative mRNA expression and protein expression levels of Sesn2 were upregulated after treatment with EMPA (Figures 4A,B). Additionally, the protein expression levels of p-AMPK and p-mTOR were altered after EMPA treatment, similar to findings in the animal model (Figures 4B–E). To determine the molecular mechanism by which EMPA influences lipid generation, we evaluated the mRNA expression patterns of Srebp-1c, PPARα, and FAS transcriptional factors in HepG2 cells. These genes were increased in PA-stimulated cells, compared with control cells. However, these mRNA expression levels were significantly altered in EMPA-treated HepG2 cells ($p < 0.05$; Figure 4F). qPCR analysis indicated that mRNA expression levels of IL-18, IL-6, IL-1β, TNF-α and MCP-1 in HepG2 cells were significantly increased by PA stimulation; these mRNA expression levels were significantly downregulated after treatment with EMPA ($p < 0.05$; Figure 4G). Consistent with the *in vivo* results, our *in vitro* findings demonstrated the anti-inflammatory and anti-oxidative effects of EMPA against PA-stimulated HepG2 cells. These data showed that EMPA protected against fatty acid β-oxidation and inflammation; it also upregulated Sesn2 expression and activated the AMPK pathway in PA-stimulated HepG2 cells.

EMPA activated the AMPK-mTOR signaling pathway by upregulating Sesn2 to protect against liver injury

To explore whether Sesn2 was responsible for the beneficial effects of EMPA on hepatocytes, we transfected HepG2 cells with siRNA targeting Sesn2 (siSESN2) or with negative control siRNA (siNC). Transfection with siSESN2 downregulated Sesn2 expression in both PA-stimulated and PA-stimulated + EMPA-treated cells (Figures 5A–C). Additionally, EMPA did not activate p-AMPK or inhibit p-mTOR and HO-1, while it downregulated Sesn2 (Figures 5D–I); these findings indicated that EMPA activates AMPK via Sesn2. Notably, we did not observe decreased inflammatory factors in EMPA-treated HepG2 cells that had been subjected to Sesn2 knockdown (Figures 5J–L). Furthermore, Sesn2 downregulation led to enhanced lipid generation but not reduced fatty acid oxidation (PPARα) in PA-stimulated HepG2 cells; however, EMPA treatment partly reversed these changes (Figures 5M,N; Supplementary Figure S2). Taken together, our findings demonstrate that Sesn2 plays a critical role in inflammation and mediates the beneficial effect of EMPA on intracellular lipid metabolism in PA-stimulated cells.

EMPA reduced lipid accumulation in PA-stimulated HepG2 cells

To confirm the beneficial effects of EMPA on lipid accumulation, we performed *in vitro* experiments using PA-stimulated HepG2 cells. After stimulation with PA, HepG2 cells were cultured either alone or in combination with EMPA for 24 h; lipid contents were examined by ORO staining. The results showed that lipid accumulation in HepG2 increased after stimulation with PA. However, the addition of EMPA led to significant reduction of lipid accumulation (Figures 6A–C). Moreover, to examine lipid peroxidation after PA stimulation in HepG2 cells, we measured the MDA content; EMPA significantly reduced MDA content in PA-stimulated cells (Figure 6D).

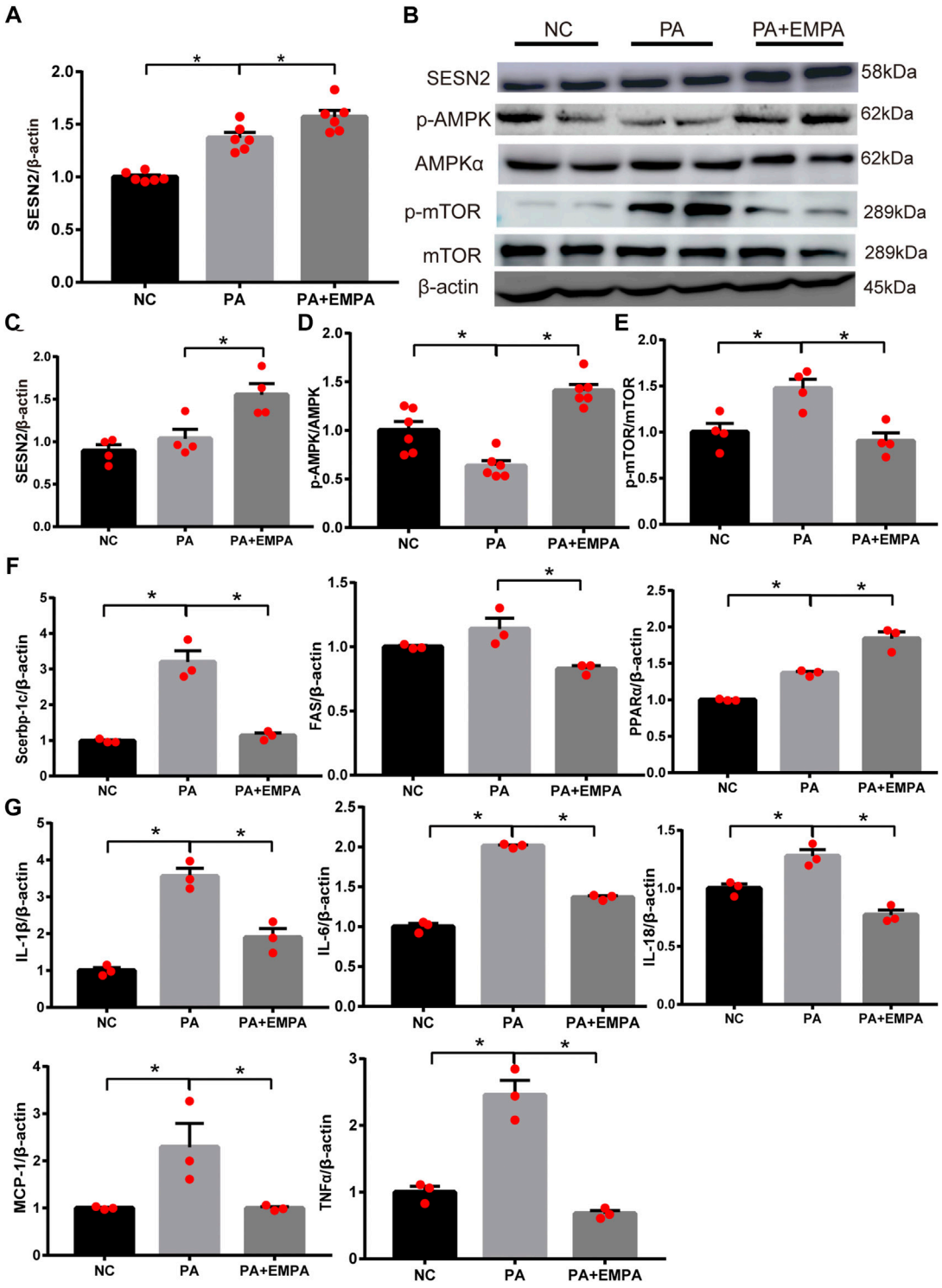

FIGURE 4
Effects of empagliflozin on palmitate-induced HepG2 cells. **(A)** Sestrin2 was quantified by qPCR. **(B–E)** Sestrin2, p-AMPK and p-mTOR protein levels. **(F)** The expressions of SREBP-1c, PPARα and fatty acid synthase (FAS) were quantified by qPCR. **(G)** Expression of inflammatory cytokines and chemokines in HepG2 cell. Data represent means ± SEM. *$p < 0.05$.

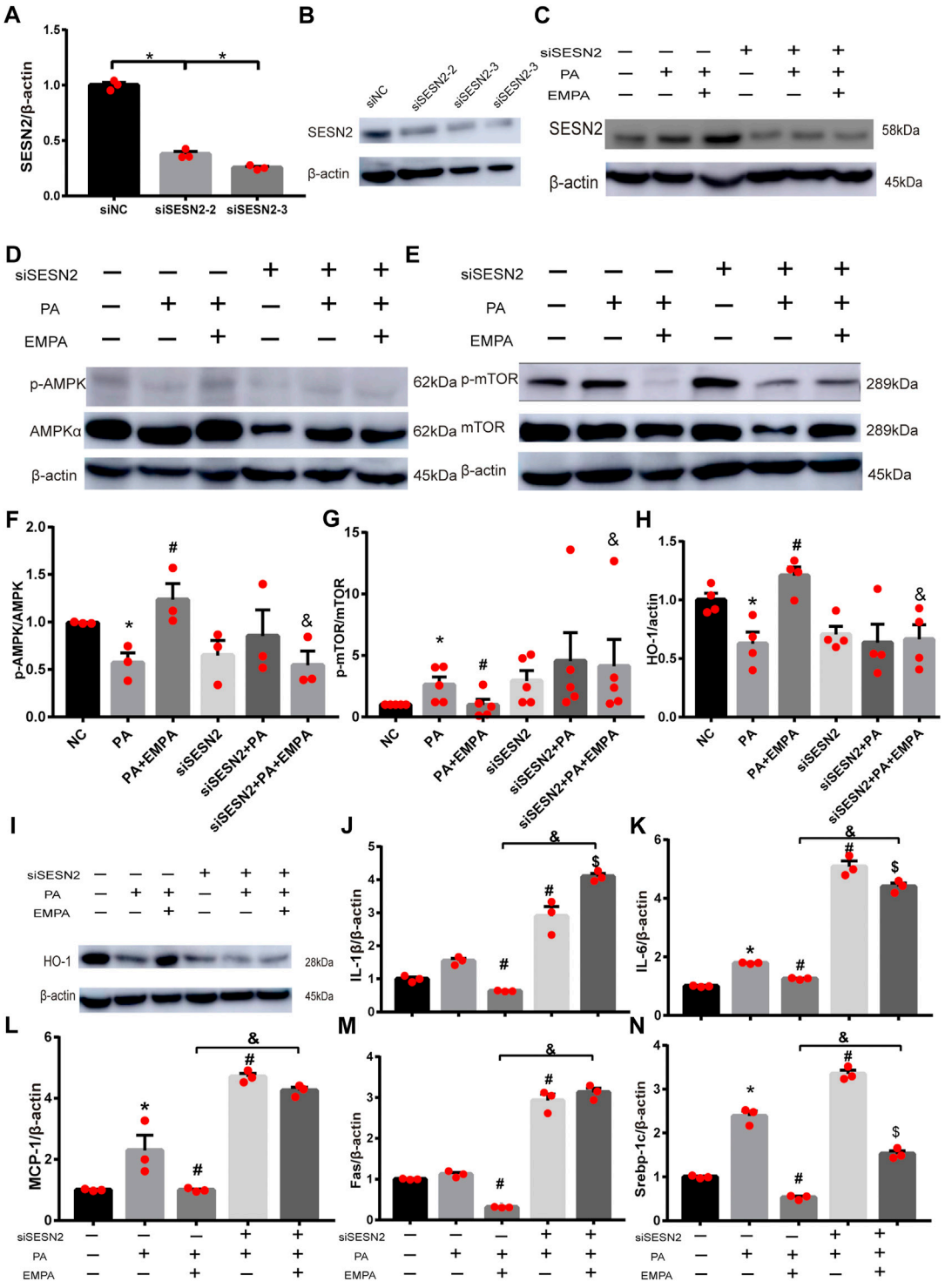

FIGURE 5
SESN2 knockdown weakened the effects of EMPA on inflammation and lipid accumulation. **(A)** The hepatocytes were transfected with siSESN2 for 48h, followed by qPCR analysis. **(B)** Western blot detection of SESN2 in HepG2 cells expressing SESN2-siRNA or control-siRNA. **(C)** Western blot analysis of SESN2 protein levels treated with or without EMPA after transfected with SESN2-siRNA or control-siRNA. **(D–I)** Western blot analysis of p-mTOR, p-AMPK and HO-1 protein levels after transfected with SESN2-siRNA or control-siRNA. **(J, K)** Inflammatory factors partly did not decrease in HepG2 cells with EMPA-siSESN2. **(L–N)** Fatty acid generation and β-oxidation in HepG2 cells treated with EMPA after SESN2-siRNA or control-siRNA. The data are expressed as the mean ± SEM; *$p < 0.05$ vs. siNC and #$p < 0.05$. siNC + PA group; $$p < 0.05$ vs. siSESN2 002B; PA; &$p < 0.05$ vs. siNC + PA + EMPA group.

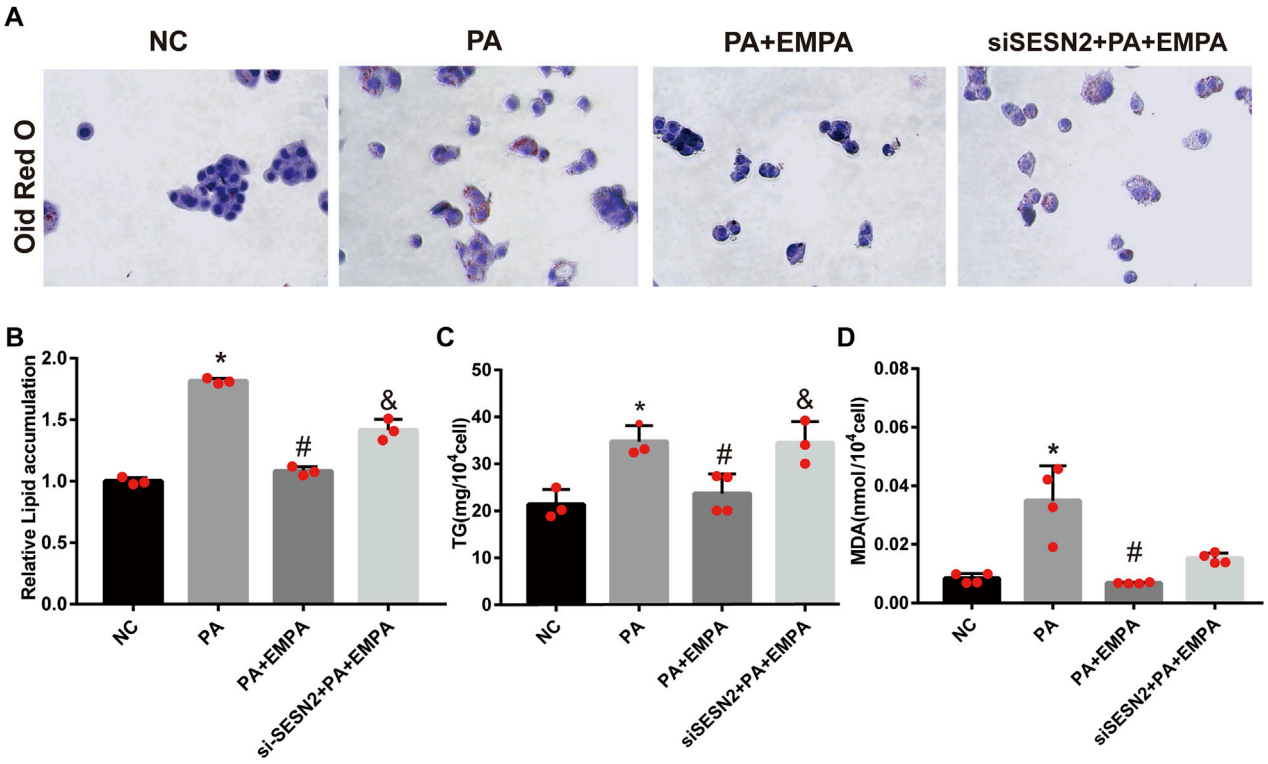

FIGURE 6
Empagliflozin reduces lipid accumulation in palmitate-induced HepG2 cells. **(A)** Lipid droplets in HepG2 cells were stained with Oil Red O. **(B)** Lipid accumulation was quantified by the absorbance value of the extracted Oil Red O dye at 495 nm. **(C)** TG in HepG2 cells. **(D)** MDA in HepG2 cells. Data are means ± SEM (n = 3-4/group). $^{*}p < 0.05$ vs. NC and $^{\#}p < 0.05$ vs. PA group; $^{\&}p < 0.05$ vs. PA + EMPA group.

Discussion

The present study demonstrated that EMPA treatment could attenuate HFD-induced NAFLD by activating Sesn2-mediated AMPK-mTOR signaling; this alleviated abnormal hepatic function and inflammation. Our results demonstrated the vital role for Sesn2 in EMPA-mediated changes in lipid metabolism and inflammation in models of NAFLD.

NAFLD has a complex pathogenesis. It is most prominently characterized by abnormal liver function and extensive lipid accumulation, particularly in patients with obesity (Saponaro et al., 2015). Excess FFA production causes disorders of lipid metabolism, lipid oxidation, and inflammation (Haukeland et al., 2006). In this study, HFD mice exhibited serum and hepatic lipid dysfunction, along with increases in body weight and fat mass. Moreover, HFD mice showed abnormal liver function with increased lipid drops in ORO staining and significant steatosis in H&E staining regarding the liver injury. These findings confirmed that HFD administration could induce NAFLD.

EMPA, an SGLT2i, has shown unprecedented benefits in clinical trials of patients with diabetes who have either established cardiovascular disease or NAFLD events (Cowie and Fisher, 2020; Sumida et al., 2020). Several pilot studies have shown that EMPA improves liver dysfunction or severe liver pathology through reductions of body weight, transaminase activity, fatty liver index, inflammatory response, and liver histopathology (steatosis or fibrosis) (Komiya et al., 2016; Seko et al., 2017; Sattar et al., 2018). Here, we found that EMPA improved hepatic function and alleviated hepatic lipid accumulation in HFD mice. The beneficial effects of EMPA might include reductions of inflammation and pro-inflammatory cytokine production, decreased lipid peroxidation, and increased energy utilization (Xu et al., 2017; Xu and Ota, 2018; Cowie and Fisher, 2020). However, the mechanism underlying these effects has not been fully elucidated. Our study confirmed that the NAFLD-related inflammation occurred in our *in vivo* model, as demonstrated by the significantly increased levels of IL-18, TNF-α, IL-6, MCP-1, and IL-1β; these levels were reduced after treatment with EMPA. This result is also confirmed by recent finding that EMPA treatments ameliorated hepatic pro-inflammatory cytokine genes (IL-1b, IL-6, and IFN-γ) and inflammatory chemokines (MCP-1, C-C motif chemokine ligand) in NAFLD mouse models (Lee et al., 2022).

Consistent with the findings in previous studies, our *in vitro* experiments suggested that EMPA could reduce inflammation in PA-stimulated HepG2 cells.

Although inflammation is a major pathological component of NAFLD, the mechanism by which EMPA protects against NAFLD-related inflammation is not entirely clear. To explore this mechanism, we investigated the Sesn2-related signaling pathway. Sesn2 is a stress-responsive gene implicated in anti-oxidative processes. Several studies have demonstrated that Sesn2 controls physiological or pathophysiological processes through the AMPK/mTOR signaling pathway. Additionally, Sesn2 inhibits the accumulation of reactive oxygen species by activating Nrf2/HO-1 (Kim et al., 2017). Furthermore, Sesn2 reportedly rescued ischemic tolerance in aged hearts and promoted sensitivity to ischemic insults through the AMPK signaling pathway (Quan et al., 2018; Yan et al., 2021). The literature thus far suggests that Sesn2 is involved in controlling oxidative stress and hypoxia in multiple tissues (Sun X. et al., 2020). In our work, we found that EMPA upregulated Sesn2 to alleviate inflammation, while regulating downstream signals, including p-AMPK, p-mTOR, and Nrf2/HO-1. The *in vitro* findings showed that Sesn2 knockdown could aggravate the inflammatory response in PA-stimulated hepatocytes. Conversely, EMPA-mediated changes in inflammatory factors and AMPK/mTOR signaling were significantly inhibited by Sesn2 knockdown in PA-stimulated HepG2 cells. These findings suggested that EMPA-mediated effects on inflammation were partly dependent on Sesn2 expression.

EMPA has been reported to attenuate the accumulation of triglycerides and FFAs. The proposed mechanism depends partly on enhanced energy expenditure and increased fatty acid oxidation (Hawley et al., 2016; Xu et al., 2017). Lee *et al.* found that EMPA could alter the hepatic lipidome towards a protective profile (Lee et al., 2022). AMPK and mTOR complex (mTORC1 and mTORC2) primarily regulate cellular energy homeostasis (Garcia and Shaw, 2017; Liu and Sabatini, 2020). PA inhibits fatty acid oxidation via decreasing AMPKα Thr172 phosphorylation and its downstream target ACC phosphorylation (Mukhopadhyay et al., 2015). Hawley *et al.* showed that SGLT2i treatment activated AMPKα, thus accelerating fatty acid oxidation and decreasing liver lipid content (Hawley et al., 2016). Therefore, the AMPK pathway has been proposed to have a critical role in the EMPA-mediated enhancement of fatty acid oxidation. Additionally, circulating Sesn2 was independently associated with the level of high-density lipoprotein in a previous study, demonstrating that Sesn2 has a regulatory role in lipid metabolism (Bai et al., 2019). However, the mechanisms underlying the effects of Sesn2 on lipid metabolism and fatty acid oxidation have been unclear.

Lipid metabolism contains the fatty acids and triglycerides metabolism, involving in triglycerides accumulation, fatty acid oxidation, and *de novo* lipogenesis (Jeon and Carr, 2020). Here, we observed that EMPA enhanced fatty acid oxidation, as demonstrated by the significantly increased levels of PPARα and GPX4. PPARα, as a critical transcriptional regulator, mainly participates in mitochondrial oxidation and whose ligands include FFAs and fatty acid derivatives (Mandard et al., 2004). GPX4, a lipid peroxide regulator, can protect cells from death by transforming lipid hydroperoxides into lipid alcohol (Forcina and Dixon, 2019). Our study showed that EMPA regulated lipid oxidation by enhancing GPX4 and PPARα. Moreover, we explored the related oxidation pathway such as Nrf2/HO-1pathway. After Nrf2 enters the nucleus, its downstream targets, including HO-1(HMOX1) and GCLC, appear to be induced (Koyani et al., 2016). In our study, we accessed the lipid oxidation pathway; the results indicated that EMPA activated the Nrf2/HO-1/GCLC axis to reduce oxidation. However, the mechanisms underlying the effects of Sesn2 on lipid and fatty acid oxidation have been unclear. Although we identified that EMPA ameliorates lipid oxidation via Sesn2 knockdown, PPARα was not inhibited after treatment with EMPA. This suggested that Sesn2 did not improve lipid oxidation by regulating PPARα.

Additionally, we observed that EMPA reduced lipid metabolism, as demonstrated by the significantly reduced levels of FAS and Srebp-1c and decreased TG and FFA levels. FAS and Srebp-1c are the essential genes involved in *de novo* lipogenesis (Obara et al., 2010). Furthermore, silencing of Sesn2 caused upregulation of lipogenic processes and increased TG and FFA levels. After treatment with EMPA, the FAS and Srebp-1c levels were significantly decreased but remained higher than in cells with unaltered Sesn2 expression. Meanwhile, EMPA could not reduce lipid accumulation (ORO), TG and FFA levels in HepG2 cells after silencing Sesn2. These findings suggested that EMPA ameliorates changes in lipid metabolism partly through downregulation of lipogenic processes via upregulation of Sesn2.

This study had a few limitations. First, we did not perform experiments in Sesn2 knock-out mice. Second, we did not fully explore how EMPA activates Sesn2. Third, this study does not determine whether EMPA alleviated lipid metabolism and synthesis via Sesn2 or whether PPARα/AMPK is dependent on these alterations. Finally, although we explored p-AMPK (Thr172) and p-mTOR (mTORC1), the downstream targets acetyl-CoA carboxylase and mTORC2 were not identified. Therefore, further studies are needed to elucidate the mechanism and explore the effects of Sesn2 silencing in an *in vivo* model.

In summary, our results showed that EMPA activates Sestrin2-mediated AMPK/mTOR pathway and ameliorates lipid accumulation in obesity-related nonalcoholic fatty liver disease. Thus, we propose Sesn2 as a target for treatment of NAFLD through its effects on the AMPK/mTOR signaling pathway.

Data availability statement

The original contributions presented in the study are included in the article/Supplementary Material, further inquiries can be directed to the corresponding authors.

Ethics statement

The animal study was reviewed and approved by Animal Ethics Committee of Weifang Medical University.

Author contributions

YM and CK participated in the study design, data collection, and in the writing of the draft manuscript. XS and GZ conceived and designed the study, participated in the revision and final approval of the manuscript. Other authors participated in the partial data collection.

Funding

This study was supported by grants from National Natural Science Foundation of China (81870593, 82170865), Natural Science Foundation of Shandong Province of China (ZR2020MH106, ZR202102240146).

Conflict of interest

The authors declare that the research was conducted in the absence of any commercial or financial relationships that could be construed as a potential conflict of interest.

Publisher's note

Supplementary material

The Supplementary Material for this article can be found online at: https://www.frontiersin.org/articles/10.3389/fphar.2022.944886/full#supplementary-material

References

Bai, L., Sun, C., Zhai, H., Chen, C., Hu, X., Ye, X., et al. (2019). Investigation of urinary Sestrin2 in patients with obstructive sleep apnea. *Lung* 197 (2), 123–129. doi:10.1007/s00408-019-00205-8

Chu, X., Liu, L., Na, L., Lu, H., Li, S., Li, Y., et al. (2013). Sterol regulatory element-binding protein-1c mediates increase of postprandial stearic acid, a potential target for improving insulin resistance, in hyperlipidemia. *Diabetes* 62 (2), 561–571. doi:10.2337/db12-0139

Coelho, F. D. S., Borges-Canha, M., von, H. M., Neves, J. S., Vale, C., Leite, A. R., et al. (2020). Effects of sodium-glucose co-transporter 2 inhibitors on liver parameters and steatosis: A meta-analysis of randomized clinical trials. *Diabetes. Metab. Res. Rev.* 37, e3413. doi:10.1002/dmrr.3413

Cowie, M. R., and Fisher, M. (2020). SGLT2 inhibitors: Mechanisms of cardiovascular benefit beyond glycaemic control. *Nat. Rev. Cardiol.* 17 (12), 761–772. doi:10.1038/s41569-020-0406-8

Fitchett, D., Inzucchi, S. E., Cannon, C. P., McGuire, D. K., Scirica, B. M., Johansen, O. E., et al. (2019). Empagliflozin reduced mortality and hospitalization for heart failure across the spectrum of cardiovascular risk in the EMPA-REG OUTCOME trial. *Circulation* 139 (11), 1384–1395. doi:10.1161/CIRCULATIONAHA.118.037778

Garcia, D., and Shaw, R. J. (2017). AMPK: Mechanisms of cellular energy sensing and restoration of metabolic balance. *Mol. Cell.* 66, 789–800. doi:10.1016/j.molcel.2017.05.032

Gong, L., Wang, Z., Wang, Z., and Zhang, Z. (2021). Sestrin2 as a potential target for regulating metabolic-related diseases. *Front. Endocrinol.* 12, 751020. doi:10.3389/fendo.2021.751020

Han, X., Ding, C., Zhang, G., Pan, R., Liu, Y., Huang, N., et al. (2020). Liraglutide ameliorates obesity-related nonalcoholic fatty liver disease by regulating Sestrin2-mediated Nrf2/HO-1 pathway. *Biochem. Biophys. Res. Commun.* 525 (4), 895–901. doi:10.1016/j.bbrc.2020.03.032

Haukeland, J. W., Damås, J. K., Konopski, Z., Loberg, E. M., Haaland, T., Goverud, I., et al. (2006). Systemic inflammation in nonalcoholic fatty liver disease is characterized by elevated levels of CCL2. *J. Hepatol.* 44 (6), 1167–1174. doi:10.1016/j.jhep.2006.02.011

Hawley, S. A., Ford, R. J., Smith, B. K., Gowans, G. J., Mancini, S. J., Pitt, R. D., et al. (2016). The Na+/Glucose cotransporter inhibitor canagliflozin activates AMPK by inhibiting mitochondrial function and increasing cellular AMP levels. *Diabetes* 65 (9), 2784–2794. doi:10.2337/db16-0058

Hsiang, J. C., and Wong, V. W. (2020). SGLT2 inhibitors in liver patients. *Clin. Gastroenterol. Hepatol.* 18 (10), 2168–2172. doi:10.1016/j.cgh.2020.05.021

Hwang, H. J., Jung, T. W., Choi, J. H., Lee, H. J., Chung, H. S., Seo, J. A., et al. (2017). Knockdown of sestrin2 increases pro-inflammatory reactions and ER stress in the endothelium via an AMPK dependent mechanism. *Biochim. Biophys. Acta. Mol. Basis Dis.* 1863 (6), 1436–1444. doi:10.1016/j.bbadis.2017.02.018

Jegal, K. H., Kim, E. O., Kim, J. K., Park, S. M., Jung, D. H., Lee, G. H., et al. (2020). Luteolin prevents liver from tunicamycin-induced endoplasmic reticulum stress via nuclear factor erythroid 2-related factor 2-dependent sestrin 2 induction. *Toxicol. Appl. Pharmacol.* 399, 115036. doi:10.1016/j.taap.2020.115036

Jeon, S., and Carr, R. (2020). Alcohol effects on hepatic lipid metabolism. *J. Lipid Res.* 61, 470–479. doi:10.1194/jlr.R119000547

Kim, H. J., Joe, Y., Kim, S. K., Park, S. U., Park, J., Chen, Y., et al. (2017). Carbon monoxide protects against hepatic steatosis in mice by inducing sestrin-2 via the PERK-eIF2α-ATF4 pathway. *Free Radic. Biol. Med.* 110, 81–91. doi:10.1016/j.freeradbiomed.2017.05.026

Kishimoto, Y., Kondo, K., and Momiyama, Y. (2021). The protective role of Sestrin2 in atherosclerotic and cardiac diseases. *Int. J. Mol. Sci.* 22 (3), 1200. doi:10.3390/ijms22031200

Komiya, C., Tsuchiya, K., Shiba, K., Miyachi, Y., Furuke, S., Shimazu, N., et al. (2016). Ipragliflozin improves hepatic steatosis in obese mice and liver dysfunction in type 2 diabetic patients irrespective of body weight reduction. *PLoS One* 11 (3), e0151511. doi:10.1371/journal.pone.0151511

Koyani, C. N., Kitz, K., Rossmann, C., Bernhart, E., Huber, E., Trummer, C., et al. (2016). Activation of the MAPK/Akt/Nrf2-Egr1/HO-1-GCLc axis protects MG-63

osteosarcoma cells against 15d-PGJ2-mediated cell death. *Biochem. Pharmacol.* 104, 29–41. doi:10.1016/j.bcp.2016.01.011

Kramer, C. K., and Zinman, B. (2019). Sodium-glucose cotransporter-2 (SGLT-2) inhibitors and the treatment of type 2 diabetes. *Annu. Rev. Med.* 70, 323–334. doi:10.1146/annurev-med-042017-094221

Lee, N., Heo, Y. J., Choi, S. E., Jeon, J. Y., Han, S. J., Kim, D. J., et al. (2022). Hepatoprotective effects of gemigliptin and empagliflozin in a murine model of diet-induced non-alcoholic fatty liver disease. *Biochem. Biophys. Res. Commun.* 588, 154–160. doi:10.1016/j.bbrc.2021.12.065

Li, S., Vandvik, P. O., Lytvyn, L., Guyatt, G. H., Palmer, S. C., Rodriguez-Gutierrez, R., et al. (2021). SGLT-2 inhibitors or GLP-1 receptor agonists for adults with type 2 diabetes: A clinical practice guideline. *BMJ* 373, n1091. doi:10.1136/bmj.n1091

Liu, G. Y., and Sabatini, D. M. (2020). mTOR at the nexus of nutrition, growth, ageing and disease. *Nat. Rev. Mol. Cell. Biol.* 21, 183–203. doi:10.1038/s41580-019-0199-y

Liu, J., Jin, X., Yu, C. H., Chen, S. H., Li, W. P., and Li, Y. M. (2010). Endoplasmic reticulum stress involved in the course of lipogenesis in fatty acids-induced hepatic steatosis. *J. Gastroenterol. Hepatol.* 25 (3), 613–618. doi:10.1111/j.1440-1746.2009.06086.x

Lucero, D., Zago, V., López, G. I., Graffigna, M., Fainboim, H., Miksztowicz, V., et al. (2011). Pro-inflammatory and atherogenic circulating factors in non-alcoholic fatty liver disease associated to metabolic syndrome. *Clin. Chim. Acta.* 412 (1-2), 143–147. doi:10.1016/j.cca.2010.09.025

Mandard, S., Müller, M., and Kersten, S. (2004). Peroxisome proliferator-activated receptor alpha target genes. *Cell. Mol. Life Sci.* 61, 393–416. doi:10.1007/s00018-003-3216-3

Mantovani, A., Petracca, G., Csermely, A., Beatrice, G., and Targher, G. (2020). Sodium-glucose cotransporter-2 inhibitors for treatment of nonalcoholic fatty liver disease: A meta-analysis of randomized controlled trials. *Metabolites* 11 (1), 22. doi:10.3390/metabo11010022

Marra, F., and Lotersztajn, S. (2013). Pathophysiology of NASH: Perspectives for a targeted treatment. *Curr. Pharm. Des.* 19 (29), 5250–5269. doi:10.2174/13816128113199990344

Mota, M., Banini, B. A., Cazanave, S. C., and Sanyal, A. J. (2016). Molecular mechanisms of lipotoxicity and glucotoxicity in nonalcoholic fatty liver disease. *Metabolism.* 65 (8), 1049–1061. doi:10.1016/j.metabol.2016.02.014

Mukhopadhyay, S., Saqcena, M., Chatterjee, A., Garcia, A., Frias, M. A., and Foster, D. A. (2015). Reciprocal regulation of AMP-activated protein kinase and phospholipase D. *J. Biol. Chem.* 290, 6986–6993. doi:10.1074/jbc.M114.622571

Neuschwander-Tetri, B. A. (2017). Non-alcoholic fatty liver disease. *BMC Med.* 15 (1), 45. doi:10.1186/s12916-017-0806-8

Obara, N., Fukushima, K., Ueno, Y., Wakui, Y., Kimura, O., Tamai, K., et al. (2010). Possible involvement and the mechanisms of excess trans-fatty acid consumption in severe NAFLD in mice. *J. Hepatol.* 53, 326–334. doi:10.1016/j.jhep.2010.02.029

Park, H. W., Park, H., Ro, S. H., Jang, I., Semple, I. A., Kim, D. N., et al. (2014). Hepatoprotective role of Sestrin2 against chronic ER stress. *Nat. Commun.* 5, 4233. doi:10.1038/ncomms5233

Quan, N., Wang, L., Chen, X., Luckett, C., Cates, C., Rousselle, T., et al. (2018). Sestrin2 prevents age-related intolerance to post myocardial infarction via AMPK/PGC-1α pathway. *J. Mol. Cell. Cardiol.* 115, 170–178. doi:10.1016/j.yjmcc.2018.01.005

Saponaro, C., Gaggini, M., and Gastaldelli, A. (2015). Nonalcoholic fatty liver disease and type 2 diabetes: Common pathophysiologic mechanisms. *Curr. Diab. Rep.* 15 (6), 607. doi:10.1007/s11892-015-0607-4

Sattar, N., Fitchett, D., Hantel, S., George, J. T., and Zinman, B. (2018). Empagliflozin is associated with improvements in liver enzymes potentially consistent with reductions in liver fat: Results from randomised trials including the EMPA-REG OUTCOME® trial. *Diabetologia* 61, 2155–2163. doi:10.1007/s00125-018-4702-3

Seko, Y., Sumida, Y., Tanaka, S., Mori, K., Taketani, H., Ishiba, H., et al. (2017). Effect of sodium glucose cotransporter 2 inhibitor on liver function tests in Japanese patients with non-alcoholic fatty liver disease and type 2 diabetes mellitus. *Hepatol. Res.* 47 (10), 1072–1078. doi:10.1111/hepr.12834

Sumida, Y., Yoneda, M., Tokushige, K., Kawanaka, M., Fujii, H., Yoneda, M., et al. (2020). Antidiabetic therapy in the treatment of nonalcoholic steatohepatitis. *Int. J. Mol. Sci.* 21 (6), E1907. doi:10.3390/ijms21061907

Sun, W., Wang, Y., Zheng, Y., and Quan, N. (2020). The emerging role of Sestrin2 in cell metabolism, and cardiovascular and age-related diseases. *Aging Dis.* 11, 154–163. doi:10.14336/AD.2019.0320

Sun, X., Han, F., Lu, Q., Li, X., Ren, D., Zhang, J., et al. (2020). Empagliflozin ameliorates obesity-related cardiac dysfunction by regulating sestrin2-mediated AMPK-mTOR signaling and redox homeostasis in high-fat diet-induced obese mice. *Diabetes* 69 (6), 1292–1305. doi:10.2337/db19-0991

Tuttle, K. R., Brosius, F. C., 3rd, Cavender, M. A., Fioretto, P., Fowler, K. J., Heerspink, H., et al. (2021). SGLT2 inhibition for CKD and cardiovascular disease in type 2 diabetes: Report of a scientific workshop sponsored by the national kidney foundation. *Diabetes* 70 (1), 1–16. doi:10.2337/dbi20-0040

Viganò, L., Lleo, A., and Aghemo, A. (2018). Non-alcoholic fatty liver disease, non-alcoholic steatohepatitis, metabolic syndrome and hepatocellular carcinoma-a composite scenario. *Hepatobiliary Surg. Nutr.* 7 (2), 130–133. doi:10.21037/hbsn.2018.01.01

Xu, L., Nagata, N., Nagashimada, M., Zhuge, F., Ni, Y., Chen, G., et al. (2017). SGLT2 inhibition by empagliflozin promotes fat utilization and browning and attenuates inflammation and insulin resistance by polarizing M2 macrophages in diet-induced obese mice. *EBioMedicine* 20, 137–149. doi:10.1016/j.ebiom.2017.05.028

Xu, L., and Ota, T. (2018). Emerging roles of SGLT2 inhibitors in obesity and insulin resistance: Focus on fat browning and macrophage polarization. *Adipocyte* 7 (2), 121–128. doi:10.1080/21623945.2017.1413516

Yan, C., Tian, X., Li, J., Liu, D., Ye, D., Xie, Z., et al. (2021). A high-fat diet attenuates AMPK α1 in adipocytes to induce exosome shedding and nonalcoholic fatty liver development *in vivo*. *Diabetes* 70 (2), 577–588. doi:10.2337/db20-0146

Yang, J. H., Kim, K. M., Cho, S. S., Shin, S. M., Ka, S. O., Na, C. S., et al. (2019). Inhibitory effect of Sestrin2 on hepatic stellate cell activation and liver fibrosis via blocking transforming growth factor-β signaling. *Antioxidants Redox Signal.* 31 (3), 243–259. doi:10.1089/ars.2018.7559

Younossi, Z. M. (2019). Non-alcoholic fatty liver disease - a global public health perspective. *J. Hepatol.* 70 (3), 531–544. doi:10.1016/j.jhep.2018.10.033

Zámbó, V., Simon-Szabó, L., Szelényi, P., Kereszturi, E., Bánhegyi, G., and Csala, M. (2013). Lipotoxicity in the liver. *World J. Hepatol.* 5 (10), 550–557. doi:10.4254/wjh.v5.i10.550

frontiers | Frontiers in Pharmacology

TYPE Review
PUBLISHED 09 September 2022
DOI 10.3389/fphar.2022.951004

OPEN ACCESS

EDITED BY
Marilia Seelaender,
University of São Paulo, Brazil

REVIEWED BY
Faming Zhang,
Nanjing Medical University, China
Jianye Yuan,
Shanghai University of Traditional Chinese Medicine, China

*CORRESPONDENCE
Xudong Tang,
txdly@sina.com

†These authors have contributed equally to this work and share first authorship

SPECIALTY SECTION
This article was submitted to Gastrointestinal and Hepatic Pharmacology, a section of the journal Frontiers in Pharmacology

RECEIVED 23 May 2022
ACCEPTED 19 August 2022
PUBLISHED 09 September 2022

CITATION
Zhang T, Zhang B, Tian W, Wang F, Zhang J, Ma X, Wei Y and Tang X (2022), Research trends in ulcerative colitis: A bibliometric and visualized study from 2011 to 2021.
Front. Pharmacol. 13:951004.
doi: 10.3389/fphar.2022.951004

Research trends in ulcerative colitis: A bibliometric and visualized study from 2011 to 2021

Tai Zhang[1,2†], Beihua Zhang[1,2†], Wende Tian[1,3†], Fengyun Wang[1,2], Jiaqi Zhang[1,2], Xiangxue Ma[1,2], Yuchen Wei[1,2] and Xudong Tang[4*]

[1]Xiyuan Hospital, China Academy of Chinese Medical Sciences, Beijing, China, [2]Department of Gastroenterology, Xiyuan Hospital, China Academy of Traditional Chinese Medical Sciences, Beijing, China, [3]National Clinical Research Center for Chinese Medicine Cardiology, Xiyuan Hospital, China Academy of Chinese Medical Sciences, Beijing, China, [4]China Academy of Chinese Medical Sciences, Beijing, China

Background: Ulcerative colitis (UC) is an idiopathic inflammatory bowel disease with repeated relapses and remissions. Despite decades of effort, numerous aspects, including the initiating event and pathogenesis of UC, still remain ambiguous, which requires ongoing investigation. Given the mass of publications on UC, there are multidimensional challenges to evaluating the scientific impact of relevant work and identifying the current foci of the multifaceted disease. Accordingly, herein, we aim to assess the global growth of UC research production, analyze patterns of research areas, and evaluate trends in this area.

Methods: The Web of Science Core Collection of Clarivate Analytics was searched for articles related to UC published from 2011 to 2021. Microsoft Office Excel 2019 was used to visualize the number of publications over time. Knowledge maps were generated using CiteSpace and VOSviewer to analyze collaborations among countries, institutions, and authors and to present the journey of UC research as well as to reveal the current foci of UC research.

Results: A total of 5,088 publications were evaluated in the present study. China had the most publications (1,099, 22.5%). Univ Calif San Diego was the most productive institution (126, 2.48%). William J Sandborn published the greatest number of articles (100, 1.97%). Toshifumi Hibi was the most influential author in the field with a betweenness centrality of 0.53. *Inflammatory bowel diseases* was identified as the most prolific journal (379, 7.45%). *Gastroenterology* was the most co-cited journal (3,730, 4.02%). "Vedolizumab," "tofacitinib," "*Faecalibacterium prausnitzii*," "fecal microbiota transplantation (FMT)," "toll-like receptor 4," and "nucleotide-binding oligomerization domain-like receptor protein 3 inflammasome" were considered the hot topics.

Conclusion: In UC research, manuscripts that had high impacts on the scientific community provided an evidence base. UC therapy has entered the era of personalized and precision therapy. As research on FMT, anti-integrin

antibodies, Janus kinase inhibitors, and anti-tumor necrosis factor drugs continues to grow, their use in the clinical setting may also expand.

KEYWORDS

ulcerative colitis, bibliometrics, trends, therapy, mechanisms

Introduction

Crohn's disease (CD) and ulcerative colitis (UC), two idiopathic gastrointestinal diseases characterized by chronic inflammation of the gastrointestinal tract, are examples of inflammatory bowel disease (IBD). Both pediatric and adult populations are experiencing a rise in IBD incidence worldwide (Actis et al., 2019). By 2025, IBD is expected to affect 30 million individuals worldwide (Kaplan, 2015). Samuel Wilks' first description of UC in 1859 (Wilks, 1859), characterized by such highly consistent features that at once appear to be key clues, has not yet uncovered a complete understanding of its pathogenesis. There is a relapsing and remitting mucosal inflammation that originates in the rectal region and extends proximally in an uninterrupted manner, ending with an abrupt delineation and transition into normal colonic mucosa. If left untreated, or inadequately treated, the chronic inflammation throughout the intestine can lead to impaired quality of life, frequent need for surgery and hospitalization, and even colorectal cancer (Viola et al., 2021).

UC is a subject of continued interest, with a huge body of research published per year in relation to etiology, histopathology, epidemiology, and therapeutics. Nevertheless, the exponentially increasing number of literature studies makes it impossible to keep up to date with the latest findings regarding all issues. Therefore, the bibliometric approach is proposed to acquire the numerical growth trend, gauge the contributions of countries, institutions, and authors, reveal the evolution trend of the field, apprehend the body of knowledge on the subject, and obtain hot topics of research. Bibliometric analysis of the extant literature will be carried out to assess global trends and developments in UC research.

Materials and methods

Source of the data and search strategy

A search was conducted on the Science Citation Index Expanded of the Web of Science Core Collection (WOSCC) of Clarivate Analytics. The entire electronic search was conducted on 7 July 2022. As part of the comprehensive search strategy, we searched meta-analysis studies and scientometric and bibliometric analyses. Based on the search strategies employed in these studies (Connelly et al., 2016; Schöffel et al., 2016; Nguyen et al., 2018; Lucaciu et al., 2021; Schöffel et al., 2021), we used advanced search to identify publications relevant to UC with the following query: TOPIC: [(ulcerativ* AND colitis) OR (ulcerativ* AND enteritis) OR (colitis ulcerosa) OR (enteritis ulcerosa) OR (idiopathic proctocolitis) OR (colitis gravis) OR (colitis chronica purulenta) OR (colitis polyposa) OR (gastroenteritis ulcerosa) OR (backwash ileitis)] AND Language: (English). Timespan: 2011–2012.

This study focused, for the purpose of this analysis, on articles (*document types*) that included original research articles, case reports, and case series out of the different types of documents indexed in the database (article, proceedings paper, review, meeting abstract, correction, letter, editorial material, note, book chapter, news item, and correction addition). Preprints and non-peer-reviewed publications were also removed. The results of the search were restricted to publications containing the search terms in the title, as the objective was to find the entire scientific output of content solely related to the topic of UC (Connelly et al., 2016; Schöffel et al., 2016; Schöffel et al., 2021). In "TOPIC" searches, the term would also show up in abstracts, author keywords, and keywords plus, which would result in an array of publications that were off-topic. Furthermore, "IBD" was not considered as a retrieval term under the advanced search option, as such a word may cause a more or less broader topic to handle indeterminate IBD and CD, which are ineligible for inclusion; individually screening the titles or abstracts to make a distinction between literature exclusively discussing UC and other IBD type-specific publications would be a challenging task given that types of IBD are generally presented and discussed together in documents containing "IBD" in the "title."

Bibliographic records were downloaded in plain text, including titles, abstracts, author information, affiliations, keywords, date of publication, and cited references, for analysis with CiteSpace and VOSviewer.

Data analysis

In the present study, we used CiteSpace, a document visualization and analysis software developed by Professor Chaomei Chen of Drexel University. The core concepts of CiteSpace include burst detection, betweenness centrality, and heterogeneous networks, which help to identify the nature of a given research front and to label a specialty while also identifying emerging trends and abrupt changes in real time (Chen, 2006).

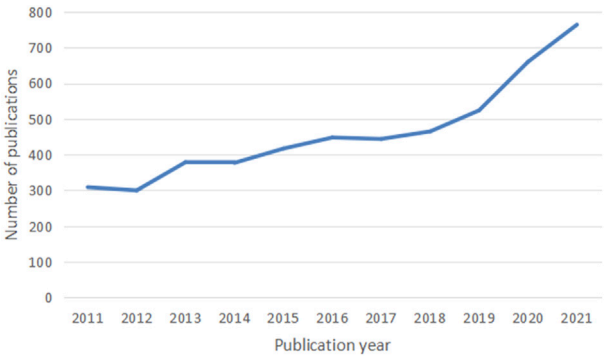

FIGURE 1
Number of articles published annually in UC research. Countries or regions and institution analysis.

VOSviewer, another bibliometric software developed by Professors van Eck and Waltman from Leiden University, has text mining capabilities to process large-scale data for mapping and clustering of the scientific literature (Van Eck and Waltman, 2010).

CiteSpace was used to 1) visualize collaborations among countries, institutions, and authors using knowledge maps; 2) perform a co-citation analysis of references; and 3) detect the citation bursts of references and keywords. VOSviewer was used to visually analyze keyword co-occurrence.

Citation numbers are presumed to be a constant parameter in the modern academic world, correlated with scientific achievement, career success, and academic reputation. One kind of citation is self-citation, which involves citations of one's own work (Aksnes, 2003). Multiple subtypes of self-citation exist, including author self-citation, journal self-citation, institutional self-citation, and publisher self-citation (Bardeesi et al., 2021). Self-citations will be analyzed from the perspective of the institution and the author in this study. Results for the WOSCC were limited to the names of the selected institutions and authors in the "refine" section. Next, the data were imported into Microsoft Excel 2019 and analyzed after being extracted from the "citation report" section of the database. Journal Citation Reports (JCR) (clarivate.com/products/web-of-science) provide the impact factor (IF) of sources. Furthermore, Microsoft Excel 2019 was applied to analyze and plot the annual publication output.

Results

Publication output

A total of 5,088 publications were finally included in our study. The number of publications per year is presented in Figure 1. In terms of volume growth, the overall trend has kept increasing from 2011 to 2021 and roughly falls into three phases.

From 2011 to 2016, it was the initial period where the publication number showed a steady increasing trend, except in 2012 and 2014. The number of publications (448) reached a peak in 2016. During the second stage from 2016 to 2018, the field entered a stable stage of publications, and no apparent research trend was identified. An outbreak in UC research was witnessed during the third stage from 2018 through 2021. Notably, a large amount of scientific literature was published from 2019 to 2021. The output reached its maximum in 2021 (764).

There were a total of 5,088 publications co-authored by 419 institutions from 100 countries or regions. The top 20 countries or regions and institutions according to the number of publications and betweenness centrality are listed in Table 1. Researchers from East Asia, North America, and Western Europe authored the majority of the articles. Specifically, China had the most publications, with 1,099 (21.60%) documents, followed by the United States (1,096, 21.54%), Japan (672, 12.32%), and Italy (335, 6.58%).

As for the analysis of institutions, Univ Calif San Diego in the United States ranked first with 126 articles (2.48). It was Mayo Clin in the United States that came in second with 87 publications (1.71%) and Hyogo Coll Med in Japan came in third with 78 publications (1.53%).

As defined by Freeman's betweenness centrality metric, betweenness centrality determines how often a node (e.g., an article or an author) is on the shortest path between other nodes (Freeman, 1977). The node with a high degree of betweenness centrality often connects components of the network that would otherwise be disconnected if it was removed.

The top countries or regions by betweenness centrality were South Korea (0.18), India (0.17), England (0.16), and Belgium (0.13). The highest-ranked institution by betweenness centrality was Univ Calif San Diego (0.19), Kitasato Univ (0.12), and Harvard Univ (0.14).

The visualized results of the international collaboration among countries or regions of co-authors are presented in Figure 2. In summary, active collaborations that were centered on Asian and European countries were observed in the network. For example, South Korea cooperated frequently with Slovenia, Malta, Lithuania, Serbia, Ukraine, Pakistan, Sudan, Singapore, Palau, China, and Thailand. England worked closely with Denmark, Germany, Italy, Switzerland, the Netherlands, Malta, Sri Lanka, Saudi Arabia, Singapore, Argentina, Egypt, South Africa, Australia, Canada, and the United States.

The presence of a red tree ring demonstrates a citation burst. Hence, Turkey was detected with strong citation bursts, revealing high scholarly activity over a brief period.

The collaboration network of co-author institutions is shown in Figure 3. The analysis of the network showed two main groups

TABLE 1 Top productive 20 countries or regions and institutions involved in UC research.

Rank	Country	Centrality	Count (% of 5,088)	Rank	Institutions	Centrality	Count (% of 5,088)
1	China	0	1,099 (21.60)	1	Univ Calif San Diego (the United States)	0.19	126 (2.48)
2	United States	0	1,096 (21.54)	2	Mayo Clin (the United States)	0.02	87 (1.71)
3	Japan	0.01	627 (12.32)	3	Hyogo Coll Med (Japan)	0.07	78 (1.53)
4	Italy	0.01	335 (6.58)	4	Icahn Sch Med Mt Sinai (the United States)	0.09	75 (1.47)
5	England	0.16	316 (6.21)	5	Univ Toronto (Canada)	0.05	72 (1.42)
6	Canada	0.01	312 (6.13)	6	Univ Calgary (Canada)	0.04	64 (1.26)
7	Germany	0.03	270 (4.07)	7	Massachusetts Gen Hosp (the United States)	0.07	63 (1.24)
8	Spain	0.04	204 (4.01)	8	Harvard Med Sch (the United States)	0	56 (1.10)
9	France	0.09	191 (3.75)	9	Keio Univ (Japan)	0.01	55 (1.08)
10	Belgium	0.13	181 (3.56)	9	Kitasato Univ (Japan)	0.12	55 (1.08)
10	Netherlands	0.01	175 (3.44)	10	Univ Penn (the United States)	0.05	54 (1.06)
11	South Korea	0.18	165 (3.24)	11	Univ Amsterdam (the Netherlands)	0.01	53 (1.04)
12	Sweden	0.06	148 (2.91)	12	Hosp Clin Barcelona (Spain)	0.08	52 (1.02)
13	India	0.17	142 (2.79)	12	Katholieke Univ Leuven (Belgium)	0.01	52 (1.02)
14	Denmark	0.01	130 (2.56)	13	Cleveland Clin (the United States)	0.01	51 (1.00)
15	Iran	0	119 (2.34)	14	Shanghai Jiao Tong Univ (China)	0.02	50 (0.98)
16	Australia	0.08	118 (2.32)	14	Tel Aviv Univ (Israel)	0.08	50 (0.98)
17	Poland	0	103 (1.91)	15	Toho Univ (Japan)	0.02	49 (0.96)
18	Turkey	0	102 (2.02)	16	Univ Ulsan (South Korea)	0	48 (0.94)
19	Israel	0.1	94 (1.85)	16	Tokyo Med and Dent Univ (Japan)	0.05	48 (0.94)
20	Switzerland	0.02	77 (1.51)	17	Nanjing Univ Chinese Med (China)	0	46 (0.90)
				17	Shanghai Univ Tradit Chinese Med (China)	0	46 (0.90)
				18	Univ Chicago (the United States)	0	45 (0.88)
				18	Harvard Univ (the United States)	0.14	45 (0.88)
				19	Univ Tokyo (Japan)	0.04	44 (0.86)
				20	Mt Sinai Hosp (United States)	0.02	43 (0.85)

Note: Centrality refers to betweenness centrality. Betweenness centrality was computed by CiteSpace. To rank an influential entity (e.g., a country, region, or institution) in a graph, betweenness centrality was calculated as the unweighted shortest path between all pairs of nodes in the graph; a node with a higher betweenness centrality (> 0.1) possesses greater control over the network. Count refers to the total number of publications.

of collaborators: the North America and Europe group and the Japanese group.

As member institutions of the collaborative community of North American and European institutions, Univ Calif San Diego and Harvard Univ played central roles.

Univ Calif San Diego had close communication with Univ Penn, McMaster Univ (Canada), Dartmouth Hitchcock Med Ctr (Lebanon), Univ Amsterdam, Acad Med Ctr (the Netherlands), Hosp Clin Barcelona, Univ Calgary, Icahn Sch Med Mt Sinai, Univ Chicago, Univ Western Ontario (Canada), Mayo Clin, Janssen Res and Dev LLC (the United States), Western Univ (Canada), Med Univ Vienna (Austria), and John Radcliffe Hosp (England).

The major collaborators with Harvard Univ were Massachusetts Gen Hosp, Ghent Univ Hosp (Belgium), Tel Aviv Univ (Israel), Univ Calif Los Angeles (the United States), Univ Southern Denmark (Denmark), Beth Israel Deaconess Med Ctr (the United States), Brigham and Women's Hosp (the United States), Cincinnati Children's Hosp Med Ctr (the United States), Univ Copenhagen (Denmark), Children's Hosp Philadelphia (the United States), Univ Michigan (the United States), Univ N Carolina (the United States), and Connecticut Children's Med Ctr (the United States).

In addition, intense collaborations were seen among Japanese institutions. For instance, there were collaborative structures among Kitasato Univ, Univ Hosp Leuven (Belgium), Osaka City Univ (Japan), Keio Univ, Toho Univ, Tokyo Med and Dent Univ, Fukuoka Univ (Japan), Hyogo Coll Med, Niigata Univ (Japan), Kurume Univ (Japan), Jikei Univ (Japan), and Tokyo Women's Med Univ (Japan).

Strong citation bursts were detected for Mie Univ (Japan), Univ Chicago, Harvard Univ, Nanjing Univ Chinese Med, Humanitas Univ (Italy), Univ Gothenburg (Sweden), Univ Amsterdam, Cleveland Clin, Massachusetts Gen Hosp, and Univ Western Ontario, signifying their large increases in recent publications.

As Table 2 shows, the highly productive institutions that had the highest self-citation rates during the studied period were as

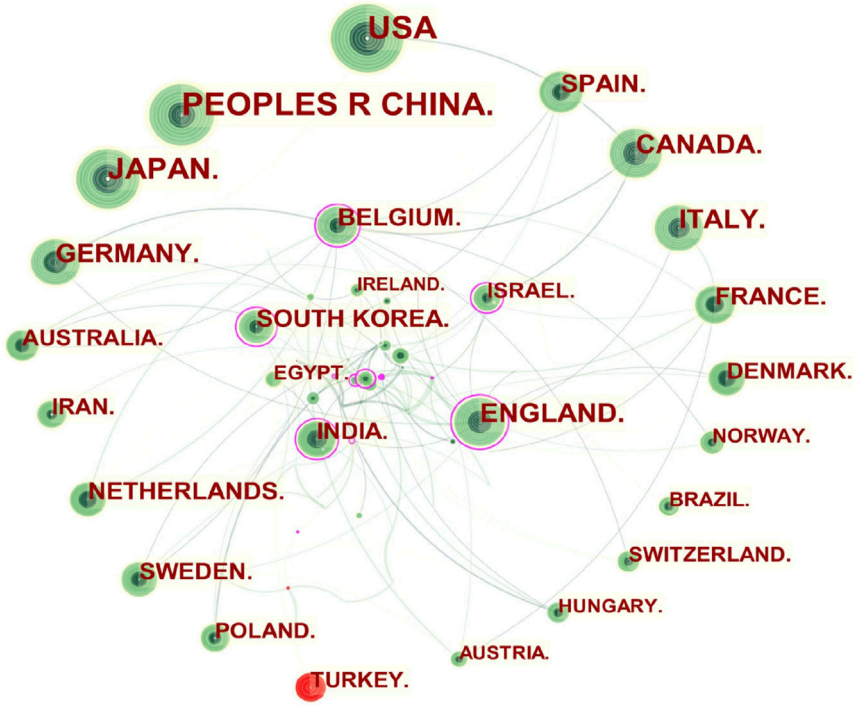

FIGURE 2
Network of countries and regions engaged in UC research. Note: An individual node represents a country or region on the network map. The greater the area of the node, the more publications there are. The thicker the curved line connecting nodes, the more frequent their co-occurrence, as this indicates a collaborative relationship. An isolated node with no link lacks all collaboration. When a node has a high betweenness centrality (> 0.1) (i.e., when it is connected to more than 10% of the other nodes), it exerts significant influence over others as it controls most resources within their collaborative networks (Cobo et al., 2011). The presence of a purple rim also indicates a high degree of betweenness centrality. Red tree rings indicate bursts of citation, indicating high scholarly activity. Red tree rings with a greater thickness show a greater burst for a corresponding node.

follows: Hyogo Coll Med (3.66%), Kitasato Univ (3.23%), Keio Univ (2.42%), Univ Calif San Diego (2.36%), Univ Calgary (1.73%), Icahn Sch Med Mt Sinai (1.61%), Massachusetts Gen Hosp (1.35%), Univ Toronto (1.30%), Mayo Clin (1.16%), Univ Penn (1.05%), and Harvard Med Sch (0.41%).

Authors

A total of 435 authors were involved in the UC-related studies. As shown in Table 3, William J Sandborn published the most articles (100, 1.97%), followed by Severine Vermeire (69, 1.36%), and Silvio Danese (62, 1.22%). It can be seen that similar to the landscape of the research output of countries, the high-yield authors mainly came from East Asia, North America, and Western Europe. The top authors by betweenness centrality were Toshifumi Hibi (0.53), Edward V Loftus Jr (0.39), Stefan Schreiber (0.35), Yasuo Suzuki (0.2), Suk-Kyun Yang (0.11), and Jean-Frédéric Colombel (0.11). Supplementary Table S1 presents the number of articles published by the top 20 productive authors in different institutions.

The international collaboration network is presented in Figure 4. Strong collaborations were seen among Edward V Loftus Jr, Stefan Schreiber, Rafał Filip (Poland), Toshifumi Hibi, Jean-Frédéric Colombel, William J Sandborn, Bruce E Sands, Serap Sankoh (the United States), William J Tremaine (the United States), Alan R Zinsmeister (the United States), Ali M Abbas (the United States), Brihad Abhyankar (England), and Eric J Dozois (the United States). Close scientific cooperations were observed among Stefan Schreiber, Edward V Loftus Jr, Dermot P B McGovern (the United States), Andre Franke (Germany), Silvio Danese, Julián Panés, Iris Dotan (Israel), Bernd Bokemeyer (Germany), and David Ellinghaus (Germany). Jean-Frédéric Colombel worked closely with Brian G Feagan, Peter R Gibson (Australia), William J Sandborn, Gert Van Assche, Maria Rosario (the United States), Subrata Ghosh (England), Freddy Cornillie (Switzerland), Karen Lasch (the United States), Parambir S Dulai (the United States), Serap Sankoh, Edward V Loftus Jr, George Philip (the United States), Bruce E Sands, and Toshifumi Hibi.

Toshifumi Hibi was at the center of a domestic research structure, working in partnership with Yasuo Suzuki, Soichiro Ishihara (Japan), Toshiaki Watanabe (Japan), Rafał Filip, Shunji

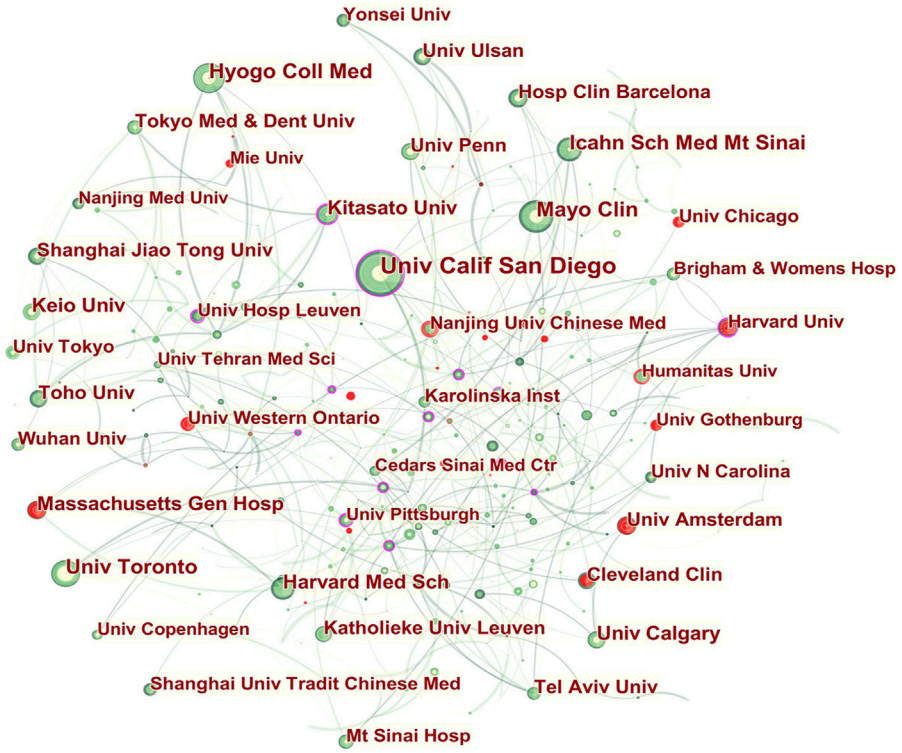

FIGURE 3
Network of institutions engaged in UC research. Note: An individual node represents an institution on the network map. The greater the area of the node, the more publications there are. The thicker the curved line connecting nodes, the more frequent their co-occurrence, as this indicates a collaborative relationship. An isolated node with no link lacks all collaboration. When a node has a high betweenness centrality (> 0.1) (i.e., when it is connected to more than 10% of the other nodes), it exerts significant influence over others as it controls most resources within their collaborative networks (Cobo et al., 2011). The presence of a purple rim also indicates a high degree of betweenness centrality. Red tree rings indicate bursts of citation, indicating high scholarly activity. Red tree rings with a greater thickness show a greater burst for a corresponding node.

TABLE 2 Self-citations of the top productive institutions involved in UC research.

Institutions	Total citations	Self-citations	Self-citation rate (%)
Univ Calif San Diego (United States)	15,745	372	2.36
Mayo Clin (United States)	4,121	48	1.16
Hyogo Coll Med (Japan)	1,502	55	3.66
Icahn Sch Med Mt Sinai (the United States)	8,274	133	1.61
Univ Toronto (Canada)	7,896	103	1.30
Univ Calgary (Canada)	5,142	89	1.73
Massachusetts Gen Hosp (the United States)	4,972	67	1.35
Harvard Med Sch (the United States)	1,445	6	0.41
Keio Univ (Japan)	2,151	52	2.42
Kitasato Univ (Japan)	1,608	52	3.23
Univ Penn (the United States)	4,665	49	1.05

Note: The rate of self-citation was determined by dividing the number of self-citations in institution X by the total number of citations received by that institution.

Ishihara (Japan), Jean-Frédéric Colombel, Mamoru Watanabe, Haruhiko Ogata (Japan), Roopal B Thakkar (the United States), Tadakazu Hisamatsu (Japan), Taku Kobayashi (Japan), Jewel Johanns (the United States), Bunei Iizuka (Japan), Gerhard Rogler (Switzerland), Edward V Loftus Jr, Omoniyi J Adedokun (the United States), and Katsuyoshi Matsuoka (Japan).

TABLE 3 Top productive 20 authors in UC research.

Rank	Author	Count (% of 5,088)	Centrality
1	William J Sandborn (the United States)	100 (1.97)	0.05
2	Severine Vermeire (Belgium)	69 (1.36)	0.09
3	Silvio Danese (Italy)	62 (1.22)	0.06
4	Laurent Peyrin-Biroulet (France)	57 (1.12)	0.04
5	Toshifumi Hibi (Japan)	54 (1.06)	0.53
6	Brian G Feagan (Canada)	51 (1.00)	0.1
7	Jean-Frédéric Colombel (the United States)	45 (0.88)	0.11
8	Walter Reinisch (Austria)	44 (0.86)	0.04
9	Julián Panés (Spain)	42 (0.83)	0.09
9	Bruce E Sands (the United States)	42 (0.83)	0.1
10	David T Rubin (the United States)	41 (0.81)	0.01
11	Byong Duk Ye (South Korea)	39 (0.77)	0.01
12	Paul Rutgeerts (Belgium)	38 (0.75)	0.02
13	Ashwin N Ananthakrishnan (the United States)	36 (0.71)	0
13	Suk-Kyun Yang (South Korea)	36 (0.71)	0.11
13	Yasuo Suzuki (Japan)	36 (0.71)	0.2
13	Hiroki Ikeuchi (Japan)	36 (0.71)	0.01
14	Mamoru Watanabe (Japan)	35 (0.69)	0.01
15	Stefan Schreiber (Germany)	34 (0.67)	0.35
16	Motoi Uchino (Japan)	33 (0.65)	0.03
17	Gert Van Assche (Belgium)	32 (0.63)	0.03
17	Takayuki Matsumoto (Japan)	32 (0.63)	0.01
18	Remo Panaccione (Canada)	31 (0.61)	0.01
18	Marc Ferrante (Belgium)	31 (0.61)	0.04
19	Bo Shen (the United States)	30 (0.59)	0.03
19	Makoto Naganuma (Japan)	30 (0.59)	0
20	Edward V Loftus Jr (the United States)	29 (0.57)	0.39
20	Masato Kusunoki (Japan)	29 (0.57)	0.06
20	Takanori Kanai (Japan)	29 (0.57)	0.02

Note: Centrality refers to betweenness centrality. Betweenness centrality was computed by CiteSpace. To rank an influential author in a graph, betweenness centrality was calculated as the unweighted shortest path between all pairs of nodes in the graph; a node with a higher betweenness centrality (> 0.1) possesses greater control over the network. Count refers to the total number of publications.

Active domestic collaborations were also observed among Yasuo Suzuki, Masakazu Nagahori (Japan), Kitaro Futami (Japan), Katsuyoshi Matsuoka (Japan), Michio Itabashi (Japan), Kenji Watanabe (Japan), Reiko Kunisaki (Japan), Keisuke Hata (Japan), Hideaki Kimura (Japan), and Toshifumi Hibi; another cooperative network consisted of Suk-Kyun Yang, Kyung-Jo Kim (South Korea), Jung Ho Bae (South Korea), Soo-Kyung Park (South Korea), Jong Wook Kim (South Korea), Jeong-Sik Byeon (South Korea), Chang Sik Yu (South Korea), Dong-Hoon Yang (South Korea), Kee Wook Jung (South Korea), Sang Hyoung Park (South Korea), Seung-Jae Myung (South Korea), Jae Seung Soh (South Korea), Jin-Ho Kim (South Korea), Yong Sik Yoon (South Korea), Seohyun Lee (South Korea), Ho-Su Lee (South Korea), Hyo Jeong Lee (South Korea), Byong Duk Ye (South Korea), and Dermot P B McGovern (the United States).

Paul Rutgeerts, Gert Van Assche, Mark S Silverberg (Canada), Bo Shen, Toshimitsu Araki (Japan), Yoshiki Okita (Japan), and Masato Kusunoki exhibited strong citation bursts, indicating that they have actively published in this area recently.

According to Table 4, the highest and lowest self-citation rates were recorded by Byong Duk Ye (9.62%) and Edward V Loftus Jr (0.44%), respectively.

Journals and co-cited academic journals

A total of 937 journals published literature in the field of UC. Among the top 10 journals listed in Table 5, the top three prolific journals were *Inflammatory Bowel Diseases* (379, 7.45%), *Journal of Crohn's and Colitis* (298, 5.86%), and *World Journal of Gastroenterology* (159, 3.13%). The publishers of these

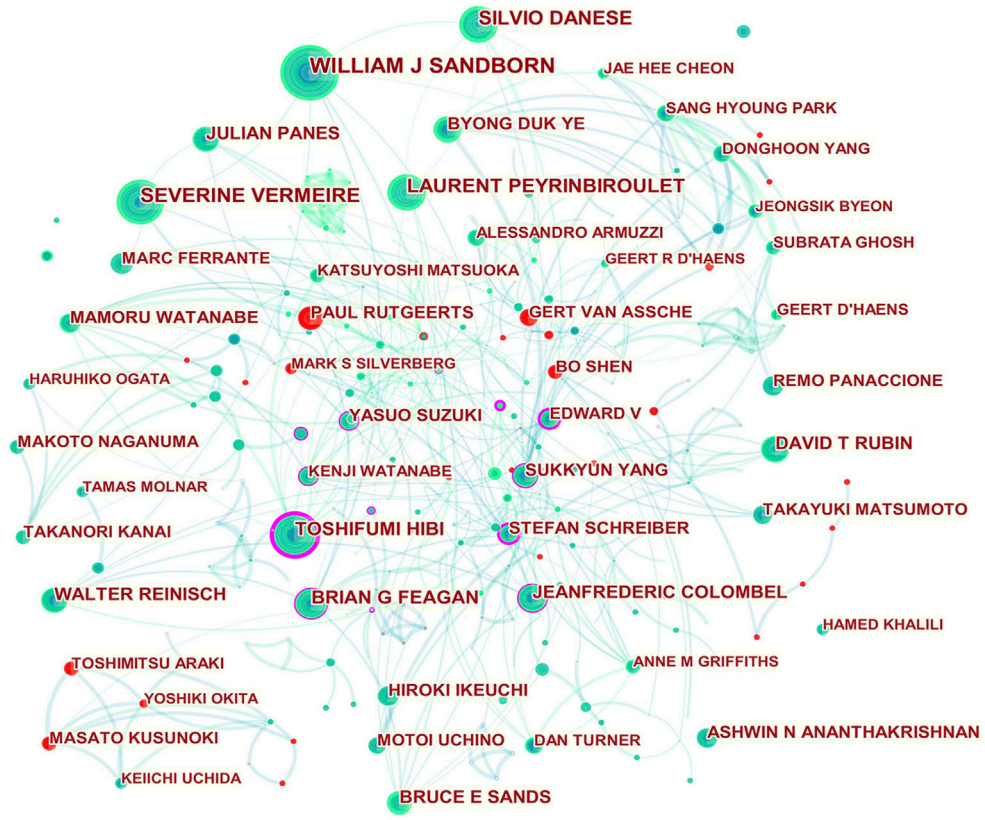

FIGURE 4
Network of authors in UC research. Note: An individual node represents an author on the network map. The greater the area of the node, the more publications there are. The thicker the curved line connecting nodes, the more frequent their co-occurrence, as this indicates a collaborative relationship. An isolated node with no link lacks all collaboration. When a node has a high betweenness centrality (> 0.1) (i.e., when it is connected to more than 10% of the other nodes), it exerts significant influence over others as it controls most resources within their collaborative networks (Cobo et al., 2011). The presence of a purple rim also indicates a high degree of betweenness centrality. Red tree rings indicate bursts of citation, indicating high scholarly activity. Red tree rings with a greater thickness show a greater burst for a corresponding node.

productive journals are located in either the United States or England.

The co-citation relationship exists when two journals are cited simultaneously in one or more identical publications. In this instance, the two journals cited by the same third journal are regarded to have an intellectual affinity. The co-citation analysis of journals can be used to map out the journals that are influential within a particular field. Among 1,041 co-cited academic journals, *Gastroenterology* had the most co-citations (3,730, 4.02%), followed by *Inflammatory Bowel Diseases* (3,624, 3.91%), and *Gut* (3,344, 3.61%).

Co-cited references and references with citation bursts

Referencing other scientific works is a regular feature of scientific publications. A co-citation network, for example, results from this process (Kessler, 1963). Two papers are cited in paper A: paper B and paper C (Figure 5). In light of these two citations, Paper B and Paper C are considered "co-cited" by Paper A. A co-citation relationship indicates similar content between these two papers. There is a greater likelihood of Paper B and C being similar when they are co-cited by more papers (e.g., Paper D, E, and F). An analysis of co-citations assumes that references co-cited in a paper are intellectually related, thereby mapping research areas, for example, the knowledge base for a research field (Marshakova, 1973; Small, 1973). Different levels of co-citation analysis can be performed: that of the publications per se; that of the cited authors; and that of the cited journals.

Of the 895 co-cited references retrieved, papers that had been co-cited with a high frequency are listed in Table 6. Of the top 10 co-cited references, *adalimumab induces and maintains clinical remission in patients with moderate-to-severe ulcerative*

TABLE 4 Self-citations of the top productive authors involved in UC research.

Author	Total citations	Self-citations	Self-citation rate (%)
William J Sandborn (the United States)	12,623	301	2.38
Severine Vermeire (Belgium)	7,607	75	0.99
Silvio Danese (Italy)	6,114	70	1.14
Laurent Peyrin-Biroulet (France)	4,015	55	1.37
Toshifumi Hibi (Japan)	2,364	51	2.16
Brian G Feagan (Canada)	230	5	2.17
Jean-Frédéric Colombel (the United States)	9,223	90	0.98
Walter Reinisch (Austria)	8,268	96	1.16
Julián Panés (Spain)	1,645	25	1.52
Bruce E Sands (the United States)	1,070	14	1.31
David T Rubin (the United States)	1,777	31	1.74
Byong Duk Ye (South Korea)	686	66	9.62
Paul Rutgeerts (Belgium)	8,169	68	0.83
Ashwin N Ananthakrishnan (the United States)	2,841	44	1.55
Suk-Kyun Yang (South Korea)	690	62	8.99
Yasuo Suzuki (Japan)	847	21	2.48
Hiroki Ikeuchi (Japan)	510	20	3.92
Mamoru Watanabe (Japan)	1,039	18	1.73
Stefan Schreiber (Germany)	4,361	23	0.53
Motoi Uchino (Japan)	453	15	3.31
Gert Van Assche (Belgium)	6,783	47	0.69
Takayuki Matsumoto (Japan)	454	4	0.88
Remo Panaccione (Canada)	3,559	47	1.32
Marc Ferrante (Belgium)	2,167	30	1.38
Bo Shen (the United States)	788	9	1.14
Makoto Naganuma (Japan)	641	35	5.46
Edward V Loftus Jr (the United States)	1,812	8	0.44
Masato Kusunoki (Japan)	273	9	3.30
Takanori Kanai (Japan)	867	31	3.58

Note: The rate of self-citation was determined by dividing the number of self-citations by author X by the total number of citations received by that author.

colitis (Sandborn et al., 2012a), published in *Gastroenterology*, was the most frequently co-cited (103), followed by *tofacitinib as induction and maintenance therapy for ulcerative colitis* (Sandborn et al., 2017), published in *The New England Journal of Medicine* (99), and *vedolizumab as induction and maintenance therapy for ulcerative colitis* (Feagan et al., 2013), published in *The New England Journal of Medicine* (97).

Keyword analysis

Keywords summarize the main points of a document in a highly condensed and generalized form. Keywords are therefore indicative of the topics of scientific output. In the co-occurrence analysis, the number of times that keywords appear in the same paper is counted pairwise in order to identify the strong association between the keywords. The co-occurrence analysis demonstrates the statistical link between two keywords within a dataset under investigation; the more frequently two keywords occur together, the greater their expected logical relationship is. The co-occurrence keyword analysis is based on the assumption that by describing the contents of documents, co-occurring keywords capture those semantic or conceptual groups of topics that can portray a field. By calculating similarity matrices and proximity indices based on the keyword co-occurrence network, it is possible to identify the clusters with the most central co-occurring keywords. The greater the co-word relationship, the greater the likelihood that two keywords will belong to the same cluster.

In the study, a total of 713 keywords were extracted. After the exclusion of keywords with an occurrence of fewer than 10 times and the merging of equivalent keywords, 331 keywords were identified.

In Figure 6, the keyword co-occurrence was visualized in a timeline. The year corresponds to the earliest year when each keyword occurred. There are nodes on the map that represent keywords. Co-occurrences of keywords are represented by the links. UC research topics have evolved over time, as indicated by the chronological order in which keywords appear.

In the early years from 2011 to 2013, UC research began to focus on (1) cystic fibrosis, asthma, breast cancer, and osteoporosis; (2) primary sclerosing cholangitis, rheumatoid arthritis, systemic lupus erythematosus, and ankylosing spondylitis; (3) celiac disease, pouchitis, and familial adenomatous polyposis; (4) abnormal motility, colonic permeability, and enteric nervous system; (5) adipose tissue; (6) epidemiology, gene polymorphism, susceptibility loci, drug delivery, and activity index; (7) dextran sulfate sodium (DSS) and acetic acid; (8) guinea pig; (9) N-acetylcysteine, fish oil, and vitamin D; (10) 5-aminosalicylic acid (5-ASA), sulfasalazine, olsalazine, and chitosan; (11) cyclosporin, 6-mercaptopurine, methotrexate, and azathioprine; (12) certolizumab pegol, infliximab, etanercept, adalimumab, and tacrolimus; (13) Adacolumn, leukocytapheresis, and apheresis; (14) probiotics, antibiotic therapy, curcumin, traditional Chinese medicine, and electroacupuncture; (15) colectomy, ileostomy, and ileal pouch–anal anastomosis; (16) liver transplantation; (17) confocal laser endomicroscopy and PillCam colon capsule endoscopy; (18) C-reactive protein, lactoferrin, and fecal calprotectin; (19) E-cadherin; (20) Epstein–Barr virus and cytomegalovirus infection; (21) *Helicobacter pylori*, gut microbiota, *Escherichia coli*, and *Clostridium difficile* infection; (22) short-chain fatty acids, butyrate, and bile acid; (23) innate immunity; (24) regulatory T (T_{reg}) cell, T helper 17 (Th17) cell, natural killer T cell, and mast cell; (25) enterochromaffin cell; (26) antineutrophil cytoplasmic antibody and anti-*Saccharomyces cerevisiae* antibody; (27) angiogenesis, oxidative stress, apoptosis, chromosomal instability, and DNA methylation; (28) *ATG16L1* and *Cd14*; (29) β-catenin, nuclear factor kappa B (NF-κB), and p53; (30) cyclooxygenase-2, peroxisome proliferator-activated receptor gamma, tumor necrosis factor-α (TNF-α), interleukin (IL)-6, IL-22, and mucosal addressin cell adhesion molecule-1 (MAdCAM-1); (31) immunoglobulin G4, hydrogen sulfide, hydrogen peroxide, and nitric oxide.

The middle stage from 2013 to 2016 focused on (1) bone marrow; (2) irritable bowel syndrome (IBS); (3) depression, anxiety, and obesity; (4) endoscopic activity; (5) trinitrobenzene sulfonic acid; (6) polypectomy, mucosal proctectomy, and appendectomy; (7) intestinal eosinophil; (8) tofacitinib and golimumab; (9) leucocytapheresis; (10) bifidobacteria-fermented milk; (11) *Faecalibacterium prausnitzii (F. prausnitzii)* and opportunistic infection; (12) lipopolysaccharide and cytosin–guanosin dinucleotide motif; (13) IBD5 locus and cytochrome P450 3A4; (14) microRNA; (15) CD98, S100 protein, transforming growth factor-β, nuclear factor erythroid 2 p45-related factor 2, IL-23 receptor, IL-8, IL-17, IL-33, β-arrestin, and myeloperoxidase.

From 2016 to 2019, researchers shifted their focus to (1) bioelectrical impedance analysis; (2) Ulcerative Colitis Endoscopic Index of Severity; (3) atherosclerosis; (4) collagenous colitis, lymphocytic colitis, backwash ileitis, and intestinal fibrosis; (5) endoscopic remission and clinical remission; (6) antiviral therapy; (7) cholecystectomy; (8) alpha-tocopherol, green tea, HMPL-004, flavonoid, coumarin, and resveratrol; (9) polyunsaturated fatty acid; (10) vedolizumab; (11) fecal microbiota transplantation (FMT); (12) macrophage, dendritic cell, and stem cell; (13) tight junction; (14) endoplasmic reticulum stress, cell death, and epithelial-to-mesenchymal transition; (15) aryl hydrocarbon receptor, toll-like receptor (TLR) 4, granulocyte macrophage colony-stimulating factor, and sphingosine 1-phosphate; (16) NLRP3 (NOD-, LRR-, and pyrin-domain containing protein 3) inflammasome; (15) claudin-2; (16) polymeric nanoparticles (NPs) and poly-(lactic-co-glycolic acid) NPs.

From 2019 to 2021, the field turned to research on (1) psoriatic arthritis; (2) iron; (3) Qing Dai, baicalin, β-sitosterol, polysaccharide, polyphenol, and berberine; (4) long noncoding RNA; (5) dectin-1, caspase-1, cytotoxic T-lymphocyte antigen 4, adenosine monophosphate-activated protein kinase, mitogen-activated protein kinase, signal transducer and activator of transcription 3 (STAT3), phosphatase and tensin homolog, and bcl-2-associated X protein; (6) Janus kinase-2; (7) IL-1β, IL-17, and IL-13.

Table 7 presents the meaningful keywords with a high frequency in UC research. The most frequent keywords were colorectal cancer (619), risk (612), management (455), infliximab (427), inflammation (409), epidemiology (366), colectomy (358), and remission (327).

The network visualization of co-occurring keywords based on VOSviewer is presented in Figure 7. A minimum occurrence of at least five times of all keywords resulted in five clusters. The size of a node represents the number of articles that use a specific keyword. A cluster is identified by a distinct color and is made up of nodes with common characteristics, which in this case pertain to pathogenesis, infliximab, surgery, 5-ASA, and assessment of endoscopic severity.

Kleinberg's algorithm for burst detection is an effective analytical tool for identifying sudden spikes in the frequency of references or keywords within a specified time frame (Kleinberg, 2003). In this way, citation bursts provide an opportunity to identify keywords characterized by rapid citation growth. Keywords with citation bursts shown in Figure 8 were considered research hot topics over time. Among them, the keywords whose citation bursts ended in

TABLE 5 Top 10 prolific journals and top 10 co-cited journals in UC research.

Rank	Journal	Count (% of 5,088)	IF	JCR	Co-cited journal	Count (% of 92,729)	IF	JCR
1	*Inflammatory Bowel Diseases* (England)	379 (7.45)	7.290	Q1	*Gastroenterology* (the United States)	3,730 (4.02)	33.883	Q1
2	*Journal of Crohn's and Colitis* (England)	298 (5.86)	10.020	Q1	*Inflammatory Bowel Diseases* (England)	3,624 (3.91)	7.290	Q1
3	*World Journal of Gastroenterology* (the United States)	159 (3.13)	5.374	Q2	*Gut* (the United States)	3,344 (3.61)	31.793	Q1
4	*Alimentary Pharmacology and Therapeutics* (England)	130 (2.56)	9.524	Q1	*The American Journal of Gastroenterology* (the United States)	2,753 (2.97)	12.045	Q1
5	*Digestive Diseases and Sciences* (the United States)	125 (2.26)	3.487	Q3	*Journal of Crohn's and Colitis* (England)	2,218 (2.39)	10.020	Q1
6	*PLOS One* (the United States)	107 (2.23)	3.752	Q2	*The New England Journal of Medicine* (the United States)	2,055 (2.22)	176.079	Q1
7	*Scandinavian Journal of Gastroenterology* (England)	94 (1.96)	3.027	Q4	*World Journal of Gastroenterology* (the United States)	2,041 (2.20)	5.374	Q2
8	*BMC Gastroenterology* (England)	78 (1.47)	2.847	Q4	*Alimentary Pharmacology and Therapeutics* (England)	1,972 (2.13)	9.524	Q1
9	*Clinical Gastroenterology and Hepatology: the official clinical practice journal of the American Gastroenterological Association* (the United States)	69 (1.42)	13.576	Q1	*Lancet* (England)	1,702 (1.84)	202.731	Q1
10	*Gastroenterology* (the United States)	66 (1.24)	33.883	Q1	*Clinical Gastroenterology and Hepatology: the official clinical practice journal of the American Gastroenterological Association* (the United States)	1,609 (1.74)	13.576	Q1

Note: We recorded the 2021 Journal Citation Reports (JCR) Journal Impact Factor (JIF) of a journal from the Web of Science. The JIF, is calculated by dividing the number of citations to a journal's articles published in the two preceding years by the number of (citable) articles published in the journal during those 2 years. To represent a journal's quality, all journals in a certain subject are grouped in descending order by IF, value from the previous year, and then divided into four quartiles: Q1, Q2, Q3, and Q4. Journal co-citation occurs when a journal is co-cited (cited together) with another journal in a research paper, often indicating similar topics between the two journals. The journal co-citation analysis is used to determine the most influential journals. Count refers to the total number of publications.

2020 or later represented topics that are actively discussed, which included vedolizumab, NLRP3 inflammasome, FMT, TLR-4, tofacitinib, and *F. prausnitzii*.

Discussion

General information

UC takes a toll on both patients and their caregivers beyond its clinical consequences. The disorder results in one-quarter million physician visits, 30,000 hospitalizations, and the loss of over one million workdays per year on a global scale (Cohen et al., 2010). UC is estimated to have a total economic burden in the United States between $8.1 and $14.9 billion and in Europe between €12.5 and 29.1 billion annually (Cohen et al., 2010). Table 1 indicates that European countries were the main providers of publications in the field. An IBD review found that the highest incidence and prevalence of UC in North America and Europe between 1990 and 2016 (Ng et al., 2017). Based on the study by Burisch et al. (2020), the mean annual cost for Crohn's and UC in Western Europe was double than that in Eastern Europe. The cost of biological treatments for IBD was lower in Eastern Europe than in Western Europe. Nonetheless, the rates of surgery and disease progression in Western and Eastern Europe were similar, despite the higher use of biotherapies in Western Europe (Burisch et al., 2020). Thus, much effort is being made by healthcare providers and policy-makers in these most burdened countries or regions (e.g., England, Spain, France, Belgium, the Netherlands, and Switzerland) to research UC.

Deviating from the geographic distribution of the high-yield countries, the majority of the top highly productive institutions were distributed among North American countries and East Asian countries. Among them, most universities or institutes contributing to UC research are located in the United States and Japan. The productive European institutions were also mostly in Western Europe.

As previously described, in bibliometric analysis, betweenness centrality is a crucial element. It is possible to determine the relative importance of each entity within a co-cited network by utilizing the centrality indicator. A node with a high degree of centrality can, for example, be considered a "bridge" between two others because it represents the shortest path between them. The degree of betweenness centrality demonstrated that some entities dominated and influenced others in a research topic. These entities are likely to initiate collaborative relationships and, in most cases, provide central financial or resource assistance in their network community clusters. The elimination of such nodes would lead to network fragmentation and an overall deterioration in the research field. Therefore, a high betweenness centrality (above 0.1 or represented by the purple halo in the network) indicates a high

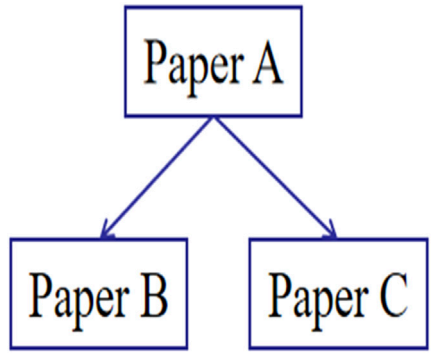

FIGURE 5
A basic example of co-citation.

level of engagement with other entities as well as the potential for influence within the academic community.

As shown in Figure 2, in the network of co-authors' countries, the landmark nodes are outlined in purple, that is, those contributing ground-breaking research, including England, Belgium, South Korea, India, and Israel. In this vein, they were considered consistently influential in UC research. In particular, England and Belgium were likely to initiate collaborations and act as connecting links for European collaborators.

The number of publications by South Korea, India, and Israel did not place them in the top 10, but these countries cooperated highly and diversely. For instance, South Korea had close cooperation with Palau, Singapore, Malta, Thailand, China, Pakistan, Lithuania, Serbia, Ukraine, and Slovakia. India worked closely with Slovakia, France, Malta, Greece, Ukraine, Brazil, Trinidad and Tobago, the United Arab Emirates, Bahrain, Malaysia, Iraq, Saudi Arabia, and Israel. Israel cooperated closely with the United States, Canada, Brazil, India, Malta, Singapore, Romania, Portugal, Spain, Estonia, Norway, Croatia, Hungary, Greece, Poland, Finland, Chile, and Cyprus. It may be explained in part by the scientific excellence of these countries, as well as that of England and France, that the foundation for excellent research is good partnerships and transnational collaboration between investigators.

Interestingly, despite their high scientific output, the United States, China, and Japan had less influence in UC research from a macro-national standpoint. These countries' poor performance in international collaborations could hinder future progress in understanding the etiopathogenesis and management of UC.

In Figure 3, the meso-institutional cooperation network pictured the dominance of American institutions over others in UC research overall. Although nearly half of the top institutions with regard to publication output were US-based, only two of them were central to this domain of research. In particular, Univ Calif San Diego and Harvard Univ appeared to hold significant influence worldwide. Institutions in Japan are mostly partnered with domestic entities led by Kitasato Univ. In addition, inter- and intra-regional cooperation for Chinese institutions, such as high-yield institutions like Nanjing Univ Chinese Med, Shanghai Jiao Tong Univ, and Shanghai Univ Tradit Chinese Med, was far from sufficient.

It is not uncommon for researchers who focus on a specific field to self-cite at all levels of publication, particularly if they have been productive in their field for a while (Livas et al., 2021). Excessive and superfluous self-citations are inappropriate since they artificially inflate citation-based metrics and self-promotion. However, genuine self-citations offer multiple benefits since they offer authors the opportunity

TABLE 6 Top 10 co-cited references in UC research.

Rank	References	Co-citation	Publishing year
1	Adalimumab induces and maintains clinical remission in patients with moderate-to-severe ulcerative colitis	103	2012
2	Tofacitinib as induction and maintenance therapy for ulcerative colitis	99	2017
3	Vedolizumab as induction and maintenance therapy for ulcerative colitis	97	2013
4	Early mucosal healing with infliximab is associated with improved long-term clinical outcomes in ulcerative colitis	96	2011
5	Beyond endoscopic mucosal healing in UC: histological remission better predicts corticosteroid use and hospitalization over 6 years of follow-up	85	2016
6	Subcutaneous golimumab maintains clinical response in patients with moderate-to-severe ulcerative colitis	84	2014
7	Subcutaneous golimumab induces clinical response and remission in patients with moderate-to-severe ulcerative colitis	82	2014
8	Adalimumab for induction of clinical remission in moderate-to-severe active ulcerative colitis: results of a randomized controlled trial	76	2011
9	Colectomy rate comparison after treatment of ulcerative colitis with placebo or infliximab	61	2009
9	Ciclosporin vs. infliximab in patients with severe ulcerative colitis refractory to intravenous steroids: a parallel, open-label, randomized controlled trial	61	2012
10	Combination therapy with infliximab and azathioprine is superior to monotherapy with either agent in ulcerative colitis	58	2014
10	Development and validation of the Nancy histological index for UC	58	2017

Note: Document co-citation occurs when two publications are co-cited (cited together) in subsequent publications, suggesting intellectual closeness between the two articles. The purpose of this analysis is to determine the time evolution of the most influential publications and the most pursued themes over time. Count refers to the total number of publications.

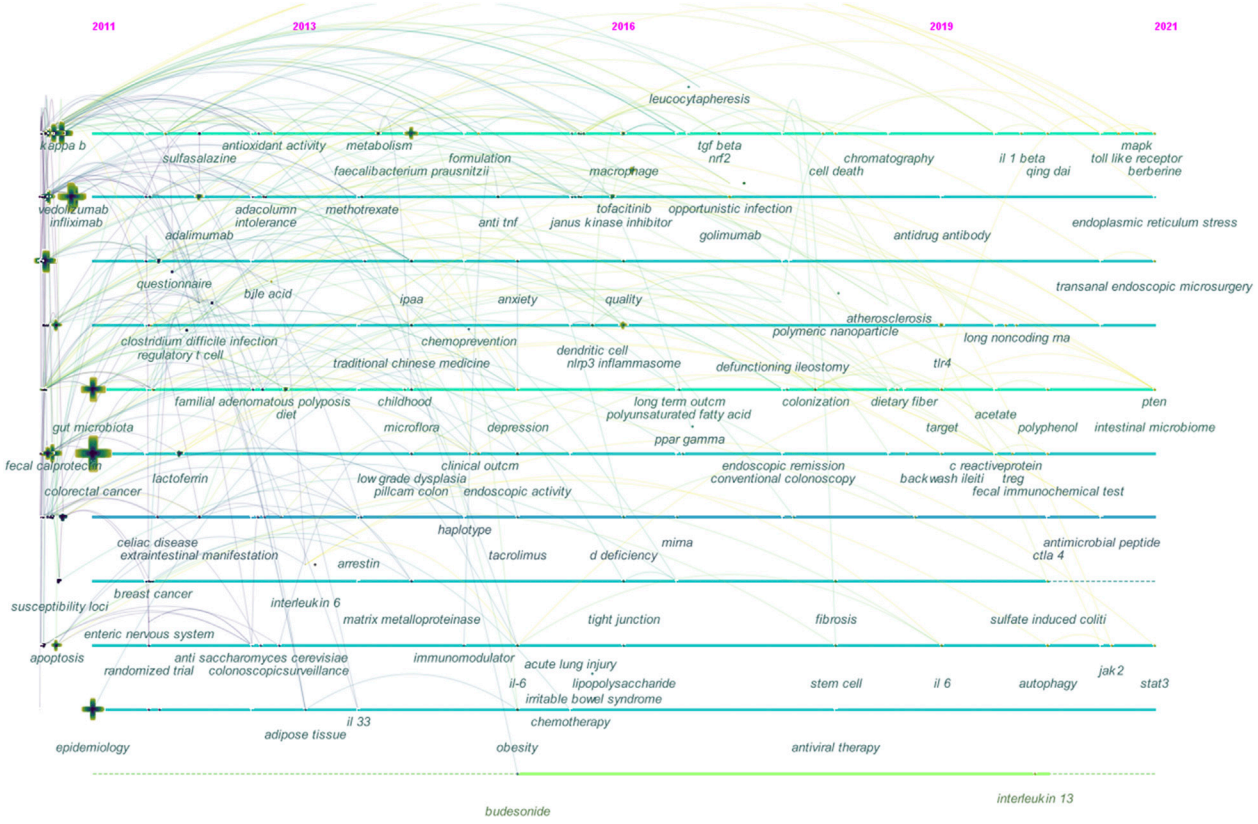

FIGURE 6
Timeline view of co-occurring keywords in UC research. Note: Each node represents a keyword, and the colors represent the node's average year of publication. Each cross represents a citation burst of a keyword co-occurrence. Time zones are represented chronologically by vertical lines spread from left to right in the timeline view. In the leftmost position are the earliest nodes, whereas the rightmost positions are the most recent. In this view, the horizontal arrangement of nodes is restricted to the time zones they occupy, but the nodes are permitted to have vertical connections with nodes in other time zones. The vertical connections between nodes indicate the co-occurrence of keywords from different clusters.

to expand on previous hypotheses, construct new methodologies, and justify further investigation (Gami et al., 2004; Glänzel and Thijs, 2004).

As seen in Table 2, 1.78% (1,026) of all citations to the scientific output of the top institutions were self-citations, out of a total of 57,521. Generally, 10–20% of self-citation in scientific work is acceptable; self-citation of more than 20% is considered ostentation and a self-overpaying attitude (Hyland, 2003; Krell, 2014; Pearce, 2016). There was an appropriate level of self-citation for the studied organizations. Of note, Hyogo Coll Med had fewer citations (1,502) but received the highest self-citation rate (3.66).

Prolific authors and micro-author cooperation networks are shown in Table 3 and Figure 4, respectively. Toshifumi Hibi was identified as the most influential researcher in the collaboration network's knowledge flow, indicating that his scholarship gave him credibility among peers. It was found that the research papers by Japanese scholar Yasuo Suzuki influenced UC research in this decade. Another Asian researcher, Su-Kyun Yang, made an influential contribution to this field as well.

This field also benefited greatly from the academic contributions of Western scholars such as Jean-Frédéric Colombel, Stefan Schreiber, and Edward V Loftus Jr.

Dermot P B McGovern (0.26 betweenness centrality), Kenji Watanabe (Japan; 0.18 betweenness centrality), Yasushi Iwao (Japan; 0.12 betweenness centrality), Akira Sugita (Japan; 0.12 betweenness centrality), Kitaro Futami (Japan; 0.11 betweenness centrality), and Gerhard Rogler (0.12 betweenness centrality) also conducted exemplary studies that contributed significantly to UC research, despite not ranking among the top 20 researchers in terms of scientific output.

In Table 4, interestingly, self-citation rates are highest among researchers who have published less research and received fewer total citations. For example, with 39 publications and 686 total citations, Byong Duk Ye had the highest self-citation rate

(9.62%). The second highest self-citation rate (8.99%) was received by Suk-Kyun Yang, with 36 documents and 690 total citations. In addition, Makoto Naganuma (30 publications; 641 total citations; 5.46% self-citation rate) is ranked third, followed by Hiroki Ikeuchi (36 publications; 510 total citations; 3.92% self-citation rate), Takanori Kanai (29 publications; 867 total citations; 3.58% self-citation rate), and Masato Kusunoki (29 publications; 273 total citations; 3.30% self-citation rate). Therefore, Asian researchers are more prone to self-cite than their counterparts.

In contrast, even with their higher total citations and greater scientific output, Severine Vermeire and Jean-Frédéric Colombel demonstrated only 0.99 and 0.98% of self-citations, respectively. Overall, the rate of author self-citations was logical, as it was noted earlier that a self-citation rate of under 20% is considered acceptable.

Table 5 shows that UC literature was mostly published in gastroenterological journals from Western countries in Q1 or Q2, indicative of the fact that high-quality and well-designed studies comprised the evidence base for UC research.

As a bibliometric indicator, the number of co-citations is used to assess research performance and to quantify their impact on the scientific community. A journal with a high co-citation frequency is typically referred to as a mainstream journal. Co-citations were found mostly in journals with a high IF and in Q1 journals, indicating that articles published in top-tier journals have attracted constant academic interest.

There are some overlaps between the productive journals and the highly co-cited ones, such as *Inflammatory Bowel Diseases*, *Journal of Crohn's and Colitis*, *World Journal of Gastroenterology*, *Alimentary Pharmacology & Therapeutics*, and *Clinical Gastroenterology and Hepatology: the official clinical practice journal of the American Gastroenterological Association*, and *Gastroenterology*. In this regard, they were considered core journals in the field since their high co-citations allowed them to influence the research area due to their heightened attention from scholars, and they were also suitable for monitoring research progress because of their high volume.

Knowledge base

Numerous articles published on UC in the last 10 years have discussed many aspects of the pathogenesis and management of UC. These references (Sandborn et al., 2012; Sandborn et al., 2017; Feagan et al., 2013; Colombel et al., 2011; Bryant et al., 2016; Sandborn et al., 2014; Reinisch et al., 2011; Sandborn et al., 2009; Laharie et al., 2012; Panaccione et al., 2014; Marchal-Bressenot et al., 2017) shown in Table 6 have been recognized as knowledge carriers by the scientific community, which serves as a starting point for further research aimed at producing new knowledge. An overview of these articles is provided in Supplementary Table S2 with a summary of their key findings or conclusions. The majority are randomized controlled trials evaluating the efficacy of biologic medications as an induction therapy or a maintenance therapy. The most extensively studied of these agents are TNF antagonists (infliximab; adalimumab; golimumab). In line with this, a bibliometric analysis conducted by Xiong et al. (2022) on immunotherapy and biotherapy for IBD revealed that anti-TNF therapy, specifically, infliximab, has been a major research area for the last decade. The corroborative findings from Figure 7, which indicate that infliximab constitutes a key component of knowledge, are also indicative of this point.

In addition, as noted in these co-cited sources, anti-α4β7 antibody (vedolizumab) and tofacitinib, a pan-JAK inhibitor, have significantly contributed to the expansion of this condition's therapeutic arsenal. Biologics and small molecules have therefore become the cornerstone of induction and maintenance of remission in patients with moderately to severely active UC over the past 10 years. As compared to conventional therapies, such as 5-ASA, corticosteroids, and immunomodulators, these medications have shown greater success (Panaccione et al., 2014). Biologic medications and small molecules have thus revolutionized UC treatment paradigms.

Hot topics

Zooming in on keywords frequently used by authors in Table 7, interesting trends, and the future of evidence synthesis emerged, including lines of research on: 1) identification of risk factors, surveillance methods, and surveillance intervals for UC-associated colorectal cancer (Hata et al., 2019; Zhou et al., 2019; Zhang and Gan, 2021); 2) anti-TNF drugs for UC induction of remission and maintenance therapy (Guo et al., 2019; Vande Casteele et al., 2019); 3) surgical treatment of UC which include proctocolectomy with ileal pouch–anal anastomosis (Drews et al., 2019; Luo et al., 2020); 4) dysbiosis of the gut microbiota (predominantly bacteria) in the pathogenesis of UC and FMT as a therapeutic strategy for UC (Blanchaert et al., 2019; Khan et al., 2019; Guo et al., 2020; Liu et al., 2021); 5) diagnostic criteria and differential diagnoses for UC (Smith et al., 2020; Wang et al., 2021); 6) NF-κB signaling pathway in the pathogenesis of UC and its clinical implication (Lu and Zhao, 2020; Dejban et al., 2021).

Citation bursts are events that are detected during bursts of activity. It is possible to detect citation bursts by observing the surge of citations associated with a particular entity. Accordingly, keywords that are experiencing ongoing citation bursts are indicative of areas of active research or emerging trends. As identified in Figure 8, the following keywords whose citation

TABLE 7 Top 20 keywords with the highest count in UC research.

Rank	Keyword	Count	Rank	Keyword	Count
1	Colorectal cancer	619	11	Induction	281
2	Risk	612	12	Efficacy	277
3	Management	455	13	Gut microbiota	269
4	Infliximab	427	14	Pathogenesis	248
5	Inflammation	409	15	Ileal-pouch anal anastomosis	237
6	Epidemiology	366	16	Quality of life	218
7	Colectomy	358	17	NF-κB	215
8	Remission	327	18	TNF-α	212
9	Diagnosis	307	19	Fecal calprotectin	160
10	Maintenance therapy	305	20	Oxidative stress	147

Note: Count refers to the frequency at which keywords appear.

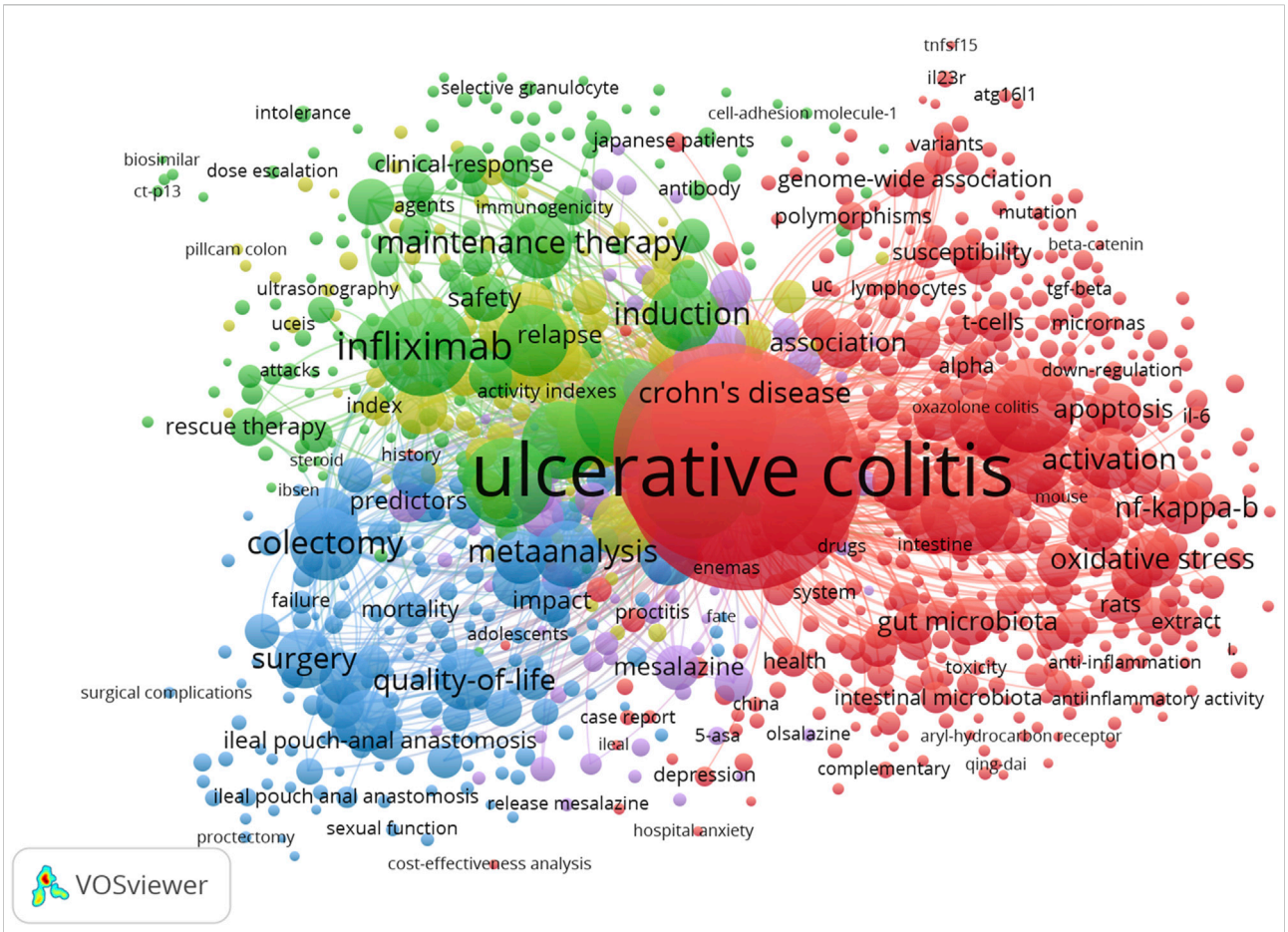

FIGURE 7
Map of co-occurring keyword clustering with a minimum of 5 occurrences in UC. Note: Minimum number of co-occurrences of a keyword = 5 and minimum links strength = 10. There are 5 clusters of keywords. The proximity of mapped keywords is determined by the keyword's relatedness to each other. The node size represents the frequency of keyword occurrence, whereas the node color shows the category in which co-occurring keywords belong. Lines linking nodes indicate co-occurrence of keywords. The thicker the line, the greater the frequency with which the keywords co-occur.

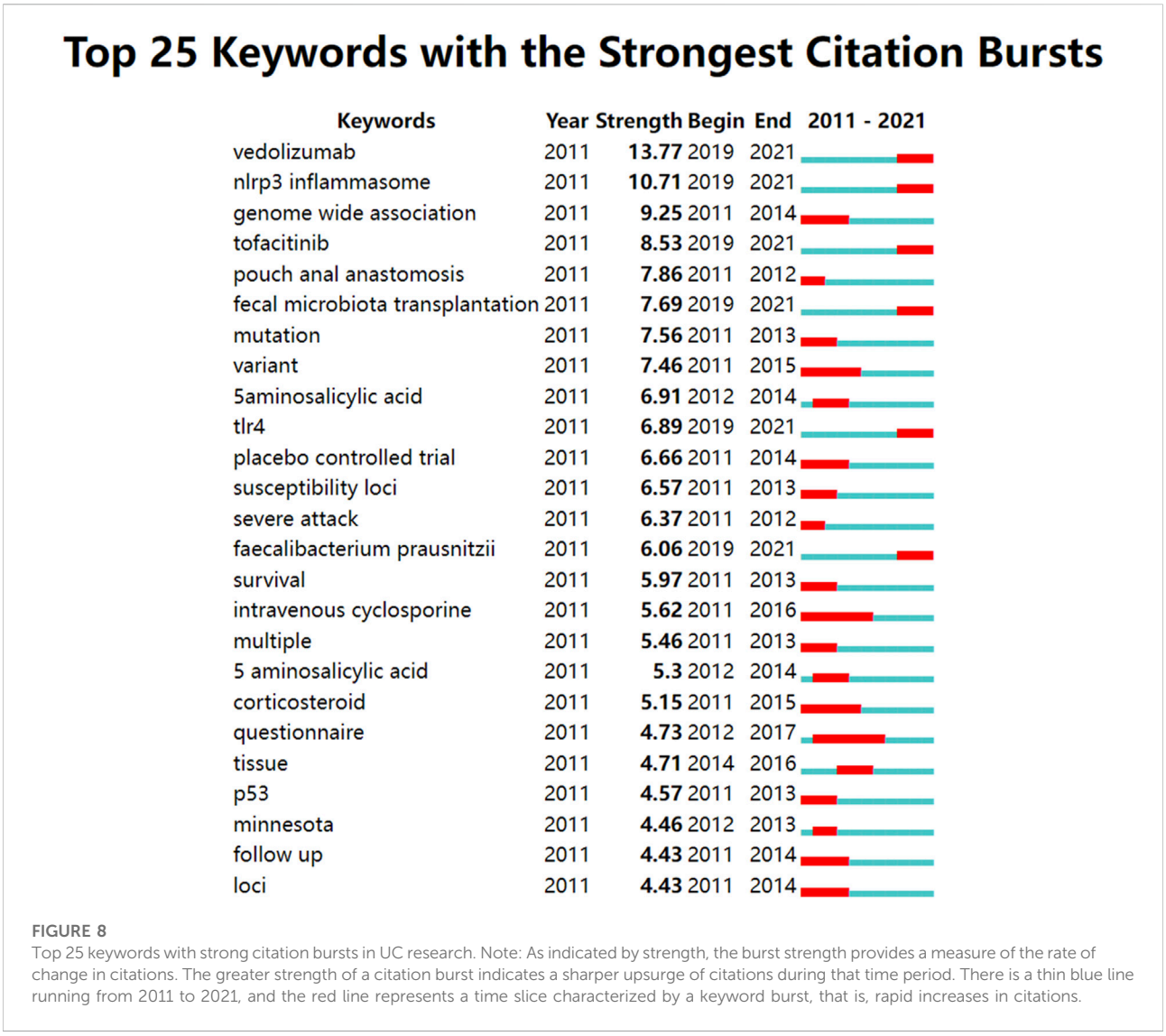

FIGURE 8
Top 25 keywords with strong citation bursts in UC research. Note: As indicated by strength, the burst strength provides a measure of the rate of change in citations. The greater strength of a citation burst indicates a sharper upsurge of citations during that time period. There is a thin blue line running from 2011 to 2021, and the red line represents a time slice characterized by a keyword burst, that is, rapid increases in citations.

bursts lasted until 2020 or later are illustrated as recent interest areas of the field as follows.

Vedolizumab

Vedolizumab, a humanized monoclonal antibody targeting the integrin α4β7, blocks the interaction between MAdCAM-1 and α4β7, thereby preventing lymphocyte trafficking into the gut (Feagan et al., 2013; Sandborn et al., 2013; Sands et al., 2014). Vedolizumab has been found to be effective in the induction and maintenance treatment of UC in the GEMINI 1 trial, a randomized, double-blind, placebo-controlled study in UC patients (Feagan et al., 2013). Study results showed a higher rate of clinical response, clinical remission, and mucosal healing when compared to placebo-treated patients (Feagan et al., 2013).

The results of real-world studies add further credibility to the effectiveness and safety of vedolizumab in UC. For example, a study by Yarur et al. (2019) retrospectively assessed the safety and effectiveness of vedolizumab by comparing it to anti-TNF agents in a cohort of biologic-naïve patients with UC. There was no significant difference in the rates of clinical response, clinical remission, and mucosal healing between the vedolizumab and anti-TNF groups after 2 years. Vedolizumab, however, provided higher treatment persistence ($p < 0.01$), and anti-TNF agents are associated with higher dose escalation ($p < 0.05$).

Though already approved for the treatment of UC, the molecular mechanisms of vedolizumab in humans are not yet well understood and further study is needed. In the study by Zeissig et al. (2019), vedolizumab had only minimal effects on the abundance and activation of intestinal T cells, the colonic T cell receptor repertoire, and intestinal trafficking of labeled

leucocytes. However, the study by Binder et al. (2018) showed that $CD4^+$ T cells from donors with UC adhered to MAdCAM-1 and vedolizumab significantly reduced dynamic adhesion; this is in agreement with the current mechanisms of its action since vedolizumab inhibits α4β7-expressing T cells in high endothelial venules of the gut and reduces infiltration of inflammatory cells. An investigation of the functional effect of α4β7 integrin and the G protein-coupled receptor GPR15 on intestinal homing of effector T (T_{eff}) or T_{reg} cells found that α4β7 mediates homing of T_{reg} cells, whereas α4β7 and GPR15 mediate homing of T_{eff} cells; vedolizumab reduces intestinal homing of both T_{eff} cells and T_{reg} cells by blocking α4β7 (Fischer et al., 2016). In a study by Rath and others, they investigated factors associated with vedolizumab efficacy in patients with IBD and found that vedolizumab treatment reduces the expression of the α4β7 integrin on Th1, Th2, and Th17 polarized cluster of differentiation $CD4^+$ T cells (Rath et al., 2018). In addition, UC patients in remission at baseline had significantly higher levels of α4β7-expressing cells in the lamina propria than non-responders (Rath et al., 2018). These data imply that vedolizumab may function by inhibiting the migration of particular T cell subtypes to the gut. In a study that performed immunophenotyping of peripheral and mucosal immune cells in IBD patients on vedolizumab, it was found that immunosuppression caused by antibodies against α4β7 integrin extends beyond T cells and primarily involves modulation of innate immunity, including changes in macrophage populations (e.g., changes in macrophage M1 to M2 profiles in patients who achieved remission specifically with vedolizumab) and changes in the expression of molecules that are involved in microbial sensing, chemoattraction, and innate effector responses (Zeissig et al., 2019). Thus, the integrin-binding property of vedolizumab is thought to alter gene expression in monocytes, skewing the population toward a wound-healing phenotype and away from an inflammatory one. However, further research on other immune cell subpopulations is needed to gain a deeper understanding of vedolizumab's mechanism of action.

Tofacitinib

Tofacitinib is an inhibitor of JAK-1, JAK-3, and, to a lesser extent, JAK-2 (Meyer et al., 2010; Hodge et al., 2016). Tofacitinib was first studied as part of a phase II trial in which 194 adult patients with moderate to severe UC were either treated with a placebo or four different doses of tofacitinib (0.5, 3, 10, or 15 mg twice daily) for 8 weeks (Sandborn et al., 2012b). In this study, the primary endpoint was the clinical response, defined as a reduction of 3 or more points in the Mayo score over 8 weeks from baseline. There was a statistically significant difference in the primary endpoint between the 15 mg group and the placebo group (78% vs. 42%, $p < 0.001$). Furthermore, the 10 and 15 mg groups showed significantly higher rates of clinical remission (48 and 41%, respectively), as well as endoscopic remission (30 and 27%, respectively), than the placebo group (10 and 2%, respectively).

The efficacy of tofacitinib in patients with UC was later validated in three phase III trials: OCTAVE Induction 1 and 2 as well as OCTAVE Sustain (Sandborn et al., 2017). At week 8, in the OCTAVE Induction 1 trial, 18.5% of the patients receiving tofacitinib achieved remission, vs. only 8.2% in the placebo group ($p = 0.007$), while in the OCTAVE Induction 2 trial, 16.6% achieved remission vs. 3.6% ($p < 0.001$). In the tofacitinib 10 mg group, mucosal healing was greater than that in the placebo group. According to the subgroup analysis, those who had experience with anti-TNFs did not differ significantly from those who were naïve in terms of both their primary and secondary outcomes. In light of the reduced sample size, this should be interpreted with caution. In the OCTAVE Sustain trial, the remission rates for those on 5 and 10 mg twice daily were higher at week 52 than those on placebo (34.3 and 40.6% vs. 11.1%, $p < 0.001$).

As tofacitinib real-world data have emerged, a growing body of evidence shows that it is effective in more complex and diverse patient populations. According to a systematic review of 17 real-world studies involving 1,162 patients with UC, the clinical response rate at week 8 was 62% (95% confidence interval [CI] 55–69%), with similar rates at week 12–16 (64%; 95% CI 56–73%) (Taxonera et al., 2022). In terms of clinical remission, 35% (95% CI 24–45%) was achieved at week 8, and 47% (95% CI 40%–54%) at week 12–16. The outcomes align with those seen in clinical trials, apart from the fact that the meta-analysis cohort which was looked at in the real world was a more refractory one, with 88% having biological experience and two-thirds failing both anti-TNF and vedolizumab, compared to 51% of the OCTAVE cohort having anti-TNF experience and none having prior vedolizumab experience (Sandborn et al., 2017; Taxonera et al., 2022).

F. prausnitzii

As part of the normal human microbiome, *F. prausnitzii* bacteria occupy 6–8%, even as high as 20% (Eckburg et al., 2005; Walker et al., 2011). In IBD, a longitudinal study has demonstrated an overall reduction in short-chain fatty acids, including butyrate, in those with a perturbed gut microbiome (Lloyd-Price et al., 2019). These reductions were closely related in magnitude to a reduction in *F. prausnitzii*, the main producer of butyrate (Lloyd-Price et al., 2019). There is evidence that *F. prausnitzii* plays a potent anti-inflammatory role by interfering with various immune pathways, including inhibiting IL-17 (Zhang et al., 2014a), skewing human dendritic cells to prime IL-10-producing T cells (Rossi et al., 2016), influencing Th17 differentiation (Huang et al., 2016), expanding T_{reg}

populations in the gut (Patterson et al., 2017), and inhibiting NF-κB activation (Sokol et al., 2008; Sarrabayrouse et al., 2014), thus stimulating genes involved in enterocyte differentiation, proliferation, and regeneration (Martín et al., 2018). Through its anti-inflammatory mechanisms, *F. prausnitzii* appears to play a key role in protecting colonic functions.

As compared with healthy individuals, UC patients had lower counts of *F. prausnitzii* species (Sokol et al., 2009; Li et al., 2016; Yao et al., 2016). For example, the presence of *F. prausnitzii* was determined in 28 healthy controls, 45 patients with CD, 28 patients with UC, and 10 patients with IBS (Lopez-Siles et al., 2014). *F. prausnitzii* was found to be a specific marker for IBD as its abundance was significantly lower in patients with IBD than in IBS patients and healthy controls ($p < 0.001$) (Lopez-Siles et al., 2014). As demonstrated by Prosberg et al. (2016), in their random-effects meta-analysis of 231 patients with CD and 392 patients with UC, *F. prausnitzii* abundance was reduced in active disease than in remission, suggesting *F. prausnitzii* may be a reliable indicator of disease activity. In addition, patients with UC experienced remission after 5-ASA treatment, and the abundance of *F. prausnitzii* in the intestine increased gradually (Varela et al., 2013). Moreover, in the same study, the authors found that a low level of *F. prausnitzii* was associated with frequent relapses (more than one relapse per year) and that the recovery of the *F. prausnitzii* population after relapse was associated with maintaining clinical remission (Varela et al., 2013). In the study by Magnusson et al. (2016) on UC patients, *F. prausnitzii* abundance increased during infliximab induction in treatment responders ($p = 0.01$). The presence of this bacterium was higher in responders to infliximab at week 6 than in non-responders ($p = 0.003$) (Magnusson et al., 2016). The results of a meta-analysis that included 427 CD patients, 560 UC patients, and 682 healthy controls from 16 studies have shown a negative correlation between the abundance of *F. prausnitzii* and IBD activity (Zhao et al., 2021). However, a cut-off level of *F. prausnitzii* for diagnosis and starting treatment of IBD has not been determined. As far as microbiota-based strategies are concerned, identification of deficiency in relevant anti-inflammatory bacteria, such as *F. prausnitzii*, may lead to augmentation of bacteria or administration of molecules, such as a microbial anti-inflammatory molecule, to counter the inflammation (Ramirez-Farias et al., 2009; Quévrain et al., 2016).

In addition, *Faecalibacterium*, often considered a sign of a healthy gut microbiome, was found in greater abundance at baseline in both infliximab and ustekinumab responders than non-responders (Rajca et al., 2014; Magnusson et al., 2016; Doherty et al., 2018). Therefore, a high abundance of *F. prausnitzii* is associated with improved treatment response to IBD, suggesting that the gut microbiota may contribute to explaining the heterogeneity of response to treatments (Radhakrishnan et al., 2022). In practice, however, the use of microbiota profiles to predict IBD treatment response is still in its infancy to be clinically relevant.

FMT

Following FMT's initial success in inducing remission in primary UC in 1989 (Bennet and Brinkman, 1989), randomized controlled trials (RCTs) have provided a more convincing case for its potential as a treatment for UC. The results of five RCTs showed that FMT significantly improved the clinical remission rate of UC in comparison with placebo or autologous fecal transplant at 8–12 weeks, suggesting that FMT may be beneficial in the treatment of the disorder (Moayyedi et al., 2015; Paramsothy et al., 2017; Costello et al., 2019; Sood et al., 2019; Crothers et al., 2021). Contrary to this, one study found a clinical and endoscopic response among 30% of patients with UC who received allogeneic treatment and 20% of those who received autologous fecal material; however, these differences were not significant (Rossen et al., 2015). Furthermore, another study linked FMT with worse clinical remission outcomes in UC patients than 5-ASA, though both agents had similar clinical response rates (Schierová et al., 2020). In evaluating FMT's effectiveness, these studies seem inconsistent. However, as evidenced in resultant meta-analyses, FMT had a better result than placebo for inducing remission in UC (Costello et al., 2017; Narula et al., 2017; Caldeira et al., 2020; Liu et al., 2021).

It has been observed or suspected that many factors influence FMT effectiveness. In the study by Schierová et al. (2020), FMT treatment was only successful for one female with stool donated by a man, suggesting that gender may affect the efficacy of FMT in particular. Previously, it was suggested that colonoscopic or enema administration offered superior results over upper gastrointestinal administration; however, encouraging results have recently been reported on oral lyophilized FMT in UC (Paramsothy et al., 2017; Tang et al., 2020; Haifer et al., 2021). Liu et al. (2021) conducted a meta-analysis involving five RCTs with 292 participants to conclude that FMT *via* the lower gastrointestinal tract results in better outcomes for both primary (combined clinical remission with endoscopic remission/response) and secondary outcomes (clinical remission and endoscopic response). In contrast, the effects of FMT performed *via* the upper gastrointestinal tract were not found to be beneficial in any of the subgroup analyses comparing FMT with controls (Liu et al., 2021). Treatment with multiple donors is considered more effective than treatment with individual donors because of the increased microbial diversity involved (Paramsothy et al., 2017; Levy and Allegretti, 2019). In addition, a new diagnosis of UC was generally treated successfully, possibly because of the lesser impact the disease has on the microbiome.

In conclusion, the extent to which FMT is effective appears to depend on the method of donor material delivery, the source of donor material (from a healthy normal donor or a super donor; fresh or frozen), the number of procedures (a single FMT or repeated sessions), previous treatment, and the severity of the

UC. As well, in light of the large heterogeneity of the cohorts of participants studied and the FMT protocols used, it is difficult to determine which patient population should be treated or how to implement the best FMT methodology. FMT studies are also often limited by the lack of long-term follow-up of study participants. Limited long-term follow-up reports indicate that FMT effects gradually fade over 3 months (Damman et al., 2015; Wei et al., 2016). Multicenter studies with sufficiently large sample sizes and detailed microbiome analyses of patients and donors will be needed to further our understanding of UC treatment.

In light of the complexity of the fecal microbiota mixture and the multitude of compositions that can be involved in the regulation of the microbiome, including bacteria, yeast, parasites, and viruses, there is uncertainty as to which fecal microbiota components are beneficial and which may pose a risk by transferring antibiotic resistance or producing genotoxic compounds. Although FMT has been shown to be relatively safe in the short term for the treatment of patients with active UC (Liu et al., 2021), it is associated with some adverse reactions due to its complex composition.

Using 20 RCTs and 109 non-RCTs over a 20-year period, a recent meta-analysis showed that 19% of patients experienced FMT-related adverse events (AEs) and 1.39% of patients experienced FMT-related SAE (Marcella et al., 2021). There were most frequently reported AEs of diarrhea (10%), abdominal discomfort (7%), nausea, vomiting, and flatulence (3.3%); in regard to SAE, bacteremia and death occurred in 0.09% of patients; these complications were more common in patients who sustained mucosal barrier injuries ($p < 0.05$) (Marcella et al., 2021). The bacteria, including multidrug-resistant pathogens and other harmful species, are relatively harmless to a healthy donor, but they can pose a threat to an immunocompromised or otherwise vulnerable recipient. It has been observed that there have been a small number of serious complications with capsule-delivered FMT, such as bacteremia and intermittent UC flares, as well as one death as a result of infection by *Escherichia coli* producing extended-spectrum beta-lactamase (DeFilipp et al., 2019). Pathogen screening is routine and should effectively eliminate the risk, but identifying detrimental bacteria specific to a particular individual is considerably more challenging.

It is, however, feasible to microfilter feces to eliminate solids, parasites, and fungi from fecal suspensions due to the advent of washed microbiota transplantation (WMT) (Shi, 2020). By increasing intestinal mucosal permeability and decreasing proinflammatory metabolites, it has been demonstrated that washing preparation contributes to reducing the incidence rate of FMT-related AEs. Based on metabolism analysis, it has been shown that washing significantly reduces pro-inflammatory metabolites, including prostaglandin G2, leukotriene B4, corticosterone, and transient receptor potential vanilloid 1, as well as differentially enriched metabolic pathways that are associated with fever and inflammation (Lu et al., 2022). Thus, in the context of UC, WMT is primarily concerned with reducing transplantation-related AEs associated with the preparation of washed microbiota (Zhang et al., 2020a). Additionally, washed microbiota preparation allows for delivering a precise dose of enriched microbiota rather than relying on stool weight as an indicator of dose (Zhang et al., 2020a) It might be possible to resolve the bias between studies caused by differences in stool dosage by applying this technique in the future.

Through clinical trials, animal experiments, and *in vitro* tests, Zhang et al. (2020a) concluded that WMT provides superior safety, quality control, and precise bacteria enrichment to FMT. An open-label prospective study conducted by Chen et al. (2020a) demonstrated that wash-treated FMT was safe and effective in achieving clinical responses in 77.8% (7/9) of the UC patients within 2 weeks; clinical and endoscopic remissions were achieved in 55.6% (5/9) and 33.3% (3/9) of cases, respectively, by week 12. Wu et al. (2021) reported the case of a 31-year-old male with refractory UC and recurrent invasive fungal infections who did not respond to antifungal therapy. Interesting to note was the rapid decrease in inflammatory markers that occurred during the hospitalization and follow-up period after WMT within 1 week, and that fecal fungal cultures were consistently negative throughout. As reported in a recent study by Wang et al. (2022), the frequency and duration of treatment for WMT were considerably lower than those of crude FMT in a 25-year-old man with refractory UC. It is also possible that clinical remission time increases continuously with increasing interval WMTs, although more evidence is needed to support this (Schierová et al., 2020). Nevertheless, this study suggests the potential benefit of repeating interval WMTs as a long-term treatment strategy for refractory UC. Another retrospective study of 21 female patients with IBD found a higher pregnancy rate in the WMT group than in the non-WMT group ($p = 0.047$) (Zhao et al., 2022). Most of the time to pregnancy in the WMT group was less than 6 months, significantly shorter than in the non-WMT group ($p = 0.017$) (Zhao et al., 2022). In this way, the results of this pilot study suggest the possibility that WMT could have a beneficial effect on fertility in patients with IBD.

Furthermore, the microbial analysis of clinical samples of FMT provides valuable insights regarding how FMT affects the microbiome and its mechanisms of action. FMT significantly increased bacterial diversity, which correlated well with clinical responses, according to bacterial taxa analysis (Paramsothy et al., 2017). There were several bacterial taxa associated with remission after FMT, such as *Clostridium* clusters IV and XVIII, whereas Proteobacteria (*Sutterella* spp.) and *Fusobacterium* species were found to be associated with non-remission (Paramsothy et al., 2017). Researchers found that patients who were in remission following FMT had enriched *Eubacterium hallii* and *Roseburia inulivorans*, increased levels of short-chain fatty acid biosynthesis and secondary bile acids in their metagenomic and metabolomic

analyses (Paramsothy et al., 2019). *Fusobacterium*, *Sutterella*, and *Escherichia* species were significantly higher in remission-failing patients, and their heme and lipopolysaccharide (LPS) synthesis levels were significantly higher (Paramsothy et al., 2019). Enhanced levels of butyrate-producing bacteria and recovered short-chain fatty acids were also associated with sustained remission following FMT treatment (Fuentes et al., 2017). In patients with IBD, *Akkermansia muciniphila* (*A. muciniphila*) was significantly less abundant and colonized than in healthy individuals (Zhang et al., 2020b). The colonization rate of *A. muciniphila* has increased significantly after WMT as compared to pre-WMT. It appears that *A. muciniphila* abundance may be closely related to WMT's effectiveness in treating IBD (Zhang et al., 2020b). As inter-individual microbial variation and inherent microbial metabolic redundancy are likely to be more important in dictating outcomes than exactly what microbial shifts occurred, the functional changes will likely play an even greater role.

TLR-4

As well as serving as a primary pattern recognition receptor, TLR4 has also been identified as the canonical receptor for LPS of Gram-negative bacteria, and there is emerging research showing that TLR4 participates in the initiation of UC (Takahashi et al., 2009). Antigen-presenting cells in the intestine, such as macrophages and dendritic cells, as well as enterocytes and lymphocytes, express TLR4 (Jilling et al., 2006). Auxiliary molecules such as LPS binding protein (LBP), CD14, and myeloid differentiation factor 2 (MD-2) play a role in the TLR4 receptor complex as co-receptors (Pandey et al., 2018). When LPS is identified, the LBP transfers LPS to the cell surface CD14, which then binds to the TLR4/MD-2 receptor complex (Pandey et al., 2018). A consequence of the LPS/MD-2/TLR4 complex is that two distinct intracellular adaptor proteins are recruited, including myeloid differentiation 88 (MyD88)/MyD88-like adaptor molecule as well as toll-interleukin receptor (TIR) domain-containing adaptor protein-inducing interferon-β (TRIF)/TRIF-related adaptor molecule, which then activates two parallel signaling pathways, the TRIF-dependent pathway and the MyD88-dependent pathway (Kawasaki and Kawai, 2014), facilitating the activation of NF-κB and mitogen-activated protein kinase, leading to the production of proinflammatory cytokines, such as TNF-α and IL-6, IL-8, and IL-12, and the initiation of IBD (Chow et al., 1999; Miggin and O'Neill, 2006).

TLR4 mRNA and protein levels were significantly increased in the colonic mucosa of UC and CD patients when compared with healthy controls (Brown et al., 2014). In patients with UC at the active phase, TLR4 has also been identified on the lamina propria and submucosa of inflammatory cells but not in healthy controls (Tan et al., 2014). TLR4 expression was also found to be linked to disease activity indices, endoscopic scores, and histopathological scores (Tan et al., 2014).

Due to the pathological role played by TLR4 downstream signaling in inflammation, anti-inflammatory agents that target TLR4 signaling may be helpful to treat UC. Through the use of TLR4 antagonists, including paeoniflorin, monoclonal antibodies, and CRX-526, DSS-induced intestinal inflammation has been reduced with respect to disease activity and histopathological scores (Fort et al., 2005; Liu et al., 2010; Zhang et al., 2014b). However, other studies have shown that blocking TLR4 does not result in improved clinical symptoms or histological scores during chronic intestinal inflammation (Fukata et al., 2005), despite the opposite being true for acute inflammation (Ungaro et al., 2009), likely due to the low involvement of innate immunity in chronic inflammation (Wardill et al., 2019). In addition, it has been shown that although the production of chemokines, including C-C motif chemokine ligand 2 (CCL2), CCL20, and Cys-X3-Cys chemokine ligand 1, and the infiltration of macrophages and dendritic cells were depressed in anti-TLR4 antibody-treated mice, tissue repair was thwarted, suggesting that TLR4 acts as a mediator for both mucosal repair and inflammation (Ungaro et al., 2009).

A diverse range of plant-derived molecules with TLR4 specificity and inhibitory properties are being examined for their potential as TLR4 antagonists (Schink et al., 2018). The modulation of TLR4 with herbal extracts kicked off a large area of research to assess their potential as a treatment for UC (Dai et al., 2022). However, promising phytochemicals as TLR4 antagonists may be in UC treatment, but there remain challenges in their bioavailability and administration. Furthermore, few clinical trials targeting UC pathobiology have been conducted with TLR4 modulators, which suggests the need for further experiments and clinical trials focusing on UC therapy through anti-TLR4 therapies.

NLRP3 inflammasome

A plausible hypothesis for UC's etiology and pathogenesis is that of unregulated immune activation of both the innate and adaptive immune systems, possibly in response to resident gut microbes. NLRP3 inflammasome plays a primary role in the host defense response against microbial pathogens by controlling their ingress through the intestinal tract.

There is evidence suggesting that mice lacking the NLRP3 inflammasome components exhibit exacerbated colitis when challenged with DSS or 2,4,6-trinitrobenzene sulfonic acid for the induction of experimental colitis (Allen et al., 2010; Zaki et al., 2010; Hirota et al., 2011), as characterized by increased mortality, compromised epithelial integrity, an increase in commensal bacterial translocation from the gut to the bloodstream, and a decline in cytokines, including IL-1β.

These studies found that mice with NLRP3 inflammasome deficiency exhibited enhanced intestinal leukocyte infiltration, whereas macrophages isolated from knockout mice were incapable of mounting an immune response against bacterial muramyl dipeptide, and neutrophils had enhanced apoptosis and impaired chemotaxis to neutrophil chemotaxis factors. In addition, the intestinal microbiota of nlrp3−/− mice differed from that of wild-type mice, with some strains of Enterobacteriaceae and *Mycobacterium* species showing signs of pathogenicity (Hirota et al., 2011).

Even though many studies have demonstrated that inflammasome activation reduces UC pathology, other studies, however, have highlighted an opposite tendency in disease severity in mice lacking NLRP3 inflammasome components and related pro-inflammatory cytokines (Ruiz et al., 2017; Mai et al., 2019; Zhang et al., 2019). NLRP3, IL-1β, caspase-1, and apoptosis-associated speck-like protein containing a caspase recruitment domain (ASC) were highly expressed in UC and CD biopsies from quiescent and active patients (Ranson et al., 2018). In a study by Hanaei et al. (2018), they investigated NLRP3 single nucleotide polymorphisms (SNPs) in blood samples from healthy subjects and UC patients and demonstrated a significant association between the genotype rs10754558 of the NLRP3 SNP and UC. Diverse factors might account for these discrepancies, including the genetic background of the mice or humans studied, microbiome composition across animal facilities, modified experimental colitis protocols, and differences in NLRP3 ablation methods (Bauer et al., 2012; Wagatsuma and Nakase, 2020). There are two potential mechanisms through which an activated inflammasome could contribute to gut homeostasis, and the activation response of the inflammasome depends on the normal function of the intestinal epithelium. The activation of NLRP3 inflammasome in the intestinal epithelial cells is supposed to play a beneficial role in maintaining homeostasis; however, it may be detrimental if the epithelial barrier is damaged, leading to impaired sensing of commensal microbiota or bacterial clearance, thus inducing inflammation of the mucosa (Zambetti and Mortellaro, 2014).

It has been suggested so far that specific inhibitors of NLRP3 or those that reduce the levels of NLRP3 are being most evaluated as a therapeutic approach in UC. Mice treated with MCC950, a specific NLRP3 inhibitor, experienced resolution of acute or chronic colitis by inhibiting ASC oligomerization, caspase-1 dependent activation of IL-1β and IL-18, and reducing pro-inflammatory cytokines (Perera et al., 2018; Wu et al., 2018). In the study by Saber and El-Kader (2021), metformin and MCC950 combined had a protective effect on UC and might become a treatment of choice in the future. The researchers found that metformin/MCC950 attenuated DSS-induced colitis by inhibiting NLRP3 inflammasome *via* autophagy-mediated interactions between heat shock protein 90 and NLRP3 (Saber and El-Kader, 2021).

A growing body of evidence suggests that some natural products might act by targeting the NLRP3 inflammasome to affect colonic inflammation in colitis models. The anti-inflammatory effect of cardamonin was demonstrated in an animal model of DSS-induced colitis, which was shown to alleviate body weight loss, diarrhea, colon shortening, and histological damage (Ren et al., 2015). Inhibition of NLRP3 inflammasome activation through suppressing TLR4 and NF-κB was responsible for this protective effect (Ren et al., 2015). The therapeutic effects of cardamonin, evodiamine, walnut oil, and palmatine have been demonstrated in experimental mouse models of colitis as well. Their anti-inflammatory effects are related to their antioxidant properties, activation of autophagy, promotion of mitophagy, and inhibition of apoptosis (Wang et al., 2018; Mai et al., 2019; Ding et al., 2020; Miao et al., 2021).

As demonstrated in a DSS-induced colitis mouse model, adipose-derived stem cells (ASCs) were also shown to suppress NLRP3 inflammasome formation and regulate the M1 macrophage population through prostaglandin E2, raising the possibility that ASCs may suppress colitis by modulating the NLRP3 inflammasome (Park et al., 2018).

Additionally, Chen et al. (2020b) showed that pretreatment with heat-killed probiotic *Enterococcus faecalis* attenuated colitis and inflammation-associated colon carcinogenesis. In macrophages, *Enterococcus faecalis* can suppress NLRP3 inflammasome activation, caspase-1 activation, and IL-1β maturation (Chen et al., 2020b). Consequently, *Enterococcus faecalis* attenuated phagocytosis, which is essential for the activation of NLRP3 inflammasome in response to commensal microorganisms (Chen et al., 2020b).

In conclusion, in UC patients with specific genetic abnormalities and in several experimental models of colitis, excessive activation of NLRP3 inflammasome augments colonic inflammation. Accordingly, targeting this inflammasome for the treatment of UC appears to be promising. However, it is not clear whether shutting off the NLRP3 inflammasome in the gut abruptly and completely will result in severe side effects or even exacerbate the inflammatory condition since this inflammasome also plays a key role in maintaining gut immune homeostasis and that inflammasome disruption could trigger an inflammatory response.

Limitations

There are several limitations to this study, most of which are the same as those of other bibliometric studies performed. First, the search terms without "IBD" included would result in potential missing publications. Second, despite the WoSCC containing over 12,000 of the journals with the highest impact and open-access journals selected based on rigorous and qualified editorial standards (Tam et al., 2012), the bibliometric analysis was conducted solely using the WoSCC as the source of data, and we did not use Scopus; thus, documents published in non-WoSCC-cited journals were not included, and they might

contribute to scientific productivity in the field. Furthermore, only English publications were included, which may have decreased the number of retrieved documents. Lastly, the field delineation methods that rely on bibliometrics used in the present study have their weaknesses; co-citation, as an example, is a retrospective analysis that occurs only for articles with references and citations, so it is less effective with newer articles without citations. Due to their age, more recent articles are underrepresented since they have not received as many citations as older articles.

Conclusion

A bibliometric profile of UC in the last decade aims to identify, evaluate, and depict publications related to qualitative, semi-qualitative, and chronological aspects. In terms of qualitative, quantitative, and collaborative variables, we showed that Europe and North America held the leading positions in UC research. There has been a poor record of institutional, regional, and national cooperation among high-yield Asian countries, such as Japan and China. A change in this stifling trend is necessary to facilitate future advancements in this field of study, and future collaborative efforts should be supported, promoted, and implemented globally. Anti-integrins, JAK inhibitors, and FMT were described in the manuscripts as research foci for UC therapies. Gut microbiota and associated inflammatory signaling pathways as well as the NLRP3 inflammasome regulation were hot issues in basic research.

Author contributions

XT and FW led the team and were responsible for all aspects of the project. TZ, BZ, and WT substantially contributed to the methods, data acquisition, results, and interpretation. JZ, XM, and YW participated in designing and writing the manuscript. TZ, BZ, WT, and JZ revised this manuscript critically for important intellectual content. XT gave final approval of the manuscript. All authors contributed to the article and approved the submitted version.

Funding

This work was supported by the National Natural Science Foundation of China (No. 81830118), China Academy of Chinese Medical Sciences Innovation Fund (No. CI 2021A01012), and China Academy of Chinese Medical Sciences Basic Research Fund for Outstanding Young Technical Talents (Innovation) Training Program (No. ZZ15-YQ-002).

Conflict of interest

The authors declare that the research was conducted in the absence of any commercial or financial relationships that could be construed as a potential conflict of interest.

Publisher's note

All claims expressed in this article are solely those of the authors and do not necessarily represent those of their affiliated organizations, or those of the publisher, the editors, and the reviewers. Any product that may be evaluated in this article, or claim that may be made by its manufacturer, is not guaranteed or endorsed by the publisher.

Supplementary material

The Supplementary Material for this article can be found online at: https://www.frontiersin.org/articles/10.3389/fphar.2022.951004/full#supplementary-material

References

Actis, G. C., Pellicano, R., Fagoonee, S., and Ribaldone, D. G. (2019). History of inflammatory bowel diseases. *J. Clin. Med.* 8 (11), 1970. doi:10.3390/jcm8111970

Aksnes, D. (2003). A macro study of self-citation. *Scientometrics* 56, 235–246. doi:10.1023/a:1021919228368

Allen, I. C., TeKippe, E. M., Woodford, R. M., Uronis, J. M., Holl, E. K., Rogers, A. B., et al. (2010). The NLRP3 inflammasome functions as a negative regulator of tumorigenesis during colitis-associated cancer. *J. Exp. Med.* 207 (5), 1045–1056. doi:10.1084/jem.20100050

Bardeesi, A. M., Jamjoom, A. A., Algahtani, A., and Jamjoom, A. (2021). The impact of country self-citation rate among medical specialties in Saudi Arabia. *Cureus* 13 (1), e12487. doi:10.7759/cureus.12487

Bauer, C., Duewell, P., Lehr, H. A., Endres, S., and Schnurr, M. (2012). Protective and aggravating effects of Nlrp3 inflammasome activation in IBD models: Influence of genetic and environmental factors. *Dig. Dis.* 30, 82–90. doi:10.1159/000341681

Bennet, J. D., and Brinkman, M. (1989). Treatment of ulcerative colitis by implantation of normal colonic flora. *Lancet* 1 (8630), 164. doi:10.1016/s0140-6736(89)91183-5

Binder, M. T., Becker, E., Wiendl, M., Schleier, L., Fuchs, F., Leppkes, M., et al. (2018). Similar inhibition of dynamic adhesion of lymphocytes from IBD patients to MAdCAM-1 by vedolizumab and etrolizumab-s. *Inflamm. Bowel Dis.* 24 (6), 1237–1250. doi:10.1093/ibd/izy077

Blanchaert, C., Strubbe, B., and Peeters, H. (2019). Fecal microbiota transplantation in ulcerative colitis. *Acta Gastroenterol. belg.* 82 (4), 519

Brown, M., Hughes, K. R., Moossavi, S., Robins, A., and Mahida, Y. R. (2014). Toll-like receptor expression in crypt epithelial cells, putative stem cells and intestinal myofibroblasts isolated from controls and patients with inflammatory bowel disease. *Clin. Exp. Immunol.* 178 (1), 28–39. doi:10.1111/cei.12381

Bryant, R. V., Burger, D. C., Delo, J., Walsh, A. J., Thomas, S., von Herbay, A., et al. (2016). Beyond endoscopic mucosal healing in UC: Histological remission

better predicts corticosteroid use and hospitalisation over 6 years of follow-up. *Gut* 65 (3), 408–414. doi:10.1136/gutjnl-2015-309598

Burisch, J., Vardi, H., Schwartz, D., Friger, M., Kiudelis, G., Kupčinskas, J., et al.Epi-IBD group (2020). Health-care costs of inflammatory bowel disease in a pan-European, community-based, inception cohort during 5 years of follow-up: A population-based study. *Lancet. Gastroenterol. Hepatol.* 5 (5), 454–464. doi:10.1016/S2468-1253(20)30012-1

Caldeira, L. F., Borba, H. H., Tonin, F. S., Wiens, A., Fernandez-Llimos, F., and Pontarolo, R. (2020). Fecal microbiota transplantation in inflammatory bowel disease patients: A systematic review and meta-analysis. *PLoS One* 15 (9), e0238910. doi:10.1371/journal.pone.0238910

Chen, C. M. (2006). CiteSpace II: Detecting and visualizing emerging trends and transient patterns in scientific literature. *J. Am. Soc. Inf. Sci. Technol.* 57, 359–377. doi:10.1002/asi.20317

Chen, M., Liu, X. L., Zhang, Y. J., Nie, Y. Z., Wu, K. C., and Shi, Y. Q. (2020). Efficacy and safety of fecal microbiota transplantation by washed preparation in patients with moderate to severely active ulcerative colitis. *J. Dig. Dis.* 21 (11), 621–628. doi:10.1111/1751-2980.12938

Chen, Z., Zhang, Y., Lin, R., Meng, X., Zhao, W., Shen, W., et al. (2020). Cronobacter sakazakii induces necrotizing enterocolitis by regulating NLRP3 inflammasome expression via TLR4. *J. Med. Microbiol.* 69 (5), 748–758. doi:10.1099/jmm.0.001181

Chow, J. C., Young, D. W., Golenbock, D. T., Christ, W. J., and Gusovsky, F. (1999). Toll-like receptor-4 mediates lipopolysaccharide-induced signal transduction. *J. Biol. Chem.* 274 (16), 10689–10692. doi:10.1074/jbc.274.16.10689

Cobo, M. J., López-Herrera, A. G., Herrera-Viedma, E., and Herrera, F. (2011). An approach for detecting, quantifying, and visualizing the evolution of a research field: A practical application to the fuzzy sets theory field. *J. Inf.* 5 (1), 146–166. doi:10.1016/j.joi.2010.10.002

Cohen, R. D., Yu, A. P., Wu, E. Q., Xie, J., Mulani, P. M., and Chao, J. (2010). Systematic review: The costs of ulcerative colitis in western countries. *Aliment. Pharmacol. Ther.* 31 (7), 693–707. doi:10.1111/j.1365-2036.2010.04234.x

Colombel, J. F., Rutgeerts, P., Reinisch, W., Esser, D., Wang, Y., Lang, Y., et al. (2011). Early mucosal healing with infliximab is associated with improved long-term clinical outcomes in ulcerative colitis. *Gastroenterology* 141 (4), 1194–1201. doi:10.1053/j.gastro.2011.06.054

Connelly, T. M., Devane, L., Kelly, J. C., Wrafter, P., and Messaris, E. (2016). The 100 classic papers in ulcerative colitis: A bibliometric analysis. *Expert Rev. Gastroenterol. Hepatol.* 10 (10), 1187–1195. doi:10.1080/17474124.2016.1216786

Costello, S. P., Hughes, P. A., Waters, O., Bryant, R. V., Vincent, A. D., Blatchford, P., et al. (2019). Effect of fecal microbiota transplantation on 8-week remission in patients with ulcerative colitis: A randomized clinical trial. *JAMA* 321 (2), 156–164. doi:10.1001/jama.2018.20046

Costello, S. P., Soo, W., Bryant, R. V., Jairath, V., Hart, A. L., and Andrews, J. M. (2017). Systematic review with meta-analysis: Faecal microbiota transplantation for the induction of remission for active ulcerative colitis. *Aliment. Pharmacol. Ther.* 46 (3), 213–224. doi:10.1111/apt.14173

Crothers, J. W., Chu, N. D., Nguyen, L. T. T., Phillips, M., Collins, C., Fortner, K., et al. (2021). Daily, oral FMT for long-term maintenance therapy in ulcerative colitis: Results of a single-center, prospective, randomized pilot study. *BMC Gastroenterol.* 21 (1), 281. doi:10.1186/s12876-021-01856-9

Dai, W., Long, L., Wang, X., Li, S., and Xu, H. (2022). Phytochemicals targeting Toll-like receptors 4 (TLR4) in inflammatory bowel disease. *Chin. Med.* 17 (1), 53. doi:10.1186/s13020-022-00611-w

Damman, C. J., Brittnacher, M. J., Westerhoff, M., Hayden, H. S., Radey, M., Hager, K. R., et al. (2015). Low level engraftment and improvement following a single colonoscopic administration of fecal microbiota to patients with ulcerative colitis. *PLoS One* 10 (8), e0133925. doi:10.1371/journal.pone.0133925

DeFilipp, Z., Bloom, P. P., Torres Soto, M., Mansour, M. K., Sater, M. R. A., Huntley, M. H., et al. (2019). Drug-resistant *E. coli* bacteremia transmitted by fecal microbiota transplant. *N. Engl. J. Med.* 381 (21), 2043–2050. doi:10.1056/NEJMoa1910437

Dejban, P., Nikravangolsefid, N., Chamanara, M., Dehpour, A., and Rashidian, A. (2021). The role of medicinal products in the treatment of inflammatory bowel diseases (IBD) through inhibition of TLR4/NF-kappaB pathway. *Phytother. Res.* 35 (2), 835–845. doi:10.1002/ptr.6866

Ding, W., Ding, Z., Wang, Y., Zhu, Y., Gao, Q., Cao, W., et al. (2020). Evodiamine attenuates experimental colitis injury via activating autophagy and inhibiting NLRP3 inflammasome assembly. *Front. Pharmacol.* 11, 573870. doi:10.3389/fphar.2020.573870

Doherty, M. K., Ding, T., Koumpouras, C., Telesco, S. E., Monast, C., Das, A., et al. (2018). Fecal microbiota signatures are associated with response to ustekinumab therapy among Crohn's disease patients. *mBio* 9 (2), e02120-17–17. doi:10.1128/mBio.02120-17

Drews, J. D., Onwuka, E. A., Fisher, J. G., Huntington, J. T., Dutkiewicz, M., Nogalska, A., et al. (2019). Complications after proctocolectomy and ileal pouch-anal anastomosis in pediatric patients: A systematic review. *J. Pediatr. Surg.* 54 (7), 1331–1339. doi:10.1016/j.jpedsurg.2018.08.047

Eckburg, P. B., Bik, E. M., Bernstein, C. N., Purdom, E., Dethlefsen, L., Sargent, M., et al. (2005). Diversity of the human intestinal microbial flora. *Science* 308 (5728), 1635–1638. doi:10.1126/science.1110591

Feagan, B. G., Rutgeerts, P., Sands, B. E., Hanauer, S., Colombel, J. F., Sandborn, W. J., et al.GEMINI 1 Study Group (2013). Vedolizumab as induction and maintenance therapy for ulcerative colitis. *N. Engl. J. Med.* 369 (8), 699–710. doi:10.1056/NEJMoa1215734

Fischer, A., Zundler, S., Atreya, R., Rath, T., Voskens, C., Hirschmann, S., et al. (2016). Differential effects of α4β7 and GPR15 on homing of effector and regulatory T cells from patients with UC to the inflamed gut *in vivo*. *Gut* 65 (10), 1642–1664. doi:10.1136/gutjnl-2015-310022

Fort, M. M., Mozaffarian, A., Stöver, A. G., Correia Jda, S., Johnson, D. A., Crane, R. T., et al. (2005). A synthetic TLR4 antagonist has anti-inflammatory effects in two murine models of inflammatory bowel disease. *J. Immunol.* 174 (10), 6416–6423. doi:10.4049/jimmunol.174.10.6416

Freeman, L. C. (1977). *A set of measures of centrality based on betweenness. Sociometry.* 40 (1), 35–41. doi:10.2307/3033543

Fuentes, S., Rossen, N. G., van der Spek, M. J., Hartman, J. H., Huuskonen, L., Korpela, K., et al. (2017). Microbial shifts and signatures of long-term remission in ulcerative colitis after faecal microbiota transplantation. *ISME J.* 11 (8), 1877–1889. doi:10.1038/ismej.2017.44

Fukata, M., Michelsen, K. S., Eri, R., Thomas, L. S., Hu, B., Lukasek, K., et al. (2005). Toll-like receptor-4 is required for intestinal response to epithelial injury and limiting bacterial translocation in a murine model of acute colitis. *Am. J. Physiol. Gastrointest. Liver Physiol.* 288 (5), G1055–G1065. doi:10.1152/ajpgi.00328.2004

Gami, A. S., Montori, V. M., Wilczynski, N. L., and Haynes, R. B. (2004). Author self-citation in the diabetes literature. *CMAJ* 170 (13), 1925–1927. doi:10.1503/cmaj.1031879

Glänzel, W., and Thijs, B. (2004). Does co-authorship inflate the share of self-citations? *Scientometrics* 61, 395–404. doi:10.1023/B:SCIE.0000045117.13348.b1

Guo, C., Wu, K., Liang, X., Liang, Y., and Li, R. (2019). Infliximab clinically treating ulcerative colitis: A systematic review and meta-analysis. *Pharmacol. Res.* 148, 104455. doi:10.1016/j.phrs.2019.104455

Guo, X. Y., Liu, X. J., and Hao, J. Y. (2020). Gut microbiota in ulcerative colitis: Insights on pathogenesis and treatment. *J. Dig. Dis.* 21 (3), 147–159. doi:10.1111/1751-2980.12849

Haifer, C., Saikal, A., Paramsothy, S., Borody, T. J., Ghaly, D. S., Kaakoush, N. O., et al. (2021). 680 lyophilized orally administered fecal microbiota transplantation in the management of ulcerative colitis (Lotus study) – results from the induction phase of A randomized controlled trial. *Gastroenterology* 160–135. doi:10.1016/s0016-5085(21)01074-x

Hanaei, S., Sadr, M., Rezaei, A., Shahkarami, S., Ebrahimi Daryani, N., Bidoki, A. Z., et al. (2018). Association of NLRP3 single nucleotide polymorphisms with ulcerative colitis: A case-control study. *Clin. Res. Hepatol. Gastroenterol.* 42 (3), 269–275. doi:10.1016/j.clinre.2017.09.003

Hata, K., Anzai, H., Ikeuchi, H., Futami, K., Fukushima, K., Sugita, A., et al. (2019). Surveillance colonoscopy for ulcerative colitis-associated colorectal cancer offers better overall survival in real-world surgically resected cases. *Am. J. Gastroenterol.* 114 (3), 483–489. doi:10.14309/ajg.0000000000000117

Hirota, S. A., Ng, J., Lueng, A., Khajah, M., Parhar, K., Li, Y., et al. (2011). NLRP3 inflammasome plays a key role in the regulation of intestinal homeostasis. *Inflamm. Bowel Dis.* 17 (6), 1359–1372. doi:10.1002/ibd.21478

Hodge, J. A., Kawabata, T. T., Krishnaswami, S., Clark, J. D., Telliez, J. B., Dowty, M. E., et al. (2016). The mechanism of action of tofacitinib - an oral Janus kinase inhibitor for the treatment of rheumatoid arthritis. *Clin. Exp. Rheumatol.* 34 (2), 318

Huang, X. L., Zhang, X., Fei, X. Y., Chen, Z. G., Hao, Y. P., Zhang, S., et al. (2016). Faecalibacterium prausnitzii supernatant ameliorates dextran sulfate sodium induced colitis by regulating Th17 cell differentiation. *World J. Gastroenterol.* 22 (22), 5201–5210. doi:10.3748/wjg.v22.i22.5201

Hyland, K. (2003). Selfcitation and self-reference: Credibility and promotion in academic publication. *J. Am. Soc. Inf. Sci. Technol.* 54 (3), 251–259. doi:10.1002/asi.10204

Jilling, T., Simon, D., Lu, J., Meng, F. J., Li, D., Schy, R., et al. (2006). The roles of bacteria and TLR4 in rat and murine models of necrotizing enterocolitis. *J. Immunol.* 177 (5), 3273–3282. doi:10.4049/jimmunol.177.5.3273

Kaplan, G. G. (2015). The global burden of IBD: From 2015 to 2025. *Nat. Rev. Gastroenterol. Hepatol.* 12 (12), 720–727. doi:10.1038/nrgastro.2015.150

Kawasaki, T., and Kawai, T. (2014). Toll-like receptor signaling pathways. *Front. Immunol.* 5, 461. doi:10.3389/fimmu.2014.00461

Kessler, M. M. (1963). Bibliographic coupling between scientific papers. *Amer. Doc.* 14 (1), 10–25. doi:10.1002/asi.5090140103

Khan, I., Ullah, N., Zha, L., Bai, Y., Khan, A., Zhao, T., et al. (2019). Alteration of gut microbiota in inflammatory bowel disease (IBD): Cause or consequence? IBD treatment targeting the. *Pathogens* 8 (3), 126. doi:10.3390/pathogens8030126

Kleinberg, J. (2003). Bursty and hierarchical structure in streams. *Data Min. Knowl. Discov.* 7, 373–397. doi:10.1023/A:1024940629314

Krell, F. T. (2014). Losing the numbers game: Abundant self-citations put journals at risk for a life without an impact factor. *Eur. Sci. Ed.* 40 (2), 36–38.

Laharie, D., Bourreille, A., Branche, J., Allez, M., Bouhnik, Y., Filippi, J., et al. (2012). Ciclosporin versus infliximab in patients with severe ulcerative colitis refractory to intravenous steroids: A parallel, open-label randomised controlled trial. *Lancet* 380 (9857), 1909–1915. doi:10.1016/S0140-6736(12)61084-8

Levy, A. N., and Allegretti, J. R. (2019). Insights into the role of fecal microbiota transplantation for the treatment of inflammatory bowel disease. *Ther. Adv. Gastroenterol.* 12, 1756284819836893. doi:10.1177/1756284819836893

Li, K. Y., Wang, J. L., Wei, J. P., Gao, S. Y., Zhang, Y. Y., Wang, L. T., et al. (2016). Fecal microbiota in pouchitis and ulcerative colitis. *World J. Gastroenterol.* 22 (40), 8929–8939. doi:10.3748/wjg.v22.i40.8929

Liu, X., Li, Y., Wu, K., Shi, Y., and Chen, M. (2021). Fecal microbiota transplantation as therapy for treatment of active ulcerative colitis: A systematic review and meta-analysis. *Gastroenterol. Res. Pract.*, 2021, 6612970. doi:10.1155/2021/6612970

Liu, Y., Zhang, Z., Wang, L., Li, J., Dong, L., Yue, W., et al. (2010). TLR4 monoclonal antibody blockade suppresses dextran-sulfate-sodium-induced colitis in mice. *J. Gastroenterol. Hepatol.* 25 (1), 209–214. doi:10.1111/j.1440-1746.2009.06046.x

Livas, C., Delli, K., and Pandis, N. (2021). Author self-citation in orthodontics is associated with author origin and gender. *Prog. Orthod.* 22 (1), 1. doi:10.1186/s40510-020-00348-y

Lloyd-Price, J., Arze, C., Ananthakrishnan, A. N., Schirmer, M., Avila-Pacheco, J., Poon, T. W., et al. (2019). Multi-omics of the gut microbial ecosystem in inflammatory bowel diseases. *Nature* 569 (7758), 655–662. doi:10.1038/s41586-019-1237-9

Lopez-Siles, M., Martinez-Medina, M., Busquets, D., Sabat-Mir, M., Duncan, S. H., Flint, H. J., et al. (2014). Mucosa-associated Faecalibacterium prausnitzii and *Escherichia coli* co-abundance can distinguish irritable bowel syndrome and inflammatory bowel disease phenotypes. *Int. J. Med. Microbiol.* 304 (3-4), 464–475. doi:10.1016/j.ijmm.2014.02.009

Lu, G., Wang, W., Li, P., Wen, Q., Cui, B., and Zhang, F. (2022). Washed preparation of faecal microbiota changes the transplantation related safety, quantitative method and delivery. *Microb. Biotechnol.* doi:10.1111/1751-7915.14074

Lu, P. D., and Zhao, Y. H. (2020). Targeting NF-κB pathway for treating ulcerative colitis: Comprehensive regulatory characteristics of Chinese medicines. *Chin. Med.* 15, 15. doi:10.1186/s13020-020-0296-z

Lucaciu, L. A., Constantine-Cooke, N., Plevris, N., Siakavellas, S., Derikx, L. A. A. P., Jones, G. R., et al. (2021). Real-world experience with tofacitinib in ulcerative colitis: A systematic review and meta-analysis. *Ther. Adv. Gastroenterol.* 14, 17562848211064004. doi:10.1177/17562848211064004

Luo, W. Y., Singh, S., Cuomo, R., and Eisenstein, S. (2020). Modified two-stage restorative proctocolectomy with ileal pouch-anal anastomosis for ulcerative colitis: A systematic review and meta-analysis of observational research. *Int. J. Colorectal Dis.* 35 (10), 1817–1830. doi:10.1007/s00384-020-03696-7

Magnusson, M. K., Strid, H., Sapnara, M., Lasson, A., Bajor, A., Ung, K. A., et al. (2016). Anti-TNF therapy response in patients with ulcerative colitis is associated with colonic antimicrobial peptide expression and microbiota composition. *J. Crohns Colitis* 10 (8), 943–952. doi:10.1093/ecco-jcc/jjw051

Mai, C. T., Wu, M. M., Wang, C. L., Su, Z. R., Cheng, Y. Y., and Zhang, X. J. (2019). Palmatine attenuated dextran sulfate sodium (DSS)-induced colitis via promoting mitophagy-mediated NLRP3 inflammasome inactivation. *Mol. Immunol.* 105, 76–85. doi:10.1016/j.molimm.2018.10.015

Marcella, C., Cui, B., Kelly, C. R., Ianiro, G., Cammarota, G., and Zhang, F. (2021). Systematic review: The global incidence of faecal microbiota transplantation-related adverse events from 2000 to 2020. *Aliment. Pharmacol. Ther.* 53 (1), 33–42. doi:10.1111/apt.16148

Marchal-Bressenot, A., Salleron, J., Boulagnon-Rombi, C., Bastien, C., Cahn, V., Cadiot, G., et al. (2017). Development and validation of the Nancy histological index for UC. *Gut* 66 (1), 43–49. doi:10.1136/gutjnl-2015-310187

Marshakova, I. V. (1973). System of document connections based on references. *Nauchno-Tekhnicheskaya Inf. Seriya 2-Informatsionnye Protsessy I Sist.* (6), 3

Martín, R., Bermúdez-Humarán, L. G., and Langella, P. (2018). Searching for the bacterial effector: The example of the multi-skilled commensal bacterium Faecalibacterium prausnitzii. *Front. Microbiol.* 9, 346. doi:10.3389/fmicb.2018.00346

Meyer, D. M., Jesson, M. I., Li, X., Elrick, M. M., Funckes-Shippy, C. L., Warner, J. D., et al. (2010). Anti-inflammatory activity and neutrophil reductions mediated by the JAK1/JAK3 inhibitor, CP-690, 550, in rat adjuvant-induced arthritis. *J. Inflamm.* 7, 41. doi:10.1186/1476-9255-7-41

Miao, F., Shan, C., Ma, T., Geng, S., and Ning, D. (2021). Walnut oil alleviates DSS-induced colitis in mice by inhibiting NLRP3 inflammasome activation and regulating gut microbiota. *Microb. Pathog.* 154, 104866. doi:10.1016/j.micpath.2021.104866

Miggin, S. M., and O'Neill, L. A. (2006). New insights into the regulation of TLR signaling. *J. Leukoc. Biol.* 80 (2), 220–226. doi:10.1189/jlb.1105672

Moayyedi, P., Surette, M. G., Kim, P. T., Libertucci, J., Wolfe, M., Onischi, C., et al. (2015). Fecal microbiota transplantation induces remission in patients with active ulcerative colitis in a randomized controlled trial. *Gastroenterology* 149 (1), 102–109. doi:10.1053/j.gastro.2015.04.001

Shi, Q. (2020). Nanjing consensus on methodology of washed microbiota transplantation. *Chin. Med. J.* 133, 2330–2332. doi:10.1097/CM9.0000000000000954

Narula, N., Kassam, Z., Yuan, Y., Colombel, J. F., Ponsioen, C., Reinisch, W., et al. (2017). Systematic review and meta-analysis: Fecal microbiota transplantation for treatment of active ulcerative colitis. *Inflamm. Bowel Dis.* 23 (10), 1702–1709. doi:10.1097/MIB.0000000000001228

Ng, S. C., Shi, H. Y., Hamidi, N., Underwood, F. E., Tang, W., Benchimol, E. I., et al. (2017). Worldwide incidence and prevalence of inflammatory bowel disease in the 21st century: A systematic review of population-based studies. *Lancet* 390 (10114), 2769–2778. doi:10.1016/S0140-6736(17)32448-0

Nguyen, N. H., Fumery, M., Dulai, P. S., Prokop, L. J., Sandborn, W. J., Murad, M. H., et al. (2018). Comparative efficacy and tolerability of pharmacological agents for management of mild to moderate ulcerative colitis: A systematic review and network meta-analyses. *Lancet. Gastroenterol. Hepatol.* 3 (11), 742–753. doi:10.1016/S2468-1253(18)30231-0

Panaccione, R., Ghosh, S., Middleton, S., Márquez, J. R., Scott, B. B., Flint, L., et al. (2014). Combination therapy with infliximab and azathioprine is superior to monotherapy with either agent in ulcerative colitis. *Gastroenterology* 146 (2), 392–400. doi:10.1053/j.gastro.2013.10.052

Pandey, N., Chauhan, A., and Jain, N. (2018). TLR4 polymorphisms and expression in solid cancers. *Mol. Diagn. Ther.* 22 (6), 683–702. doi:10.1007/s40291-018-0361-9

Paramsothy, S., Kamm, M. A., Kaakoush, N. O., Walsh, A. J., van den Bogaerde, J., Samuel, D., et al. (2017). Multidonor intensive faecal microbiota transplantation for active ulcerative colitis: A randomised placebo-controlled trial. *Lancet* 389 (10075), 1218–1228. doi:10.1016/S0140-6736(17)30182-4

Paramsothy, S., Nielsen, S., Kamm, M. A., Deshpande, N. P., Faith, J. J., Clemente, J. C., et al. (2019). Specific bacteria and metabolites associated with response to fecal microbiota transplantation in patients with ulcerative colitis. *Gastroenterology* 156 (5), 1440–1454. doi:10.1053/j.gastro.2018.12.001

Park, H. J., Kim, J., Saima, F. T., Rhee, K. J., Hwang, S., Kim, M. Y., et al. (2018). Adipose-derived stem cells ameliorate colitis by suppression of inflammasome formation and regulation of M1-macrophage population through prostaglandin E2. *Biochem. Biophys. Res. Commun.* 498 (4), 988–995. doi:10.1016/j.bbrc.2018.03.096

Patterson, A. M., Mulder, I. E., Travis, A. J., Lan, A., Cerf-Bensussan, N., Gaboriau-Routhiau, V., et al. (2017). Human gut symbiont Roseburia hominis promotes and regulates innate immunity. *Front. Immunol.* 8, 1166. doi:10.3389/fimmu.2017.01166

Pearce, J. (2016). Are you overpaying your academic executive team? A method for detecting unmerited academic executive compensation. *Tert. Educ. Manag.* 22 (3), 189–201. doi:10.1080/13583883.2016.1181198

Perera, A. P., Fernando, R., Shinde, T., Gundamaraju, R., Southam, B., Sohal, S. S., et al. (2018). MCC950, a specific small molecule inhibitor of NLRP3 inflammasome attenuates colonic inflammation in spontaneous colitis mice. *Sci. Rep.* 8 (1), 8618. doi:10.1038/s41598-018-26775-w

Prosberg, M., Bendtsen, F., Vind, I., Petersen, A. M., and Gluud, L. L. (2016). The association between the gut microbiota and the inflammatory bowel disease activity: A systematic review and meta-analysis. *Scand. J. Gastroenterol.* 51 (12), 1407–1415. doi:10.1080/00365521.2016.1216587

Quévrain, E., Maubert, M. A., Michon, C., Chain, F., Marquant, R., Tailhades, J., et al. (2016). Identification of an anti-inflammatory protein from Faecalibacterium prausnitzii, a commensal bacterium deficient in Crohn's disease. *Gut* 65 (3), 415–425. doi:10.1136/gutjnl-2014-307649

Radhakrishnan, S. T., Alexander, J. L., Mullish, B. H., Gallagher, K. I., Powell, N., Hicks, L. C., et al. (2022). Systematic review: The association between the gut microbiota and medical therapies in inflammatory bowel disease. *Aliment. Pharmacol. Ther.* 55 (1), 26–48. doi:10.1111/apt.16656

Rajca, S., Grondin, V., Louis, E., Vernier-Massouille, G., Grimaud, J. C., Bouhnik, Y., et al. (2014). Alterations in the intestinal microbiome (dysbiosis) as a predictor of relapse after infliximab withdrawal in Crohn's disease. *Inflamm. Bowel Dis.* 20 (6), 978–986. doi:10.1097/MIB.0000000000000036

Ramirez-Farias, C., Slezak, K., Fuller, Z., Duncan, A., Holtrop, G., and Louis, P. (2009). Effect of inulin on the human gut microbiota: Stimulation of bifidobacterium adolescentis and Faecalibacterium prausnitzii. *Br. J. Nutr.* 101 (4), 541–550. doi:10.1017/S0007114508019880

Ranson, N., Veldhuis, M., Mitchell, B., Fanning, S., Cook, A. L., Kunde, D., et al. (2018). NLRP3-Dependent and -independent processing of interleukin (IL)-1β in active ulcerative colitis. *Int. J. Mol. Sci.* 20 (1), 57. doi:10.3390/ijms20010057

Rath, T., Billmeier, U., Ferrazzi, F., Vieth, M., Ekici, A., Neurath, M. F., et al. (2018). Effects of anti-integrin treatment with vedolizumab on immune pathways and cytokines in inflammatory bowel diseases. *Front. Immunol.* 9, 1700. doi:10.3389/fimmu.2018.01700

Reinisch, W., Sandborn, W. J., Hommes, D. W., D'Haens, G., Hanauer, S., Schreiber, S., et al. (2011). Adalimumab for induction of clinical remission in moderately to severely active ulcerative colitis: Results of a randomised controlled trial. *Gut* 60 (6), 780–787. doi:10.1136/gut.2010.221127

Ren, G., Sun, A., Deng, C., Zhang, J., Wu, X., Wei, X., et al. (2015). The anti-inflammatory effect and potential mechanism of cardamonin in DSS-induced colitis. *Am. J. Physiol. Gastrointest. Liver Physiol.* 309 (7), G517–G527. doi:10.1152/ajpgi.00133.2015

Rossen, N. G., Fuentes, S., van der Spek, M. J., Tijssen, J. G., Hartman, J. H., Duflou, A., et al. (2015). Findings from a randomized controlled trial of fecal transplantation for patients with ulcerative colitis. *Gastroenterology* 149 (1), 110–118. doi:10.1053/j.gastro.2015.03.045

Rossi, O., van Berkel, L. A., Chain, F., Tanweer Khan, M., Taverne, N., Sokol, H., et al. (2016). Faecalibacterium prausnitzii A2-165 has a high capacity to induce IL-10 in human and murine dendritic cells and modulates T cell responses. *Sci. Rep.* 6, 18507. doi:10.1038/srep18507

Ruiz, P. A., Morón, B., Becker, H. M., Lang, S., Atrott, K., Spalinger, M. R., et al. (2017). Titanium dioxide nanoparticles exacerbate DSS-induced colitis: Role of the NLRP3 inflammasome. *Gut* 66 (7), 1216–1224. doi:10.1136/gutjnl-2015-310297

Saber, S., and El-Kader, E. M. A. (2021). Novel complementary coloprotective effects of metformin and MCC950 by modulating HSP90/NLRP3 interaction and inducing autophagy in rats. *Inflammopharmacology* 29 (1), 237–251. doi:10.1007/s10787-020-00730-6

Sandborn, W. J., Feagan, B. G., Marano, C., Zhang, H., Strauss, R., Johanns, J., et al.PURSUIT-SC Study Group (2014). Subcutaneous golimumab induces clinical response and remission in patients with moderate-to-severe ulcerative colitis. *Gastroenterology* 146 (1), 85–95. doi:10.1053/j.gastro.2013.05.048

Sandborn, W. J., Feagan, B. G., Rutgeerts, P., Hanauer, S., Colombel, J. F., Sands, B. E., et al.GEMINI 2 Study Group (2013). Vedolizumab as induction and maintenance therapy for Crohn's disease. *N. Engl. J. Med.* 369 (8), 711–721. doi:10.1056/NEJMoa1215739

Sandborn, W. J., Ghosh, S., Panes, J., Vranic, I., Su, C., Rousell, S., et al. (2012). Tofacitinib, an oral Janus kinase inhibitor, in active ulcerative colitis. *N. Engl. J. Med.* 367 (7), 616–624. doi:10.1056/NEJMoa1112168

Sandborn, W. J., Rutgeerts, P., Feagan, B. G., Reinisch, W., Olson, A., Johanns, J., et al. (2009). Colectomy rate comparison after treatment of ulcerative colitis with placebo or infliximab. *Gastroenterology* 137 (4), 1250–1260. doi:10.1053/j.gastro.2009.06.061

Sandborn, W. J., Su, C., Sands, B. E., D'Haens, G. R., Vermeire, S., Schreiber, S., et al. (2017). Tofacitinib as induction and maintenance therapy for ulcerative colitis. *N. Engl. J. Med.* 376 (18), 1723–1736. doi:10.1056/NEJMoa1606910

Sandborn, W. J., van Assche, G., Reinisch, W., Colombel, J. F., D'Haens, G., Wolf, D. C., et al. (2012). Adalimumab induces and maintains clinical remission in patients with moderate-to-severe ulcerative colitis. *Gastroenterology* 142 (2), 257–265. doi:10.1053/j.gastro.2011.10.032

Sands, B. E., Feagan, B. G., Rutgeerts, P., Colombel, J. F., Sandborn, W. J., Sy, R., et al. (2014). Effects of vedolizumab induction therapy for patients with Crohn's disease in whom tumor necrosis factor antagonist treatment failed. *Gastroenterology* 147 (3), 618–627. doi:10.1053/j.gastro.2014.05.008

Sarrabayrouse, G., Bossard, C., Chauvin, J. M., Jarry, A., Meurette, G., Quévrain, E., et al. (2014). CD4CD8αα lymphocytes, a novel human regulatory T cell subset induced by colonic bacteria and deficient in patients with inflammatory bowel disease. *PLoS Biol.* 12 (4), e1001833. doi:10.1371/journal.pbio.1001833

Schierová, D., Březina, J., Mrázek, J., Fliegerová, K. O., Kvasnová, S., Bajer, L., et al. (2020). Gut microbiome changes in patients with active left-sided ulcerative colitis after fecal microbiome transplantation and topical 5-aminosalicylic acid therapy. *Cells* 9 (10), 2283. doi:10.3390/cells9102283

Schink, A., Neumann, J., Leifke, A. L., Ziegler, K., Fröhlich-Nowoisky, J., Cremer, C., et al. (2018). Screening of herbal extracts for TLR2- and TLR4-dependent anti-inflammatory effects. *PLoS One* 13 (10), e0203907. doi:10.1371/journal.pone.0203907

Schöffel, N., Bendels, M. H., and Groneberg, D. A. (2016). Ulcerative colitis: A scientometric approach to the global research output and network. *Eur. J. Intern. Med.* 34, e41–e43. doi:10.1016/j.ejim.2016.06.019

Schöffel, N., Brüggmann, D., Klingelhöfer, D., Bendels, M. H. K., and Groneberg, D. A. (2021). Ulcerative colitis: A critical approach to the global research output employing density-equalizing mapping and scientometric methods. *J. Clin. Gastroenterol.* 55 (3), e19–e26. doi:10.1097/mcg.0000000000001351

Small, H. (1973). Co-citation in the scientific literature: A new measure of the relationship between two documents. *J. Am. Soc. Inf. Sci.* 24 (4), 265–269. doi:10.1002/asi.4630240406

Smith, R. L., Taylor, K. M., Friedman, A. B., Gibson, R. N., and Gibson, P. R. (2020). Systematic review: Clinical utility of gastrointestinal ultrasound in the diagnosis, assessment and management of patients with ulcerative colitis. *J. Crohns Colitis* 14 (4), 465–479. doi:10.1093/ecco-jcc/jjz163

Sokol, H., Pigneur, B., Watterlot, L., Lakhdari, O., Bermúdez-Humarán, L. G., Gratadoux, J. J., et al. (2008). Faecalibacterium prausnitzii is an anti-inflammatory commensal bacterium identified by gut microbiota analysis of Crohn disease patients. *Proc. Natl. Acad. Sci. U. S. A.* 105 (43), 16731–16736. doi:10.1073/pnas.0804812105

Sokol, H., Seksik, P., Furet, J. P., Firmesse, O., Nion-Larmurier, I., Beaugerie, L., et al. (2009). Low counts of Faecalibacterium prausnitzii in colitis microbiota. *Inflamm. Bowel Dis.* 15 (8), 1183–1189. doi:10.1002/ibd.20903

Sood, A., Mahajan, R., Singh, A., Midha, V., Mehta, V., Narang, V., et al. (2019). Role of faecal microbiota transplantation for maintenance of remission in patients with ulcerative colitis: A pilot study. *J. Crohns Colitis* 13 (10), 1311–1317. doi:10.1093/ecco-jcc/jjz060

Takahashi, K., Sugi, Y., Hosono, A., and Kaminogawa, S. (2009). Epigenetic regulation of TLR4 gene expression in intestinal epithelial cells for the maintenance of intestinal homeostasis. *J. Immunol.* 183 (10), 6522–6529. doi:10.4049/jimmunol.0901271

Tam, W. W. S., Wong, E. L. Y., Wong, F. C. Y., and Cheung, A. W. L. (2012). Citation classics in the integrative and complementary medicine literature: 50 frequently cited articles. *Eur. J. Integr. Med.* 4 (1), e77–e83. doi:10.1016/j.eujim.2011.12.004

Tan, Y., Zou, K. F., Qian, W., Chen, S., and Hou, X. H. (2014). Expression and implication of toll-like receptors TLR2, TLR4 and TLR9 in colonic mucosa of patients with ulcerative colitis. *J. Huazhong Univ. Sci. Technol. Med. Sci.* 34 (5), 785–790. doi:10.1007/s11596-014-1353-6

Tang, L. L., Feng, W. Z., Cheng, J. J., and Gong, Y. N. (2020). Clinical remission of ulcerative colitis after different modes of faecal microbiota transplantation: A meta-analysis. *Int. J. Colorectal Dis.* 35 (6), 1025–1034. doi:10.1007/s00384-020-03599-7

Taxonera, C., Olivares, D., and Alba, C. (2022). Real-world effectiveness and safety of tofacitinib in patients with ulcerative colitis: Systematic review with meta-analysis. *Inflamm. Bowel Dis.* 28 (1), 32–40. doi:10.1093/ibd/izab011

Ungaro, R., Fukata, M., Hsu, D., Hernandez, Y., Breglio, K., Chen, A., et al. (2009). A novel Toll-like receptor 4 antagonist antibody ameliorates inflammation but impairs mucosal healing in murine colitis. *Am. J. Physiol. Gastrointest. Liver Physiol.* 296 (6), G1167–G1179. doi:10.1152/ajpgi.90496.2008

Van Eck, N. J., and Waltman, L. (2010). Software survey: VOSviewer, a computer Program for bibliometric mapping. *Scientometrics* 84 (2), 523–538. doi:10.1007/s11192-009-0146-3

Vande Casteele, N., Jeyarajah, J., Jairath, V., Feagan, B. G., and Sandborn, W. J. (2019). Infliximab exposure-response relationship and thresholds associated with endoscopic healing in patients with ulcerative colitis. *Clin. Gastroenterol. Hepatol.* 17 (9), 1814–1821. doi:10.1016/j.cgh.2018.10.036

Varela, E., Manichanh, C., Gallart, M., Torrejón, A., Borruel, N., Casellas, F., et al. (2013). Colonisation by Faecalibacterium prausnitzii and maintenance of clinical remission in patients with ulcerative colitis. *Aliment. Pharmacol. Ther.* 38 (2), 151–161. doi:10.1111/apt.12365

Viola, A., Fiorino, G., Costantino, G., and Fries, W. (2021). Epidemiology and clinical course of late onset inflammatory bowel disease. *Minerva Gastroenterol (Torino)*. doi:10.23736/S2724-5985.21.02890-4

Wagatsuma, K., and Nakase, H. (2020). Contradictory effects of NLRP3 inflammasome regulatory mechanisms in colitis. *Int. J. Mol. Sci.* 21 (21), 8145. doi:10.3390/ijms21218145

Walker, A. W., Ince, J., Duncan, S. H., Webster, L. M., Holtrop, G., Ze, X., et al. (2011). Dominant and diet-responsive groups of bacteria within the human colonic microbiota. *ISME J.* 5 (2), 220–230. doi:10.1038/ismej.2010.118

Wang, K., Lv, Q., Miao, Y. M., Qiao, S. M., Dai, Y., and Wei, Z. F. (2018). Cardamonin, a natural flavone, alleviates inflammatory bowel disease by the inhibition of NLRP3 inflammasome activation via an AhR/Nrf2/NQO1 pathway. *Biochem. Pharmacol.* 155, 494–509. doi:10.1016/j.bcp.2018.07.039

Wang, W., Wu, L., Wu, X., Li, K., Li, T., Xu, B., et al. (2021). Combined analysis of serum SAP and PRSS2 for the differential diagnosis of CD and UC. *Clin. Chim. Acta.* 514, 8–14. doi:10.1016/j.cca.2020.12.014

Wang, Y., Cui, B., and Zhang, F. (2022). Refractory ulcerative colitis stabilized by interval washed microbiota transplantation: Less is more. *Curr. Med. Res. Opin.* 38 (4), 531–534. doi:10.1080/03007995.2022.2030563

Wardill, H. R., Choo, J. M., Dmochowska, N., Mavrangelos, C., Campaniello, M. A., Bowen, J. M., et al. (2019). Acute colitis drives tolerance by persistently altering the epithelial barrier and innate and adaptive immunity. *Inflamm. Bowel Dis.* 25 (7), 1196–1207. doi:10.1093/ibd/izz011

Wei, Y., Gong, J., Zhu, W., Tian, H., Ding, C., Gu, L., et al. (2016). Pectin enhances the effect of fecal microbiota transplantation in ulcerative colitis by delaying the loss of diversity of gut flora. *BMC Microbiol.* 16 (1), 255. doi:10.1186/s12866-016-0869-2

Wilks, S. (1859). Morbid appearances in the intestines of miss bankes. *Med. Times Gaz.* 2, 264

Wu, D., Wu, K., Zhu, Q., Xiao, W., Shan, Q., Yan, Z., et al. (2018 Jan 820182018 Sep 6201). Formononetin administration ameliorates dextran sulfate sodium-induced acute colitis by inhibiting NLRP3 inflammasome signaling pathway. *Mediat. Inflamm.* 304853. doi:10.1155/2018/3048532

Wu, X., Cui, B. T., and Zhang, F. M. (2021). Washed microbiota transplantation for the treatment of recurrent fungal infection in a patient with ulcerative colitis. *Chin. Med. J.* 134 (6), 741–742. doi:10.1097/CM9.0000000000001212

Xiong, J. Q., Fu, Y. F., Qiu, J. H., Liao, W. D., Luo, L. Y., and Chen, S. H. (2022). Global research trends of immunotherapy and biotherapy for inflammatory bowel disease: A bibliometric analysis from 2002 to 2021. *Biomed. Eng. Online* 21 (1), 42. doi:10.1186/s12938-022-01011-9

Yao, P., Cui, M., Wang, H., Gao, H., Wang, L., Yang, T., et al. (2016). Quantitative analysis of intestinal flora of uygur and han ethnic Chinese patients with ulcerative colitis. *Gastroenterol. Res. Pract.* 2016, 9186232. doi:10.1155/2016/9186232

Yarur, A., Mantzaris, G., Silverberg, M., Walshe, M., Zezos, P., Stein, D., et al. (2019). P573 real-world effectiveness and safety of vedolizumab and anti-TNF in biologic-naive ulcerative colitis patients: Results from the EVOLVE study. *J. Crohn's. Colitis* 13, S400–S401. doi:10.1093/ecco-jcc/jjy222.697

Zaki, M. H., Boyd, K. L., Vogel, P., Kastan, M. B., Lamkanfi, M., and Kanneganti, T. D. (2010). The NLRP3 inflammasome protects against loss of epithelial integrity and mortality during experimental colitis. *Immunity* 32 (3), 379–391. doi:10.1016/j.immuni.2010.03.003

Zambetti, L. P., and Mortellaro, A. (2014). NLRPs, microbiota, and gut homeostasis: Unravelling the connection. *J. Pathol.* 233 (4), 321–330. doi:10.1002/path.4357

Zeissig, S., Rosati, E., Dowds, C. M., Aden, K., Bethge, J., Schulte, B., et al. (2019). Vedolizumab is associated with changes in innate rather than adaptive immunity in patients with inflammatory bowel disease. *Gut* 68 (1), 25–39. doi:10.1136/gutjnl-2018-316023

Zhang, J., Dou, W., Zhang, E., Sun, A., Ding, L., Wei, X., et al. (2014). Paeoniflorin abrogates DSS-induced colitis via a TLR4-dependent pathway. *Am. J. Physiol. Gastrointest. Liver Physiol.* 306 (1), G27–G36. doi:10.1152/ajpgi.00465.2012

Zhang, L., and Gan, H. (2021). Secondary colon cancer in patients with ulcerative colitis: a systematic review and meta-analysis. *J. Gastrointest. Oncol.* 12 (6), 2882–2890. doi:10.21037/jgo-21-800

Zhang, M., Qiu, X., Zhang, H., Yang, X., Hong, N., Yang, Y., et al. (2014). Faecalibacterium prausnitzii inhibits interleukin-17 to ameliorate colorectal colitis in rats. *PLoS One* 9 (10), e109146. doi:10.1371/journal.pone.0109146

Zhang, T., Li, P., Wu, X., Lu, G., Marcella, C., Ji, X., et al. (2020). Alterations of Akkermansia muciniphila in the inflammatory bowel disease patients with washed microbiota transplantation. *Appl. Microbiol. Biotechnol.* 104 (23), 10203–10215. doi:10.1007/s00253-020-10948-7

Zhang, T., Lu, G., Zhao, Z., Liu, Y., Shen, Q., Li, P., et al. (2020). Washed microbiota transplantation vs. manual fecal microbiota transplantation: clinical findings, animal studies and *in vitro* screening. *Protein Cell.* 11 (4), 251–266. doi:10.1007/s13238-019-00684-8

Zhang, Z., Li, S., Cao, H., Shen, P., Liu, J., Fu, Y., et al. (2019). The protective role of phloretin against dextran sulfate sodium-induced ulcerative colitis in mice. *Food Funct.* 10 (1), 422–431. doi:10.1039/c8fo01699b

Zhao, H., Xu, H., Chen, S., He, J., Zhou, Y., and Nie, Y. (2021). Systematic review and meta-analysis of the role of faecalibacterium prausnitzii alteration in inflammatory bowel disease. *J. Gastroenterol. Hepatol.* 36 (2), 320–328. doi:10.1111/jgh.15222

Zhao, Z., Ji, X., Zhang, T., Li, Q., Marcella, C., Wen, Q., et al. (2022). Washed microbiota transplantation improves the fertility of patients with inflammatory bowel disease. *Chin. Med. J.* doi:10.1097/CM9.0000000000002284

Zhou, Q., Shen, Z. F., Wu, B. S., Xu, C. B., He, Z. Q., Chen, T., et al. (2019). Risk of colorectal cancer in ulcerative colitis patients: A systematic review and meta-analysis. *Gastroenterol. Res. Pract.*, 5363261. doi:10.1155/2019/5363261

Advantages of publishing in Frontiers

OPEN ACCESS
Articles are free to read for greatest visibility and readership

FAST PUBLICATION
Around 90 days from submission to decision

HIGH QUALITY PEER-REVIEW
Rigorous, collaborative, and constructive peer-review

TRANSPARENT PEER-REVIEW
Editors and reviewers acknowledged by name on published articles

Frontiers
Avenue du Tribunal-Fédéral 34
1005 Lausanne | Switzerland

Visit us: www.frontiersin.org
Contact us: frontiersin.org/about/contact

REPRODUCIBILITY OF RESEARCH
Support open data and methods to enhance research reproducibility

DIGITAL PUBLISHING
Articles designed for optimal readership across devices

FOLLOW US
@frontiersin

IMPACT METRICS
Advanced article metrics track visibility across digital media

EXTENSIVE PROMOTION
Marketing and promotion of impactful research

LOOP RESEARCH NETWORK
Our network increases your article's readership